AD-A101 143 AIR FORCE INST OF TECH WRIGHT-PATTERSON AFB OH SCHOO--ETC F/G 17/9
MULTIPLE ARRESTED SYNTHETIC APERTURE RADAR.(U)
MAY 81 J S SHUSTER
UNCLASSIFIED AFIT/DS/EE/81-3 NL

1 OF 5
AD A
101143

AFIT/DS/EE/81-1

LEVEL II

AD A101143

DTIC FILE COPY

MULTIPLE ARRESTED

SYNTHETIC APERTURE RADAR

DISSERTATION

AFIT/DS/EE/81-1

Jerrold S. Shuster
Major USAF

Approved for public release; distribution unlimited

DTIC
ELECTE
JUL 9 1981
S D
D

UNCLASSIFIED

SECURITY CLASSIFICATION OF THIS PAGE (When Data Entered)

REPORT DOCUMENTATION PAGE		READ INSTRUCTIONS BEFORE COMPLETING FORM
1. REPORT NUMBER AFIT/DS/EE/81-1	2. GOVT ACCESSION NO. AD-A101143	3. RECIPIENT'S CATALOG NUMBER
4. TITLE (and Subtitle) MULTIPLE ARRESTED SYNTHETIC APERTURE RADAR		5. TYPE OF REPORT & PERIOD COVERED Doctoral Dissertation 6. PERFORMING ORG. REPORT NUMBER
7. AUTHOR(s) Jerrold S. Shuster, Major, USAF		8. CONTRACT OR GRANT NUMBER(s)
9. PERFORMING ORGANIZATION NAME AND ADDRESS Air Force Institute of Technology (AFIT/ENG) Wright-Patterson AFB, OH 45433		10. PROGRAM ELEMENT, PROJECT, TASK AREA & WORK UNIT NUMBERS 2305J402
11. CONTROLLING OFFICE NAME AND ADDRESS Deputy for Electronic Technology (RADC/EE) Hanscom AFB, MA 01731		12. REPORT DATE May 1981 13. NUMBER OF PAGES 295
14. MONITORING AGENCY NAME & ADDRESS(if different from Controlling Office)		15. SECURITY CLASS. (of this report) Unclassified 15a. DECLASSIFICATION DOWNGRADING SCHEDULE

16. DISTRIBUTION STATEMENT (of this Report)

Approved for public release; distribution unlimited

17 JUN 1981

17. DISTRIBUTION STATEMENT (of the abstract entered in Block 20, if different from Report)

APPROVED FOR PUBLIC RELEASE AFR 190-17.

Fredric C. Lynch

FREDRIC C. LYNCH, Major, USAF
Director of Public Affairs
Air Force Institute of Technology (ATC)
Wright-Patterson AFB, OH 45433

18. SUPPLEMENTARY NOTES

19. KEY WORDS (Continue on reverse side if necessary and identify by block number)

Radar
Synthetic Aperture
Moving Target
Detection
Clutter
Quadratic Forms
Optimization
Modeling

20. ABSTRACT (Continue on reverse side if necessary and identify by block number)

This report contains the formulation and analysis of an airborne synthetic aperture radar scheme which employs a multiplicity of antennas with the displaced phase center antenna technique to detect slowly moving targets embedded in a severe clutter environment. The radar is evaluated using the target to clutter power ratio as the measure of performance. Noise is ignored in the analysis. An optimization scheme which maximizes this ratio is employed to obtain the optimum processor weighting. The performance of the MASAR processor with optimum weights (over)

DD FORM 1473 1 JAN 73 EDITION OF 1 NOV 65 IS OBSOLETE

UNCLASSIFIED

SECURITY CLASSIFICATION OF THIS PAGE (When Data Entered)

20. (cont'd)

is compared against that using target weights (composed of the target signal) and that using binomial weights (which, effectively, form an n-pulse canceller). Both the target and the clutter are modeled with the electric field backscattering coefficient. The target is modeled simply as a deterministically moving point scatterer with the same albedo as a point of clutter. The clutter is modeled as a homogeneous, isotropic, two-dimensional, spatiotemporal random field for which only the correlation properties are required. The analysis shows that this radar, with its optimum weighting scheme, is a promising synthetic aperture concept for the detection of slowly moving targets immersed in strong clutter environments.

Accession For	
NTIS GRA&I	☒
DTIC TAB	☐
Unannounced	☐
Justification	
By	
Distribution/	
Availability Codes	
Dist	Avail and/or Special
A	

AFIT/DS/EE/81-1

MULTIPLE ARRESTED SYNTHETIC APERTURE RADAR

DISSERTATION

Presented to the Faculty of the School of Engineering
of the Air Force Institute of Technology
Air University
in Partial Fulfillment of the
Requirements for the Degree of
Doctor of Philosophy

by

Jerrold S. Shuster, B.S., M.S.
Major USAF

May 1981

Approved for public release; distribution unlimited

AFIT/DS/EE/81-1

MULTIPLE ARRESTED
SYNTHETIC APERTURE RADAR

DISSERTATION

by

Jerrold S. Shuster, B.S., M.S.

Major USAF

Approved:

Stanley R. Robinson Chairman	1 June 1981
Donn G. Shankland	9 June 1981
Robert E. Fontana	8 June 1981
Ronald J. Carpinella	8 June 1981
John N. Schindler	27 May 1981

Accepted:

J S Przemieniecki Dean, School of Engineering	9 June 1981

ACKNOWLEDGEMENTS

Dr John K. Schindler started me on a "passage" which profoundly affected my life (little did I realize how much it would!) by introducing me to the concept of Arrested Synthetic Aperture Radar. Though the way--for me--was fraught with every kind of humam emotion, this manuscript brings that passage to a very satisfying conclusion and I thank him for it.

There was a particular "dark period" the source of which shall be described simply as the "exigencies of the Service". Therein, I was forced into a state of psuedo-limbo (or, continuing intermittent hiatus) in the course of my research. I was literally rescued from this by two exceptionally concerned people: Lt Col David C. Luke and Col Pat J. O'Toole. They isolated and protected me for one full year. That was the crucial turning point. During that time, I was able to get my ideas to coalesce and I was able to completely formulate the MASAR model. To them I owe my deepest gratitude, for--in plain fact--without their intervention I never could have completed this work.

I am proud to have had the opportunity to associate with some very fine people (who are equally fine scientists) during my research and I am most grateful for their technical advice and counsel. At one time or another, they listened patiently while I expounded my ideas and then provided me with helpful criticism. Dr Schindler is one I have already mentioned. Dr Ronald L. Fante was my laboratory "next-door neighbor" and he graciously permitted me to use him as a "sounding board" for my ideas. He followed me through my early formulations of the MASAR model and provided me with many constructive comments and helpful suggestions.

Mr John F. McIlvenna literally ran me through (nearly 2000 miles of) my paces, during which my research was a continuing topic of conversation. He enlightened me with an appreciation for the optimization scheme which is a central theme of this work. He also introduced me to several key computational algorithms and time-saving "tricks" which I found very useful in the early stages of the computer analysis. Later, Dr Kenneth C. Chen provided me with many helpful insights into the closed-form evaluation of the clutter cross-power correlation integral, which is a substantial part of this work. The final breakthrough in obtaining that integration came to me after Dr Kendall Casey introduced me to the book by Davis and Rabinowitz (which has an excellent section on the integration of highly oscillatory functions and a superb appendix, "On the Practical Evaluation of Integrals," by Milton Abramowitz: entry 32 in the Bibliography). Dr Casey also thoroughly critiqued early drafts of this manuscript and provided many helpful suggestions to improve the exposition.

I apologize (in the informal sense) to Dr J. Philip Castillo for leading him to believe I was "almost done" with my thesis when I first came to the Air Force Weapons Lab. (I really thought I was!) He once told me (jokingly, right Phil?) he believed I was "addicted" to my thesis and doubted I'd ever come to finish it! Nevertheless, he graciously (or mercifully) allowed me brief intervals of "time off" (my thanks to Mr William S. Kehrer for "covering" for me during those), extended leave, and unencumbered evenings and weekends. That time permitted me to bring this work to a worthy conclusion.

I especially thank each member of my Committee for their continued encouragement, support, guidance, and patience. Major Jurgen O. Gobien,

PhD, was my initial chairman until he was "overtaken by events"--he was transferred--and was compelled to relinquish his post. He provided me with encouragement and guidance in the early months of my candidacy. Dr Stanley R. Robinson, who (I am very proud to say) accepted the post as the new chairman of my Committee, has been a source of continual encouragement ($\nabla \cdot \text{encouragement} = \infty$). He and Dr Donn G. Shankland have had a profound impact on this work. They have caused me to think, rethink, and think again about every facet of my research. Along the way, they provided me with many helpful insights, suggestions, as well as tutorials (they steered me into several "specialty areas" that were new to me and which proved very useful). Their efforts on my behalf were most inspiring to me. Lt Col Ron Carpinella, PhD, made several useful suggestions which led me to the development of a much improved stochastic characterization of the clutter model.

Thank you gentlemen, one and all.

My special thanks to Mr Norbert R. Padilla for assisting me in the preparation of this manuscript. Using computer graphics, "Bert" composed--most expertly and artfully--every equation (there are over 230). He also photo-reduced and mounted all the computer-generated plots shown in Figures 8 through 67.

My wife, Sharon, our sons Aaron and Marshall, and our daughter, Amy, have loved and cherished me, as I have them, all the days, months and years of this task. All those seemingly endless nights and weekends they have been home alone with me "at work" are all over, now. They have greatly helped me, emotionally, to reach this enobling goal. There were many times when I thought, almost despairingly, of giving up this effort. What kept me going was the though that, if I did, I'd have

nothing to give them for all the time I'd already spent "away" from them. Well, we've got something now--something better than anything else we might have had--and we're all going to have some good times with it! To you, my lovely Sharon, and to you, Aaron, Marshall, and Amy, I give my highest tribute: to you I dedicate this work.

Contents

Page

List of Figures

Figure		Page

Figure | Page

Figure		Page

Figure		Page

List of Tables

Table		Page

List of Symbols

Number	Symbol	First Used on Page	Definition
1.	f_0	1	radar frequency
2.	λ_0	1	radar wavelength
3.	v_R	1	radar platform velocity
4.	f_d	1	target doppler
5.	θ_h	2	-3dB half angle of radar antenna pattern
6.	M	8	number of antennas
7.	K	8	inter-SAR spacing
8.	I	8	interantenna pulse spacing factor (also see symbols 87 and 107)
9.	N	8	number of synthetic elements (number of pulses per antenna)
10.	P	8	total number of consecutive pulses required to form M overlapping synthetic apertures (also see symbols 26 and 100)
11.	A	11	a square matrix; target cross-power matrix
12.	w	11	a column vector; weighting vector, see (22)
13.	λ	11	complex eigenparameter
14.	B	11	a square matrix; clutter cross-power correlation matrix
15.	a	12	a column vector; target signal vector
16.	λ_D	12	dominant eigenvalue; optimum target to clutter power ratio
17.	w_D	12	weighting vector corresponding to
18.	m	16	an index for antennas
19.	n	16	an index for synthetic elements (positions)
20.	V_n^m	17	signal return received by antenna m in synthetic position n
21.	E_n^m	17	amplitude of V_n^m

Number	Symbol	First Used on Page	Definition
22.	ϕ_n^m	17	phase of V_n^m
23.	V^m	17	weighted sum of V_n^m over n
24.	w_n^m	18	processor weighting coefficient of V_n^m
25.	V	18	combined voltage return of all M synthetic arrays
26.	P	18	power (also see symbols 10 and 100)
27.	l	18	alternate index for antennas
28.	p	18	alternate index for synthetic elements (also see symbol 94)
29.	t	19	subscript to denote target
30.	c	19	subscript to denote clutter (also see symbol 51)
31.	TP	19	combined target power
32.	$\langle \cdot \rangle$	19	expectation operator
33.	$\langle CP \rangle$	19	combined average clutter power
34.	α_{np}^{ml}	22	element of A formed by product of target signals received by antenna m in position n and antenna l in position p
35	β_{np}^{ml}	22	element of B formed by expectation of clutter signals received by antenna m in position n and antenna l in position p
36.	α_n^m	23	target signal received by antenna m in position n
37.	e_n^m	25	elemental signal return received by antenna m at synthetic position n
38.	j	25	$\sqrt{-1}$
39.	ρ,θ,ϕ	25	spherical coordinates
40.	x,y,z	25	rectangular coordinates
41.	E_{peak}^m	25	magnitude of electric field intensity at peak of m th antenna radiation pattern

Number	Symbol	First Used on Page	Definition
42.	$g^m(\cdot)$	25	normalized two-way power radiation pattern of m th antenna
43.	$\chi_n^m(\cdot)$	25	backscattering coefficient observed by antenna m in position n from scatterer at $(\cdot)$
44.	$p(\cdot)$	25	range amplitude weighting function
45.	k_0	26	free space wave number
46.	ω_0	26	radar radian frequency
47.	τ_n^m	26	time of pulse on antenna m at position n relative to antenna 1 at position 1
48.	f_{PRF}	26	radar pulse repetition frequency
49.	R_0	26	range to center of range bin of interest
50.	σ	27	pulsewidth parameter
51.	c	27	speed of light (also see symbol 30)
52.	t_p	27	temporal pulsewidth
53.	r,θ	28	polar coordinates (also see symbol 91)
54.	V_1	28	alternate notation for V_n^m
55.	$g_1(\cdot)$	28	alternate notation for $g^m(\cdot)$
56.	$\chi_1(\cdot)$	28	alternate notation for $\chi_n^m(\cdot)$
57.	V_2	29	alternate notation for V_p^1 (also see symbols 20, 27 and 28)
58.	$g_2(\cdot)$	29	alternate notation for $g^1(\cdot)$ (also see symbols 27 and 42)
59.	$\chi_2(\cdot)$	29	alternate notation for $\chi_p^1(\cdot)$ (also see symbols 27, 28 and 43)
60.	κ	29	a constant, see (45)
61.	x_1,y_1	29	see Fig. 3
62.	x_2,y_2	29	see Fig. 3
63.	$\hat{\kappa}$	29	constant of proportionality for cross-power

Number	Symbol	First Used on Page	Definition
64.	γ	30	see (46)
65.	r_1,θ_1	30	see Fig. 3 and (47)
66.	r_2,θ_2	30	see Fig. 3 and (47)
67.	$\bar{y}_1$	30	position of antenna 1 when it pulses
68.	$\bar{y}_2$	30	position of antenna 2 when it pulses
69.	v_T	30	target speed
70.	θ_T	30	target track angle
71.	$\hat{x}_1,\hat{y}_1$	31	position of target when antenna 1 pulses
72.	$\hat{x}_2,\hat{y}_2$	31	position of target when antenna 2 pulses
73.	d	31	spacing between antenna 1 when it pulses and antenna 2 when it pulses
74.	$\delta(\cdot)$	31	Dirac delta function
75.	r_n^m,θ_n^m	32	instantaneous range and azimuth to target from antenna m in position n
76.	θ_0	33	presumed azimuth of target at midpoint of observation interval
77.	τ_1	38	alternate notation for τ_n^m
78.	τ_2	38	alternate notation for τ_p^l (also see symbols 27, 28 and 47)
79.	T	38	temporal clutter correlation interval
80.	$\hat{\theta}_1,\hat{\theta}_2$	40	same as θ_1,θ_2 when $(x_1,y_1) = (x_2,y_2)$ (see Fig. 3 and symbols 65 and 66; also see (92) and (93))
81.	ζ	40	transformed coordinate, see (64a)
82.	η	40	transformed coordinate, see (64b)
83.	κ_1	44	a constant, see (79)
84.	I_ζ	45	integral over variable ζ (see symbol 81)
85.	$\tilde{\kappa}$	48	a constant, see (98)

Number	Symbol	First Used on Page	Definition
86.	I_r	50	integral over variable r (see symbol 51)
87.	I	51	clutter cross-power integral (also see symbols 8 and 107)
88.	$f(\cdot)$	51	see (108)
89.	z	51	see (109)
90.	$f^{(r)}(\cdot)$	51	rth derivative of $f(\cdot)$, see symbol 88
91.	r	51	an index used in evaluating the clutter cross-power integral (also see symbol 53)
92.	$J_n(\cdot)$	52	Bessel function of First Kind, order n
93.	$T_p(\cdot)$	52	Chebyshev polynomial of First Kind, see (114)
94.	p	52	an index of the Chebyshev polynomials and an index used in evaluating the clutter cross-power integral (also see symbol 28)
95.	b_r	52	Chebyshev polynomial coefficient, see (118)
96.	δ_p	52	coefficients of Chebyshev polynomials, see discussion and expression on page 53
97.	s	53	an index used in evaluating the clutter cross-power integral
98.	ϵ_r	53	the Neumann number; see (119)
99.	ϵ_{r-2s}	53	the Neumann number; see (121)
100.	P,Q	55	powers of cosine antenna pattern (also see symbols 10 and 26)
101.	u,v,w	57	general functions used to form generalized product
102.	$\binom{r}{s}$	57	binomial coefficient
103.	u_1	57	factor in clutter cross-power correlation integrand, see (136)
104.	u_2,u_3	57	factor in clutter cross-power correlation integrand, see (137)

Number	Symbol	First Used on Page	Definition
105.	u_4	57	factor in clutter cross-power correlation integrand, see (138)
106.	$u_i^{(r)}(\cdot)$	58-60	rth derivative of $u_i(\cdot)$ (see symbols 103-105)
107.	I	69	MASAR improvement (also see symbols 8 and 87)
108.	r_o	69	target to clutter power ratio after processing
109.	r_i	69	target to clutter power ratio before processing
110.	w_p	69	processor weighting
111.	w_T	70	target weights
112.	w_B	70	binomial weights
113.	$I_{D/T}$	72	improvement of the optimum processor relative to the target processor
114.	$I_{D/B}$	72	improvement of the optimum processor relative to the binomial processor
115.	$I_{D/Z}$	72	improvement of the optimum processor relative to itself when tuned to a fixed target
116.	$(r_o)_D$	72	target to clutter power ratio out of the optimum processor
117.	$(r_o)_T$	72	target to clutter power ratio out of the target processor
118.	$(r_o)_B$	72	target to clutter power ratio out of the binomial processor
119.	r_{nob}	104	normalized off-boresight response
120.	$\hat{a}$	104	varied target signal vector
121.	r_b	122	response to other boresight targets
122.	$\tilde{a}$	122	varied target signal vector
123.	L	156	spatial clutter correlation interval
124.	L_x, L_y	157	x and y components of L (symbol 123)

ABSTRACT

A Multiple Arrested Synthetic Aperture Radar (MASAR) for the detection of slowly moving targets in clutter is analytically conceptualized and evaluated. The radar consists of a succession of synthetic aperture antennas which are coincident in space but are displaced in time by several interpulse periods. The radar is evaluated using the target to clutter power ratio as the measure of performance. The radar is assumed to be clutter power limited, so noise is ignored in the evaluation. The evaluation consists of a comparison between three different receiver processing schemes. The first processor is a set of weights which optimizes the target to clutter power ratio and is the central feature of MASAR. The second processor is a set of weights comprising the target signal, itself; it can be construed as a "smart, ad hoc" design and is shown to be optimum for rapidly decorrelating clutter. The third processor is set of binomial weights; effectively, it reduces the system to an n-pulse canceller which, for a two antenna system, is the well known Displaced Phase Center Antenna (DPCA) radar.

In order to perform the analysis, a generalized signal return is formulated with which closed form expressions for the target signal and the clutter cross-power correlation are derived. This generalized signal return is a range-amplitude, radiation pattern weighted integration of the electric field backscattering coefficient over the backscattering region. Both the target and the clutter are modeled with the electric field backscattering coefficient: deterministically for the target, stochastically for the clutter.

The target is modeled simply as a deterministically moving point scatter with the same albedo as a point of clutter.

The clutter is modeled as a homogeneous, isotropic, two-dimensional, spatiotemporal random field. This random field represents the amplitude and phase of the electric field backscattering coefficient as a function of time for every point in the scattering region observed from positions along the MASAR flight path. Only the correlation properties of this random field are required for the analysis.

The analysis is three-fold and considers targets moving between zero and 60 miles per hour at all track angles. First, the improvement of MASAR with the optimum processor is considered relative to that with the target and the binomial processors. Second, the response of each processor to off-boresight targets is considered. Third, the response of the optimum processor to other targets on the boresight is examined.

The analysis shows that MASAR with optimum receiver weights, generating four synthetic apertures each three feet long, can extract a three mile per hour target at ten miles from slowly decorrelating clutter 45 dB better than MASAR with target weights and over 144 dB better than MASAR with binomial weights. For a 60 mile per hour target, under the same circumstances, the corresponding figures are 70 dB and 106 dB. The analysis further shows that, with longer synthetic apertures, both the target's location and velocity component parallel to the MASAR boresight can be accurately determined.

The conclusion is that MASAR, with its optimum weighting scheme, is a promising synthetic aperture radar concept for the detection of slowly moving targets immersed in strong clutter environments.

MULTIPLE ARRESTED

SYNTHETIC APERTURE RADAR

1. Introduction

Background

The problem of detecting a slowly moving target imbedded in severe clutter from an airborne side-looking radar platform is addressed in this work. Here, the adjectival phrase "slowly moving" refers to the class of targets which reflect a doppler-shifted radar signal which resides well within the radar's antenna pattern mainbeam clutter return. The fundamental problem that arises in this situation is that the target becomes virtually undetectable as it is completely masked by the strong clutter return. In this case, even antenna pattern sidelobe suppression techniques cannot help, for it is the mainlobe beamwidth of the radar antenna that is the source of the difficulty.

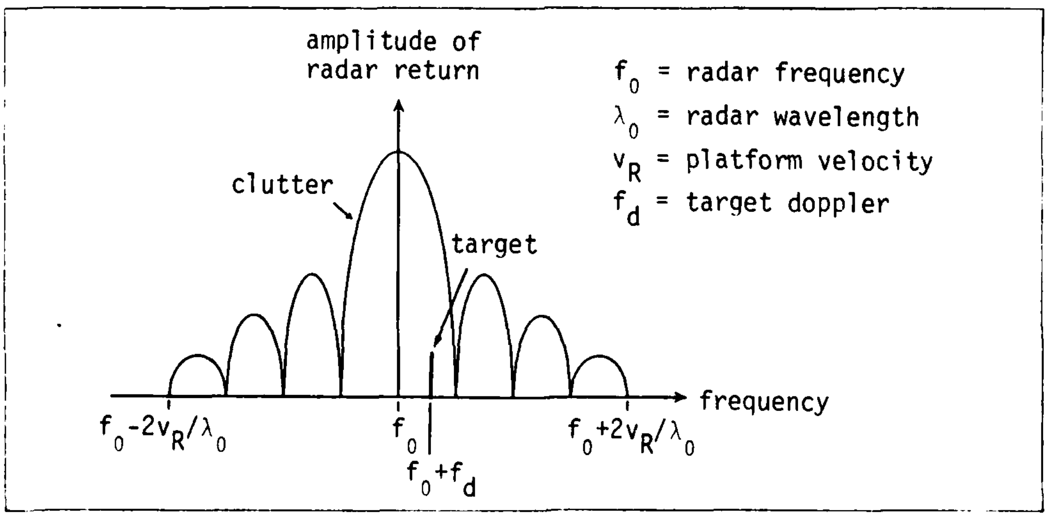

Figure 1. Frequency Spectrum of an Airborne Side-Looking Radar Return Showing a Slowly Moving Target Masked by Mainbeam Clutter

Figure 1 shows this situation. For uniformly distributed clutter, the spectral character of the frequency of the return signal is similar to the shape of the far field pattern of the radar antenna. The target return is shown masked by the mainbeam clutter return.

The mainlobe beamwidth of an antenna is proportional to the ratio of the electrical to physical length of the aperture. For an airborne side-looking antenna, the mainbeam clutter doppler spread is given as $\pm 2(V_R/\lambda_0)\sin\theta_h$, where V_R is the radar platform speed, λ_0 is the operating wavelength, and θ_h is the angle between broadside and the half-power (-3dB) point of the one-way radar antenna pattern. θ_h is directly proportional to λ_0/d where d is the antenna aperture length in the plane containing the flightpath.

Hence, there are only two ways to reduce the spread of the mainbeam clutter doppler return for a given operating frequency: (1) fly at slower speeds, and (2) use larger antennas. The first severely limits aircraft type and maneuverability, consequently, the second is usually employed. Larger antennas have smaller beamwidths but beamsteering or antenna rotation must be used to survey the normal field of interest (broadside $\pm 60^\circ$). This, in turn, requires the use of either large phased arrays or antennas requiring rotodomes, or both. These antennas are costly to install, often require a dedicated aircraft, and adversely affect aircraft performance and operating characteristics (weight and balance, flight envelope, etc.).

Alternative schemes to "see through" the mainbeam clutter have been devised which permit the use of simple, lightweight airborne antennas.

Displaced Phase Center Antenna (DPCA) techniques [1:7-9,10,13-14]* have been employed with varying degrees of success. This scheme employs two antennas, closely matched in radiation characteristics, mounted side-looking on the aircraft. The first antenna transmits and receives at a point along the flightpath. The second antenna's phase center is flown into the same position along the flightpath and it transmits and receives. Thus, the scene is viewed twice, at closely spaced--but different--times, from the same point in space. Assuming identical antenna patterns and perfectly correlated clutter, a simple subtraction of the second return from the first would eliminate the mainbeam clutter (including the sidelobe clutter). Any residual signal would be that of an object (perhaps a target) which moved during the interpulse period.

However, the performance of DPCA is limited by the ability to achieve two identical radiation patterns from antennas mounted side-by-side on an aircraft. Great pains can be taken to construct two identical antennas in the laboratory only to have their radiation characteristics unevenly and dynamically distorted by the airframe presence and flexure (of the wings, stabilizers, etc.).

A technique designed to overcome these difficulties just mentioned has been experimentally evaluated [2]. There, a two-dimensional phased array was mounted on the side of an aircraft. By taking into account mutual coupling, array element differences, and airframe presence and flexure with an intricate array element phasing algorithm, two antenna patterns identical in both amplitude and phase were to be generated from overlapping fore and aft clusters of the phased array elements. These

*Brackets enclose citations. A colon separates the citation and page references therein; commas separate multiple page references. Semicolons separate multiple citations within the brackets.

identical patterns were then to be employed in a DPCA mode. The design goal was to achieve 55dB of clutter attenuation [3:331] and MTI improvement [4:17-12; 2:331-333], and to detect targets with speeds of 2 or 3 knots at a range of 100 nautical miles. The effort met limited success. There were great difficulties in meeting and maintaining the required antenna tolerances, and the antenna array was very expensive [5].

Purpose

The purpose of this work is to formulate and analyze a method for detecting, locating, and estimating the velocity parameters of, a slowly moving target imbedded in a severe clutter environment from an airborne side-looking radar platform. The method proposed here couples synthetic aperture radar [6] and DPCA techniques with an optimization technique to achieve the best performance possible for doing this. The measure of performance for this analysis is the target to mean-clutter power ratio.

Synthetic aperture techniques allow real antennas of simple, flush-mountable construction to be used. The advantages of flush-mounted antennas are that they are less vulnerable to hostile environments, and they have minimal effect on the aircraft operating and performance characteristics.

The rationale for using synthetic aperture techniques is that differences in real antenna radiation characteristics can be easily offset, thereby obtaining better elimination of the clutter residue in a DPCA scheme. This follows from the fact that the radiation pattern of an array antenna is the product of its array pattern--which is a function of only the array geometry--and its real antenna radiation pattern. Since long synthetic arrays have array patterns which have characteristically narrow mainlobes, only a small portion of the real antenna

pattern is effectively used.

Additional rationale for the method proposed here is that the narrow mainlobe achievable with the synthetic antenna effectively illuminates a region which has an azimuthal extent far narrower than what could be achieved by any real antenna that could be used practically in an airborne operation. With this smaller region of illumination, the radar has to contend with much less clutter. In effect, the ratio of target to clutter illumination is increased. This forecasts improved detection performance.

This work conceptualizes, formulates, and analyzes a model for a displaced phase center synthetic aperture radar technique which will be called "Multiple Arrested Synthetic Aperture Radar", or MASAR (pronounced "may'sar"). MASAR specifically addresses the problem of detecting slowly moving targets imbedded in a severe clutter environment.

Herein, the analysis of the MASAR concept will be limited to comparing its theoretical performance with the same for previous slowly moving target indicator (SMTI) radar techniques and to determining its sensitivity to changes in the target and clutter environment. It will be seen that this analysis will lay a foundation upon which many further issues may be explored (see chapter VI).

Comparison and Contrast with Related Efforts

Sletten and Holt [7] first proposed a dual-antenna scheme which coupled synthetic aperture radar and DPCA techniques in order to solve the clutter problem being experienced with SMTI radars. They called it "Arrested Synthetic Aperture Radar", ASAR, but made no attempt to analyze the concept. The term "arrested" arose from the idea that both real antennas could be used to obtain two synthetic aperture "pictures"

of the scene of interest--twice arresting the action--which could then be overlaid to isolate moving targets. Chudleigh and Moulton [8], on the suggestion by Sletten, performed a cursory analysis of a rudimentary two- and three-phase center ASAR employing simple cancellation schemes. They defined clutter cancellation as the ratio of the power in the cancelled residue to the power received by any one of the synthetic apertures from distributed clutter. They found, by computer evaluation, that the addition of a third phase center reduced the clutter cancellation sensitivity of arrested synthetic aperture systems to irregularities in the flight path by an order of magnitude over a two phase center system.

MASAR is an extension of their concept to an "M" real antenna ($M \geq 2$) scheme with optimal processing. As mentioned earlier, the measure of *performance* for the analysis is the target to mean-clutter power ratio. The optimization technique employs a known scheme based on the extremal properties of the ratio of two quadratic forms [9:317-326; 10:section 10]. This scheme, which maximizes the ratio of the two quadratic forms, has been successfully applied to the maximization of array antenna gain [11; 12; 13], the maximization of array antenna gain with simultaneous controlled null placement [14; 15], and the maximization of the signal-to-interference ratio of a phased array radar [16]. This optimization scheme has not yet been applied to a synthetic aperture radar system.

MASAR is also an extension of the DPCA concept to synthetic aperture radar. Since only a small portion of the real antenna's radiation pattern is effectively used, better clutter suppression and, consequently, better SMTI performance than that achievable with conventional DPCA can be expected.

Lastly, MASAR can be implemented with simple antennas. As will be seen from the analysis, no special care need be taken to ensure matched radiation characteristics for the real elemental antennas.

Sequence of Development

In Chapter II, MASAR is conceptualized, the optimization technique is presented and an actualization of MASAR is proposed.

In Chapter III, MASAR is analytically formulated. First, a general expression is obtained for the MASAR combined signal power. Next, the models for both the target return and clutter return are derived. These models are each used in the general expression for the signal power to obtain the power for the target and clutter in quadratic form.

In Chapter IV, the results of a computer analysis of MASAR, developed from the theory in Chapter III, are presented. From these results, the performance of MASAR is discussed as a function of varying system and clutter parameters.

In Chapter V, this work is summarized and conclusions are drawn from the results presented in Chapter IV.

In Chapter VI, recommendations for further study are presented.

II. MASAR: The Conceptualization

The Conception

Consider M real antennas equally spaced on the side of an aircraft, side-looking and longitudinally aligned, so that all the antennas will traverse the same flight path. (Inflight perturbations are ignored in this analysis; they may be effectively corrected using an inertial platform). As the aircraft flies along, the antennas are sequentially pulsed from fore to aft. After the aftmost antenna (antenna M) is pulsed, the next pulse "returns" to the foremost antenna (antenna 1). The sequential pulsing is then repeated to obtain a second sequence. Assume the aircraft velocity, inter-antenna spacing, and the pulse repetition frequency (PRF) are such that on every "K"th pulse each antenna is pulsed at the same position in space where its immediate predecessor pulsed K pulses earlier. Since the antennas are pulsed sequentially fore to aft, and each antenna is pulsed at the same point in space, K is limited to

$$K = IM + 1 \tag{1}$$

where I, an integer ≥ 0, is a factor which accounts for the inter-antenna pulse spacing (the time delay between arrays). K is defined as the inter-SAR spacing; it is the number of interpulse periods between successive synthetic aperture arrays. It will take a total of

$$P = M(N-1) + (M-1)K + 1 \tag{2}$$

consecutive pulses to obtain N such "positions in space" for each of the M antennas. Each of these "positions in space" is called a synthetic element position.

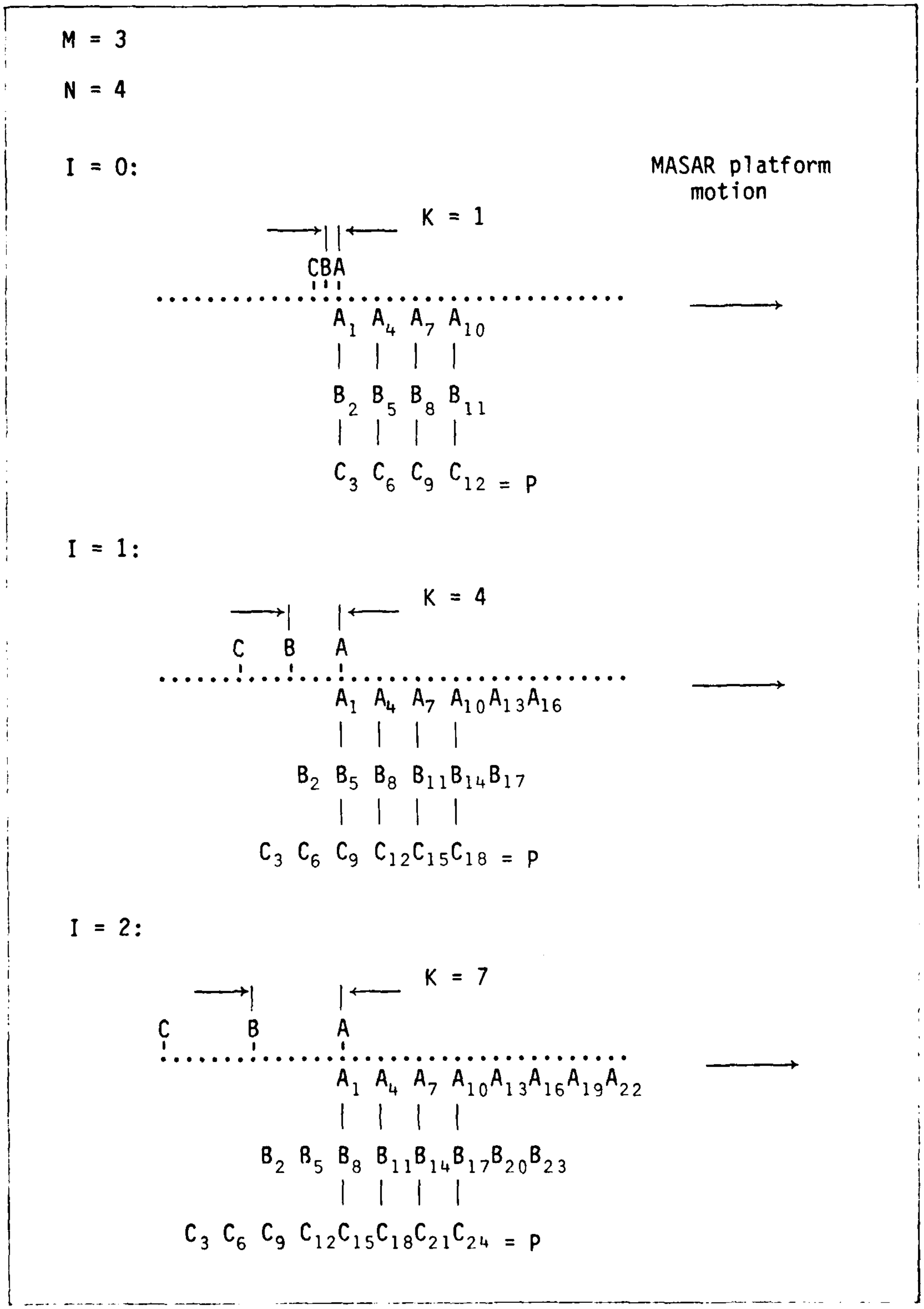

Figure 2. Illustrations of the MASAR Scheme for Generating Overlapping Synthetic Arrays.

Figure 2 on page 9 depicts three examples of this for a MASAR with $M = 3$ antennas and $N = 4$ pulses, with the inter-antenna pulse spacing factor $I = 0$, 1 and 2, top to bottom, respectively. The dotted axis represents the spatial positions of the synthetic elements if every pulse were transmitted on the same antenna. Aircraft motion is to the right. The alignment of each antenna at each synthetic element position is shown beneath the dotted axis by the letters A, B and C. The subscripts denote the number of the pulse transmitted on the antenna in that position. The antennas are shown above the dotted axis in their relative position at the time of the first pulse on antenna A. The last pulse occurs on antenna C in its rightmost position. Note that, for $I = 1$ and 2, the non-overlapping pulses at the left (beginning) and right (end) will not be used in the generation of the synthetic apertures. The pulses that are used compose the spatial intersection of the train of pulses on each antenna.

After each antenna pulses, it receives the radar return which is then stored on board the aircraft. The N synthetic element radar returns received by each antenna are then weighted and summed to form a synthetic array return. The returns for M arrays, of N synthetic elements each, are thus generated. Note that these M synthetic arrays are each displaced in time, but not in space. The temporal displacement between adjacent arrays is K/PRF.

The M synthetic array returns are then weighted and summed in a fashion which optimizes a measure of performance expressible as a ratio of two quadratic forms. As mentioned earlier, the measure of performance is the target to mean-clutter power ratio.

As with Sletten's original idea, MASAR "arrests" the scene M successive times but then performs an optimal M-fold "subtraction" to reveal the moving target.

The Optimization Procedure

The formulation of the MASAR model is closely tied to the optimization scheme. As an aid in perspective for the formulation, the optimization procedure shall be discussed here first.

The target-to-clutter power ratio is a widely used measure of performance for moving target indicating (MTI) radars, and it will be the same for MASAR. Both target and clutter power can be expressed in quadratic form. The problem here is to determine what optimizes their ratio. Here "optimum" is used in the sense that it is the absolute maximum for given target and clutter.

The optimization follows directly from the extremal properties of the ratio of two quadratic forms which shall now be summarized [9:317-326; 12:section 10; see esp. Appendix A, herein].

Consider the generalized eigenproblem,

$$Aw = \lambda Bw \tag{3}$$

where A and B are square matrices of order N and w is a column vector of dimension N. Each has complex-valued elements. λ is a complex-valued parameter. Premultiplying both sides by the transpose-conjugate of w, denoted $w^{\dagger}$, and moving all terms to the left side yields

$$w^{\dagger}Aw - \lambda w^{\dagger}Bw = 0 \tag{4}$$

The left side of (4)* is known as the pencil of two quadratic forms, where λ is the parameter of the pencil. When B is positive definite,

*Equations are referenced only by their number enclosed in parentheses.

As with Sletten's original idea, MASAR "arrests" the scene M successive times but then performs an optimal M-fold "subtraction" to reveal the moving target.

The Optimization Procedure

The formulation of the MASAR model is closely tied to the optimization scheme. As an aid in perspective for the formulation, the optimization procedure shall be discussed here first.

The target-to-clutter power ratio is a widely used measure of performance for moving target indicating (MTI) radars, and it will be the same for MASAR. Both target and clutter power can be expressed in quadratic form. The problem here is to determine what optimizes their ratio. Here "optimum" is used in the sense that it is the absolute maximum for given target and clutter.

The optimization follows directly from the extremal properties of the ratio of two quadratic forms which shall now be summarized [9:317-326; 12:section 10; see esp. Appendix A, herein].

Consider the generalized eigenproblem,

$$Aw = \lambda Bw \tag{3}$$

where A and B are square matrices of order N and w is a column vector of dimension N. Each has complex-valued elements. λ is a complex-valued parameter. Premultiplying both sides by the transpose-conjugate of w, denoted $w^{\dagger}$, and moving all terms to the left side yields

$$w^{\dagger}Aw - \lambda w^{\dagger}Bw = 0 \tag{4}$$

The left side of (4)* is known as the pencil of two quadratic forms, where λ is the parameter of the pencil. When B is positive definite,

*Equations are referenced only by their number enclosed in parentheses.

the pencil is called "regular". The determinantal equation

$$|A - \lambda B| = 0 \tag{5}$$

is the eigenequation of the pencil. It has N roots λ_i $(i = 1,2,\ldots,N)$ which are the eigenvalues of the pencil.

If the pencil is regular and A can be expressed as a Hermitian outer self-product,

$$A = aa^\dagger \tag{6}$$

where a is a column vector having complex-valued elements, then there exists only <u>one nonzero</u> eigenvalue. Furthermore, if B is Hermitian, then this eigenvalue is the <u>maximum value</u> of the ratio (the dominant eigenvalue of the regular pencil) and is found as

$$\left(\frac{w^\dagger A w}{w^\dagger B w}\right)_{max} = \lambda_D = a^\dagger B^{-1} a \tag{7}$$

And furthermore, the eigenvector corresponding to this dominant eigenvalue is given by

$$w_D = B^{-1} a \tag{8}$$

And hence, from (7) and (8),

$$\lambda_D = a^\dagger w_D \tag{9}$$

For MASAR, the vector a describes the target signal, so the matrix A comprises all cross-power terms of the target signal return; also, the matrix B comprises all cross-power terms of the clutter signal return. For a MASAR processor employing weights, w, the processed target power is $w^\dagger Aw$ and the processed clutter power is $w^\dagger Bw$.

The vector w_D is the set of processor weights which optimizes the target-to-clutter power ratio to the value λ_D. It, then, is the weight vector which characterizes the optimum processor.

However, this is not a matched filter processor in the sense of North [17]. This is because the matched filter is obtained for the maximization of signal-to-noise when the noise is white (i.e., when the noise power spectrum is constant). Here, the maximization is with respect to the target-to-clutter power, and the clutter is not white. In fact, it has long been known that, for ground-based radars, the long-time-average power spectrum of the clutter signal return approaches that of the transmitted pulse [18:297]. This is not unexpected, since the clutter signal return is the sum of many similar returns with arbitrary amplitudes and phases [19:171]. Of course, for an airborne side-looking radar, the clutter power spectrum is further "colored" by the platform motion relative to the "clutter source." An example of this spectrum is shown in Figure 1.

<u>A Noteworthy Consequence of the Optimization</u>

This optimization has a very interesting consequence. Note what happens to the target to clutter power ratio when the optimum weights are used:

$$\left.\frac{w^{\dagger}Aw}{w^{\dagger}Bw}\right|_{w = w_D} = \frac{w_D^{\dagger}Aw_D}{w_D^{\dagger}Bw_D} = \frac{w_D^{\dagger}aa^{\dagger}w_D}{w_D^{\dagger}a}$$

$$= \frac{|w_D^{\dagger}a|^2}{w_D^{\dagger}a} \tag{10}$$

where (6) and (8) have been invoked. The optimally processed target power becomes the square of the optimally processed clutter power. Their ratio, of course, is the eigenvalue (9)--the maximum achievable ratio for the target, a, immersed in the clutter, B.

A Proposed Implementation

At this point, as a further aid in perspective for the work which follows, it is interesting to postulate an airborne implementation for MASAR. The important quantity for MASAR is the optimum weighting vector, (8). It can be determined easily, once the target and clutter signals are known. However, there is no way to separate the target and clutter signals before processing; so these signals must be separately determined in another fashion.

As will be seen in the next chapter, the clutter power matrix B comprises all the cross-power correlation terms of the clutter signal return. The B matrix could be determined with a radar receiver which dynamically adapts to the clutter environment by continually sampling the clutter and estimating its second moments or cross-correlation characteristics. This is the classical correlation or covariance matrix estimation problem on which much work has been done [20; 21].

The target signal vector, a, would have to be presumed. A "tune, test, and retune" approach would have to be employed. On board the inflight MASAR aircraft, a decision would have to be made to search for a presumed target. The target signal vector, a, which matches the target would then be generated. MASAR would be, in effect, <u>tuned</u>, by the target signal vector, to the doppler <u>history</u> of the presumed target during the observation interval. The MASAR optimum weights would then be obtained from (8).

Next, the target scene would be sampled in the MASAR fashion, using the best settings for the controllable system parameters (aircraft speed, operating frequency, PRF, number of antennas, number of pulses, etc.; see chapter VI), and the returns would be processed using the

"tuned" weights. A simple threshold test could be then be performed using the actual processed signal versus the presumed target signal to determine the presence of a target.

Such an implementation of MASAR would require rapid tuning to search for a wide range of possible targets. With the various "target situations" (type, velocity, range, etc.) that would be of interest under real conditions, a seemingly tremendous amount of processing would be involved. Certainly, it seems too much for a sequential on-board processor to handle. However, multiple parallel-processors, with very-high-speed, very-large-scale-integrated technology may permit an effective realization of MASAR.

One advantage of such a scheme is, with on-board storage of the signal returns, the target scene need only be sampled once. Afterwards, the MASAR system could discriminate and adapt to the clutter, then tune and test for all targets of interest using the same set of signal returns. As targets are detected, they could be disposed to a tracking system. All the while, the target scene could be simultaneously updated with succeeding samples.

III. MASAR: The Formulation

In this chapter, an analytical model for MASAR is formulated. First, a general expression for the MASAR combined signal power is obtained with which the target and clutter powers are expressed as quadratic forms. Notational conventions are introduced and explained in this part of the exposition. Next, the MASAR signal return received by one antenna is obtained as a spatial integration over the product of factors comprising the antenna power radiation pattern, the electric field backscattering coefficient, the free-space Green's function and the range-amplitude weighting. Then, the expression for the generalized cross-power term (generalized in the sense that it can be used to describe the cross-power for either the target or the clutter) is written as the product of the signal returns received by two arbitrary MASAR antennas. From this, by explicitly characterizing the electric field backscattering coefficient for the target and for the clutter, expressions are obtained for the target signal and the clutter cross-power correlation. Whereas the closed-form expression for the target signal is obtained quite directly, the same for the clutter cross-power is obtained after much work. The chapter concludes with examples of the clutter and an abstract of the computer analysis.

Formulation of the Generalized Combined Signal Power

Recall from the preceeding chapter, that MASAR requires M antennas (real elements) and N pulses (synthetic elements) on each antenna. Here, m shall denote a member of the real elements, i.e., $m \in \{1,2,3,\ldots,M\}$ and n shall denote a member of the synthetic elements, i.e., $n \in \{1,2,3,\ldots,N\}$. Each synthetic element corresponds to a fixed

position in space and so the phrases "synthetic element position", "synthetic position", or "position" will be used frequently with common meaning.

The radar return received by real element m at synthetic element position n is converted into a complex voltage which can be characterized as an amplitude and phase:

$$V_n^m = E_n^m e^{j\phi_n^m} \tag{11}$$

The m th synthetic array return is obtained as a weighted sum of the N synthetic element returns:

$$V^m = \sum_{n=1}^{N} \tilde{w}_n^m V_n^m$$

$$= \sum_{n=1}^{N} \tilde{w}_n^m E_n^m e^{j\phi_n^m} \tag{12}$$

where the $\tilde{w}_n^m$ are the synthetic element weights. The combined return, is obtained as a weighted sum of the M synthetic array returns:

$$V = \sum_{m=1}^{M} \hat{w} V^m$$

$$= \sum_{m=1}^{M} \sum_{n=1}^{N} \hat{w}^m \tilde{w}_n^m V_n^m \tag{13}$$

where the $\hat{w}_n^m$ are the array weights. (Recalling the discussion in the proposed implementation (see pp.13ff), $|V|^2$ would be compared to a

threshold to determine the presence of a moving target.)

As shall be seen, the weighting coefficients will be determined in a manner which permits them to be combined:

$$w_n^m \triangleq \hat{w}^m \tilde{w}_n^m \tag{14}$$

Then, the combined complex voltage return of the M synthetic arrays may be expressed as

$$V = \sum_{m=1}^{M} \sum_{n=1}^{N} w_n^m V_n^m \tag{15}$$

The combined power may be written as

$$P = VV^*$$

$$= \sum_{m=1}^{M} \sum_{n=1}^{N} \sum_{l=1}^{M} \sum_{p=1}^{N} w_n^m w_p^{*l} V_n^m V_p^{*l} \tag{16}$$

where * denotes complex conjugation, the indices l and p stand for antenna l in synthetic position p, and where a constant of proportionality in units of reciprocal impedance has been ignored (it would cancel out in the target-to-clutter power ratio, anyway). This Hermitian biquadratic form can be reduced to a Hermitian quadratic form simply by combining the m and n summation indices into a single summation index i, and the l and p summation indices into a single index k:

$$P = \sum_{i=1}^{MN} \sum_{k=1}^{MN} w_i w_k^* V_i V_k^* \tag{17}$$

However, in this form the convenient real-by-syntnetic element identification is lost. Hence, even though it is more cumbersome, the biquadratic form will be retained; the inconvenience will prove to be temporary.

The radar return is a superposition of target (signal of interest) and clutter (signal of interference) and noise (random interference, generated by the environment, within the radar frequency passband). The target is assumed to be located in a field of randomly located scatterers (such as vegetation) and the radar return from these scatterers, referred to as clutter, is assumed (as was done in the Introduction) to be so large as to mask the target. Under these conditions, the further assumption can be made that noise is negligible compared to the clutter; that is, the system is assumed to have a low thermal noise floor and be clutter power limited. Noise can then be ignored here, leaving only the target and clutter signals to be considered.

The MASAR combined target and mean clutter power returns may be expressed as

$$TP = \sum_{m=1}^{M} \sum_{n=1}^{N} \sum_{l=1}^{M} \sum_{p=1}^{N} w_n^m w_p^{*l} \left(V_n^m V_p^{*l} \right)_t \tag{18}$$

and

$$\langle CP \rangle = \sum_{m=1}^{M} \sum_{n=1}^{N} \sum_{l=1}^{M} \sum_{p=1}^{N} w_n^m w_p^{*l} \left\langle \left(V_n^m V_p^{*l} \right) \right\rangle_c \tag{19}$$

where TP is the combined target power, $\langle CP \rangle$ is the combined average clutter power, and $\langle \cdot \rangle$ denotes the average, or expectation. The reason for taking the expectation of the clutter power will become apparent later (see page 33).

Not only are (18) and (19) Hermitian biquadratic forms, but also (19) can be reasonably restricted to a positive definite form. As will become clear when the clutter model is established (see pp. 33ff), (19) is at least a positive semidefinite form (also referred to in the literature as *nonnegative definite*). What this means is, there is no choice of nonzero weights for which (19) can be made negative. However, this does not exclude the case where (19) can be made identically equal to zero. Were this possible, the performance measure chosen for this analysis would not be bounded. It is well known that this kind of performance is not obtainable in an actual physical situation. (Wouldn't it be nice if the clutter could be made to vanish!) In order to be able to predict the performance of an actual system, the clutter model used in this analysis must be realistic enough to prohibit such a singularity in the performance measure. Then (19) must be restricted to a positive definite form. Even if one were (unfortunate enough) to select a clutter model which contained such a singularity, the addition of noise to each term in (19)--when m = 1 and n = p--would restore the positive definiteness of (19) without disturbing the Hermitian symm·y.

The combined target and mean clutter powers may be conveniently expressed in quadratic form as

$$\mathrm{TP} = w^{\dagger} A w \tag{20}$$

and

$$\left\langle \mathrm{CP} \right\rangle = w^{\dagger} B w \tag{21}$$

where lower case letters are used to denote vectors and upper case letters are used to denote square matrices. Here, w is a column vector

whose elements are the weights w_n^m, i.e.,

$$W = \left(W_n^m\right)_N^M = \begin{pmatrix} W_1^1 \\ W_1^2 \\ \vdots \\ W_1^M \\ W_2^1 \\ \vdots \\ W_2^M \\ \vdots \\ W_N^1 \\ \vdots \\ W_N^M \end{pmatrix} \tag{22}$$

and $w^\dagger$ denotes its transpose-conjugate, a row vector.

Throughout this work, supercripts will denote the real elements and subscripts will denote the synthetic elements.

The notation and expansion of $(w_n^m)_N^M$ in (22) is to be especially noted. M is the total number of real elements (real antennas) and its use here denotes that the upper index, m, is to take on all integer values from 1 to M. N is the total number of synthetic elements and its use here denotes that the lower index, n, is to take on all integer values from 1 to N. The expansion of $(w_n^m)_N^M$ is performed by setting the lower index at its first value, 1, and running the upper index through all its values 1 through M, then continually repeating this with the lower index incremented by 1, until the element w_N^M is reached.

In (20), the matrix A characterizes the target signal and is defined as

$$A = \left[\left[\alpha_{np}^{ml}\right]_N^M\right] = \left[\begin{array}{cccc} \left[\alpha_{11}^{ml}\right]^M & \left[\alpha_{12}^{ml}\right]^M & \cdots & \left[\alpha_{1N}^{ml}\right]^M \\ \left[\alpha_{21}^{ml}\right]^M & & & \cdot \\ \vdots & & & \vdots \\ \left[\alpha_{N1}^{ml}\right]^M & & \cdots & \left[\alpha_{NN}^{ml}\right]^M \end{array}\right] \tag{23}$$

where, for fixed indices i and j,

$$\left[\alpha_{ij}^{ml}\right]^M = \left[\begin{array}{cccc} \alpha_{ij}^{11} & \alpha_{ij}^{12} & \cdots & \alpha_{ij}^{1M} \\ \alpha_{ij}^{21} & & & \\ \vdots & & & \\ \alpha_{ij}^{M1} & & \cdots & \alpha_{ij}^{MM} \end{array}\right] \tag{24}$$

and where, from (18),

$$\alpha_{np}^{ml} = \left(V_n^m V_p^{*l}\right)_t \tag{25}$$

In (21), the matrix B characterizes the clutter signal and is defined in a similar fashion, as

$$B = \left[\left[\beta_{np}^{ml}\right]_N^M\right] \tag{26}$$

where, from (19),

$$\beta_{np}^{ml} = \left\langle\left(V_n^m V_p^{*l}\right)_c\right\rangle \tag{27}$$

That is, both the A and B matrices are constructed of N by N partitions of M by M matrices.

Note, from (11), that (25) separates,

$$\alpha_{np}^{ml} = \alpha_n^m \alpha_p^{*l} = (V_n^m)_t \, (V_p^{*l})_t \tag{28}$$

and thus,

$$A = aa^\dagger = (\alpha_n^m)_N^M (\alpha_p^l)_N^{\dagger M} \tag{29}$$

where, again, $(\cdot)^\dagger$ denotes the transpose-conjugate. That is,

$$a = (\alpha_n^m)_N^M = \begin{pmatrix} \alpha_1^1 \\ \alpha_1^2 \\ \vdots \\ \alpha_1^M \\ \alpha_2^1 \\ \vdots \\ \alpha_2^M \\ \vdots \\ \alpha_N^1 \\ \vdots \\ \alpha_N^M \end{pmatrix} \tag{30}$$

is the target signal vector. Hence, (20) may be written as

$$TP = w^\dagger a a^\dagger w = w^\dagger a (w^\dagger a)^\dagger = |w^\dagger a|^2 \tag{31}$$

Also note, from (11) and (27), that

$$\beta_{np}^{ml} = \left\langle (V_n^m)_c \, (V_p^{*l})_c \right\rangle \tag{32}$$

Note that the main diagonal of B comprises all the clutter cross-power terms of antenna m in position n with itself ($1 \le m \le M$, $1 \le n \le N$).

The task now is to characterize, in detail, the MASAR target and clutter signal returns; i.e., to obtain analytical models for α_n^m and β_{np}^{ml}.

The Model for the MASAR Signal Return

The formulation of the MASAR model shall be based on the following assumptions, which shall hold throughout this work:

a. multiple scattering shall be ignored,

b. no scatterer shall shadow any other,

c. propagation path effects shall be limited to round trip path length effects on the amplitude and phase of the electric field,

d. the electric field polarization shall remain constant,

e. antenna losses shall be ignored,

f. all scatterers shall be in the far field of the antenna, and,

g. second time around returns [3:350-352] shall be ignored (see Chapter VI for further discussion on this).

The voltage at the termination of a radar antenna, upon receipt of its signal return, is a superposition of the backscattered returns from all scatterers that lie in the scattering region. The scattering region is defined by the time of receipt of the signal return, and each of the backscattered returns are weighted by the temporal shape of the transmitted signal.

Thus, the MASAR elemental signal return received by antenna m at synthetic position n, from a scatterer which is at (x,y,z) can be written as

$$e_n^m(x,y,z) = E_{peak}^m g^m(\theta,\phi)\, \chi_n^m(x,y,z)\, \frac{e}{\rho^2}^{-j2k_0\rho} p(\rho)\, e^{j\omega_0\tau_n^m} \tag{33}$$

where $j = \sqrt{-1}$, $\rho^2 = x^2+y^2+z^2$, $\theta = \tan^{-1}(y/x)$, $\phi = \tan^{-1}(z/\rho)$, and where

E_{peak}^m is the magnitude of the electric field intensity at the peak of the m th antenna radiation pattern (this could vary with time, but here it shall be assumed a constant over all N synthetic positions) and is in volts/meter,

$g^m(\theta,\phi)$ is the complex (magnitude and phase) normalized two-way power radiation pattern of the m th antenna ($|g^m(\theta,\phi)|$ is the ratio of its directive gain to its directivity)--in units of normalized power, it is dimensionless,

$\chi_n^m(x,y,z)$ is the complex electric field backscattering coefficient from the scatterer at (x,y,z) observed by antenna m at synthetic position n--the scattering coefficient [22: 22-23] is defined as the ratio of the electric field scattered by the scatterer at (x,y,z) to the electric field scattered in the specular direction by a perfectly conducting scatterer of the same dimensions at the same angle of incidence and at the same position as the scatterer at (x,y,z), wherein the amplitude and polarization of the incident field remain the same; the backscattering coefficient is defined as the scattering coefficient in the direction of the source--and is dimensionless,

$p(\rho)$ is the real-valued range-amplitude weighting which char-

acterizes the envelope of the transmitted pulse and is dimensionless,

k_0 $= \omega_0/c$, where c is the speed of light,

ω_0 $= 2\pi f_0$; f_0 is the radar operating frequency,

τ_n^m
$$= [M(n-1)+(m-1)K]/f_{PRF} \tag{34}$$
is the time of the pulse on antenna m at position n relative to antenna 1 at position 1--see (1) and (2); f_{PRF} is the pulse repetition frequency, and

$\omega_0\tau_n^m$ accounts for the change in phase of the radar's master oscillator between synthetic element positions.

The signal return can be obtained by integrating (33) over the scattering region:

$$V_n^m = \iiint_{-\infty}^{\infty} dx\,dy\,dz\ e_n^m(x,y,z) = E_{peak}^m e^{j\omega_0\tau_n^m}$$

$$\bullet \iiint_{-\infty}^{\infty} dx\,dy\,dz\ g^m(\theta,\phi)\chi^m(x,y,z)\ \frac{e^{-j2k_0\rho}}{\rho^2}\ p(\rho) \tag{35}$$

<u>The</u> <u>Range-Amplitude</u> <u>Weighting</u>, <u>$p(\rho)$</u>. The range-amplitude weighting function, $p(\rho)$, substantially simplifies the task of the integration for the target and especially for the clutter. The alternative to this is to integrate over finite limits which rapidly leads to unrewarding pursuits for reasonable choices of the backscattering coefficient.

The range weighting is chosen to simulate a signal return from a "range bin" centered at range R_0. For tractability, the range weight-

ing is defined to be a gaussian-shaped pulse centered at range R_o:

$$p(\rho) = \frac{1}{\sqrt{2\pi}\,\sigma} e^{-(\rho-R_0)^2/2\sigma^2} \tag{36}$$

where σ characterizes the pulse width. σ, which is the distance from the center of the pulse to its inflection point, is defined as

$$\sigma = \frac{ct_p}{4} \tag{37}$$

where c is the speed of light, and

t_ρ is the temporal width of the pulse--the time between the inflection points of the pulse.

Note that, although the range width of the pulse is $ct_\rho = 4$, the effective width of the range weighting is $ct_\rho/2 = 2\sigma$ because of the round trip. The "range bin", therefore, is 2σ wide.

Hence, the signal received by the MASAR antenna m at position n is, from (35) and (36)

$$V_n^m = \frac{E_{peak}^m e^{j\omega_0 \tau_n^m}}{\sqrt{2\pi}\,\sigma} \iiint_{-\infty}^{\infty} dx\,dy\,dz \bullet g^m(\theta,\phi)\chi_n^m(x,y,z)\,\frac{e^{-\left[\frac{(\rho-R_0)^2}{2\sigma^2} + j2k_0\rho\right]}}{\rho^2} \tag{38}$$

For high resolution in range, σ is chosen to be small. Then the variation in range becomes, effectively,

$$|\rho - R_0| \gtrsim 3\sigma \tag{39}$$

and, then, the usual far field approximation [23:440] can be made,

$$\frac{1}{\rho^2} \cong \frac{1}{R_0^2} \tag{40}$$

Hence, the model for the MASAR signal return becomes

$$V_n^m = \frac{E_{peak}^m e^{j\omega_0 \tau_n^m}}{\sqrt{2\pi}\sigma R_0^2} \iiint_{-\infty}^{\infty} dx\, dy\, dz \bullet g^m(\theta,\phi) \chi_n^m(x,y,z)\, e^{-\left[\frac{(\rho - R_0)^2}{2\sigma^2} + j2k_0\rho\right]} \tag{41}$$

Without loss of generality, and to simplify the work which follows, further development of the models for the target and clutter shall be restricted to a two-dimensional space. This shall be the plane defined by the radar platform velocity vector and the synthetic antenna beam-maximum boresight: chosen here to be the x-y plane. That is,

$$V_n^m = \frac{E_{peak}^m e^{j\omega_0 \tau_n^m}}{\sqrt{2\pi}\sigma R_0^2} \iint_{-\infty}^{\infty} dx\, dy\, g^m(\theta) \chi_n^m(x,y)\, e^{-\left[\frac{(r - R_0)^2}{2\sigma^2} + j2k_0 r\right]} \tag{42}$$

where now, $r^2 = x^2+y^2$, $\theta = \tan^{-1}(y/x)$, with the x-axis along the antenna boresight, the y-axis along the platform velocity vector, and the origin at the center of antenna m.

<u>The Generalized Cross-Power Term</u>

Both α_n^m and β_{np}^{ml} can be obtained from (42). Recall from (28) and (32) that the cross-product $V_n^m V_p^{*l}$ is common. That is, for both the target power and the clutter power, the terms in their sums, (18) and (19), are--in general--weighted products of the signal received by antenna m in position n and the signal received by antenna l in position p. For notational simplicity, let

$$V_1 \equiv V_n^m,\ g_1(\cdot) \equiv g^m(\cdot),\ \chi_1 \equiv \chi_n^m,\ \text{etc.,} \tag{43a}$$

and

$$V_2 \equiv V_p^l, \; g_2(\cdot) \equiv g^l(\cdot), \; \chi_2 \equiv \chi_p^l, \; \text{etc.} \tag{43b}$$

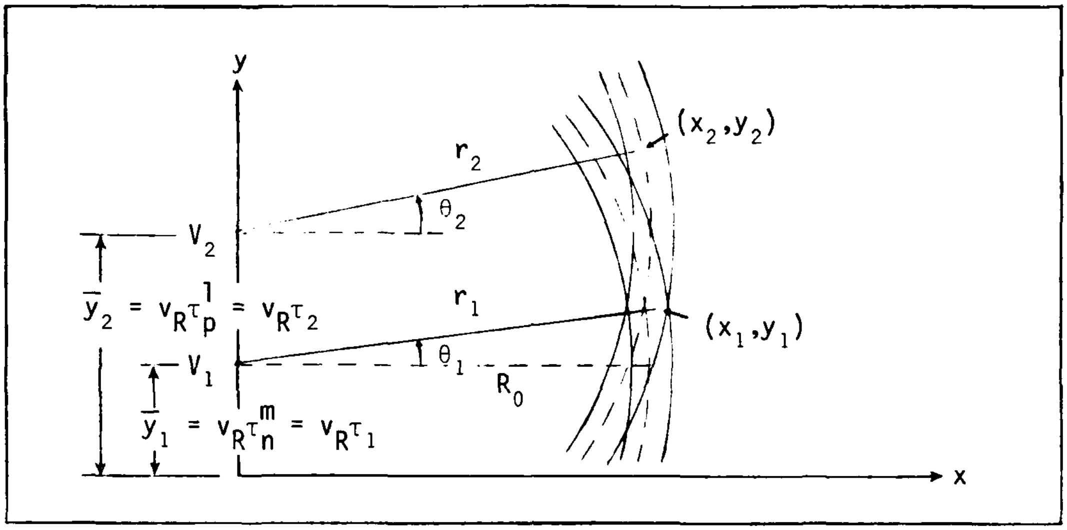

Figure 3. Geometry for the Cross-Power Term

Then, for both the target and the clutter, the term of common interest is the generalized cross-power term which can be written as, see Figure 3,

$$V_1V_2^* = \kappa \iiiint_{-\infty}^{\infty} dx_1 dy_1 \, dx_2 dy_2 \, g_1(\theta_1) \, g_2^*(\theta_2) \cdot \chi_1(x_1, y_1) \, \chi_2^*(x_2, y_2) \quad e^{-\gamma(x_1, y_1, x_2, y_2)} \tag{44}$$

where,

$$\kappa = \frac{\hat{\kappa} \, E_1 E_2 e^{j\omega_0 (\tau_1 - \tau_2)}}{2\pi\sigma^2 R_0^4} \tag{45}$$

$\hat{\kappa}$ is a constant of proportionality,

$$\gamma(x_1, y_1, x_2, y_2) = \frac{(r_1 - R_0)^2 + (r_2 - R_0)^2}{2\sigma^2} + j2k_0(r_1 - r_2) \quad (46)$$

and

$$(r_1)^2 = x_1^2 + (y_1 - \bar{y}_1)^2 \quad (47a)$$

$$\theta_1 = \tan^{-1}\left(\frac{y_1 - \bar{y}_1}{x_1}\right) \quad (47b)$$

$$(r_2)^2 = x_2^2 + (y_2 - \bar{y}_2)^2 \quad (47c)$$

$$\theta_2 = \tan^{-1}\left(\frac{y_2 - \bar{y}_2}{x_2}\right) \quad (47d)$$

where

$\bar{y}_1$ is the position of antenna 1 at $t = \tau_1$, and

$\bar{y}_2$ is the position of antenna 2 at $t = \tau_2$.

To complete the model, the backscattering coefficients must be defined for the target and the clutter. This will be done in the next two sections.

The Target Model

Throughout the generation of all M synthetic arrays, the MASAR platform shall be starboard-looking and moving with a constant velocity $\vec{v}_R$, a vector directed along the flight path. Also, the target shall be moving with a constant velocity $\vec{v}_T$, a vector directed at a track angle, θ_T, measured counterclockwise from the MASAR abeam-to-starboard direction. The target shall remain in the same MASAR range bin (see page 27)

throughout the MASAR observation interval. See Figure 4.

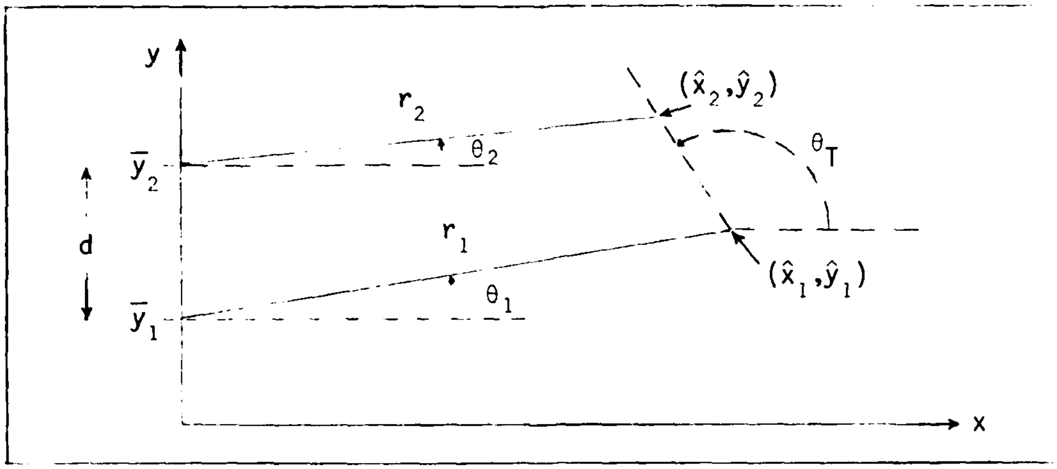

Figure 4. Geometry for the Target Model

In Figure 4,

$(\hat{x}_1,\hat{y}_1)$ is the position of the target at $t = \tau_1$ when antenna 1 pulses,

$(\hat{x}_2,\hat{y}_2)$ is the position of the target at $t = \tau_2$ when antenna 2 pulses,

$d = \bar{y}_2-\bar{y}_1$ is the spacing between antennas 1 and 2, where $\bar{y}_1$ and $\bar{y}_2$ are as described on the previous page, and where

θ_T is the target track angle.

The radar platform is moving along the y-axis in the positive direction. All angles are measured counterclockwise from abeam-to-starboard of the MASAR platform. The cross-power between antennas 1 and 2, received from the target, is obtained from (44). The target is defined quite simply as a moving isotropic scatterer:

$$\chi_1 = \delta(x_1-\hat{x}_1, y_1-\hat{y}_1) \tag{48a}$$

and

$$\chi_2 = \delta(x_2-\hat{x}_2, y_2-\hat{y}_2) \tag{48b}$$

where $\delta(\cdot)$ is the Dirac delta function. Here, χ_1 is the backscattering coefficient of the target as observed by antenna 1, and χ_2 is the same, but as observed by antenna 2.

With (48) in (44), the integration separates and is trivial:

$$V_1V_2^* = \kappa g_1\left[\tan^{-1}\left(\frac{\hat{y}_1-\bar{y}_1}{\hat{X}_1}\right)\right]g_2^*\left[\tan^{-1}\left(\frac{\hat{y}_2-\bar{y}_2}{\hat{X}_2}\right)\right]e^{-\gamma(\hat{x}_1,\hat{y}_1,\hat{x}_2,\hat{y}_2)} \tag{49}$$

with $\gamma(\cdot)$ described by (46). The relationship of (49) to (28) should be clearly evident; in fact, the target signal vector (30) can be generated from

$$\alpha_n^m = v_n^m = \frac{\sqrt{\hat{k}}E^m_{peak}}{\sqrt{2\pi}\,\sigma R_0^2}\; g^m(\theta_n^m)e^{-\frac{(r_n^m-R_0)^2}{2\sigma^2}-j2k_0r_n^m} \tag{50}$$

where r_n^m is the instantaneous range to the target from antenna m in synthetic position n, and $\theta_n^m = \tan^{-1}\left(\frac{y_n^m - \bar{y}_n^m}{x_n^m}\right)$ is the angle between r_n^m and the direction abeam-to-starboard of the MASAR platform.

Expressions for r_n^m, and θ_n^m can be easily obtained. Refer to Figure 5 for the following observations: antenna 1 is pulsed in position 1 at time $\tau_1^1 = 0$. At this time, the target is located at the tip of the radius vector $\vec{r}_1^{\,1}$ at angle θ_1^1. Antenna m is pulsed in position n at time τ_n^m; <u>however</u>, its separation from antenna 1 in position 1 along the flight path is only $d = v_R\tau_n^1$ because all antennas are pulsed at the same

synthetic positions in space. Meanwhile, the target has moved along its trajectory--determined by its speed v_T and track angle θ_T--to the tip of radius vector $\vec{r}_n^m$ at angle θ_n^m. The target has traversed a distance $r_T = v_T\tau_n^m$.

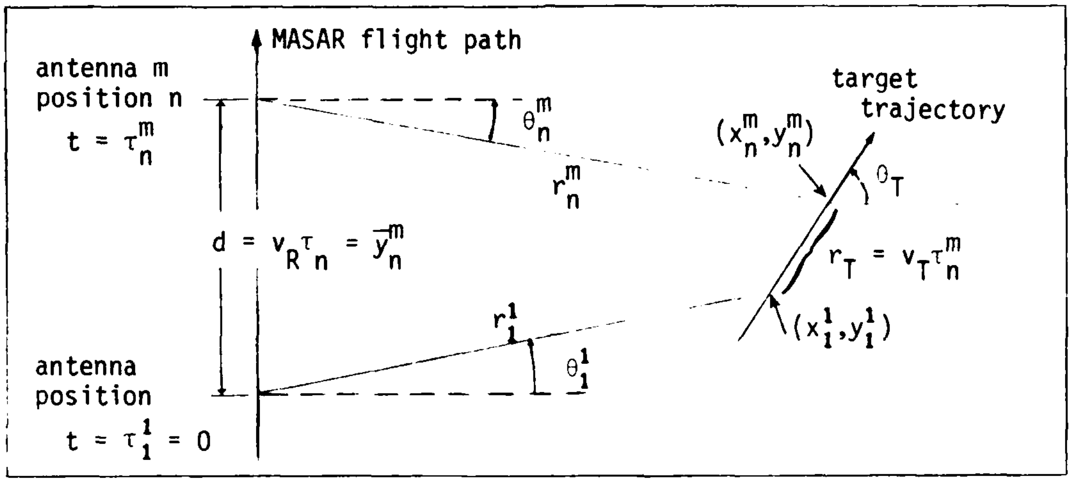

Figure 5. Geometry for the Instantaneous Target Range

From Figure 5,

$$r_n^m \cos\theta_n^m = r_1^1 \cos\theta_1^1 + v_T \tau_n^m \cos\theta_T \tag{51a}$$

and

$$r_n^m \sin\theta_n^m = r_1^1 \sin\theta_1^1 + v_T \tau_n^m \sin\theta_T - v_R \tau_n^1 \tag{51b}$$

The parameters r_n^m and θ_n^m can be computed easily given v_T and θ_T, but first r_1^1 and θ_1^1 must be established. For purposes of this model, the technique used in generating the target signal vector shall be to place the target at range R_0 along, and angle θ_0 from, the perpendicular bisector of the MASAR array at precisely the midpoint of the MASAR observation interval, as shown in Figure 6. When M antennas and N pulses are used, the midpoint of the MASAR observation interval is $(\tau_N^M - \tau_1^1)/2$. (τ_N^M is the time the last antenna pulses in the last posi-

tion and MASAR time ends.) But, $\tau_1^1 = 0$, see (34), as this is the time at which antenna 1 pulses in position 1 and MASAR time begins. Thus the midpoint of the MASAR observation interval is $\tau_N^M/2$.

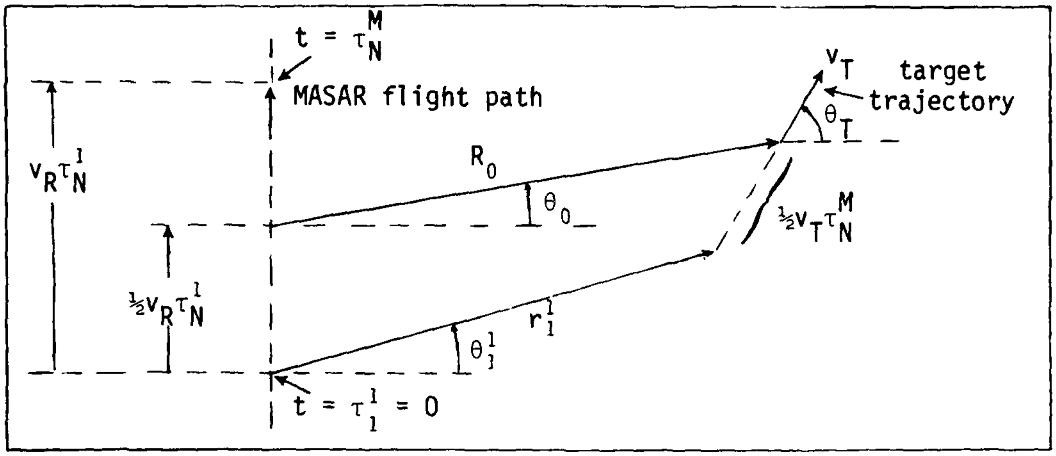

Figure 6. Geometry for Determining r_1^1 and θ_1^1

Then,

$$r_1^1 \cos\theta_1^1 = R_0 \cos\theta_0 - v_T \frac{\tau_N^M}{2} \cos\theta_T \tag{52a}$$

and

$$r_1^1 \sin\theta_1^1 = v_R \frac{\tau_N^1}{2} + R_0 \sin\theta_0 - v_T \frac{\tau_N^M}{2} \sin\theta_T \tag{52b}$$

With (52) in (51), expressions for r_n^m and θ_n^m can be obtained which hold for all m and n ($1 \leq m \leq M$, $1 \leq n \leq N$),

$$\left(r_n^m\right)^2 = \left[R_0 \cos\theta_0 + v_T \cos\theta_T \left(\tau_n^m - \frac{\tau_N^M}{2}\right)\right]^2 + \left[R_0 \sin\theta_0 \right.$$

$$\left. + \; v_R \left(\frac{\tau_N^1}{2} - \tau_n^1\right) + v_T \sin\theta_T \left(\tau_n^m - \frac{\tau_N^M}{2}\right)\right]^2 \tag{53}$$

and

$$\theta_n^m = \tan^{-1}\left[\frac{R_0 \sin\theta_0 + v_R\left(\frac{\tau^N}{2} - \tau_n^1\right) + v_T \sin\theta_T\left(\tau_n^m - \frac{\tau^N}{2}\right)}{R_0 \cos\theta_0 + v_T \cos\theta_T\left(\tau_n^m - \frac{\tau^N}{2}\right)}\right] \quad (54)$$

where care must be taken to distinguish between m, n, M, and N. For example, for 6 antennas and 50 synthetic positions, M = 6, N = 50, $1 \leq m \leq 6$, and $1 \leq n \leq 50$.

This completes the target model: the target signal vector (30) can be obtained from (50), (53) and (54) once the two-way antenna patterns $g^m(\theta)$ are defined. These shall be chosen after the clutter model is established.

The Clutter Model

As an aid in defining the clutter model, assume the MASAR platform is flying so as to overlook a heavily wooded terrain. A radar pulse, of duration t_p is transmitted. At a time corresponding to a round-trip distance for the center of the pulse of $2R_0$, the pulse return is sampled. This return is a superposition of the backscattered electric field from every scatterer in an annular ring of inner and outer radii $R_0-(ct_p)/4$ and $R_0+(ct_p)/4$, respectively. This describes the scattering region of interest.

Each point in this scattering region can be characterized by its electric field backscattering coefficient (see page 25). For a particular point, this coefficient is an amplitude and phase weighting which is applied to that part of the incident electric field which scatters back in the direction of the source. This coefficient is construed as being a random function of both time and space. That is, if one could isolate a point in the scattering region and observe its backscattering coefficient as a function of time, then one would obtain a sample function of

a random process [24:3-4]. Furthermore, different sample functions would be obtained for each of the other points in the scattering region. What is being described, here, is a random field [24:81ff; 25:243ff].

The electric field backscattering coefficient, from which the MASAR clutter signal is derived, shall be characterized as the complex (or, two-dimensional) spatiotemporal random field $\chi(x,y,t)$. This random field represents the amplitude and phase of the backscattering coefficient as a function of time for every point of the scattering region observed from positions along the MASAR flight path. The backscattering coefficient, observed by MASAR antenna m at position n shall be denoted

$$\chi_n^m(x,y) \equiv \chi(x,y,\tau_n^m) \tag{55}$$

where, for the spatial indexing parameters x and y, the x-axis lies along the antenna m boresight, the y-axis lies along the platform velocity vector, and the origin is at the intersection of these axes (at the center of antenna m). $\chi_n^m(x,y)$ assumes complex values χ with probability density $p_\chi(\chi)$ over the scattering region.

Then, the specific form for the mean clutter power B matrix elements can be obtained by taking the expectation of (44). That is; with (32), (43), (44), and (55):

$$\beta_{np}^{ml} = \langle v_n^m v_p^{*l} \rangle = \langle v_1 v_2^* \rangle = \kappa \int\int\int_{-\infty}^{\infty}\int dx_1 dy_1\, dx_2 dy_2$$

$$\bullet\ g_1(\theta_1)\, g_2^*(\theta_2) \langle \chi_1(x_1,y_1)\, \chi_2^*(x_2,y_2) \rangle e^{-\gamma(x_1,y_1,x_2,y_2)} \tag{56}$$

where κ, θ_1, θ_2, and $\gamma(\cdot)$ are described in (44). Note that if the combined clutter power was to be obtained instead of the combined <u>average</u>

clutter power, then the random field $\chi(x,y,t)$ would have to be explicitly defined and a stochastic integral would have to be evaluated.

Recall from (43) that $\langle \chi_1 \chi_2^* \rangle \equiv \langle \chi_n^m \chi_p^{*l} \rangle$. For all m and l, χ_n^m and χ_p^l have a common spatial origin when n = p, and they have different origins when n ≠ p. When n = p, the backscatter coefficient is observed twice from the same point in space, at instants τ_p^m and τ_p^l in time. When n ≠ p, the observations are from two different points in space each at instants τ_n^m and τ_p^l, respectively, in time.

It is not unreasonable to assume that, for a particular point in the scattering region, the values of the backscattering coefficient would tend to be correlated for closely spaced instants in time, and uncorrelated for widely spaced instants in time. Nor is it any less reasonable to assume that, for a particular instant in time, the values of the backscattering coefficient would tend to be correlated for closely spaced points in the scattering region, and uncorrelated for widely spaced points in the scattering region. Furthermore, within the MASAR observation interval and scattering region of interest, it may be reasonably assumed that the expected value of the backscattering coefficient is constant over time and space.

By subscribing to these assumptions, the nature of the clutter backscattering coefficient can be more explicitly defined as a random field which is both homogeneous and isotropic [24:84; 25:247]. This means that, for any two points in space or time,

$$\langle \chi(x_1,y_1,t_1)\chi^*(x_2,y_2,t_2) \rangle = f(|x_1-x_2|,|y_1-y_2|,|t_1-t_2|) \qquad (57)$$

That is, the correlation of the electric field backscattering coefficient is a function of only the distance between the space or time

points and not of the direction. (Were it a function of the direction, it would be homogeneous but not isotropic.)

By considering only the expectation of the clutter cross-power term, the task of modeling the stochastic character of the clutter backscatter is avoided. What remains is the much simpler task of modeling the correlation of the clutter backscatter coefficient, $\langle \chi_1 \chi_2^* \rangle$. This can be done by selecting any correlation function which satisfies the stochastic properties propounded in the preceeding paragraph.

For the most general sense, $\langle \chi_1 \chi_2^* \rangle$ should be chosen as a spatiotemporally weighted spatiotemporal correlation function; see chapter VI, pp. 137-138. However, both time and space for the present work are limited and it will be seen that the function chosen here, although the simplest and lending the most tractability, nevertheless leaves the evaluation of (56) to be no simple matter.

The clutter model shall be derived from the correlation function

$$\langle \chi_1 (x_1, y_1) \chi_2^* (x_2, y_2) \rangle \triangleq e^{-\frac{(\tau_1 - \tau_2)^2}{2T^2}} \delta(x_1 - x_2, y_1 - y_2) \tag{58}$$

where $\tau_1 \equiv \tau_n^m$ is the time antenna m is in position n,

$\tau_2 \equiv \tau_p^l$ is the time antenna l is in position p,

T is the temporal clutter correlation interval, and

$\delta(\cdot)$ is the Dirac delta function.

The meaning of (58) follows: all points in the clutter backscattering region are spatially uncorrelated with each other except with themselves and, even then, decorrelate as a gaussian function of the temporal spread between points of observation. The temporal correlation interval, T, determines how rapidly this decorrelation occurs.

Physically, the spatial character chosen here describes a scattering surface which tends to be everywhere discontinuous; that is, a surface with very densely packed irregularities having transitions which greatly exceed the wavelength of the source. For a 1 GHz radar, such a surface might be described by the trees (and their interspacings) of a dense forest. In contrast, this model could not be applied to spatially characterize terrain with a gently rolling surface such as a treeless region with large distances between its hills and valleys. For such terrain, one would expect some correlation between points on the surface even if they were far apart.

With (58), (56) reduces to

$$\langle V_1 V_2^* \rangle = \kappa \, e^{-\frac{(\tau_1-\tau_2)^2}{2T^2}} \int_{-\infty}^{\infty} dx \int_{-\infty}^{\infty} dy \cdot g_1\left[\tan^{-1}\left(\frac{y-\bar{y}_1}{X}\right)\right] g_2^*\left[\tan^{-1}\left(\frac{y-\bar{y}_2}{X}\right)\right] e^{-\gamma(x,y)} \tag{59}$$

where

$$\gamma(x,y) = \frac{1}{2\sigma^2}\left[(r_1-R_0)^2 + (r_2-R_0)^2\right] + j2k_0(r_1-r_2) \tag{60}$$

in which, as shown in Figure 7,

$$(r_1)^2 = x^2 + (y-y_1)^2 \tag{61}$$

$$(r_2)^2 = x^2 + (y-\bar{y}_2)^2 = (r_1)^2 - 2d(y-\bar{y}_1) + d^2 \tag{62}$$

and

$$d = \bar{y}_2 - \bar{y}_1 \tag{63}$$

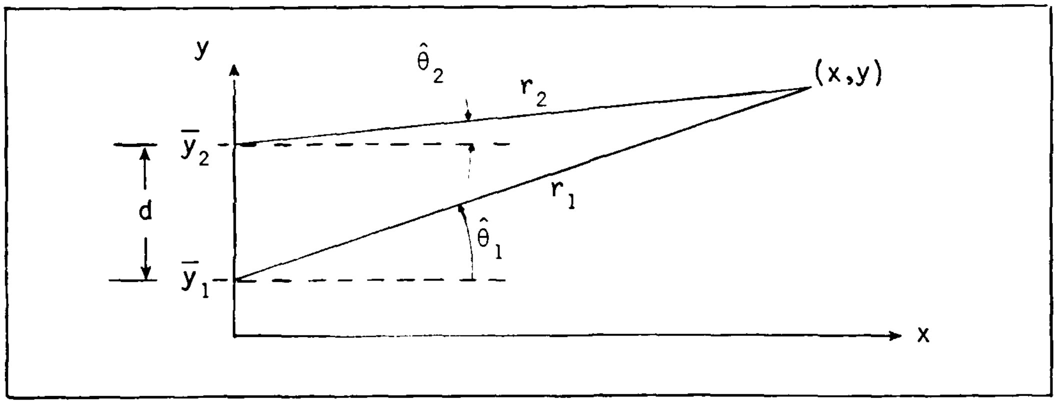

Figure 7. Geometry for Integrating the Clutter Cross-Power Correlation

Integrating the Clutter Cross-Power Correlation. The integation in (59) is greatly simplified by transforming from x,y to ζ,η:

$$\zeta = r_1 - R_0 \tag{64a}$$

$$\eta = (r_1 - r_2)/d \tag{64b}$$

First, the Jacobian of the transformation is obtained:

$$\frac{\partial(x,y)}{\partial(\zeta,\eta)} = \begin{vmatrix} \frac{\partial x}{\partial \zeta} & \frac{\partial x}{\partial \eta} \\ \frac{\partial y}{\partial \zeta} & \frac{\partial y}{\partial \eta} \end{vmatrix} \tag{65}$$

Proceeding thusly, from (61),

$$\zeta + R_0 = x \frac{\partial x}{\partial \zeta} + (y - \bar{y}_1) \frac{\partial y}{\partial \zeta} \tag{66}$$

and

$$0 = x \frac{\partial x}{\partial \eta} + (y - \bar{y}_1) \frac{\partial y}{\partial \eta} \tag{67}$$

Likewise, from (62),

$$0 = \zeta + R_0 - d\frac{\partial y}{\partial \zeta} \tag{68}$$

i.e.,

$$\frac{\partial y}{\partial \zeta} = \frac{\zeta + R_0}{d} \tag{69}$$

Also, from (62),

$$(r_2)^2 - (r_1)^2 = -2d(y - \bar{y}_1) + d^2 \tag{70}$$

or recalling (64b),

$$-(r_2 + r_1)\eta = -2(y - \bar{y}_1) + d \tag{71}$$

from which

$$\frac{\partial y}{\partial \eta} = \frac{r_1 + r_2}{2} \tag{72}$$

From (66) and (69),

$$\frac{\partial x}{\partial \zeta} = \frac{\zeta + R_0}{X} \left(1 - \frac{y - \bar{y}_1}{d}\right) \tag{73}$$

From (67) and (72),

$$\frac{\partial x}{\partial \eta} = -\frac{(y - \bar{y}_1)}{x} \frac{r_1 + r_2}{2} \tag{74}$$

Hence, the Jacobian is obtained from (65) with (69), (72), (73), and (74):

$$\frac{\partial(x,y)}{\partial(\zeta,\eta)} = \frac{\zeta + R_0}{x} \frac{r_1 + r_2}{2}$$

$$= \frac{\zeta + R_0}{x} \quad \frac{\zeta + R_0 + r_2 - r_1 + r_1}{2}$$

$$= \frac{\zeta + R_0}{x} \quad \frac{2(\zeta + R_0) - \eta d}{2} \tag{75}$$

Also, it is convenient to transform (60) at this time:

$$\gamma(\zeta,\eta) = \frac{1}{2\sigma^2}\left[\zeta^2 + (\zeta - \eta d)^2\right] + j2k_0\eta d$$

$$= \frac{1}{2\sigma^2}\left[2\zeta^2 - 2\zeta\eta d + \eta^2 d^2\right] + j2k_0\eta d \tag{76}$$

which can be more conveniently expressed by completing the square in ζ:

$$\gamma(\zeta,\eta) = \frac{1}{2\sigma^2}\, 2(\zeta - \eta d/2)^2 - \frac{\eta^2 d^2}{4\sigma^2} + \frac{\eta^2 d^2}{2\sigma^2} + j2k_0\eta d$$

$$= \frac{(\zeta - \eta d/2)^2}{\sigma^2} + \frac{\eta^2 d^2}{4\sigma^2} + j2k_0\eta d \tag{77}$$

The effect of these transformations on the limits of integration must now be considered along with a simplifying approximation. The transformation from x,y to ζ,η is isomorphic; that is, the space is not deformed. Clearly, from Figure 7 and (64b), the new variable η has finite limits: $-1 \lesssim \eta \lesssim 1$. However, in order to integrate over the entire space--as is done in (59)--in the ζ,η coordinate system, one of two possible choices for the limits of integration on ζ must be selected: either

$$\int_{-\infty}^{\infty}\!\!\int dx\ dy \rightarrow \left[\int_{-1}^{1} d\eta + \int_{1}^{-1} d\eta\right] \int_{-Ro}^{\infty} d\zeta$$

or,

$$\int_{-\infty}^{\infty}\!\!\int dx\ dy \rightarrow \int_{-1}^{1} d\eta \left[\int_{-\infty}^{-Ro} d\zeta + \int_{-Ro}^{\infty} d\zeta\right] \equiv \int_{-1}^{1} d\eta \int_{-\infty}^{\infty} d\zeta$$

In the first choice, the integration $\int_{-1}^{1} d\eta$ corresponds to an integration $\int_{-\pi/2}^{\pi/2} d\theta$, *in Figure 7, which is an integration over the forward* lobes of the real antenna patterns (remember, MASAR is starboard-looking). The integration $\int_{-1}^{1} d\eta$ corresponds to an integration $\int_{\pi/2}^{-\pi/2} d\theta$, in Figure 7, which is an integration over the back lobes of the real antenna patterns.

In the second choice, the integration $\int_{-\infty}^{-R_0} d\zeta$ corresponds to the integration over the backlobes, and the integration $\int_{-R_0}^{\infty} d\zeta$ corresponds to the integration over the front lobes. Both choices are equivalent, but the second choice is easier to work with.

Now, the simplifying approximation is made: the integration over the backlobes of the real antennas,

$$\int_{-\infty}^{0} dx \int_{-\infty}^{\infty} dy \equiv \int_{-1}^{1} d\eta \int_{-\infty}^{-Ro} d\zeta$$

is negligible. And so,

$$\iint_{-\infty}^{\infty} dx\ dy \approx \int_{-\infty}^{\infty} dy \int_{0}^{\infty} dx \equiv \int_{-1}^{1} d\eta \int_{-R_0}^{\infty} d\zeta \approx \int_{-1}^{1} d\eta \int_{-\infty}^{\infty} d\zeta$$

With this, (75) and (77); (59) becomes

$$\langle V_1 V_2^* \rangle = \kappa_1 \int_{-1}^{1} d\eta\ e^{-\left[(d/2\sigma)^2\eta^2 + j2k_0\eta d\right]}$$

$$\cdot \int_{-\infty}^{\infty} d\zeta\ g_1(\hat{\theta}_1) g_2^*(\hat{\theta}_2)\ \frac{2(\zeta+R_0)^2 - \eta\, d(\zeta+R_0)}{2x}\ e^{\frac{-(\zeta-\eta d/2)^2}{\sigma^2}} \qquad (78)$$

where,

$$\kappa_1 = \kappa\ e^{-(\tau_1-\tau_2)^2/2T^2} \qquad (79)$$

κ is defined by (45), and the variables $\hat{\theta}_1$ and $\hat{\theta}_2$ will be discussed shortly.

The integration of (78) over the variable ζ can be done asymptotically via the Method of Laplace [26:302-303]: since σ is small, and the factors $g_1(\hat{\theta}_1)$, $g_2(\hat{\theta}_2)$, and

$$\frac{2(\zeta+R_0)^2 - \eta d\ (\zeta+R_0)}{2x}$$

are smoothly and slowly varying functions of ζ, then the factor

$$e^{-(\zeta-\eta d/2)^2/\sigma^2}$$

dominates the character of the integrand. In fact, this factor drives the value of the integrand close to zero everywhere except near the

point $\zeta = \eta d/2$. Therefore, the integration on ζ can be obtained by integration over a very small interval about this point. But, with such an interval, from (78), the integration on ζ can be written as

$$
\begin{aligned}
I_\zeta &= \int_{-\infty}^{\infty} d\zeta \; g_1(\hat{\theta}_1) g_2^*(\hat{\theta}_2) \quad e^{-(\zeta-\eta d/2)^2/\sigma^2} \; \frac{2(\zeta+R_0)^2 - \eta d(\zeta+R_0)}{2x} \\
&\sim \left[g_1(\hat{\theta}_1) g_2^*(\hat{\theta}_2) \int_{-\infty}^{\infty} d\zeta \; e^{-(\zeta-\eta d/2)^2/\sigma^2} \right. \\
&\qquad \left. \bullet \; \frac{2(\zeta+R_0)^2 - \eta d(\zeta+R_0)}{2x} \right]_{\zeta=\eta d/2}
\end{aligned}
\tag{80}
$$

This last integral is simply that of a gaussian function, so

$$
\begin{aligned}
I_\zeta &\sim \sqrt{2\pi} \quad \left(\frac{\sigma}{\sqrt{2}}\right) \left[g_1(\hat{\theta}_1) g_2^*(\hat{\theta}_2) \right]_{\zeta=\eta d/2} \frac{2(\eta d/2+R_0)^2 - \eta d(\eta d/2+R_0)}{2x} \\
&= \sqrt{\pi}\sigma \; \frac{R_0(\eta d+2R_0)}{2x} \left[g_1(\hat{\theta}_1) g_2^*(\hat{\theta}_2) \right]_{\zeta=\eta d/2} \quad .
\end{aligned}
\tag{81}
$$

where x is also evaluated at $\zeta = \eta d/2$.

The parameter x can be evaluated as follows: from (61),

$$
x^2 = (r_1)^2 - (y-\bar{y}_1)^2 \tag{82}
$$

From (62),

$$
y-\bar{y}_1 = \frac{(r_2)^2 - (r_1)^2 - d^2}{-2d}
$$

$$= \frac{(r_1 - r_2)(r_1 + r_2) + d^2}{2d} \tag{83}$$

which becomes, with (64b),

$$y - \overline{y}_1 = \frac{\eta(r_1 + r_2) + d}{2} \tag{84}$$

Hence, (82) with (84) yields,

$$x^2 = (r_1)^2 - \left[\frac{\eta(r_1 + r_2) + d}{2}\right]^2 \tag{85}$$

which is to be evaluated at $\zeta = \eta d/2$. Recalling (64a),

$$r_1\Big|_{\zeta=\eta d/2} = \frac{\eta d}{2} + R_0 \tag{86}$$

Using this with (64b),

$$r_2\Big|_{\zeta=\eta d/2} = r_1\Big|_{\zeta=\eta d/2} - \eta d$$

$$= R_0 - \frac{\eta d}{2} \tag{87}$$

Adding (86) and (87),

$$(r_1 + r_2)\Big|_{\zeta=\eta d/2} = 2R_0 \tag{88}$$

Then, with (86) and (88), (85) becomes

$$x^2 = R_0^2 \left[1-\left(\frac{d}{2R_0}\right)^2\right](1-\eta^2) \tag{89}$$

or,

$$x = R_0\left[1-\left(\frac{d}{2R_0}\right)^2\right]^{1/2}\sqrt{1-\eta^2} \tag{90}$$

Hence, (81) can be written as

$$I_\zeta \sim \frac{\sqrt{\pi}\sigma R_0}{d[1-(\frac{d}{2R_0})^2]^{1/2}} \; \frac{1+\eta\left(\frac{d}{2R_0}\right)}{\sqrt{1-\eta^2}} \left[g_1(\hat{\theta}_1)g_2^*(\hat{\theta}_2)\right]_{\zeta=\eta d/2} \tag{91}$$

The arguments of $g_1(\cdot)$ and $g_2(\cdot)$ can be written from (78) with reference to (59),

$$\hat{\theta}_1 = \tan^{-1}\frac{y-\bar{y}_1}{x} \tag{92}$$

and

$$\hat{\theta}_2 = \tan^{-1}\frac{y-\bar{y}_2}{x} \tag{93}$$

which must be evaluated at $\zeta = \eta d/2$ as well. For (92), with (84), (88), and (90),

$$\tan\ \hat{\theta}_1 = \frac{2R_0\eta + d}{2x}$$

$$= \frac{\eta + \frac{d}{2R_0}}{[1-(d/2R_0)^2]^{1/2}\sqrt{1-\eta^2}} \tag{94}$$

For (93), recalling (63),

$$\tan\hat{\theta}_2 = \frac{y-\bar{y}_1+\bar{y}_1-\bar{y}_2}{x}$$

$$= \frac{y-\bar{y}_1}{x} - \frac{d}{x}$$

$$= \tan\hat{\theta}_1 - \frac{d}{x} \tag{95}$$

hence, with (90) and (94)

$$\tan\hat{\theta}_2 = \frac{\eta - \frac{d}{2R_0}}{\left[1-\left(\frac{d}{2R_0}\right)^2\right]^{1/2}\sqrt{1-\eta^2}} \tag{96}$$

With $\hat{\theta}_1$ and $\hat{\theta}_2$ so determined, and with (91), the integration over the variable ζ is completed and (78) leaves

$$\langle V_1V_2^*\rangle \sim \tilde{\kappa}\int_{-1}^{1} d\eta \; g_1(\hat{\theta}_1)g_2^*(\hat{\theta}_2)\left(1+\frac{d}{2R_0}\eta\right) e^{-\left(\frac{d}{2\sigma}\right)^2\eta^2} \frac{e^{-j2k_0\eta d}}{\sqrt{1-\eta^2}} \tag{97}$$

where, from (45), (79), and (91)

$$\tilde{\kappa} = \frac{\hat{\kappa}\, E_1E_2 e^{-\frac{(\tau_1-\tau_2)^2}{2T^2} + j\omega_0(\tau_1-\tau_2)}}{2\sqrt{\pi}\;\sigma R_0^3\left[1-\left(\frac{d}{2R_0}\right)^2\right]^{1/2}} \tag{98}$$

and where,

$$\hat{\theta}_1 = \tan^{-1}\left\{ \frac{1}{\left[1-\left(\frac{d}{2R_0}\right)^2\right]^{1/2}} \frac{\eta + \frac{d}{2R_0}}{\sqrt{1-\eta^2}} \right\} \tag{99}$$

and

$$\hat{\theta}_2 = \tan^{-1}\left\{ \frac{1}{\left[1-\left(\frac{d}{2R_0}\right)^2\right]^{1/2}} \frac{\eta - \frac{d}{2R_0}}{\sqrt{1-\eta^2}} \right\} \tag{100}$$

<u>The Clutter Integral at d = 0</u>. Eq. (97) is the halfway point in the integration of (59). Some assurance that the work so far is correct can be obtained by considering both (59) and (97) for the special case $d = \overline{y}_2 - \overline{y}_1 = 0$; i.e., when the cross-power term involves the same synthetic position (the same point in space).

Letting d = 0, and making the variable change $\eta = \sin\theta$, it is easy to obtain, from (97) through (100),

$$\langle V_1 V_2^* \rangle \sim \frac{\hat{\kappa}\, E_1 E_2 e^{-\frac{(\tau_1-\tau_2)^2}{2T^2} + j\omega_0(\tau_1-\tau_2)}}{2\sqrt{\pi}\ \sigma R_0^3} \int_{-\pi/2}^{\pi/2} d\theta\ g_1(\theta) g_2^*(\theta) \tag{101}$$

This is simply a weighted integration over the forward lobes of the product of the two-way antenna patterns.

Returning to (59) with d = 0: $\overline{y}_1 = \overline{y}_2$ from (63), which means $r_1 = r_2$ from (61) and (61), and $\arg[g_1(\cdot)] = \arg[g_2(\cdot)] = \theta$; thus, with (45) and converting to polar coordinates, (59) becomes

$$\langle V_1 V_2^* \rangle = \frac{\hat{\kappa}\, E_1 E_2 e^{-\frac{(\tau_1-\tau_2)^2}{2T^2} + j\omega_0(\tau_1-\tau_2)}}{2\pi\sigma^2 R_0^4} \int_{-\pi/2}^{\pi/2} d\theta\ g_1(\theta) g_2^*(\theta) \int_0^{\infty} dr\ r e^{-\left(\frac{r-R_0}{\sigma}\right)^2} \tag{102}$$

where the integration over the backlobes is neglected as on pages 43-44.

The integration over the variable r is done simply as follows: let $\xi/\sqrt{2} = (r - R_0)/\sigma$, then

$$I_r = \int_0^\infty dr\, r e^{-\left(\frac{r-R_0}{\sigma}\right)^2} = \frac{\sigma}{\sqrt{2}} \int_{-\sqrt{2}R_0/\sigma}^{\infty} d\xi \left(\sigma \frac{\xi}{\sqrt{2}} + R_0\right) e^{-\xi^2/2} \tag{103}$$

For R_0 large and $\sigma << R_0$, the following approximation can be made:

$$I_r \sim \frac{\sigma^2}{2} \int_{-\infty}^{\infty} \xi e^{-\xi^2/2} d\xi + \frac{\sigma R_0}{\sqrt{2}} \int_{-\infty}^{\infty} e^{-\xi^2/2} d\xi \tag{104}$$

The first integral vanishes, as it is an odd integrand integrated over even limits. The second integral is that of a standard gaussian form. Hence,

$$I_r \sim \frac{\sigma}{\sqrt{2}} R_0 \sqrt{2\pi} = \sqrt{\pi}\ \sigma\ R_0 \tag{105}$$

Thus, (102) becomes

$$\langle V_1 V_2^* \rangle \sim \frac{\hat{\kappa}\ E_1 E_2 e^{-\frac{(\tau_1-\tau_2)^2}{2T^2} + j\omega(\tau_1-\tau_2)}}{2\sqrt{\pi}\ \sigma R_0^3} \int_{-\pi/2}^{\pi/2} d\theta\ g_1(\theta) g_2^*(\theta) \tag{106}$$

which is identical to (101) and demonstrates that the same result can be obtained from both (59) and (97) when d = 0.

Continuing The Clutter Integration. Returning to the integration of the clutter cross-power correlation, from (97), let

$$I \triangleq \int_{-1}^{1} d\eta \; f(\eta) \; \frac{e^{jz\eta}}{\sqrt{1-\eta^2}} \tag{107}$$

where

$$f(\eta) = g_1(\hat{\theta}_1)g_2^*(\hat{\theta}_2)(1+\frac{d}{2R_0}\eta)\,e^{-(\frac{d}{2\sigma})^2\eta^2} \tag{108}$$

and

$$z = -2k_0 d \tag{109}$$

Noting the limits of integration, expand $f(\eta)$ in a Taylor series about zero:

$$\begin{aligned} f(\eta) &= f(0) + \frac{f^{(1)}(0)}{1!}\eta + \frac{f^{(2)}(0)}{2!}\eta^2 \\ &\quad + \cdots + \frac{f^{(r)}(0)}{r!}\eta^r + \cdots \\ &= \sum_{r=0}^{\infty} \frac{f^{(r)}(0)}{r!}\eta^r \end{aligned} \tag{110}$$

where $f^{(r)}(0)$ denotes the r th derivative of $f(\eta)$ w.r.t. η evaluated at $\eta = 0$. Then (107) can be written

$$I = \sum_{r=0}^{\infty} \frac{f^{(r)}(0)}{r!} \int_{-1}^{1} \eta^r \frac{e^{jz\eta}}{\sqrt{1-\eta^2}} \, d\eta \tag{111}$$

Letting $\eta = \cos\theta$, (111) becomes

$$I = \sum_{r=0}^{\infty} \frac{f^{(r)}(0)}{r!} \int_{0}^{\pi} \cos^r\theta \; e^{jz\cos\theta} d\theta \tag{112}$$

This looks very much like an integral form of the Bessel function of the First Kind, order n. From [27:(9.1.21)],

$$\pi j^n J_n(z) = \int_0^\pi \cos(n\theta) e^{jz\cos\theta} d\theta \tag{113}$$

where $j = \sqrt{-1}$. But, (112) involves $\cos^r\theta$. However, this can be expressed as a sum of Chebyshev poloynomials of the First Kind [27:(22.3.15)],

$$T_p(\cos\theta) = \cos(p\theta) \tag{114}$$

Thus from [27:Table 22.3],

$$\begin{aligned}\cos^r\theta &= b_r^{-1} \sum_{p=0}^{r} \delta_p \; T_p(\cos\theta) \\ &= b_r^{-1} \sum_{p=0}^{r} \delta_p \cos(p\theta)\end{aligned} \tag{115}$$

where b_r and δ_p are coefficients defined in the referenced table and will be discussed shortly. But first, in two steps, the closed form for (112) can be obtained: with (115),

$$I = \sum_{r=0}^{\infty} \frac{f^{(r)}(0)}{r!} b_r^{-1} \sum_{p=0}^{r} \delta_p \int_0^\pi \cos(p\theta) e^{jz\cos\theta} d\theta \tag{116}$$

and then, with (113),

$$I = \pi \sum_{r=0}^{\infty} \frac{f^{(r)}(0)}{r!} b_r^{-1} \sum_{p=0}^{r} j^p \delta_p \, J_p(z) \tag{117}$$

Now, from [27:Table 22.3],

$$b_r = 2^{r-1} \text{ , when } r \neq 0$$
$$= 1 \text{ , when } r=0 \qquad (118)$$

So, using the Neumann number

$$\epsilon_r = 2 \text{ , when } r=0$$
$$= 1 \text{ , otherwise} \qquad (119)$$

then, for all r,

$$b_r = \epsilon_r 2^{r-1} \qquad (120)$$

Next, the δ_p are the coefficients of the Chebyshev polynomials; they are related to the binomial coefficients. Their expression, in terms of the indicies r and p, is rather tricky to obtain. After contemplating the values for δ_p in [27:Table 22.3], with the aid of Pascal's triangle, it can be determined that, from (117),

$$\sum_{p=0}^{r} j^p \delta_p \Rightarrow \sum_{s=0}^{\left[\frac{r}{2}\right]} \frac{r!}{(r-s)!s!} \frac{j^{r-2s}}{\epsilon_{r-2s}}$$

where [r/2] means the largest integer $\leq r/2$, and where the Neumann number,

$$\epsilon_{r-2s} = 2, \text{ when } r=2s, \text{ except } r=0$$
$$= 1, \text{ otherwise} \qquad (121)$$

Hence (117) can be written

$$I = \pi \sum_{r=0}^{\infty} \frac{f^{(r)}(0)}{r!\epsilon_r 2^{r-1}} \sum_{s=0}^{\left[\frac{r}{2}\right]} \frac{r!}{(r-s)!s!} \frac{j^{r-2s}}{\epsilon_{r-2s}} J_{r-2s}(z) \tag{122}$$

Note the r!'s will cancel. Also note, from [27:(9.1.35)]

$$J_\nu(ze^{m\pi j}) = e^{m\nu\pi j} J_\nu(z) \text{ , m an integer} \tag{123}$$

and then, recalling (109),

$$\begin{aligned} J_{r-2s}(2k_0 de^{j\pi}) &= e^{(r-2s)\pi j} J_{r-2s}(2k_0 d) \\ &= (-1)^{r-2s} J_{r-2s}(2k_0 d) \end{aligned} \tag{124}$$

Thus, (122) can be written

$$I = \pi \sum_{r=0}^{\infty} \frac{f^{(r)}(0)}{\epsilon_r 2^{r-1}} \sum_{s=0}^{\left[\frac{r}{2}\right]} \frac{(-j)^{r-2s}}{(r-s)!s!} \frac{J_{r-2s}(2k_0 d)}{\epsilon_{r-2s}} \tag{125}$$

Finally, with (97), (107), and (125), the clutter cross-power correlation model can be expressed in closed form as

$$\langle V_1 V_2^* \rangle \sim \frac{\hat{\kappa}\, E_1 E_2 \sqrt{\pi}\, e^{-\frac{(\tau_1-\tau_2)^2}{2T^2} + j\omega_0(\tau_1-\tau_2)}}{2\,\sigma R_0^3\left[1-\left(\frac{d}{2R_0}\right)^2\right]^{1/2}}$$

$$\bullet \sum_{r=0}^{\infty} \frac{f^{(r)}(0)}{\epsilon_r 2^{r-1}} \sum_{s=0}^{\left[\frac{r}{2}\right]} \frac{(-j)^{r-2s}}{(r-s)!s!} \frac{J_{r-2s}(2k_0 d)}{\epsilon_{r-2s}} \tag{126}$$

All factors in (126) have been explicitly defined in the preceeding text except the antenna patterns $g_1(\cdot)$ and $g_2(\cdot)$. These must be defined in order to determine the factors $f^{(r)}(0)$ for the outside summation in (126). Recalling (108), with (99), and (100), the evaluation of the factors $f^{(r)}(0)$ can be seen to be quite complicated for even simple choices of the antenna patterns.

<u>Antennas For The MASAR Model</u>

Up to this point, the MASAR antennas have been characterized generally by the factors $g^m(\theta)$, for $m \varepsilon \{1,2,...,M\}$, having amplitude and phase both as functions of θ. Recalling the discussion in the introduction, MASAR performance as a function of the dissimilarity in antennas is among the primary interests of this work. Considering the need to evaluate the factor $f^{(r)}(0)$ for the clutter model, a tractable, sensible choice is to choose the antennas to vary in *beamwidth only*--as powers of the simple cosine pattern: i.e.,

$$g^m(\theta) = \cos^P\theta \ , \ m \ \varepsilon \ \{1,2,...M\} \tag{127a}$$

and

$$g^l(\theta) = \cos^Q\theta \ , \ l \ \varepsilon \ \{1,2,...M\} \tag{127b}$$

where P and Q are integer powers, equal when m = 1.

The use of (127a) in (50) for generation of the target signal vector is quite straightforward. There, $g^m(\theta_n^m) = \cos^P\theta_n^m$ and θ_n^m is defined by (54).

For the clutter cross-power correlation terms, however, recalling (43) and (108),

$$g^{m}(\hat{\theta}_{n}^{m}) \equiv g_{1}(\hat{\theta}_{1}) = \cos^{P}(\hat{\theta}_{1}) \tag{128a}$$

and

$$g^{l}(\hat{\theta}_{P}^{1}) \equiv g_{2}(\hat{\theta}_{2}) = \cos^{Q}(\hat{\theta}_{2}) \tag{128b}$$

Then, with (99) and (100) and some trigonometry,

$$g_{1}(\hat{\theta}_{1}) \rightarrow g_{1}(\eta) = \left[1-\left(\frac{d}{2R_{0}}\right)^{2}\right]^{P/2} \frac{(1-\eta^{2})^{P/2}}{(1+\frac{d}{2R_{0}}\eta)^{P}} \tag{129}$$

and

$$g_{2}^{*}(\hat{\theta}_{2}) \rightarrow g_{2}(\eta) = \left[1-\left(\frac{d}{2R_{0}}\right)^{2}\right]^{Q/2} \frac{(1-\eta^{2})^{Q/2}}{(1-\frac{d}{2R_{0}}\eta)^{Q}} \tag{130}$$

Then (108) can be written explicitly as

$$f(\eta) = \left[1-\left(\frac{d}{2R_{0}}\right)^{2}\right]^{\frac{P+Q}{2}} (1-\eta^{2})^{\frac{P+Q}{2}}$$

$$\bullet\ (1+\frac{d}{2R_{0}}\eta)^{-(P-1)}\ (1-\frac{d}{2R_{0}}\eta)^{-Q}\ e^{-(\frac{d}{2\sigma})^{2}\eta^{2}} \tag{131}$$

This completes the formulation of the MASAR model. The target signal vector can be obtained as described two paragraphs earlier and the clutter cross-power correlation terms can be obtained directly from (126) using (131) to obtain the factors $f^{(r)}(0)$.

<u>Computation of $f^{(r)}(0)$</u>. The evaluation of (126)--though an infinite sum--converges very rapidly, rarely requiring more than 20 terms. Nevertheless, this means that derivatives of $f(\eta)$ through the 20th or so order must be obtained. Manually differentiating (131) becomes unman-

ageable after the sixth or seventh order.

There is a better way: Liebniz's theorem for the differentiation of a product [27:(3.3.8)]

$$(uv)^{(r)} = u^{(r)}v^{(0)} + \binom{r}{1}u^{(r-1)}v^{(1)} + \binom{r}{2}u^{(r-2)}v^{(2)} + \cdots$$

$$+ \binom{r}{s}u^{(r-s)}v^{(s)} + \cdots + u^{(0)}v^{(r)} \qquad (132)$$

which can be written in the form

$$(uv)^{(r)} = \sum_{s=0}^{r} \binom{r}{s} u^{(r-s)}v^{(s)} \qquad (133)$$

where $\binom{r}{s}$ is the binomial coefficient. *This can be extended easily:* let $u = u_1$ and $v = u_2 w$, then

$$(u_1 u_2 w)^{(r)} = \sum_{s=0}^{r} \binom{r}{s} u_1^{(r-s)}(u_2 w)^{(s)}$$

$$= \sum_{s=0}^{r} \binom{r}{s}u_1^{(r-s)} \sum_{q=0}^{s} \binom{s}{q}u_2^{(s-q)} w^{(q)} \qquad (134)$$

Extend again*:* let $w = u_3 u_4$, then

$$(u_1u_2u_3u_4)^{(r)} = \sum_{s=0}^{r} \binom{r}{s}u_1^{(r-s)} \sum_{q=0}^{s} \binom{s}{q}u_2^{(s-q)} \sum_{p=0}^{q} \binom{q}{p}u_3^{(q-p)}u_4^{(p)} \qquad (135)$$

Referring to (131), let

$$u_1 = (1-\eta^2)^{\frac{P+Q}{2}} \qquad (136)$$

$$u_2 = \left(1 + \frac{d}{2R_0}\,\eta\right)^{-(P-1)} \tag{137a}$$

$$u_3 = \left(1 - \frac{d}{2R_0}\,\eta\right)^{-Q} \tag{137b}$$

and

$$u_4 = e^{-\left(\frac{d}{2\sigma}\right)^2 \eta^2} \tag{138}$$

Then (131) can be written

$$f(\eta) = \left[1 - \left(\frac{d}{2R_0}\right)^2\right]^{\frac{P+Q}{2}} (u_1 u_2 u_3 u_4) \tag{139}$$

and

$$f^{(r)}(\eta) = \left[1 - \left(\frac{d}{2R_0}\right)^2\right]^{\frac{P+Q}{2}} (u_1 u_2 u_3 u_4)^{(r)} \tag{140}$$

where (135) can be used directly. Differentiating the u_i is far more manageable. Manually obtaining about five or six orders of differentiation, each evaluated at $\eta = 0$, reveals recursive patterns from which expressions for the direct evaluation of $u_i^{(r)}(0)$ can be written.

For u_1 (note this is an even function on [-1,1], so all odd derivatives at $\eta = 0$ will vanish):

$$u_1^{(r)}(0) = \{1 - (r - [\tfrac{r}{2}]2)\}\ (-1)^{r/2} \frac{r!}{(r/2)!} \bullet \zeta(\zeta-1)(\zeta-2) \cdots (\zeta - [\tfrac{r-1}{2}]) \tag{141}$$

where again $[(\cdot)] \equiv$ largest integer $\leq (\cdot)$,

$$\zeta = \frac{P+Q}{2} \tag{142}$$

and

$$\{\bullet\} = 1, \text{ for } r \text{ even}$$
$$= 0, \text{ for } r \text{ odd} \tag{143}$$

For u_2 and u_3:

$$u_2^{(r)}(0) = \left(\frac{d}{2R_o}\right)^r \mu(\mu-1)(\mu-2) \cdots (\mu-r+1), \quad \text{for } r \geqq 1$$
$$=1, \text{ for } r=0 \tag{144}$$

where

$$\mu = -(P-1) \tag{145}$$

and

$$u_3^{(r)}(0) = \left(-\frac{d}{2R_o}\right)^r \nu(\nu-1)(\nu-2) \cdots (\nu-r+1), \quad \text{for } r \geqq 1$$
$$= 1, \text{ for } r=0 \tag{146}$$

where

$$\nu = -Q \tag{147}$$

Finally, for u_4 (also an even function on [-1,1])

$$u_4^{(r)}(0) = \{1-(r-[\tfrac{r}{2}]2)\ (-1)^{r/2} \frac{r!}{(r/2)!} \left(\frac{d}{2\sigma}\right)^r \qquad (148)$$

where $[r/2] \equiv$ largest integer $\leq r/2$, as before, and the factor in braces was defined by (143).

Examples of the Clutter

Figures 8, 9 and 10 show the magnitude and the phase of the clutter cross-power correlation for combinations of cosine-squared and cosine-fourth antenna patterns as a function of the antenna spacing. The curves are obtained by computing (126) for the values shown, and then normalizing by the factor

$$\frac{\sqrt{\hat{\kappa}}}{\sqrt{2\pi}\ \sigma R_0^2}$$

from (50) and the factor $e^{j\omega_0(\tau_1-\tau_2)}$. In the legend, PW is the pulse-width and CCT is the clutter correlation time.

Noting the phase (dashed line), the curves are seen to have a damped cosinusoidal character. (Recall that the asymptotic form of the J Bessel function for large argument is cosinusoidal [27:(9.2.1)].) The in-phase peaks of these curves are seen to be spaced at intervals of one foot, which is equal to one wavelength, for the second and succeeding peaks. These peaks arise from the beating of the Bessel functions in (126). Their argument is $2k_0 d = 4\pi d/\lambda_0$. Beginning with the second peak (the first one for nonzero d), it can be seen that 180° phase peaks occur when d is increased by integer multiples of λ_0 and zero phase peaks occur when d is increased by odd integer multiples of $\lambda_0/2$.

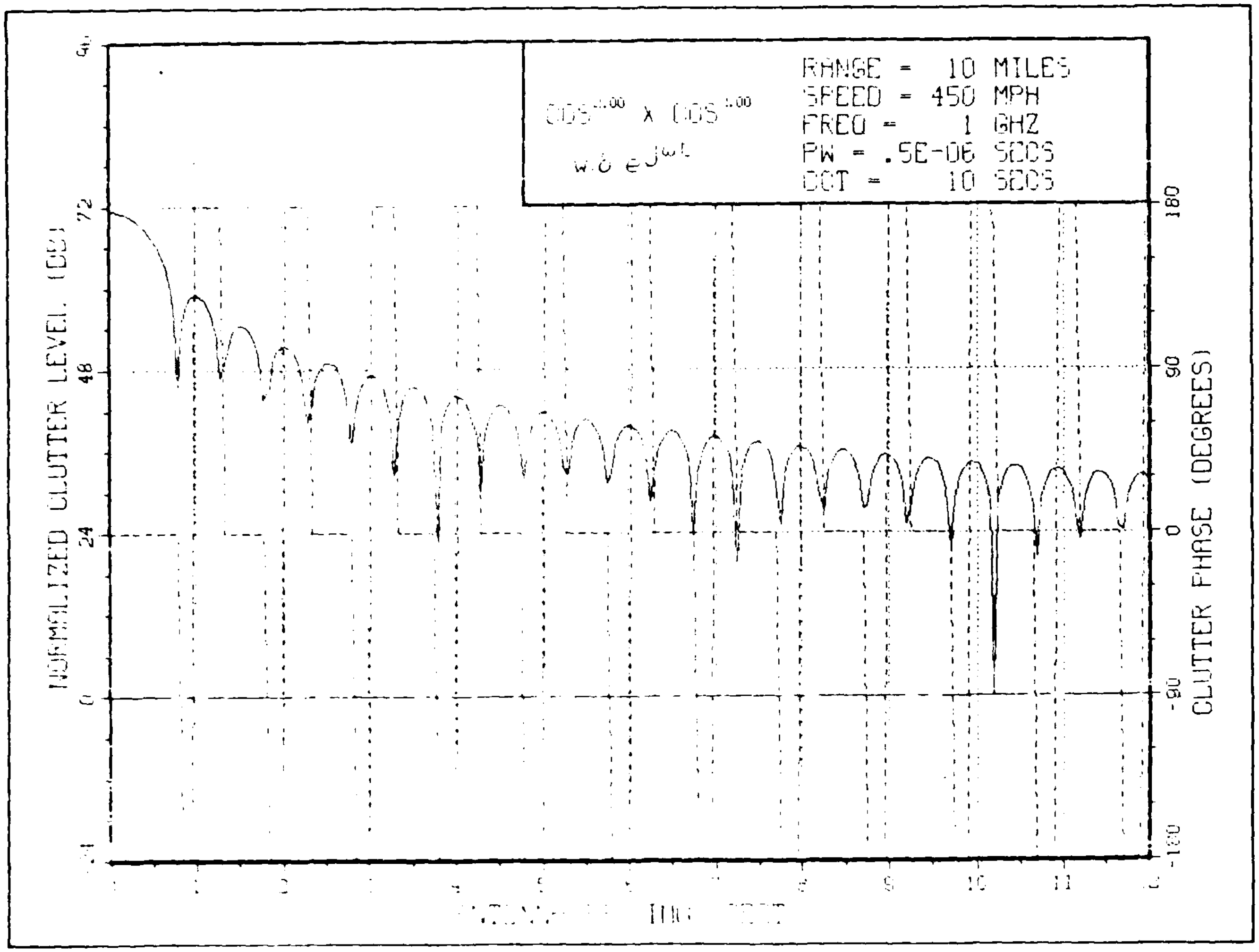

Figure 8. Magnitude (solid) and Phase (dashed) of the Clutter Cross-Power Correlation for Cos^2 by Cos^2 Cross-Products

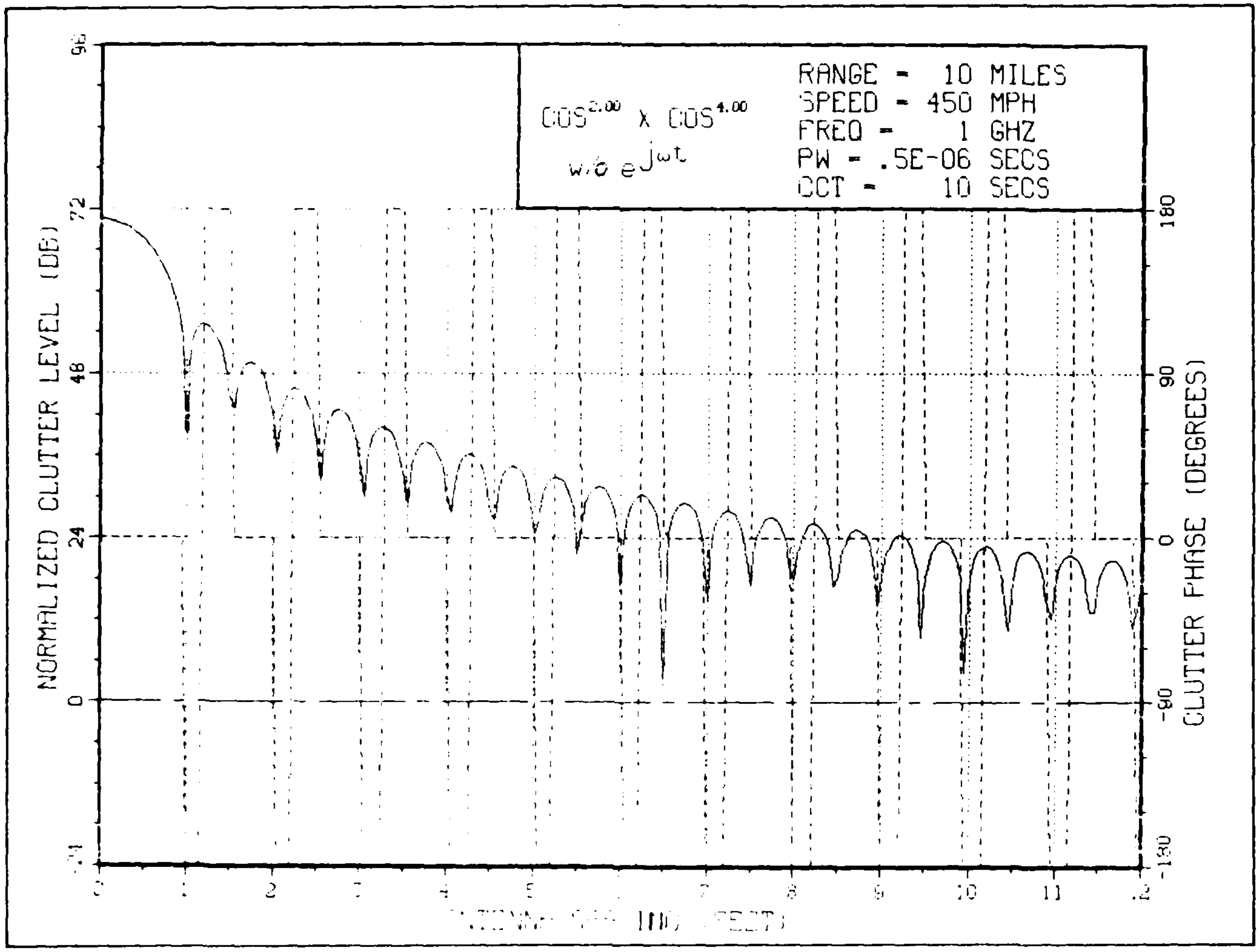

Figure 9. Magnitude (solid) and Phase (dashed) of the Clutter Cross-Power Correlation for Cos^2 by Cos^4 Cross-Products

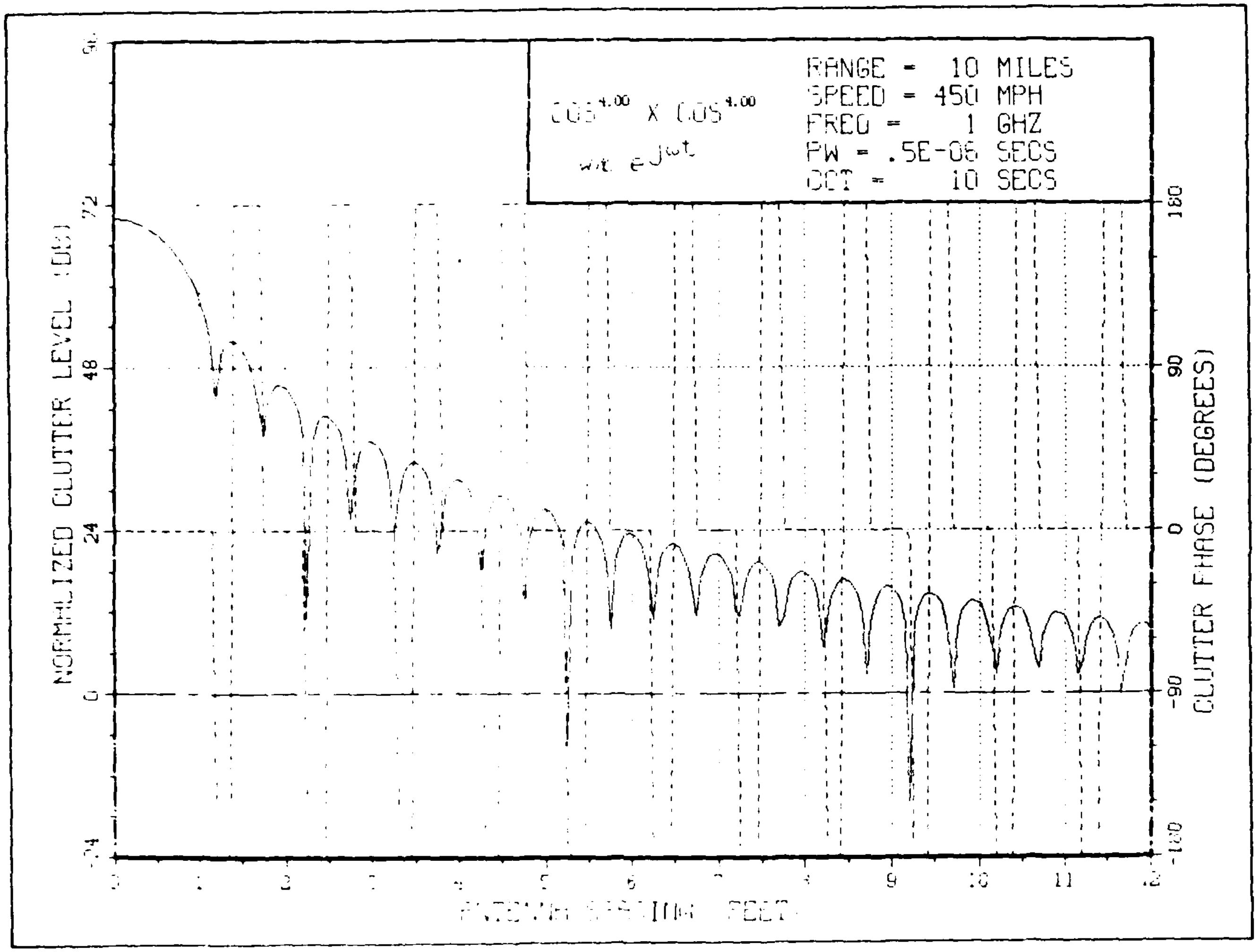

Figure 10. Magnitude (solid) and Phase (dashed) of the Clutter Cross-Power Correlation for Cos^4 by Cos^4 Cross-Products

Abstract of the Computer Analysis

An algorithm for the machine computation of the clutter cross-power terms was developed using (126) with (141) through (148) for the factors $f^{(r)}(0)$. The same was done for the target signal vector using (50), (53), (54) and (127a). Note from (48) and (58) the target has essentially the same albedo as a point of clutter.

An algorithm for the computation of the optimum weights was developed following the procedure outlined in Appendix B for the solution of the eigenproblem. A computer analysis was then performed. The results are presented in the next chapter.

IV. Analysis Of MASAR Performance

The analysis of the performance of MASAR is presented here. The performance is investigated for varying number of antennas, antenna beamwidths, number of pulses per antenna, time delay between synthetic apertures, and clutter decorrelation times.

An Overview of the Analysis Procedure

The performance is analyzed in three ways. First, the relative improvement of MASAR is examined. The improvement is defined as the ratio of the processed and unprocessed target to clutter power; i.e., the ratio of the target to clutter power ratios at the output and input to the MASAR processor. The relative improvement is defined as the ratio of the improvement obtained with the optimum processor to the improvement obtained with the target or binomial processors.

Second, the response of MASAR is examined with regard to a target which has a speed and track angle identical to the presumed target but which is positioned at azimuths which differ from the presumed azimuth. As will be seen, the direction of the effective MASAR antenna pattern mainlobe--the boresight--is automatically set by the optimum weights to the target's presumed azimuth. This part of the analysis is called "the off-boresight response to a target moving at the presumed velocity."

Third, the response of the optimum MASAR processor is examined with regard to another target which is in the vicinity of the presumed target. The velocity of this target varies from that of the presumed target. This part of the analysis is called "the response to other boresight targets."

The Cases for the Analysis

The cases for which the MASAR performance is analyzed are enumerated in Table I. There are twenty. These cases are designed to examine the performance of MASAR as a function of the parameters discussed in the opening to this chapter.

For each case, the clutter cross-power correlation matrix is generated with (126), (140) through (148) and (135). The clutter is defined by the following ten parameters:

a. radar operating frequency = 1 GHz,

b. pulsewidth = 0.5 μsec,

c. radar platform velocity = 450 mph,

d. range = 10 miles,

e. number of MASAR antennas,

f. number of pulses per antenna (number of synthetic elements per array),

g. pulse repetition frequency (PRF; see Appendix C for how this is chosen),

h. interantenna pulse spacing factor,

i. antenna patterns,

and,

j. temporal clutter correlation interval (also called the decorrelation interval).

Table I shows the values of the last six parameters listed above for each case. Henceforth, specific cases are referenced by their number shown in this table. The purpose of each case is discussed below.

Table I

Cases Used to Analyze MASAR Performance

Case Number	Number of Antennas	Number of Pulses per Antenna	PRF (Hz)	Inter-antenna Pulse Spacing Factor	Antenna Patterns (Powers of Cosine)	Clutter Correlation Interval (seconds)
1	2	8	2640	0	0,2	10
2	↓	15	↓	↓	↓	↓
3	↓	25	↓	↓	↓	↓
4	↓	8	↓	↓	2,4	↓
5	↓	15	↓	↓	↓	↓
6	↓	25	↓	↓	↓	↓
7	↓	12	↓	↓	↓	↓
8	3	8	3960	↓	2,4,6	↓
9	↓	↓	↓	2	↓	↓
10	↓	↓	↓	4	↓	↓
11	4	6	5280	0	2,4,6,8	↓
12	2	12	2640	↓	6,8	↓
13	3	8	3960	↓	4,6,8	↓
14	↓	↓	↓	↓	↓	1
15	↓	↓	↓	2	↓	↓
16	↓	↓	↓	4	↓	↓
17	↓	↓	↓	0	2,4,6	0.01
18	↓	↓	↓	2	↓	↓
19	↓	↓	↓	4	↓	↓
20	4	6	5280	0	2,4,6,8	↓

Cases 1 through 13 have a temporal clutter correlation interval of ten seconds. This is much longer than the MASAR observation interval (time from first to last processed pulse) of any Case.

Cases 1 through 6 were selected to observe MASAR performance for two antennas, varying only their beamwidths and number of pulses. Cases 1, 2 and 3 each employ isotropic and cosine-squared antenna patterns. They differ only in the number of pulses used in generating the synthetic apertures. Cases 4, 5 and 6 differ from the first three only by exchanging the isotropic pattern for a cosine-fourth power pattern to simulate the effect of a narrower beamwidth.

Cases 7 through 20 have a constant processing interval. This equals the total number of pulses processed: the number of antennas times the number of pulses.

Cases 7, 8 and 11 were chosen to observe MASAR performance as antennas are added, each having a narrower beamwidth. Cases 12, 13 and 11 were selected for the same purpose, but each added antenna has a broader beamwidth.

Cases 8, 9 and 10 each employ the same antennas and number of pulses except the time between the generation of each synthetic aperture is increased. Following (1), with M = 3, the synthetic apertures are spaced by one interpulse period in Case 8, by seven interpulse periods in Case 9, and by 13 interpulse periods in Case 10. The intent here is to observe performance as the effective time delay between synthetic aperture "looks" is increased. The target moves farther, but the clutter decorrelates more, as this delay is increased. Cases 14, 15 and 16 are for the same purpose, but the temporal clutter correlation time is shortened to 1 second. Cases 17, 18 and 19 repeat the experiment a

third time, but with a temporal clutter correlation time of 0.01 second; the order of the observation interval. Obviously, these three sets of cases can also be used to observe MASAR performance as the clutter decorrelates more rapidly.

Case 20 is the same as Case 11, except the temporal clutter correlation interval is much shorter. They can be used together to observe the change in performance of a four antenna system as the clutter decorrelates more rapidly. Case 20 can also be compared with Case 17 to observe the change in performance between a three and four antenna system, holding the processing interval constant, with rapid clutter decorrelation.

MASAR Relative Improvement

For this analysis, improvement is defined as

$$I = \frac{r_0}{r_i} \tag{149}$$

where r_i is the target to clutter power ratio at the input to the MASAR processor, and

where r_0 is the target to clutter power ratio at the output of the MASAR processor; i.e.,

$$r_0 = \frac{|w_p^\dagger a|^2}{w_p^\dagger B w_p} \tag{150}$$

where w_p is the weight vector used in the MASAR processor.

AD-A101 143 AIR FORCE INST OF TECH WRIGHT-PATTERSON AFB OH SCHOO--ETC F/G 17/9
MULTIPLE ARRESTED SYNTHETIC APERTURE RADAR.(U)
MAY 81 J S SHUSTER
UNCLASSIFIED AFIT/DS/EE/81-3 NL

2 OF 5
AD A
101143

Three different processors are considered: the optimum processor, which employs the weight vector w_D; the target processor which employs the weight vector w_T; and the binomial processor, which employs the weight vector w_B. The optimum and target weights are tabulated in Appendix E for selected cases from Table I.

The optimum weights, w_D, are determined as described in the section on the optimization procedure in Chapter II, pages 11-12 (also, their computation is discussed in Appendix B). Recall that, for a given target, these are the weights which maximize the target to clutter power ratio; i.e., they form the eigenvector that corresponds to the dominant eigenvalue of the eigenproblem characterized by (3), with $A = aa^{\dagger}$.

A "smart, ad hoc" design for MASAR is to phase the elementary antenna pulse returns so that the mainbeam of the net array is always steered to follow the target. This is precisely what the target weights do. The target weights, w_T, are simply the target signal; i.e.,

$$w_T = a \tag{151}$$

The use of w_T causes all the target signal returns to be summed in phase; consequently, the processed target power becomes

$$TP = |w_T^{\dagger} a|^2 = |a^{\dagger} a|^2 \tag{152}$$

Note, from (8), it can be seen that the target weights are <u>optimum</u> for the special case where the clutter cross-power correlation matrix is an <u>identity</u> matrix. Recall, from page 23, that the main diagonal of B comprises all the clutter cross-power correlation terms of antenna m in position n with itself ($1 \leq m \leq M$, $1 \leq n \leq N$). Then this special case

occurs when the clutter has an extremely short temporal correlation interval; e.g., from (58), when $T << (\tau_1 - \tau_2)^2$, though the clutter need not be spatially uncorrelated.

The binomial weights, w_B, simulate a multiple M-pulse canceller [3:328] for an M-antenna MASAR. The returns from the M antennas at each of the N synthetic positions are weighted by the binomial coefficients obtained from $(1-x)^{M-1}$. For example, for an M = 4 antenna, N = 2 pulse MASAR, the binomial weight vector becomes

$$w_B = (1\ \ -3\ \ 3\ \ -1\ \ 1\ \ -3\ \ 3\ \ -1)^T \tag{153}$$

where the superscript denotes the transpose.

Figuratively, the optimum weights make use of both the target and clutter information. The target weights make maximum use of the target information, but make no use of the clutter information. The binomial weights, as chosen here for an M-antenna MASAR, effectively form an M-stage, synthetic aperture, clutter canceller and make no use of the target information.

In order to obtain the unprocessed target to clutter power ratio, the unprocessed weighting vector--the weighting vector at the input to the MASAR processor--must be described. But, there is no logical way to do this. Any attempt to do so results in some sort of preprocessor which affects the target or the clutter power in some non-uniform way.

To avoid this difficulty, only the improvement of the optimum processor relative to the target and binomial processors is discussed here. The improvement of the optimum processor relative to the target processor is defined

$$I_{D/T} = \frac{I_D}{I_T} = \frac{(r_0)_D}{r_i} \div \frac{(r_0)_T}{r_i} = \frac{(r_0)_D}{(r_0)_T}$$

$$= \frac{w_D^\dagger A w_D}{w_D^\dagger B w_D} \div \frac{w_T^\dagger A w_T}{w_T^\dagger B w_T} \tag{154}$$

Similarly, the improvement of the optimum processor relative to the binomial processor is

$$I_{D/B} = \frac{(r_0)_D}{(r_0)_B} = \frac{|w_D^\dagger a|^2}{w_D^\dagger B w_D} \div \frac{|w_B^\dagger a|^2}{w_B^\dagger B w_B} \tag{155}$$

Additionally, to provide a reference datum for each case, the improvement of the optimum processor relative to itself when tuned to a fixed target is presented:

$$I_{D/Z} = \frac{(r_0)_D}{(r_0)_D|_{v_T = 0}} \tag{156}$$

Figures 11 through 30 depict these relative improvements for each of the twenty cases shown in Table I, page 67, respectively. Each curve depicts the relative improvement for on-boresight targets moving at the speeds shown along a 180 degree track (see in Figure 4, p.31) which is aligned with the perpendicular bisector of the MASAR observation interval. $I_{D/Z}$, $I_{D/T}$, and $I_{D/B}$ are depicted by the solid, broken and dashed curves, respectively. Each curve is formed by connecting the relative improvement at each three mile per hour increment by straight lines. No attempt is made to fit a smooth curve through the points.

What is of interest, here, is how the improvement varies as the system and clutter parameters vary. The system parameters that are

varied are the number of antennas, the number of pulses, the antenna beamwidths, and the effective time delay between synthetic apertures. (The PRF is varied too, but as a function of the number of antennas; see Appendix C.) The only clutter parameter that can be varied is the temporal clutter correlation interval.

Before addressing the improvement as a function of each of these parameters, some general observations will be made which are applicable to almost all the improvement curves.

First, for all cases, the performance of the optimum weights is seen to be everywhere better than or equal to the performance of the other two weighting schemes. As the target speed aproaches zero, the binomial weighting scheme does as its designed to do, which is to "cancel out" anything that doesn't move. Unfortunately, it tends to cancel out very slowly moving targets as well. This explains the sharp rise in $I_{D/B}$ as the target speed approaches zero.

As shown by the very close proximity of the $I_{D/T}$ (broken) and $I_{D/Z}$ (solid) curves in most cases, the target to clutter power ratio out of the target processor is virtually constant over all target speeds--nearly equaling that of the optimum processor tuned to a fixed target.

However, exceptions to this occur when the inter-SAR spacing is increased; i.e., when the inter-antenna pulse spacing factor is increased, which effectively increases the time delay between synthetic aperture "looks." Examples of this are shown in Figures 19 and 20. This is discussed more quantitatively in the subsection entitled "Increased Inter-SAR Spacing."

The only other exceptions occur in Cases 1, 2 and 3 (Figures 11, 12 and 13) where an isotropic antenna pattern is used. In these cases,

the target to clutter power out of the target processor is, everywhere, between three to six decibels poorer than the optimum processor. This is a consequence of the choice of the PRF, the effects of which are discussed qualitatively in the first subsection, entitled "Increased Number of Pulses."

In the following subsections, observations are made from the relative improvement curves for all twenty cases to address the performance of MASAR as a function of the system/clutter parameters shown in Table I.

Increased Number of Pulses. Cases 1 to 3, as well as Cases 4 to 7, increase the processing interval by increasing the number of pulses. The relative improvements are shown in Figures 11 through 17, respectively.

Table II

Computed Values of the Target and Clutter Powers and Their Ratios for Target and Optimum Weights: Cases 1 Through 7

Case	N	$w_T^{\dagger}Aw_T$	$w_T^{\dagger}Bw_T$	$(r_o)_T$	$w_D^{\dagger}Aw_D$	$w_D^{\dagger}Bw_D$	$(r_o)_D$
		(all values in decibels)					
1	8	24.1	90.0	-65.9	56.2	117.8	-61.6
2	15	29.5	93.6	-64.1	55.9	114.8	-58.9
3	25	34.0	96.5	-62.5	54.2	110.8	-56.6
4	8	24.1	85.6	-61.5	34.0	95.3	-61.3
5	15	29.5	88.3	-58.8	26.5	85.1	-58.6
6	25	34.0	90.6	-56.6	30.6	87.1	-56.5
7	12	27.6	87.4	-59.8	45.5	105.1	-59.6

The apparent lack of overall improvement seen in these figures as the number of pulses increases is a consequence of the normalization. Effectively, all these curves are normalized to the output target to

clutter power ratio of the optimum processor tuned to a fixed target, $(r_0)_{D|v_T=0}$. This value is tabulated in the last column of Table II above.

Table II shows the actual computed values for the target and clutter powers and their ratios, in decibels, for both the target and optimum weights for Cases 1 through 7. The number of pulses per antenna, N, is also shown for each case.

Except for the values for the target weights for Cases 1 to 3 (to be discussed later), the following relationship can be observed in the values of the target to clutter power ratios--$(r_0)_T$ and $(r_0)_D$--for Cases 1 to 3 and 4 to 7, separately:

$$(r_0)_i - (r_0)_j = 10\log_{10}\left(\frac{N_i}{N_j}\right) \tag{157}$$

where r_0 is in decibels as shown in the table, and N_i and N_j are the number of pulses for cases i and j respectively. In other words, the target to clutter power ratio increases directly as a linear function of the number of pulses when all other parameters are held fixed.

However, looking at the target weighted target power by itself, the following relationship can be observed:

$$(w_T^\dagger A w_T)_i - (w_T^\dagger A w_T)_j = 20\log_{10}\left(\frac{N_i}{N_j}\right) \tag{158}$$

where the target powers are in decibels as shown in the table. That is, the target power out of the target processor increases directly with the square of the number of pulses. This follows directly from the expression for the target weighted target power derived in Appendix D, (D.21).

There, the target power is seen to have a (sin Nx/sin x) factor which reduces to a simple function of N^2 when $\theta = \theta_0 = 180^\circ$ and $v_T = 0$ (as is the present case).

Then, the target weighted clutter power must be a linear function of N in order for (157) to hold. Inspection of these values for the cases in Table II show this to be true; i.e.,

$$(w_T^\dagger B w_T)_i - (w_T^\dagger B w_T)_j = 10\log_{10}\left(\frac{N_i}{N_j}\right) \tag{159}$$

where the clutter powers are in decibels as shown in the table.

This is not observed for the target weighted clutter powers shown for Cases 1 to 3. Consequently, the values of $(r_0)_T$ for these cases do not follow (157). Qualitatively, the reason for this stems from the use of the isotropic antennas in conjunction with the choice of the PRF. The choice of the PRF causes the first grating lobes to be centered at the azimuthal extremities of the half-space (e.g., see Figures 31 and 32). The isotropic antenna "amplifies" the grating lobe clutter return which "aliases" [28:83] with the central clutter return, causing an adverse increase in the total clutter power. If the grating lobes were not present, the target processor clutter power would be correspondingly smaller and (157) through (159) would be satisfied for these cases. (See the discussion at the end of Appendix C for why the grating lobes are present.)

The reason the effect just discussed does not manifest itself in the optimum processor target to clutter power ratios for Cases 1 to 3 is because the optimum weights are tightly coupled to both the target and clutter returns. These weights strongly attenuate the grating lobe

return at 90 degress azimuth and strongly favor the return from the target at zero degrees azimuth. Thereby, they virtually offset the adverse effect of the grating lobes.

Because of the tight coupling of the optimum weights to both the target and clutter returns, the exact dependence of both the optimally processed target and clutter powers on the number of pulses is difficult to quantify. Nevertheless, the data shows that their ratio is a direct, linear function of the number of pulses.

The last point to address in this subsection is the reason for the interesting upward cusps seen in the $I_{D/B}$ curves. They clearly increase in frequency as the number of pulses increases.

This is easily explained with the aid of (D.27), the expression derived in Appendix D for the binomially weighted target power. First, note that the binomial weights generate a constant value for the clutter power as they are independent of the target speed. The variation in the binomially weighted target to clutter power ratio occurs only in the numerator--the target power being a function of the target location, speed and track angle as seen in (D.27). Since $f_{PRF} = 2Mv_R/\lambda_0$, $\dot{\theta}_T = 180^\circ$ and $\theta = 0^\circ$, the "array factor" in (D.27) reduces to

$$\left[\frac{\sin(N\pi \frac{v_T}{v_R})}{\sin(\pi \frac{v_T}{v_R})}\right]^2$$

Upward cusps appear in the $I_{D/B}$ curve whenever this factor goes to zero. That is, when $v_T = v_R/N$, or integer multiples thereof less than v_R. For v_R = 450 mph:

N	cusps appear when v equals integer multiples of (mph)
8	56.3
12	37.5
15	30.0
25	18.0

as can be observed in the $I_{D/B}$ curves.

Increased Number of Antennas. Cases 4 and 8 reveal a dramatic relative improvement is obtained with the optimum weights when advancing from a two to three antenna MASAR. For a three mph target, the performance of the optimum processor jumps from barely better than, to 17 dB better than its closest competitor--the target processor. Here, the number of pulses remains the same, but the processing interval increases from 16 to 24.

Comparing Case 11 (note the change in the scale of the ordinate) with the two just mentioned reveals an even greater relative improvement is obtained with the optimum weights and a fourth antenna, rising to nearly 44 dB better than the target weights for a three mph target. Here, two less pulses were used--though the processing interval is the same as for Case 8.

Increased Number of Antennas for Constant Processing Interval. Cases 7, 8 and 11 show that the performance of the optimum weights increases as the number of antennas is increased from two to three to four, respectively, while holding the processing interval constant. The added antenna in each case has a narrower beamwidth. For these cases, the performance of the optimum processor relative to the target processor--as two, three, and four antennas are used--is identical to that mentioned in the previous subsection.

Cases 12, 13 and 11 also show an increase in the performance of the optimum weights, yet the added antenna has a broader beamwidth. For these cases, the improvement of the optimum processor advances from 14 dB, to 33 dB, to 44 dB better than the target processor, respectively, for a three mph target. (Note the scale of the ordinate for Case 11 is larger than the others.)

From the results of this and the previous subsection, it can be seen that, regardless of the beamwidth, adding antennas--increasing the number of synthetic aperture "looks"--significantly increases the performance of the optimum processor relative to the other two processing schemes.

Narrower Antenna Beamwidth. In Cases 4 to 7, the cosine-fourth power antenna pattern is used instead of the isotropic pattern used in Cases 1 to 3. The other antenna remains the same--the cosine-squared pattern. A slight increase in the improvement is noticed in the optimum weights relative to the target weights, with the narrower beamwidth antenna. However, as can be seen in the displacement between the $I_{D/B}$ and $I_{D/T}$ curves, the binomial weights show significantly increased improvement with the cosine-fourth pattern. Since there is less clutter with which to contend, this is expected.

The more dramatic examples of the increased improvement with narrower beamwidths is observed between Cases 7 and 12, and between Cases 8 and 13. Case 12 consists of two antennas with narrower beamwidths than those of Case 7. The optimum processor for the three mph target is 14 dB better than the target processor for Case 12, whereas it is only a little better than equal for Case 7. Case 13 differs from Case 8 by only one antenna with a narrower beamwidth. Yet, the improve-

ment of the optimum processor for the three mph target is 33 dB better than the target processor for Case 13, which is 16 dB better than the relative improvement obtained in Case 8.

Faster Clutter Decorrelation and Increased Inter-SAR Spacing. The effects of faster clutter decorrelation (smaller T) and increased inter-SAR spacing (larger K) are so closely coupled that they are discussed together, here.

By comparing the relative improvement plots for Cases 8 and 17, it can be seen that the performance of the optimum weights declines with respect to the target and binomial weights. Although the optimum weights are superior in every case, it becomes increasingly more difficult to compensate for more rapidly decorrelating clutter with them. However, the performance of the target and binomial weights (as indicated by the vertical displacement between the broken and dashed curves) remains virtually constant. This is expected, since they are not functions of the clutter. These same observations can be made by comparing the improvement shown for Cases 9 and 18; for Cases 10 and 19 (when accounting for the added effect of increased inter-SAR spacing); as well as for Cases 11 and 20. (Again, note the change in scale along the ordinate for Figure 21, Case 11.)

The effects on relative improvement between the three weighting schemes as the inter-SAR spacing (i.e., the time delay between successive synthetic aperture "looks") is increased can be seen by comparing Cases 8 to 10 (where T = 10 seconds), Cases 14 to 16 (where T = 1 second), and Cases 17 to 19 (where T = 0.01 second). For the first, second and third cases in each set, the inter-SAR spacing, K, is

one interpulse period, seven interpulse periods and 13 interpulse periods, respectively.

Although the relative improvement of the optimum processor is superior for all moving targets, the performance of the target processor as well as that of the binomial processor, shows marked improvement relative to the optimum processor as K increases. For Case 16, where T = 1 and K = 13, the binomial processor is 26 dB better than the target processor, but 20 dB poorer than the optimum processor, for a 15 mph target (see Figure 25). For Case 19, where T = 0.01 and K = 13, the binomial processor is 7 dB better than the target processor and only 3 dB poorer than the optimum processor, for the 15 mph target (see Figure 29).

The target processor, in these two examples, gains on the binomial processor (in terms of relative improvement) by 46 - 10 = 36 dB. The target processor, as is already known (see page 70), becomes equivalent to the optimum processor when the clutter rapidly decorrelates. This becomes evident upon comparing the $I_{D/T}$ curves for the long inter-SAR spacing cases: Cases 10, 16 and 19. The $I_{D/T}$ curve clearly shows a trend of approaching the zero axis as the clutter correlation interval shortens. (Note that, of all 20 cases, the clutter decorrelates the most during the MASAR observation interval in Case 19. This case has the longest inter-SAR spacing and the shortest clutter correlation interval.)

The following discussion explains the cause of the downward cusps seen in the $I_{D/T}$ curves for Cases 10 and 16, and the dip in the curve in Case 19. (The cause of the upward cusp seen in the $I_{D/B}$ curves is explained in the subsection on "Increased Number of Pulses.") Notice

that the $I_{D/Z}$ curve rises smoothly from zero dB at zero mph to its value at 60 mph in Figures 20, 26 and 29. Then, the dip in the $I_{D/T}$ curve must be caused by an upward cusp in the target to clutter power ratio out of the target processor, at the corresponding target speed. This, in turn, can only be caused by either an upward cusp in the target-weighted target power or a dip in the target-weighted clutter power, or a combination of both.

However, consider (D.21), the expression derived in Appendix D for the target-weighted target power. With $\theta_0 = \theta = 0^\circ$, $\theta_T \doteq 180^\circ$ and $f_{PRF} = 2Mv_R/\lambda_0$, which are the parameter values used for this analysis, (D.21) reduces to the constant value N^2 for all target speeds (apply L'hospital's rule to both factors of (D.21)). Hence, there must be a dip in the target-weighted clutter power.

A general analytical expression for the target-weighted clutter power can be written; from (19) with (11), (32), and (151) with (30); as

$$w_T^\dagger B w_T = \sum_{n=1}^{N} \sum_{m=1}^{M} \sum_{p=1}^{N} \sum_{l=1}^{M} \alpha_n^m \alpha_p^{*l} \beta_{np}^{ml} \tag{160}$$

The existance of a dip might be ascertained if this expression could be reduced to a product of transcendental functions. Generally, the complexity of the clutter cross-power term, β_{np}^{ml}, makes this very difficult to do. However, if one chooses $\beta_{np}^{ml} = 1$ for all m, l, n and p, then, in a manner quite similar to the derivation of (D.21), one can obtain an expression for (160) which contains the factor

$$\frac{1+\cos\theta_0^{4M}-2\cos\theta_0^{2M}\cos[2\pi K\frac{v_T}{v_R}\cos(\theta_0-\theta_T)]}{1+\cos\theta_0^4-2\cos\theta_0^2\cos[2\pi\frac{K}{M}\frac{v_T}{v_R}\cos(\theta_0-\theta_T)]}$$

For $\theta_0 = 0^\circ$ and $\theta_T = 180^\circ$, this reduces to

$$\left[\frac{\sin(\pi K\frac{v_T}{v_R})}{\sin(\frac{\pi K}{M}\frac{v_T}{v_R})}\right]^2$$

which explains the dips in the clutter power. This factor has zeros at multiples of $v_T = v_R/K$, except at multiples of $v_T = Mv_R/K$ where it equals M^2. For v_R = 450 mph and the inter-SAR spacing of K = 13, the first zero occurs at v_T = 34.6 mph. This explains the behavior of the $I_{D/T}$ curves for Cases 10, 16 and 19, as well as in Cases 9, 15 and 18 where K = 7.

[Figures 11 through 30 follow on pages 84 through 103, respectively. The text continues, with the section on "The Off-Boresight Response to a Target Moving at the Presumed Velocity," on page 204.]

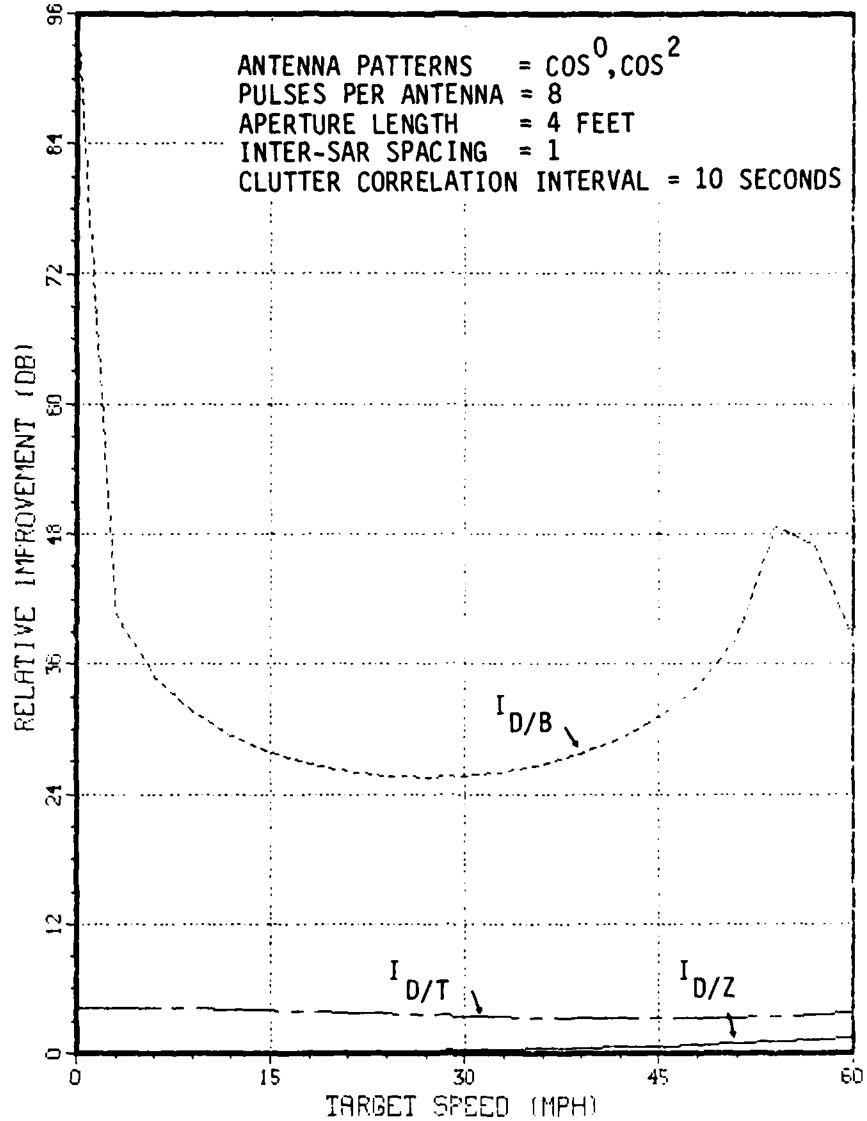

Figure 11. Relative Improvement for Case 1

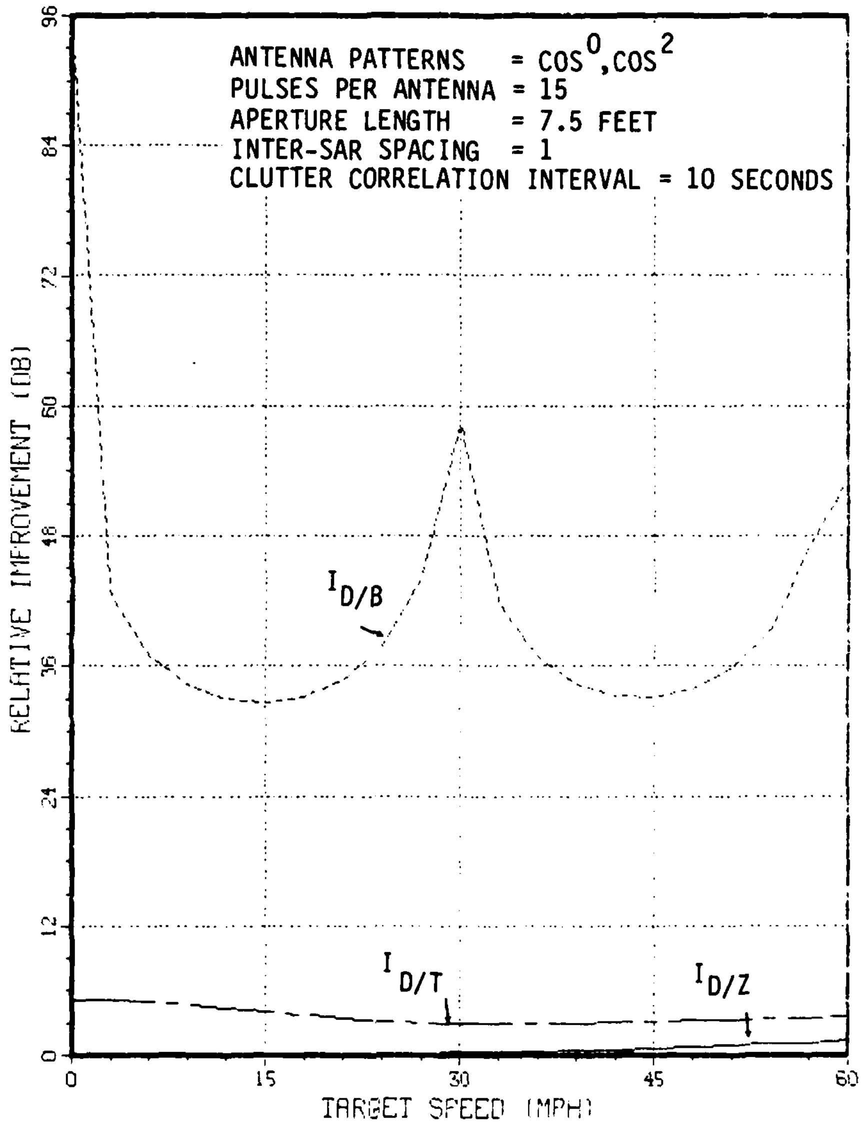

Figure 12. Relative Improvement for Case 2

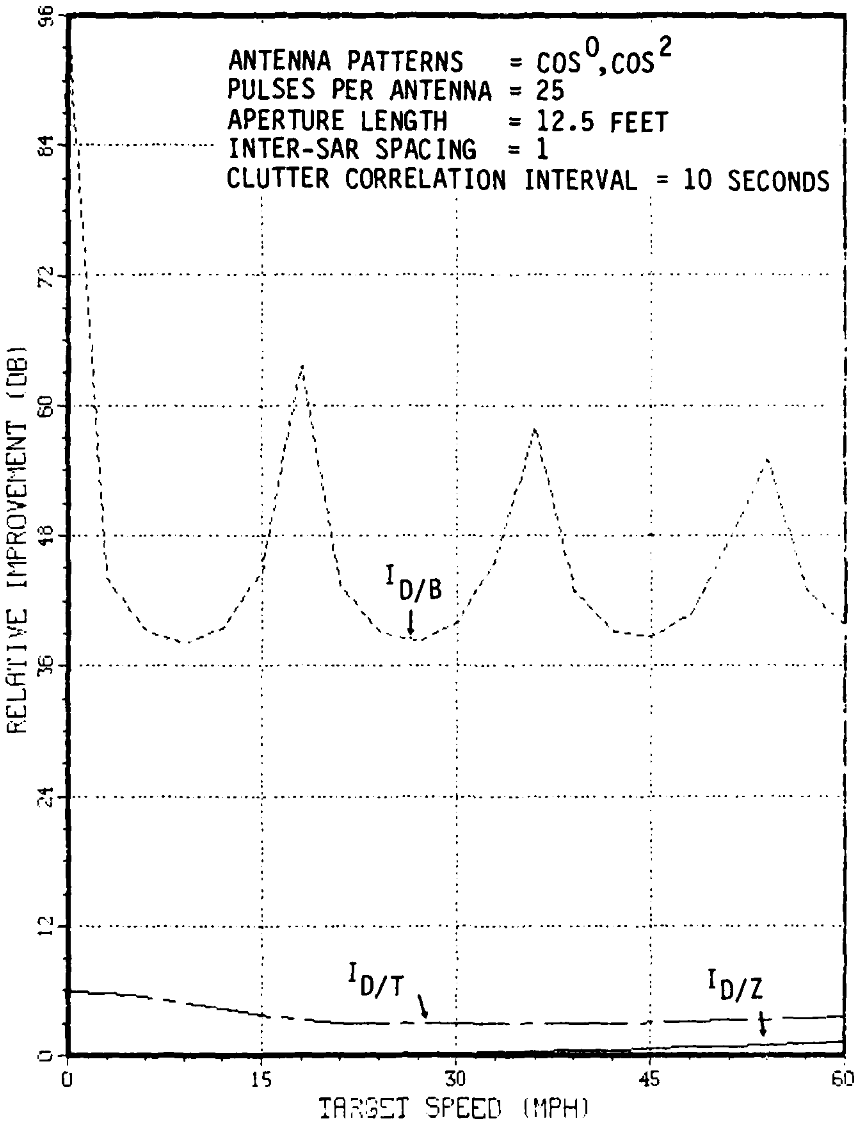

Figure 13. Relative Improvement for Case 3

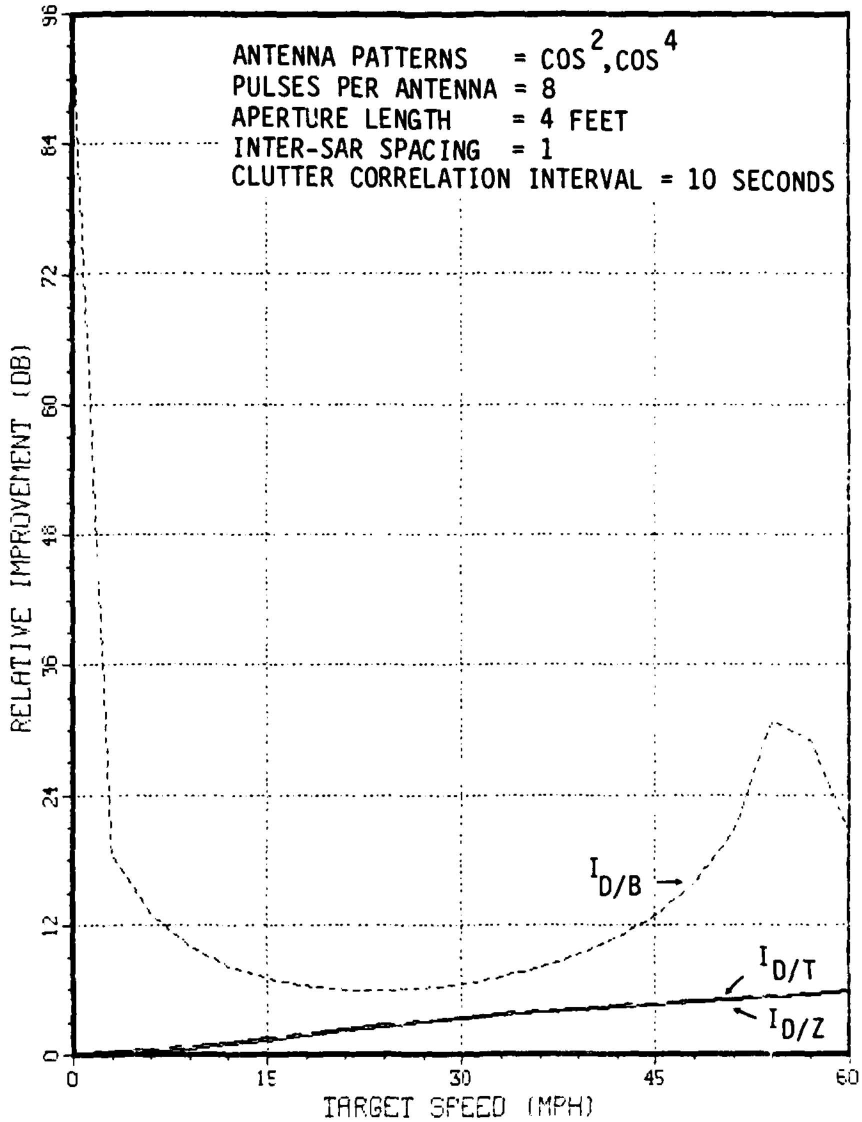

Figure 14. Relative Improvement for Case 4

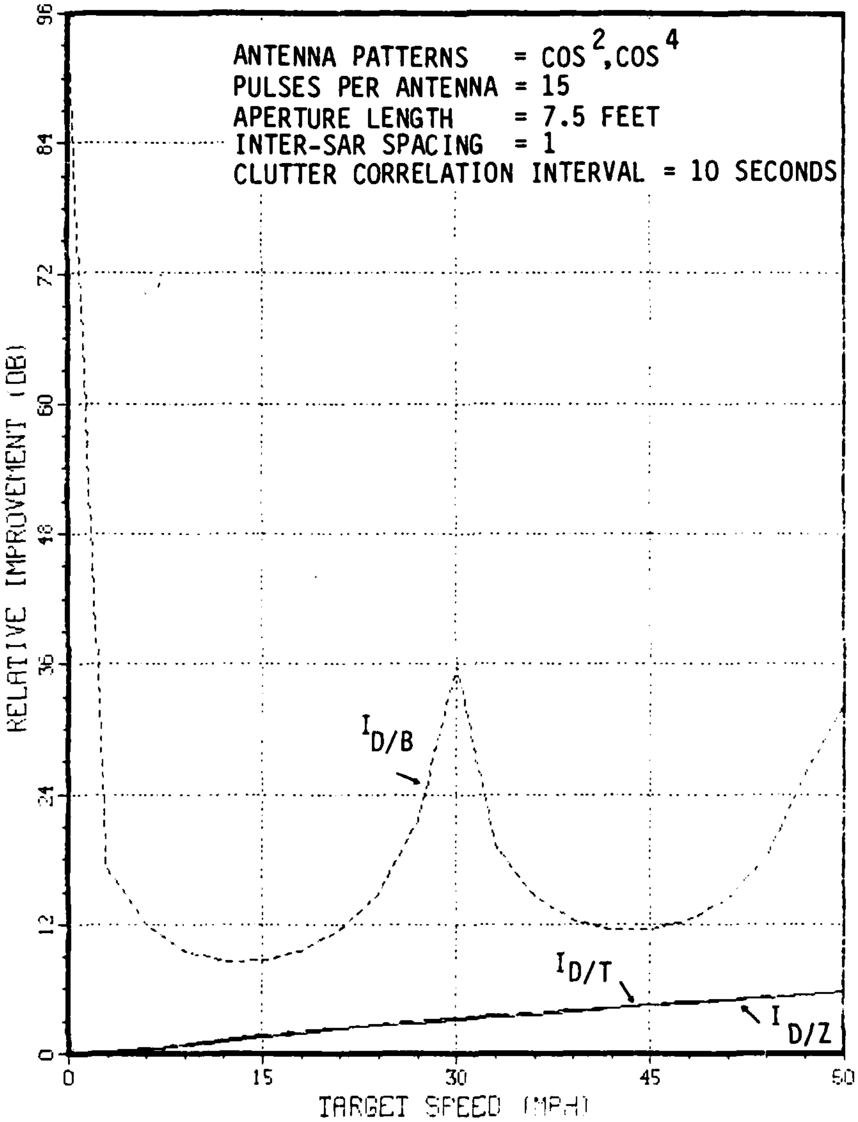

Figure 15. Relative Improvement for Case 5

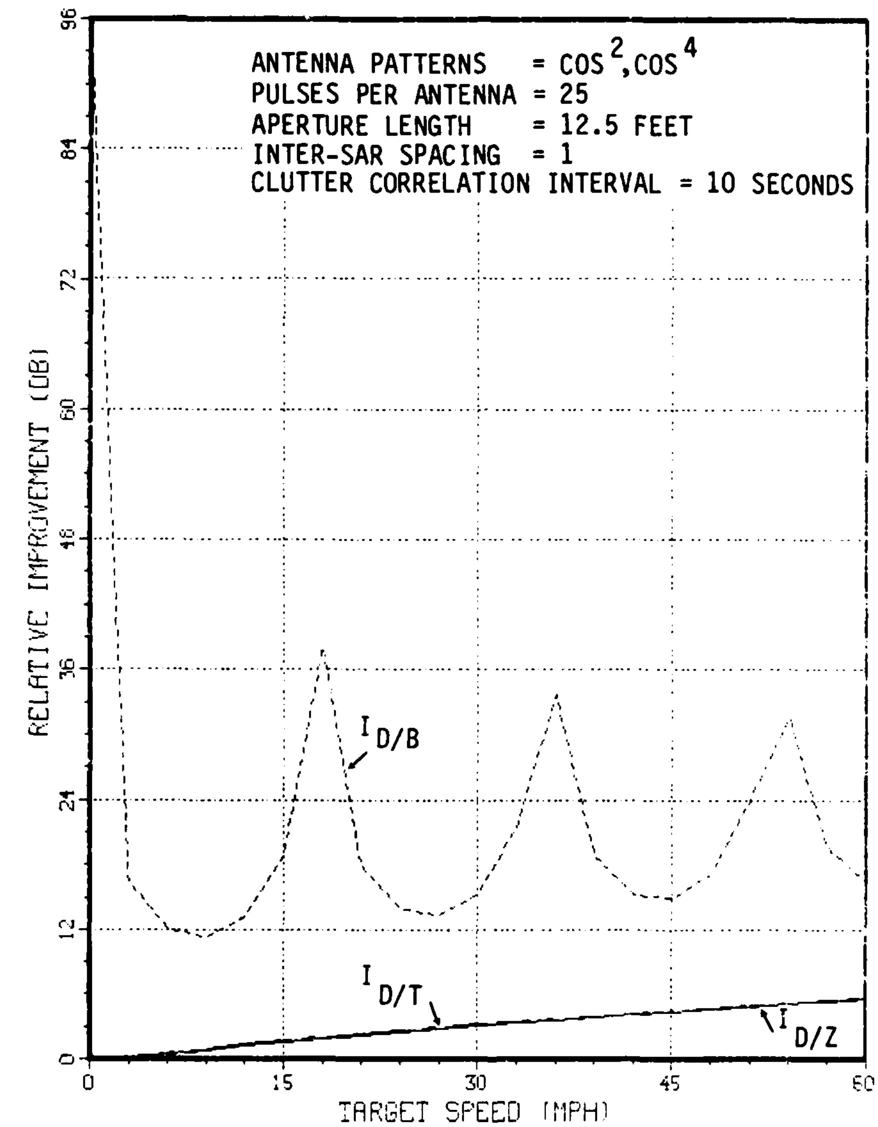

Figure 16. Relative Improvement for Case 6

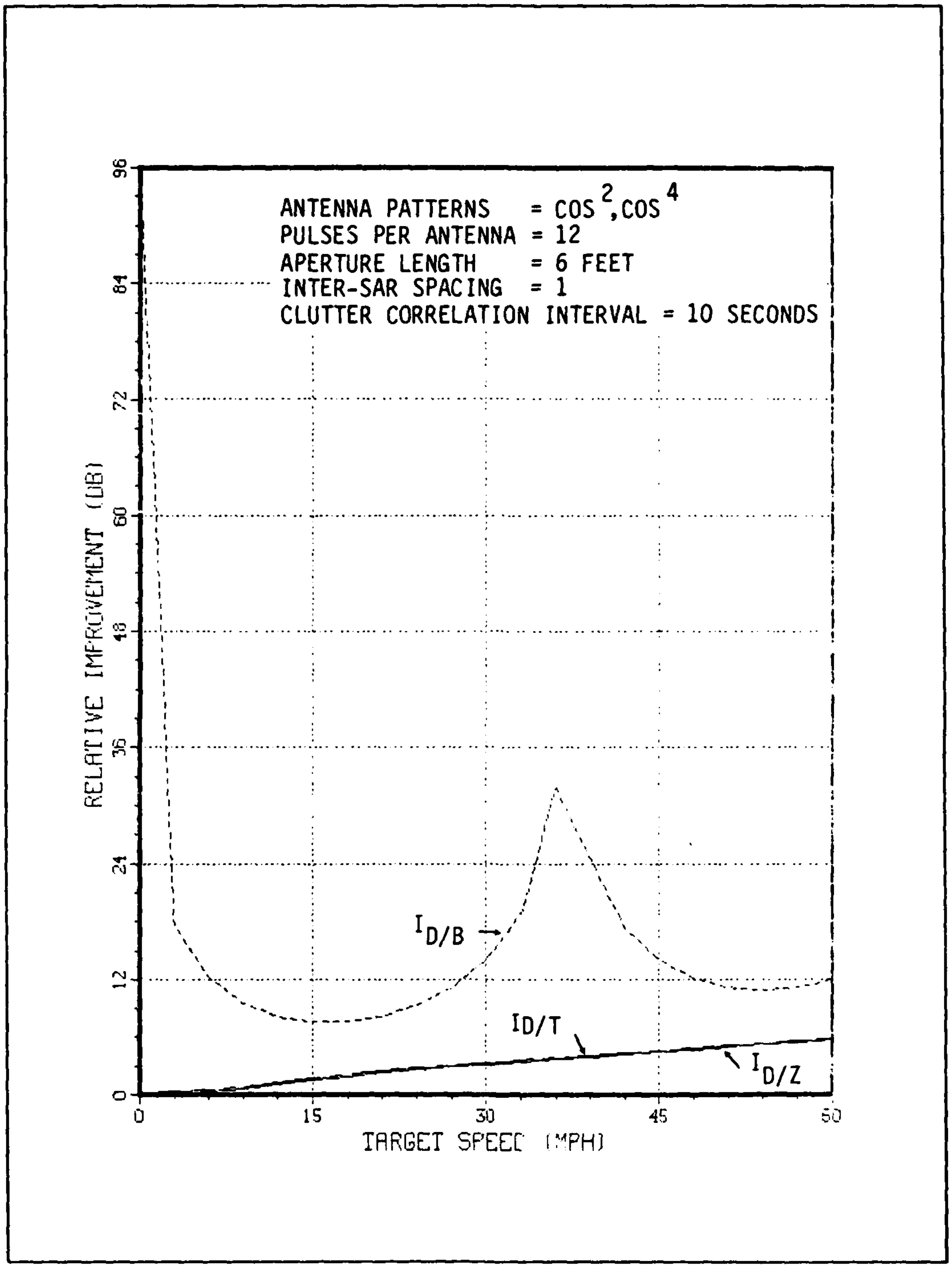

Figure 17. Relative Improvement for Case 7

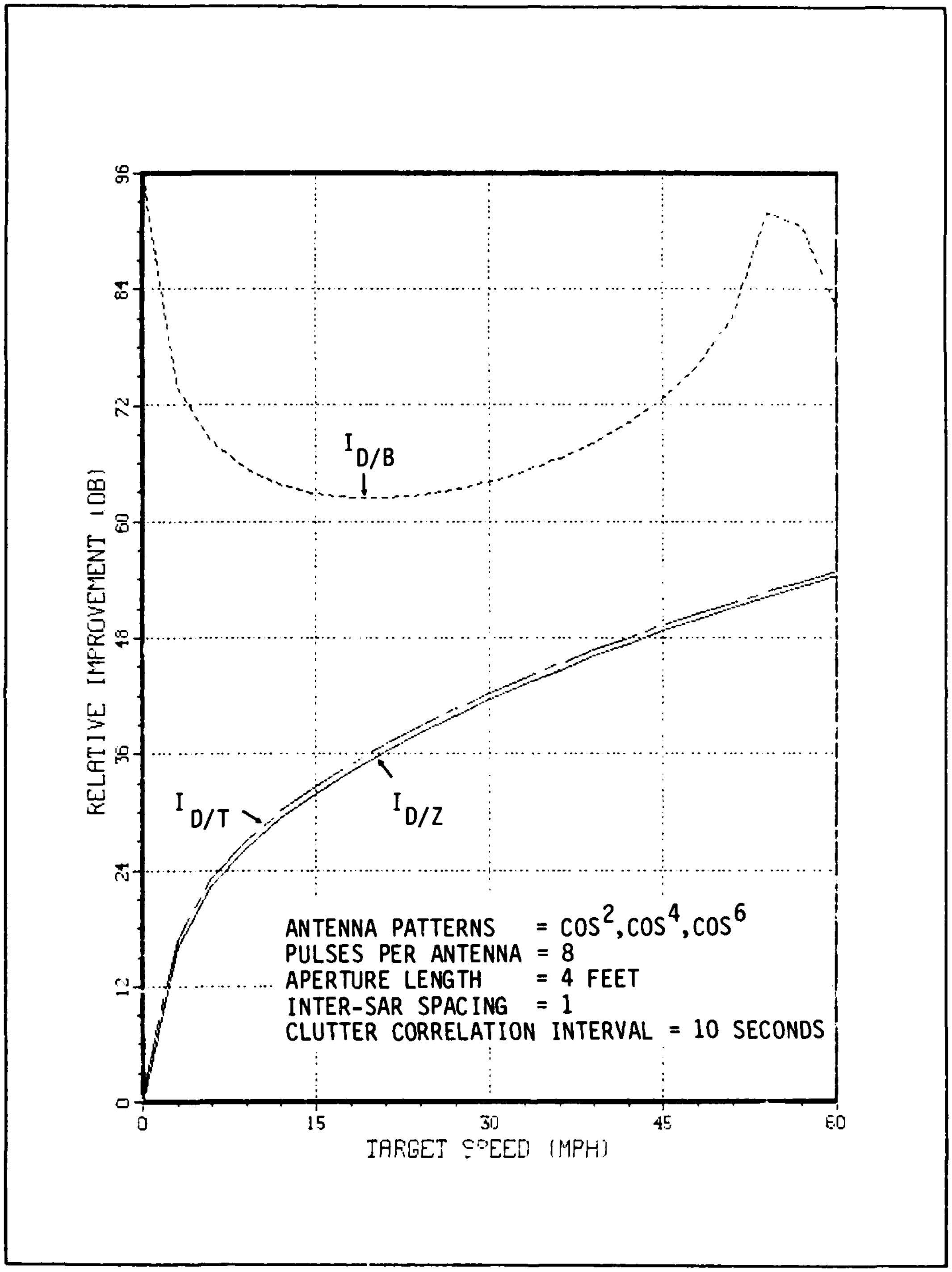

Figure 18. Relative Improvement for Case 8

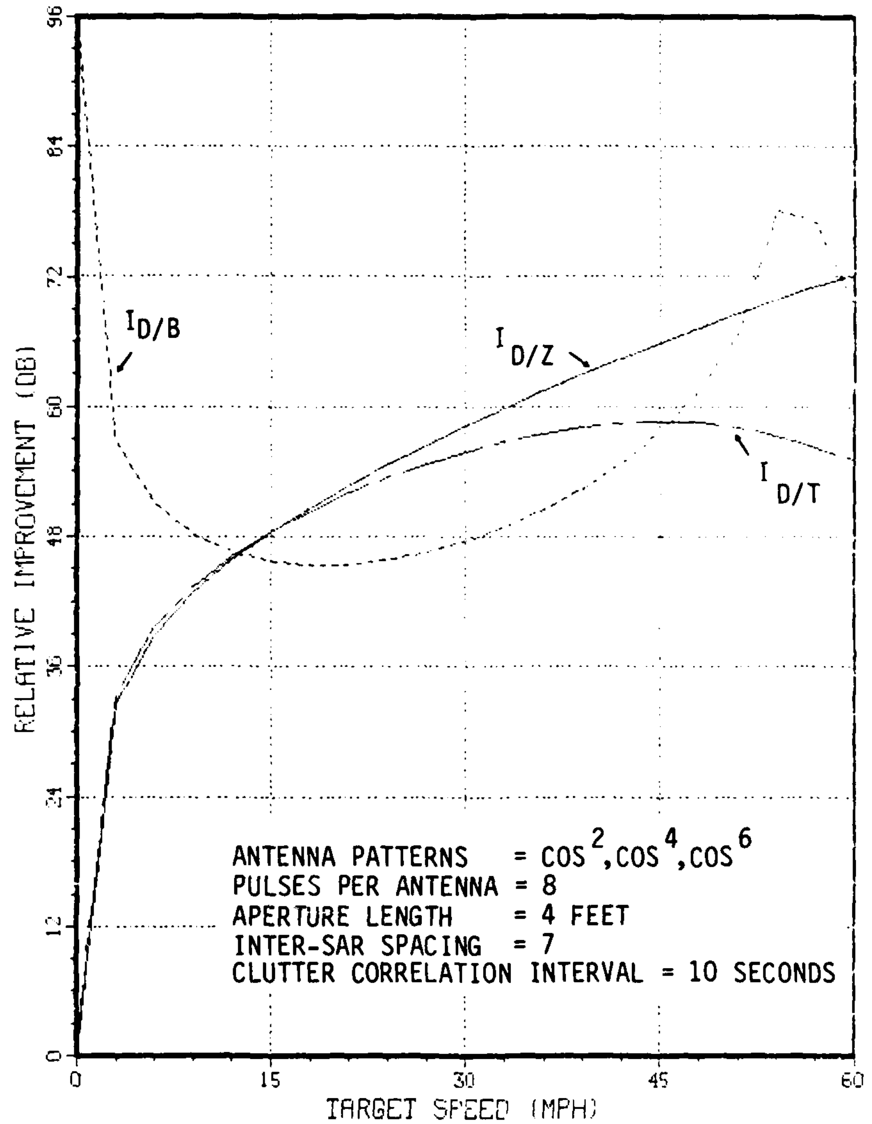

Figure 19. Relative Improvement for Case 9

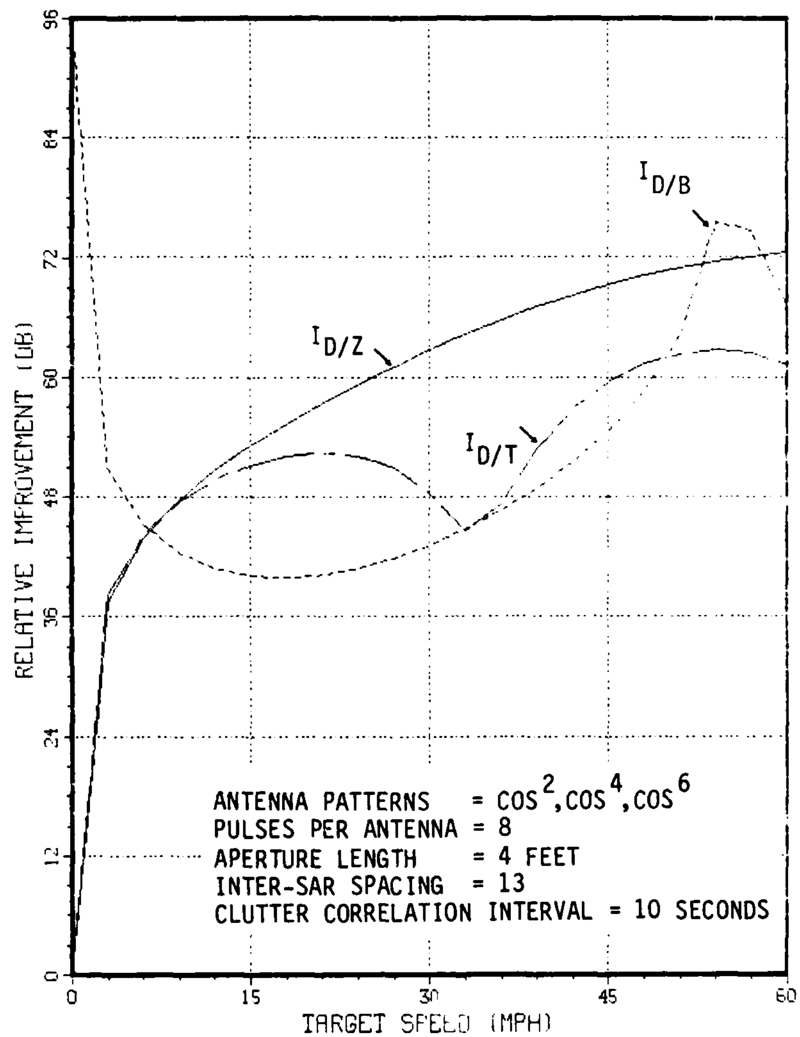

Figure 20. Relative Improvement for Case 10

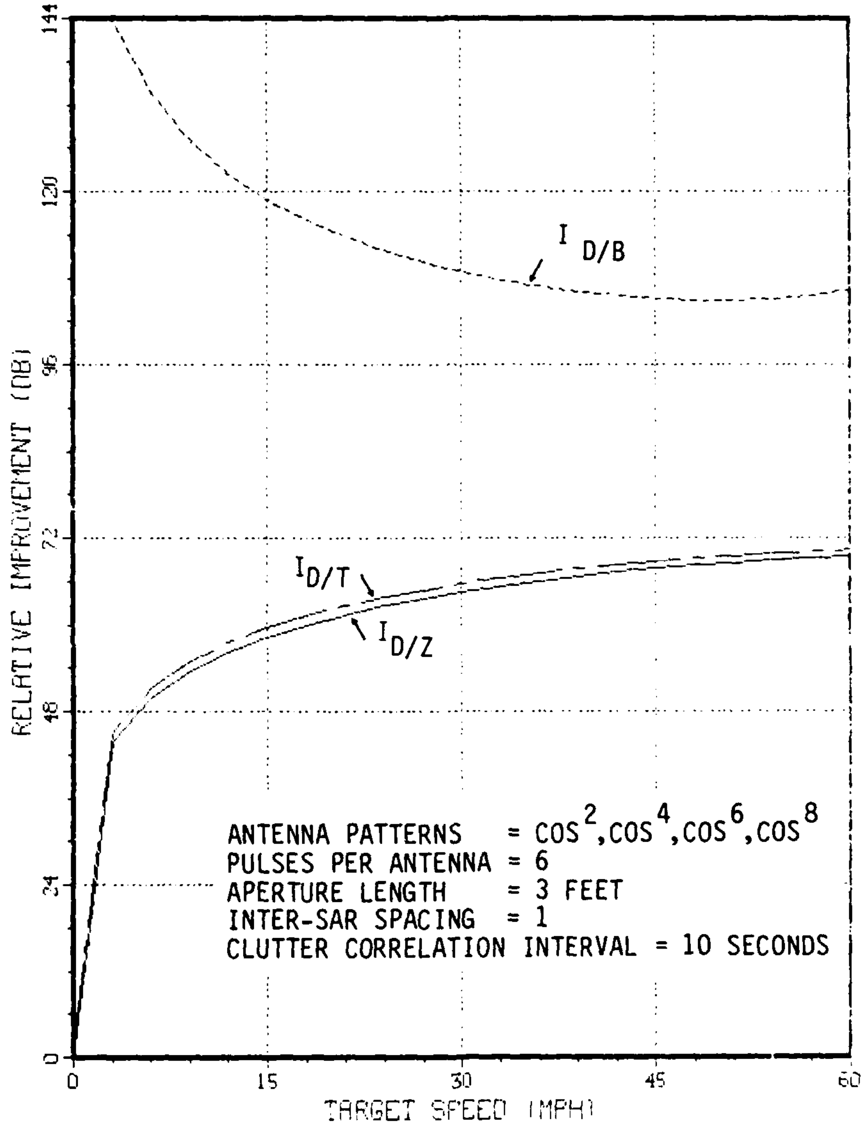

Figure 21. Relative Improvement for Case 11

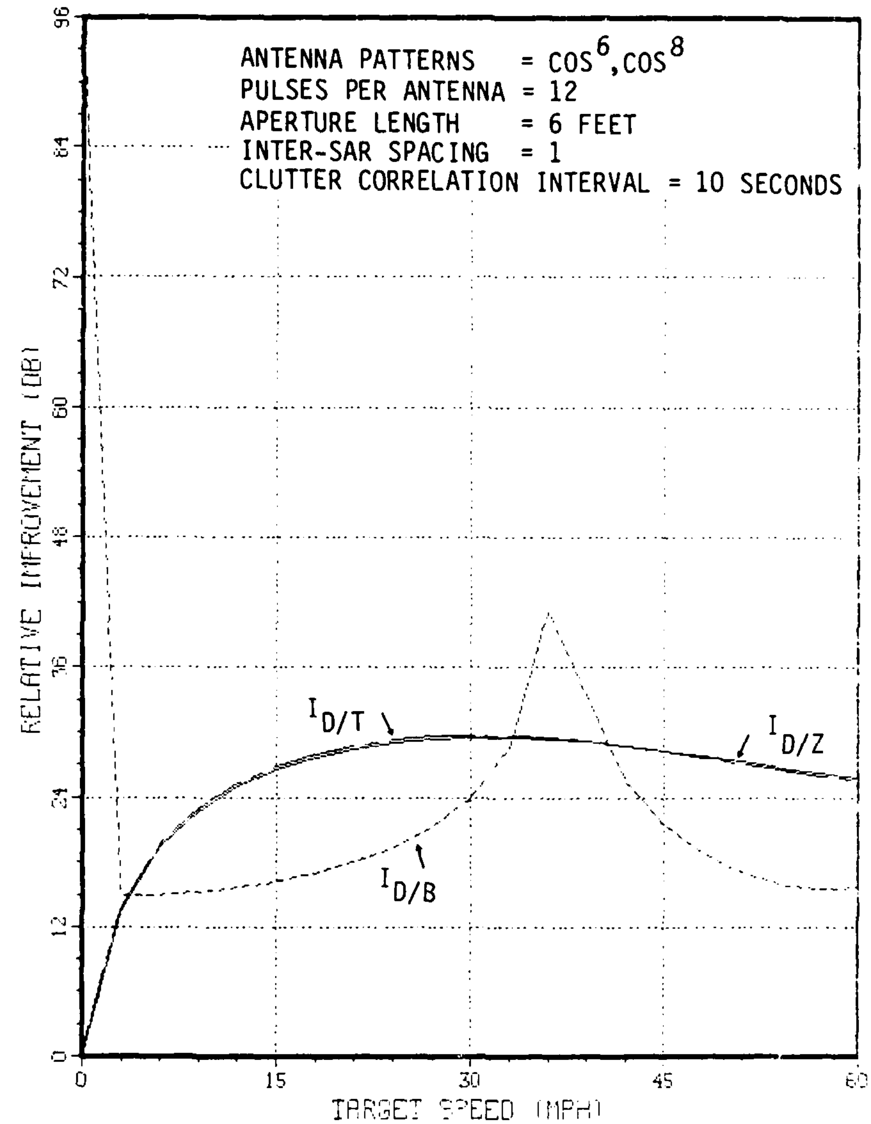

Figure 22. Relative Improvement for Case 12

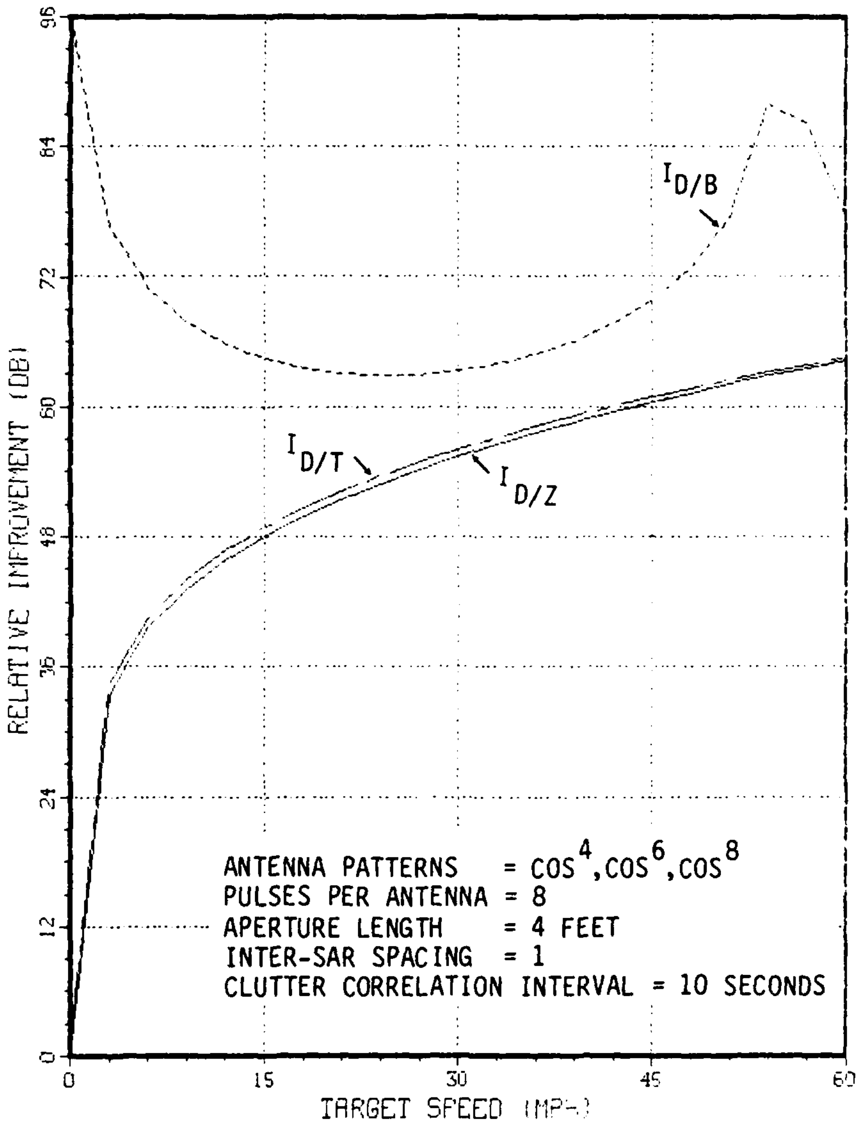

Figure 23. Relative Improvement for Case 13

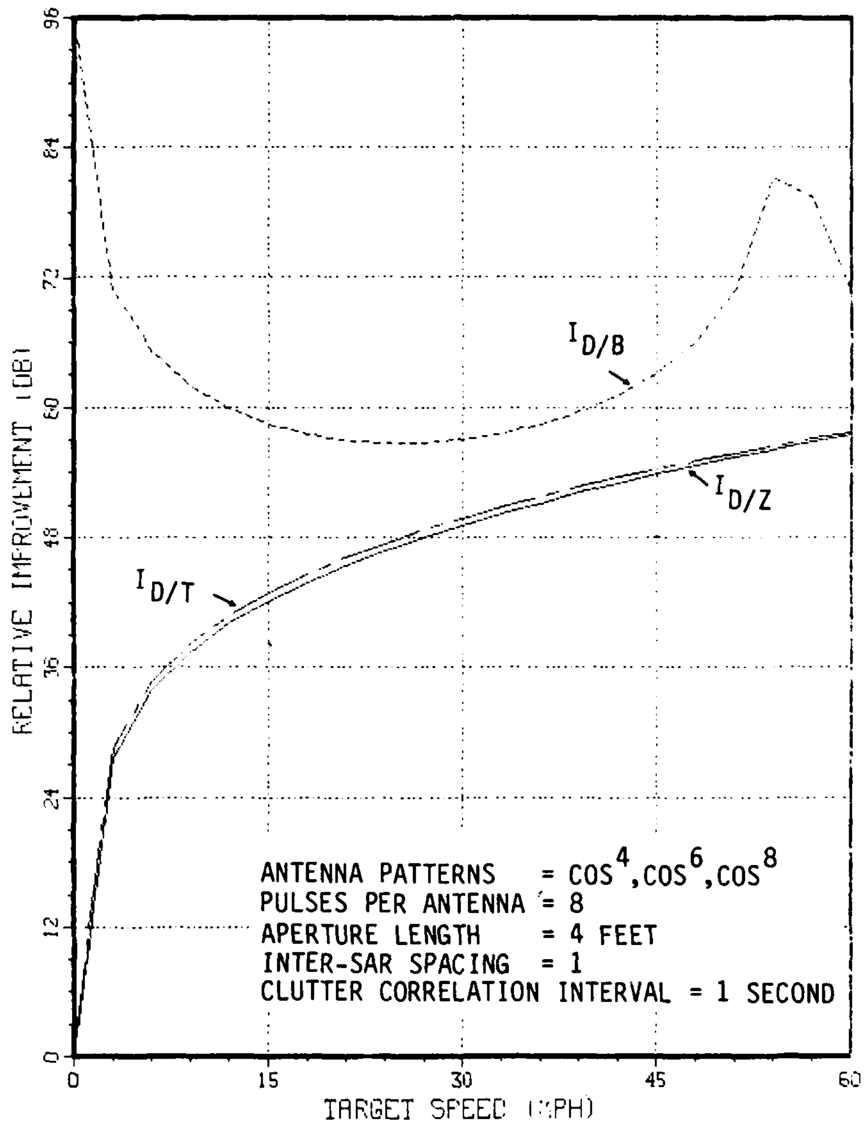

Figure 24. Relative Improvement for Case 14

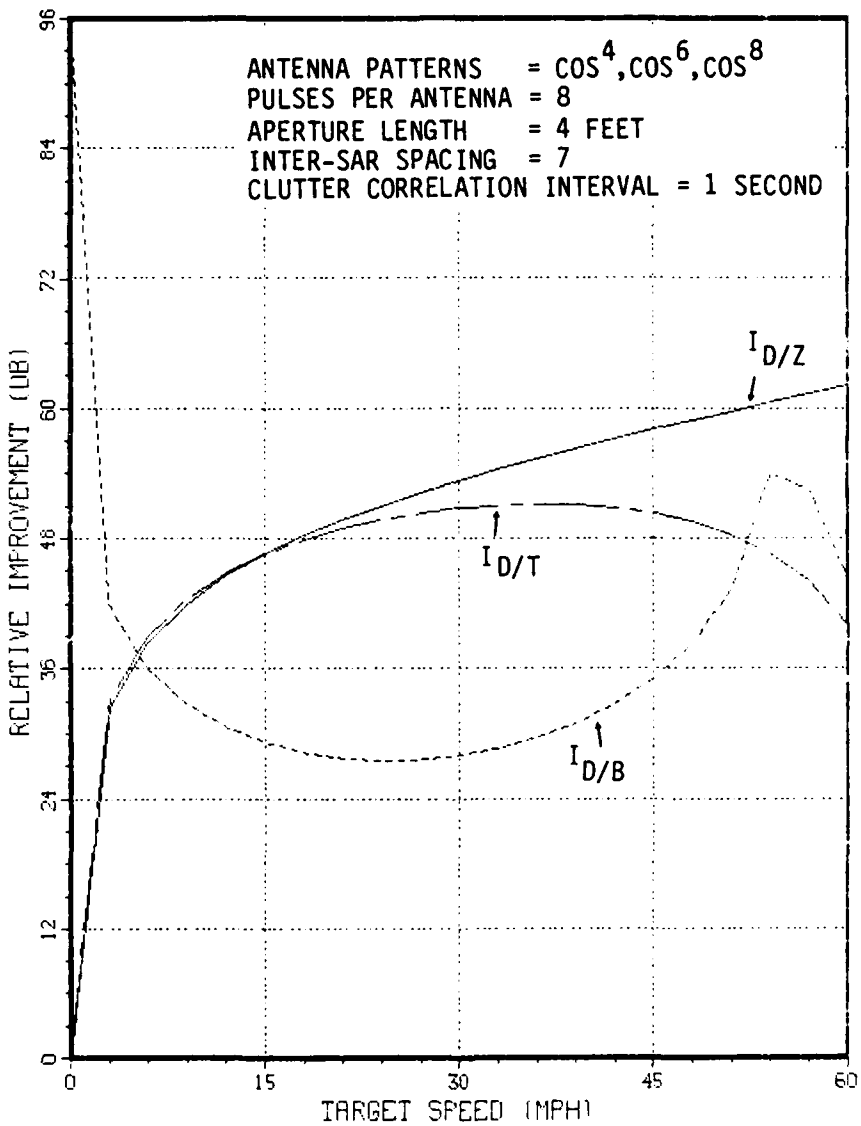

Figure 25. Relative Improvement for Case 15

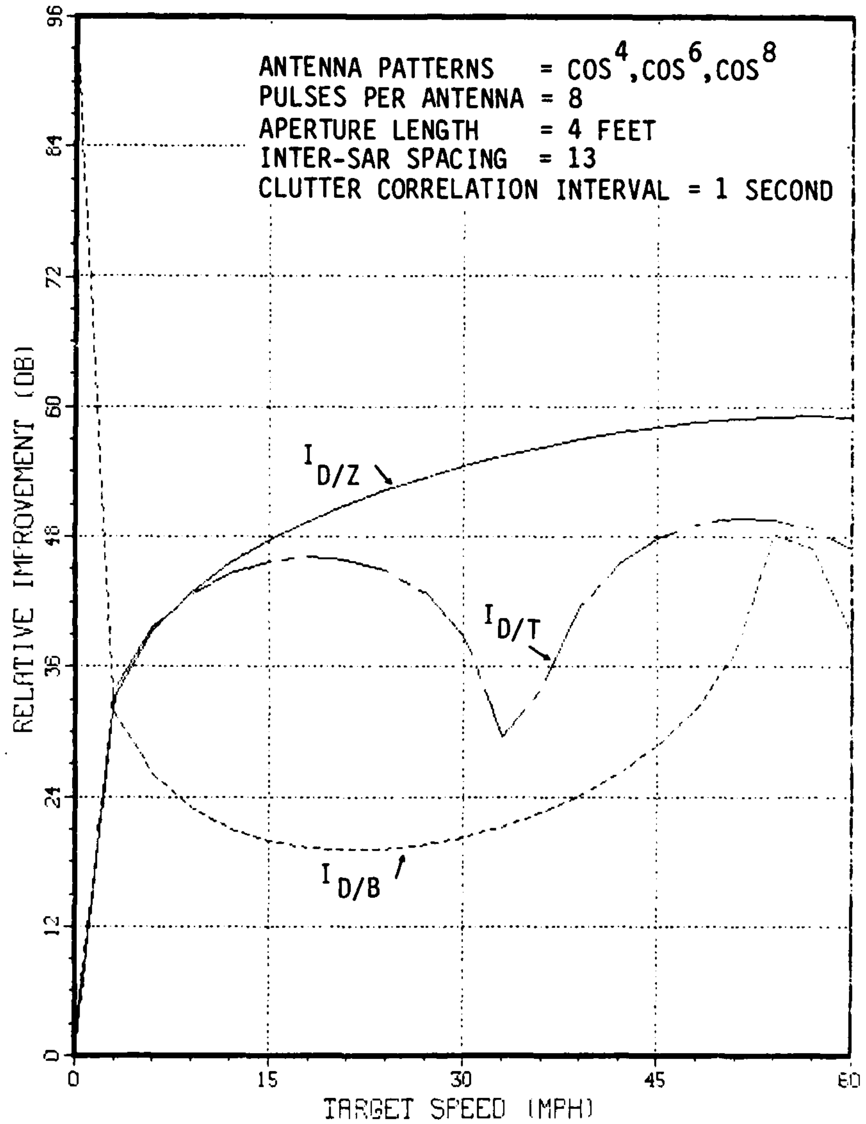

Figure 26. Relative Improvement for Case 16

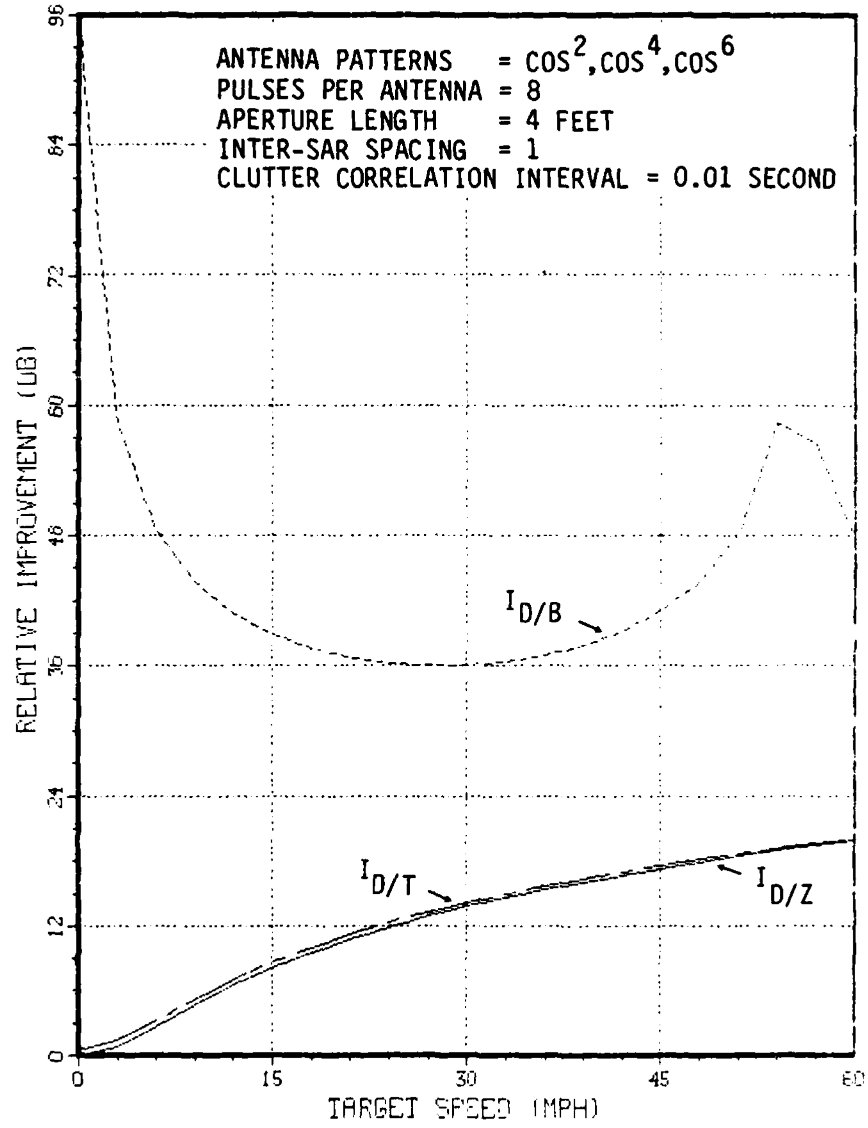

Figure 27. Relative Improvement for Case 17

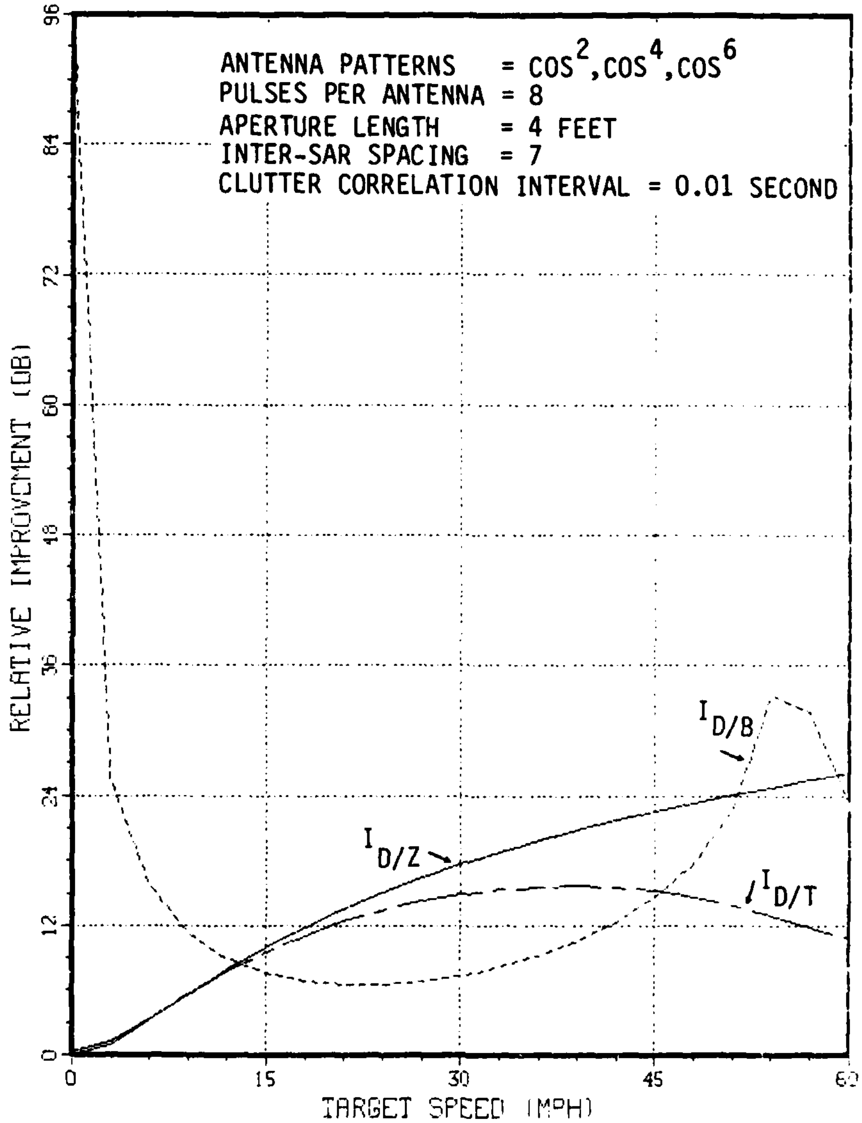

Figure 28. Relative Improvement for Case 18

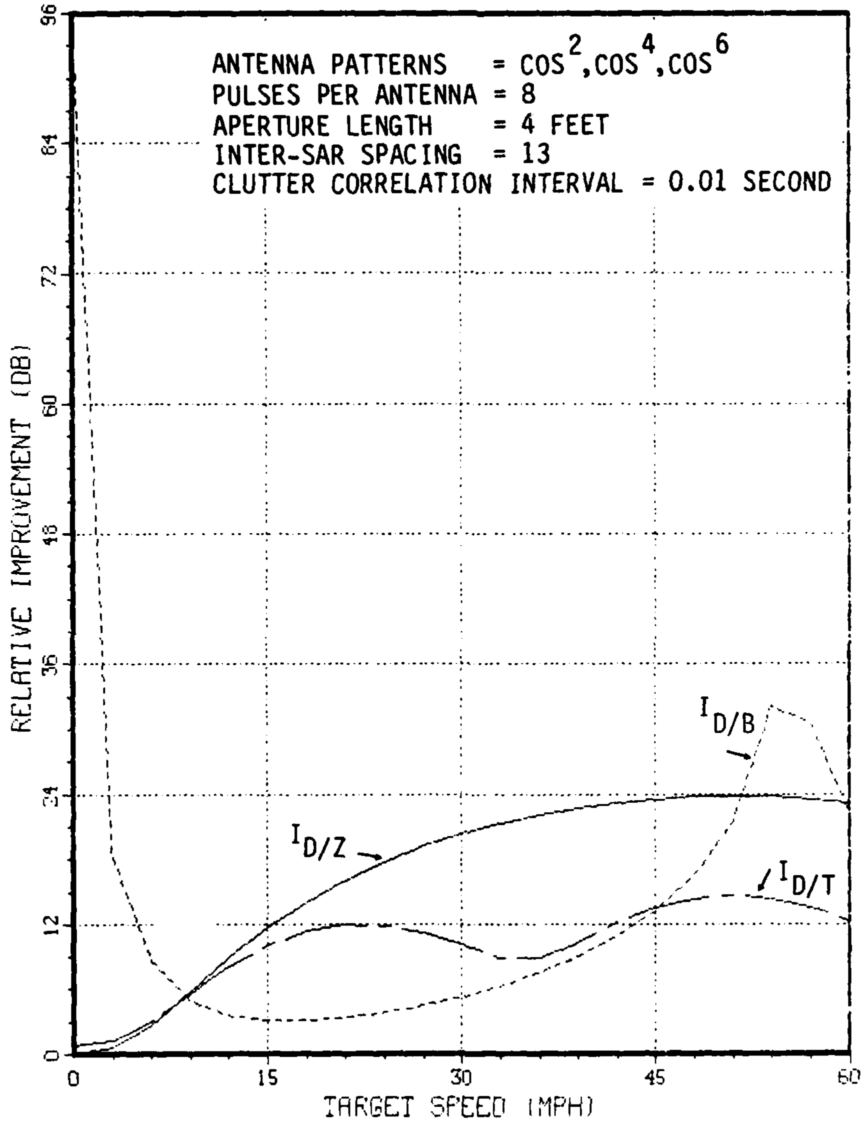

Figure 29. Relative Improvement for Case 19

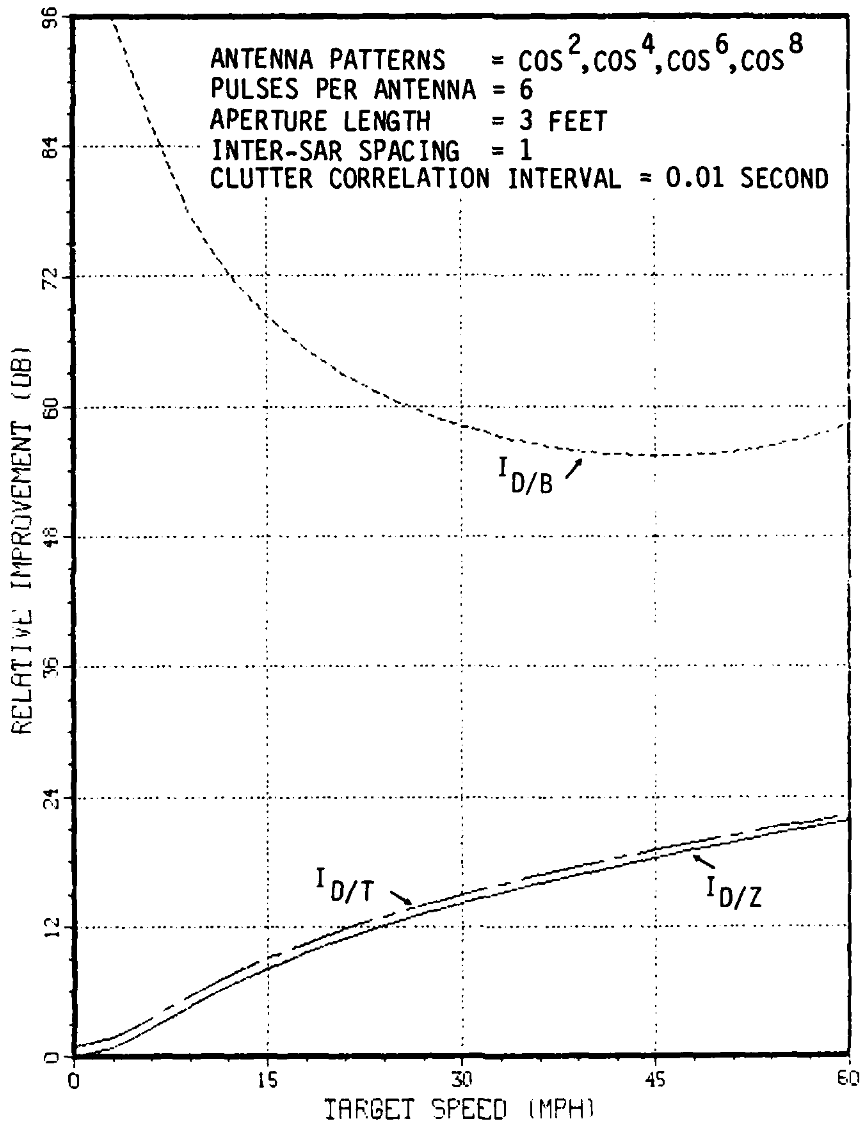

Figure 30. Relative Improvement for Case 20

The Off-Boresight Response to a Target Moving at the Presumed Velocity

The normalized off-boresight response is defined as

$$r_{nob} = \frac{1}{\lambda_D} \frac{|w_p^\dagger \hat{a}|^2}{w_p^\dagger B w_p} \tag{161}$$

where λ_D is the optimum target to clutter power ratio,

w_p is the MASAR processor weighting vector,

$w_p^\dagger B w_p$ is the processed clutter power, and

$\hat{a}$ is the target signal vector obtained by using the presumed v_T, θ_T in (53) and (54), but varying θ_0 in those equations within the half-space $-90^\circ \leq \theta_0 \leq 90^\circ$.

In other words, $\hat{a}$ is the target signal vector obtained by displacing the presumed target from its azimuthal position.

Figures 31 through 42 are examples of the off-boresight response for some representative cases. Each figure depicts the response when the optimum (w_D), target (w_T), and binomial (w_B) weights are used for w_p in (160). The response for the optimum, target, and binomial weights is shown by the solid, broken, and dashed curves, respectively. All figures depict the response to a three mile per hour target moving along a 180 degree track.

In every case, the response for the binomial weights is completely without merit. As mentioned in the previous section, the binomial weights do a good job of cancelling anything that doesn't move. Because of this, they tend to cancel slowly moving objects--such as a three mph target--as well.

These response curves resemble antenna patterns. Essentially, that's what they are. Note that the only variable in r_{nob} is the target signal vector, a; the clutter power is a constant. The target can be

thought of as a "transmitter" in the MASAR far field which is being swung azimuthally in the half-apace surrounding the MASAR platform. As this is done, the change in the output of the MASAR processor is observed. This is very much like the way conventional antenna patterns are obtained (though, applying the principle of reciprocity, the transmitter is usually held fixed and the antenna is rotated to obtain the pattern). As discussed in Appendix D for the MASAR target and binomial processors, the processed target power has factors which can be likened to the "array factors" and "element patterns" of conventional anntenna array theory.

Figures 31 through 38 depict the response when the azimuth (θ_0) of the presumed target equals zero degrees. The difference in the ordinates of these curves at zero degrees is the same as the difference in the ordinates of the corresponding improvement curves at three miles per hour.

Figures 31 and 32, and Figures 33 and 34 show the sharpening of the response as the length of the synthetic aperture increases from eight to 25 synthetic elements. This is characteristic of the beamsharpening obtained with longer antenna arrays.

Note the far out sidelobes in Figures 31 and 32 are a consequence of the isotropic pattern used in those cases in conjunction with the grating lobes which are present. (See the discussion at the end of Appendix C.) This can be verified analytically with (D.21), the expression obtained in Appendix D for the target-weighted target power. Observe that, with $\theta_0 = 0^\circ$ and $\theta = 90^\circ$, (D.21) reduces to

$$w_T^{\dagger} A w_T = \left\{ \frac{\sin[N\pi(1-\frac{v_T}{v_R})]}{\sin[\pi(1-\frac{v_T}{v_R})]} \right\}^2 \qquad (162)$$

Since v_T = 3 mph and v_R = 450 mph, this is essentially a grating lobe of amplitude approximately equal to N^2. Note that if $f_{PRF} = 4Mv_R/\lambda_0$, the grating lobes at ±90 degrees would not be present and the amplitude of the target power there would be about unity instead.

The response depicted in Figures 35 and 36 for short aperture, three and four antenna MASARs can be expected to sharpen with longer apertures. The sidelobes would be much lower, similar to the 25 pulse cases. Furthermore, the peak in the response for the optimum weights between zero and 15 degrees in Figure 35 can be expected to attenuate sharply with longer apertures. Note that, with the addition of only one antenna in Figure 36, this peak has already attenuated considerably.

As expected (see pages 70-71), Figures 37 and 38 show that the response for the optimum and target weights is comparative for very fast clutter decorrelation times.

Figures 39 through 42 depict the response when the azimuth of the presumed target is as stated in the captions. Beamsteering can be observed. In all cases, the optimum weights center the main response at the target's presumed azimuth.

Curiously, strong peaks are observed at -30 degrees for the cases where the target's presumed azimuth is +30 degrees; yet, for the cases where the target's presumed azimuth is at +60 degrees, a strong peak at -60 degrees does not appear. For these latter cases, the target weights show a puzzling response at -7.5 degrees. In fact, for the case shown

in Figure 42, the target weights have "lost" the presumed target completely. All these effects of the target weights are explainable with the aid of (D.21) from Appendix D.

First, consider the cases where the target's presumed azimuth is +30 degrees. Using $\theta_0 = 30^\circ$ in (D.21), with $\theta_T = 180^\circ$ and treating v_T/v_R as small, one finds that the "combined array factor" in (D.21) becomes

$$\left\{ \frac{\sin[N\pi\ (\sin\theta - \frac{1}{2})]}{\sin[\pi\ (\sin\theta - \frac{1}{2})]} \right\}^2$$

This explains the peaks in the response at both $\theta = +30^\circ$ and -30°.

Second, when $\theta_0 = +60^\circ$, this same factor becomes

$$\left\{ \frac{\sin[N\pi\ (\sin\theta - \frac{\sqrt{3}}{2})]}{\sin[\pi\ (\sin\theta - \frac{\sqrt{3}}{2})]} \right\}^2$$

which has no peak at $\theta = -60^\circ$. However, a peak does occur at $\sin\theta - \sqrt{3}/2 = -1$, which occurs at $\theta = -7.7^\circ$; precisely where seen in Figures 40 and 42.

These spurious peaks are clearly caused by the grating lobes which are a consequence of choosing $f_{PRF} = 2Mv_R/\lambda_0$. Had $f_{PRF} = 4Mv_R/\lambda_0$ been chosen instead, the factor above would become

$$\left\{ \frac{\sin[N\,\frac{\pi}{2}\,(\sin\theta - \sin\theta_0)]}{\sin[\frac{\pi}{2}\,(\sin\theta - \sin\theta_0)]} \right\}^2$$

which has no peaks other than at $\theta = \theta_0$. (The choice of the PRF is justified in the discussion at the end of Appendix C. If a situation arose in reality where one wished to steer the MASAR array off abeam-to-starboard of the radar platform, then the PRF would have to be carefully selected to avoid these problems.)

These peaks in the "combined array factor" for the target weights are further weighted by the "combined element pattern", the second factor of (D.21). In Figure 42, the target weight's response is lower at the "design angle" of +60 degrees than at its grating lobe at -7.7 degrees. The "combined element pattern" for this case is approximately

$$\frac{1+(\frac{1}{2}\cos\theta)^{16}-2(\frac{1}{2}\cos\theta)^{8}}{1+(\frac{1}{2}\cos\theta)^{4}-2(\frac{1}{2}\cos\theta)^{2}}\left(\frac{1}{2}\cos\theta\right)^{4}$$

At $\theta = 60^{\circ}$ this factor equals -23.5 dB, and at $\theta = -7.7^{\circ}$ it equals -9.8 dB. Then, the value of the response at $\theta = 60^{\circ}$ is 13.7 dB lower than that at $\theta = -7.7^{\circ}$; precisely as seen in Figure 42.

Note the "design angle" peak in Figure 42 does not appear exactly at $\theta = 60^{\circ}$. This is because of the added term involving v_T/v_R which was neglected in the above discussion. That is, the "combined array factor" is really

$$\left[\frac{\sin(N\pi\psi)}{\sin(\pi\psi)}\right]^2$$

where ψ is (D.22) of Appendix D.

As stated earlier, the optimum weights exhibit the same grating lobe response as the target weights for the cases where $\theta_0 = 30^{\circ}$, but--

interestingly--not for the cases where $\theta_0 = 60^\circ$. The optimum weights are complicated functions of both the target and clutter and do not lend themselves to as tractable an analysis as do the target weights. The question as to why the optimum weights are unable to neutralize the grating lobe for the cases where $\theta_0 = 30^\circ$, yet effectively neutralize the grating lobe in the cases where $\theta_0 = 60^\circ$, is left moot.

[Figures 31 through 42 follow on pages 110 through 121, respectively. The text continues with the section on "The Response of Optimum Weights to Other Boresight Targets," on page 122.]

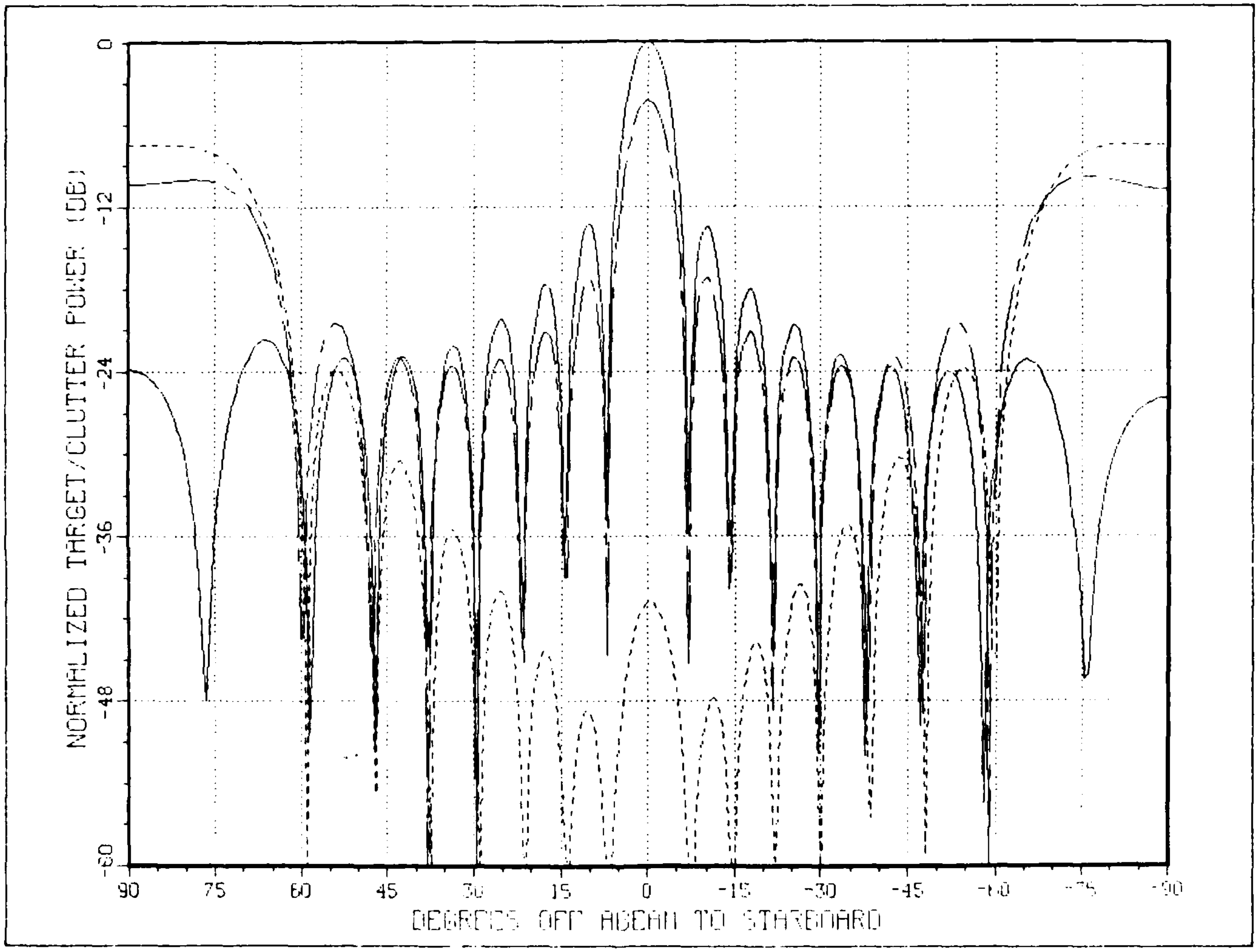

Figure 31. Off-Boresight Response for Case 1 with Optimum (solid), Target (broken) and Binomial (dashed) Weights; Presumed Target: v_T = 3 mph, $\theta_T = 180^{\circ}$, $\theta_0 = 0^{\circ}$.

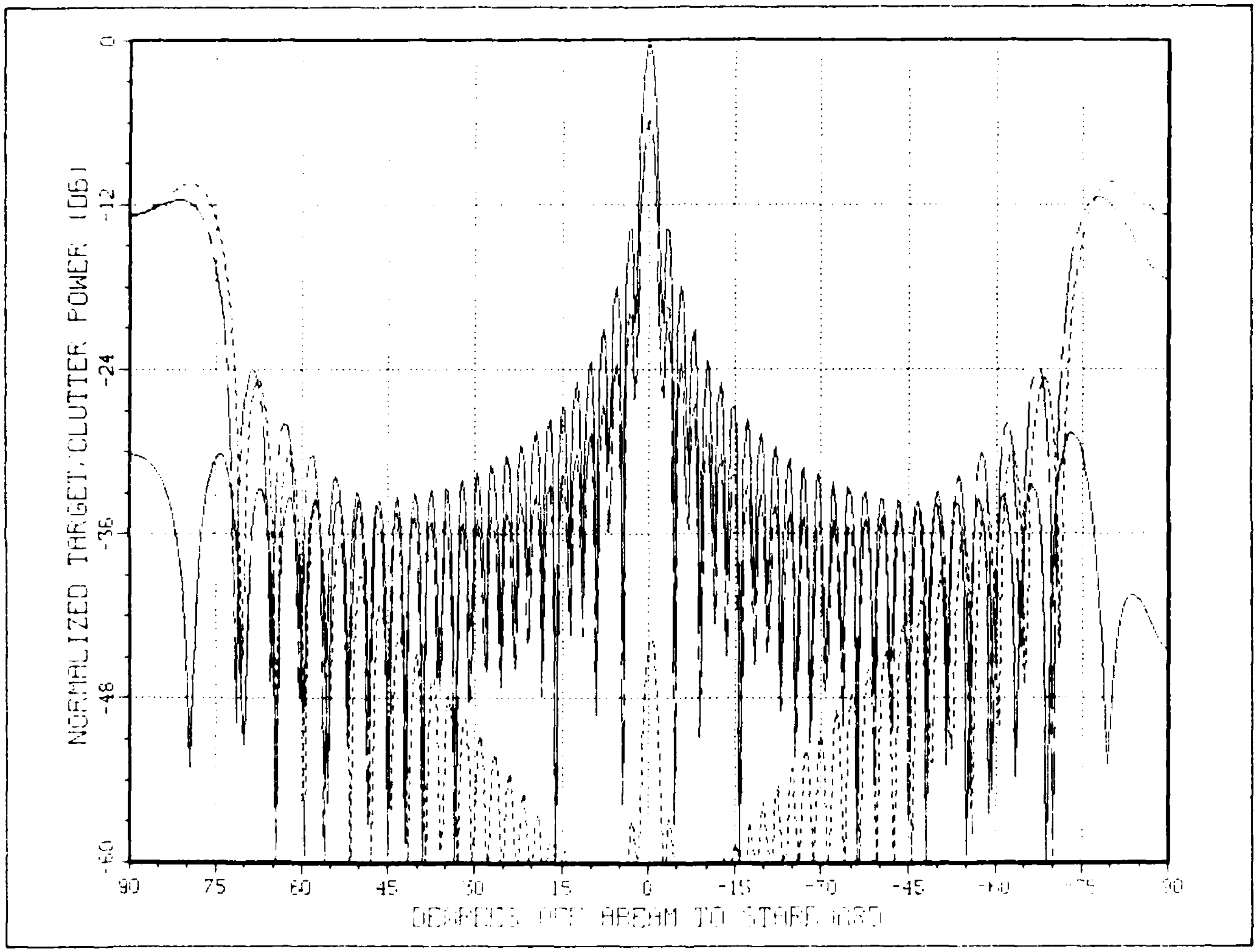

Figure 32. Off-Boresight Response for Case 3 with Optimum (solid), Target (broken) and Binomial (dashed) Weights; Presumed Target: v_T = 3 mph, θ_T = 180°, θ_n = 0°.

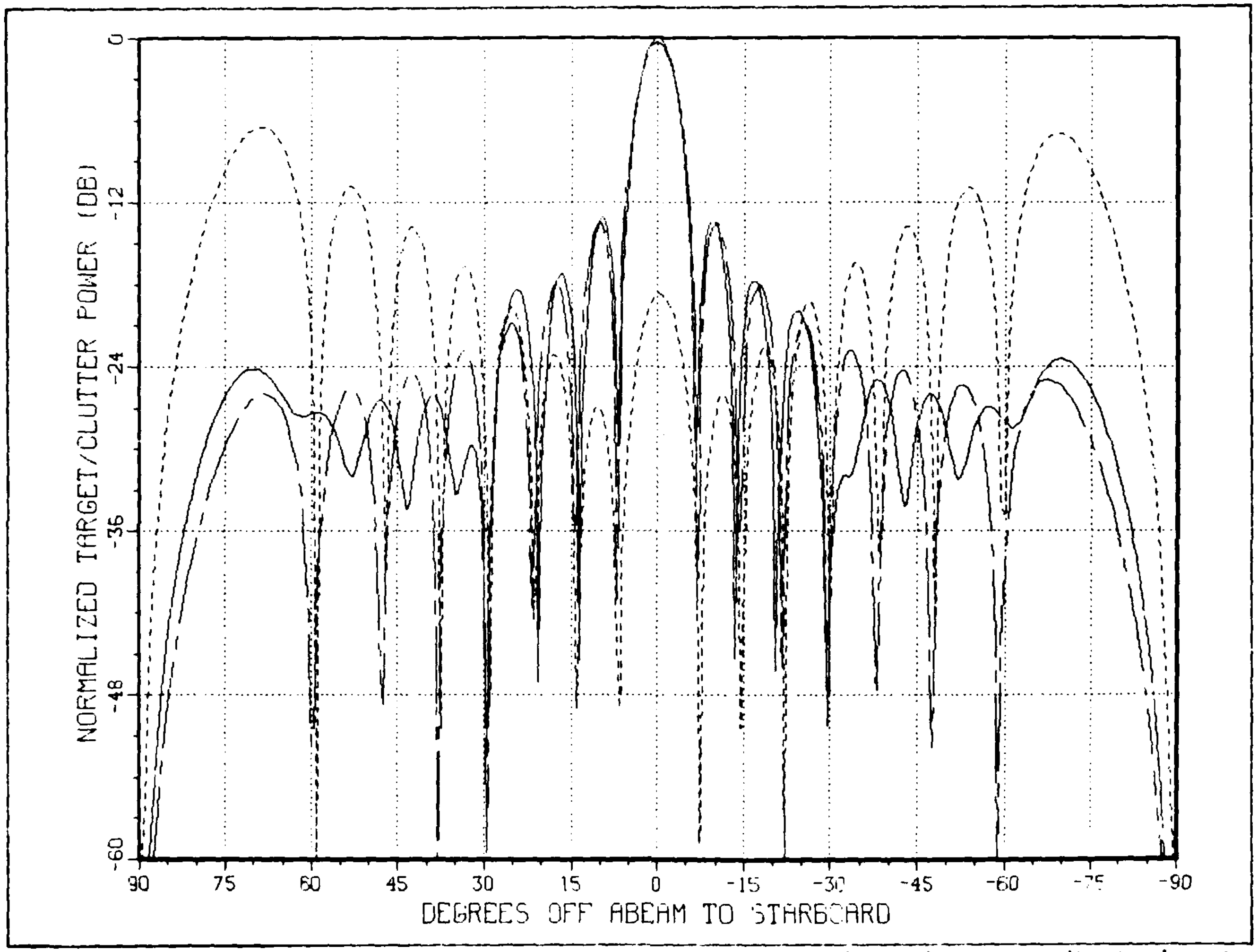

Figure 33. Off-Boresight Response for Case 4 with Optimum (solid), Target (broken) and Binomial (dashed) Weights; Presumed Target: v_T = 3 mph, θ_T = 180°, θ_0 = 0°.

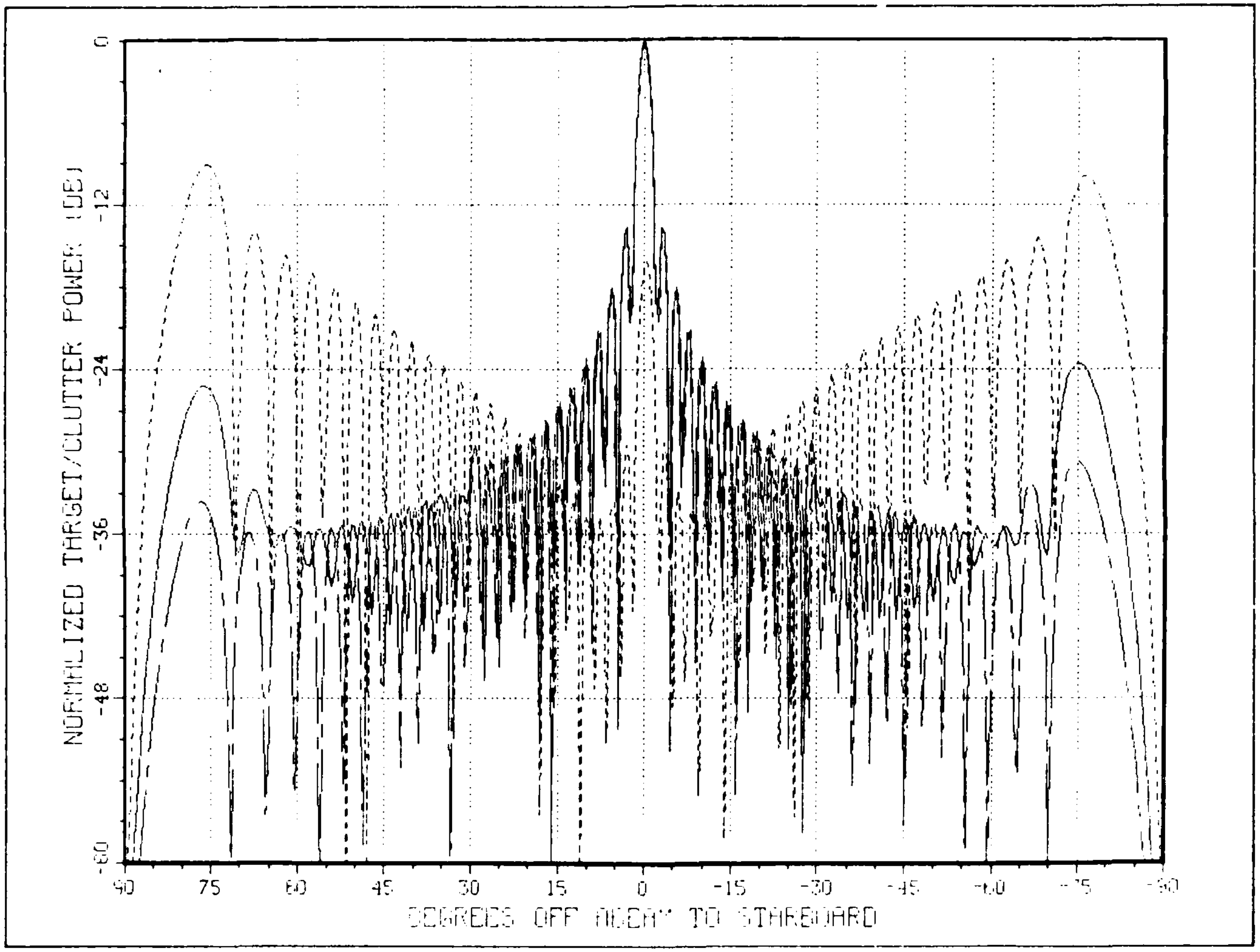

Figure 34. Off-Boresight Response for Case 6 with Optimum (solid), Target (broken) and Binomial (dashed) Weights; Presumed Target: v_T = 3 mph, $\theta_T = 180^\circ$, $\theta_0 = 0^\circ$.

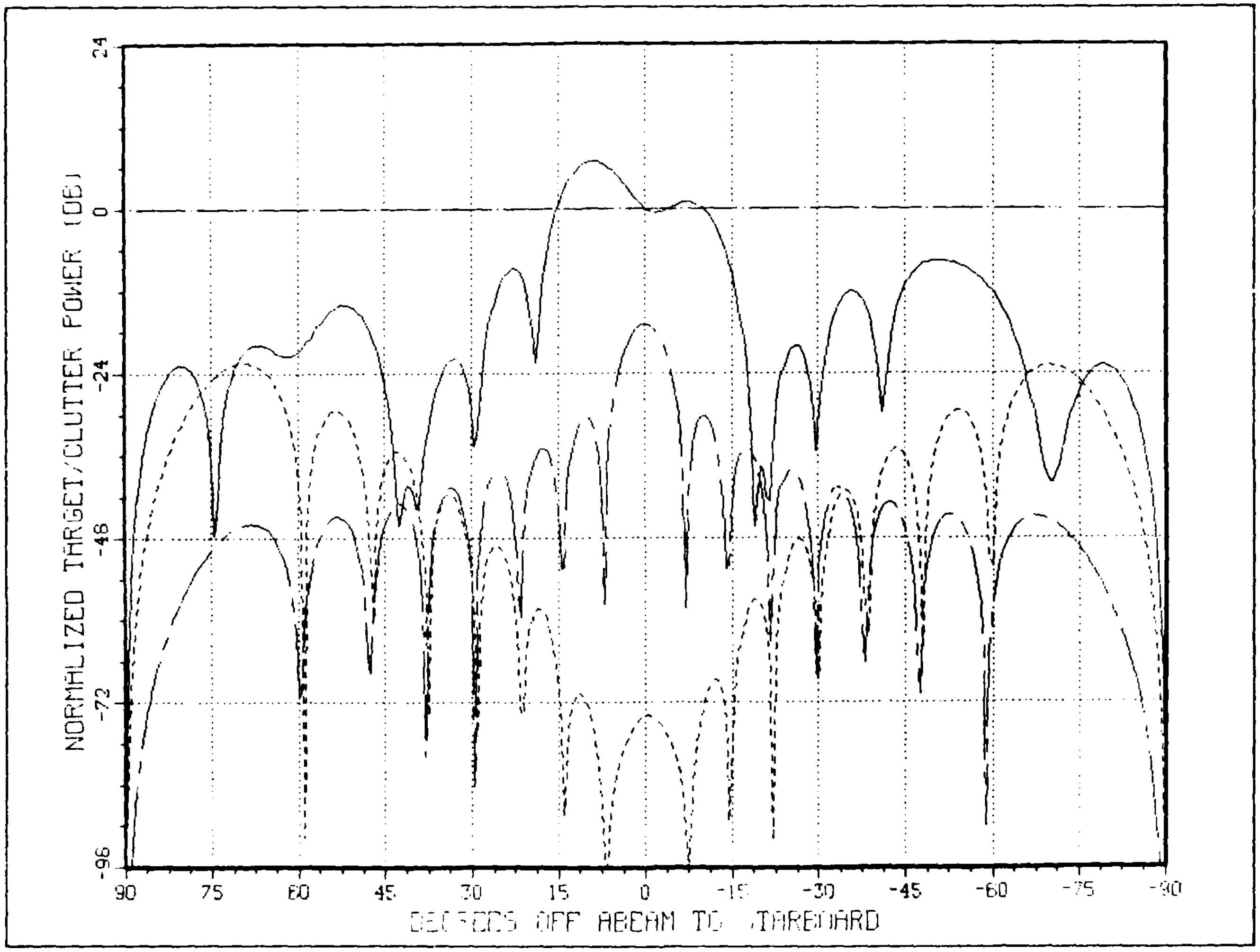

Figure 35. Off-Boresight Response for Case 8 with Optimum (solid), Target (broken) and Binomial (dashed) Weights; Presumed Target: v_T = 3 mph, $\theta_T = 180^\circ$, $\theta_0 = 0^\circ$.

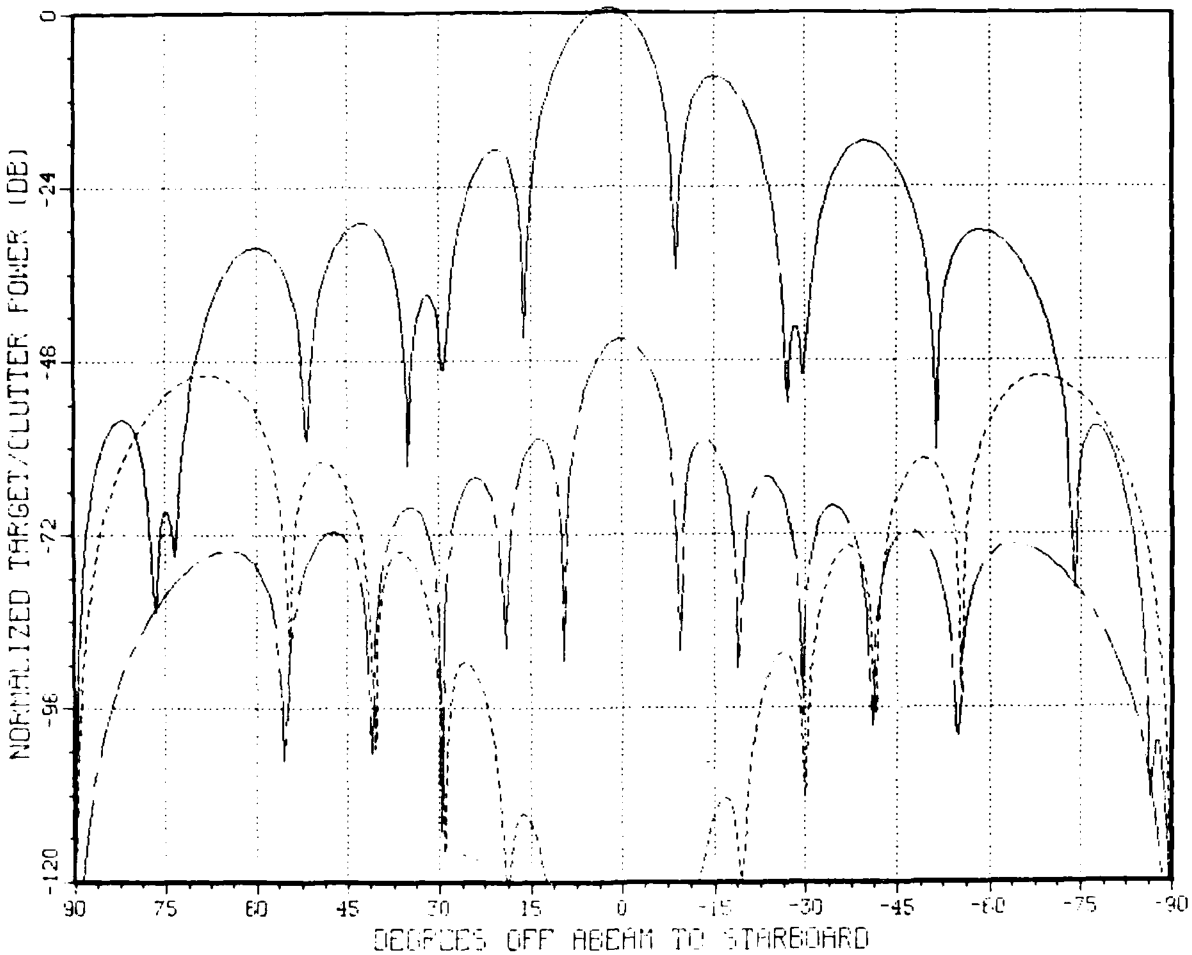

Figure 36. Off-Boresight Response for Case 11 with Optimum (solid), Target (broken) and Binomial (dashed) Weights; Presumed Target: v_T = 3 mph, $\theta_T = 180^\circ$, $\theta_0 = 0^\circ$.

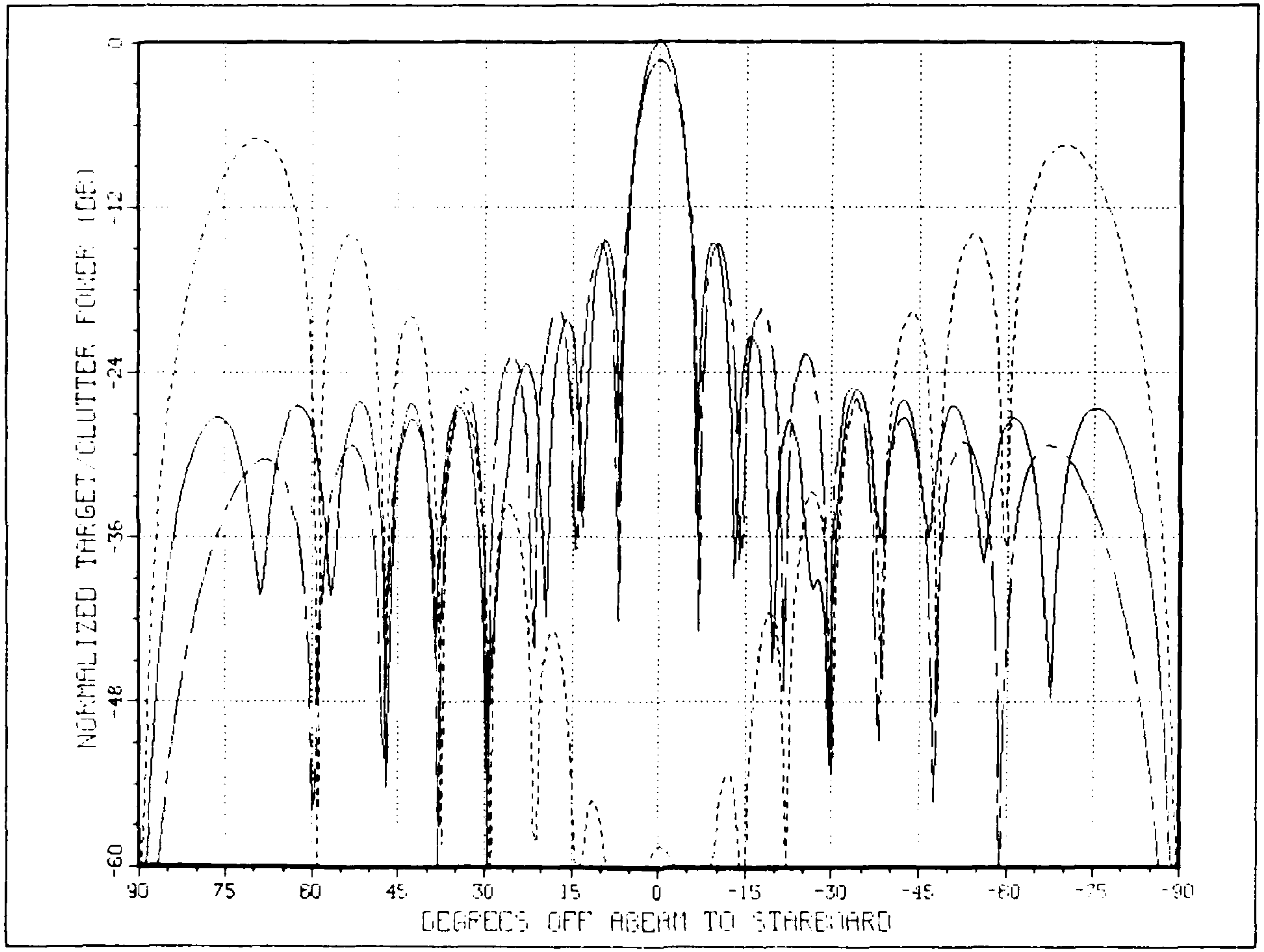

Figure 37. Off-Boresight Response for Case 17 with Optimum (solid), Target (broken) and Binomial (dashed) Weights; Presumed Target: v_T = 3 mph, θ_T = 180°, θ_0 = 0°.

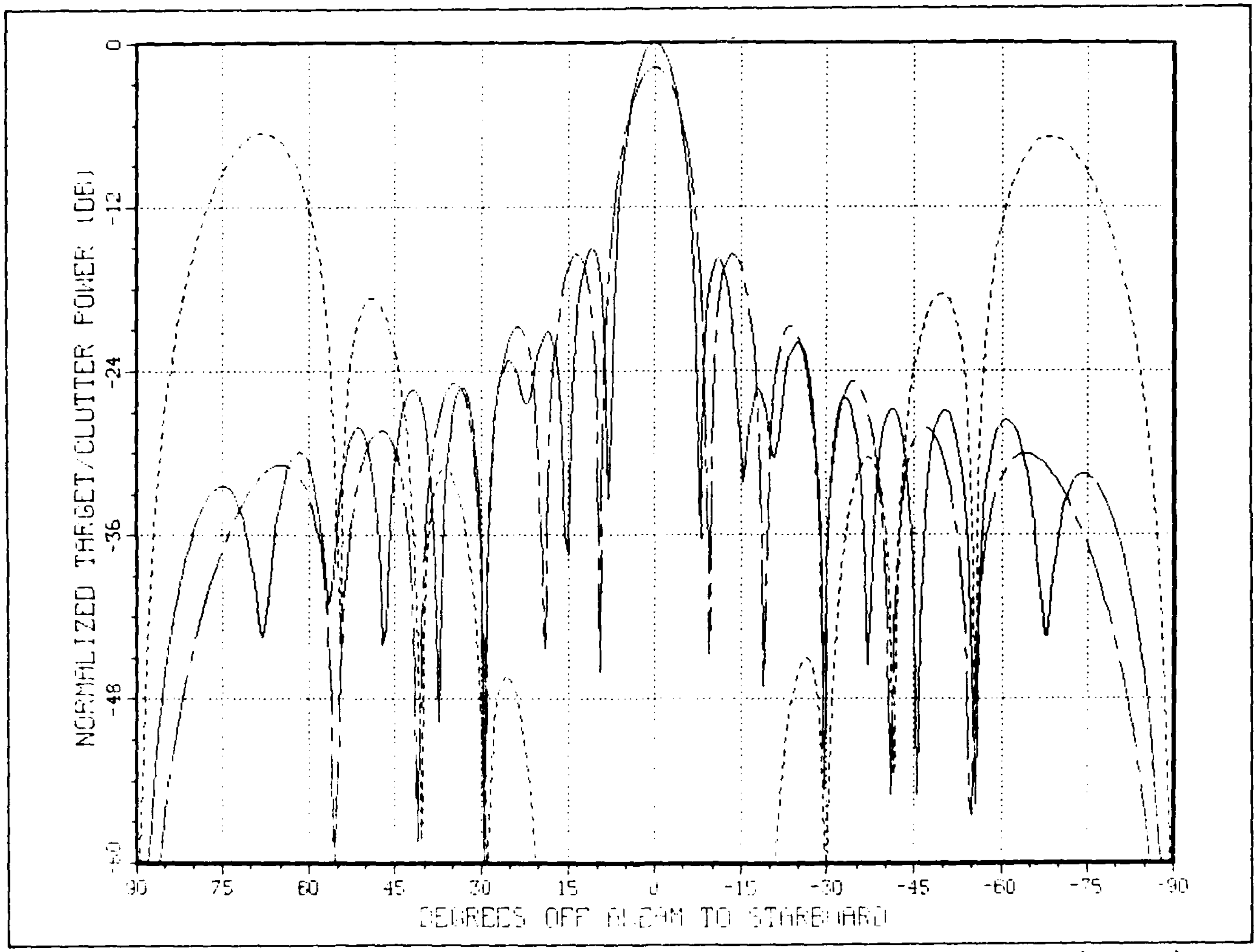

Figure 38. Off-Boresight Response for Case 20 with Optimum (solid), Target (broken) and Binomial (dashed) Weights; Presumed Target: v_T = 3 mph, $\theta_T = 180^\circ$, $\theta_0 = 0^\circ$.

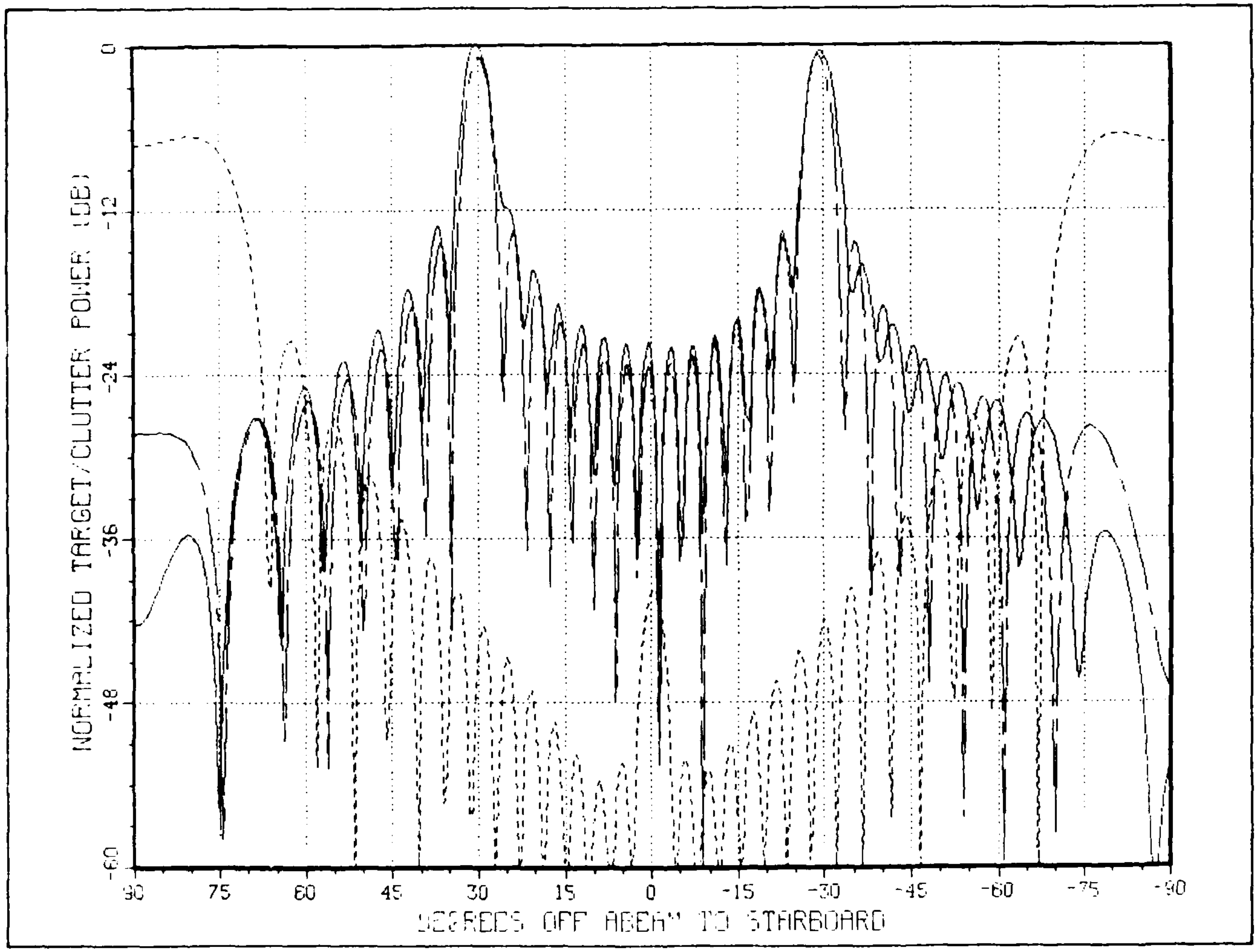

Figure 39. Off-Boresight Response for Case 2 with Optimum (solid), Target (broken) and Binomial (dashed) Weights; Presumed Target: v_T = 3 mph, $\theta_T = 180^\circ$, $\theta_0 = 30^\circ$.

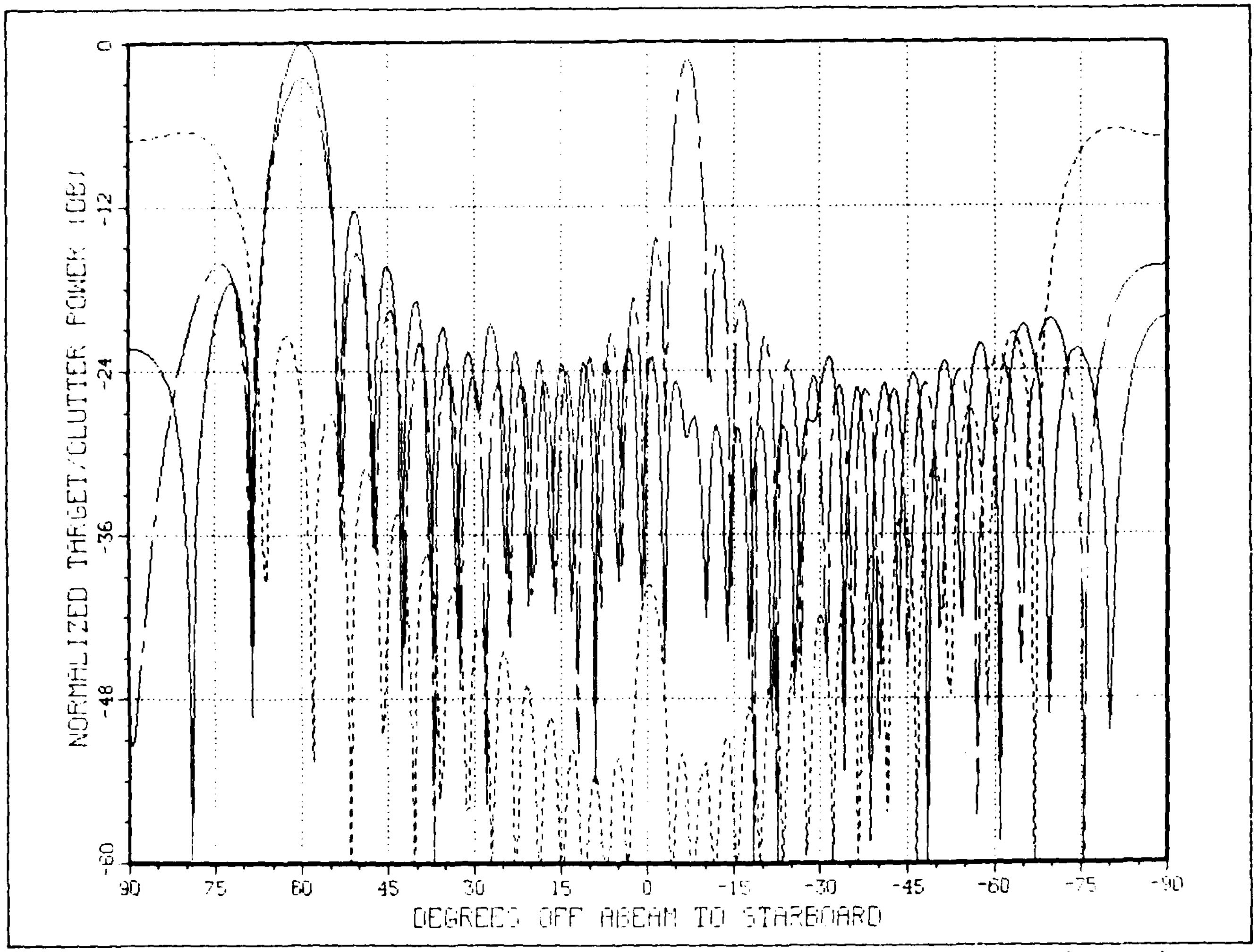

Figure 40. Off-Boresight Response for Case 2 with Optimum (solid), Target (broken) and Binomial (dashed) Weights; Presumed Target: v_T = 3 mph, $\theta_T = 180^\circ$, $\theta_0 = 60^\circ$.

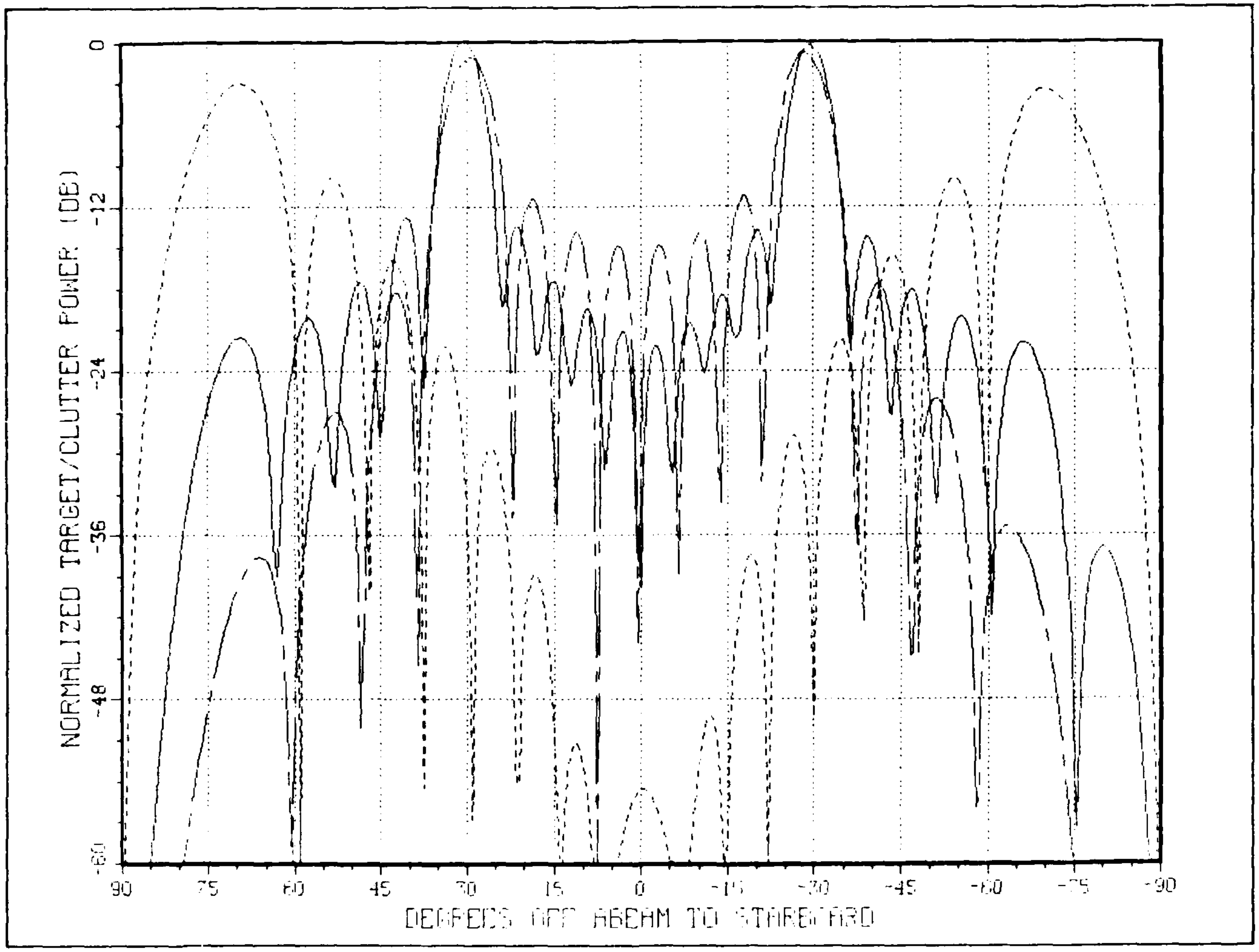

Figure 41. Off-Boresight Response for Case 17 with Optimum (solid), Target (broken) and Binomial (dashed) Weights; Presumed Target: v_T = 3 mph, $\theta_T = 180^\circ$, $\theta_0 = 30^\circ$.

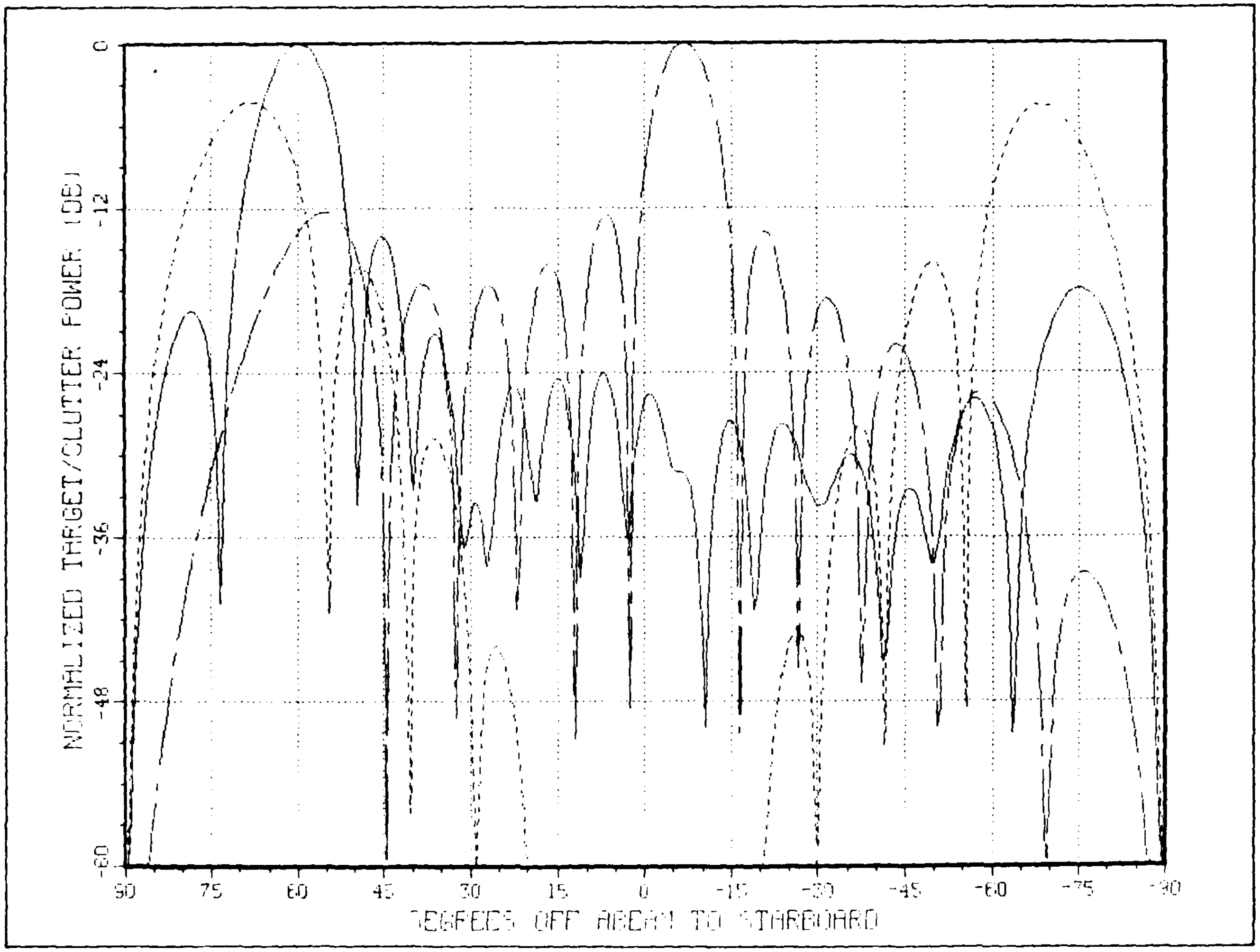

Figure 42. Off-Boresight Response for Case 20 with Optimum (solid), Target (broken) and Binomial (dashed) Weights; Presumed Target: v_T = 3 mph, θ_T = 180°, θ_0 = 60°.

Response of Optimum Weights to Other Boresight Targets

As seen in the previous section, the optimum weights steer the main response--the boresight--to the azimuth of the presumed target. The response of the optimum weights to another target on the boresight can be obtained from

$$r_b = \frac{1}{\lambda_D} \frac{|w_D^{\dagger} \tilde{a}|^2}{w_D^{\dagger} B w_D} \tag{163}$$

which is the same as (161) with the optimum weights, and

where $\tilde{a}$ is the target signal vector obtained by fixing θ_0 in (53) and (54) at the azimuth of the presumed target while varying v_T over a selected range of speeds and θ_T over the range $0^\circ \leq \theta_T \leq 360^\circ$.

Since the optimum weights are used in (163), and recalling (8), (9) and (10), then

$$\begin{aligned} r_b &= \frac{|w_D^{\dagger} \tilde{a}|^2}{\lambda_D^2} \\ &= \frac{|w_D^{\dagger} \tilde{a}|^2}{|w_D^{\dagger} a|^2} \end{aligned} \tag{164}$$

which is simply the varied target power normalized by the presumed target power.

The three-dimensional surfaces shown in Figures 43 through 67 were obtained by computing r_b over the range of target speeds and track angles shown. Constant track angle contours are shown every ten degrees and constant speed contours are shown every three miles per hour. In viewing these surfaces, the reader must imagine to be positioned looking obliquely down upon a cube. The lower visible orthogonal edges form the

X (target speed) and Y (track angle) axes, while the leftmost visible vertical edge forms the Z (target to clutter power) axis. The vertical axis is the normalized target to clutter power in the sense of (163). In each figure, the top, middle and bottom surfaces depict the response to other targets when the optimum weights for targets moving along a 180 degree track at 3, 15, and 30 miles per hour, respectively, are used.

The arrows shown in each figure extend from the -48 dB floor vertically upward to the response on the 180 degrees track for the 3, 15, and 30 mile per hour targets, left to right, respectively. Since the zero dB level is the response relative to the presumed target, the arrow for the presumed target is the length of the vertical axis. Note that, in some cases, the upper tip of the arrow points to a hidden part of the surface (see, e.g., the 30 mph arrow on the upper surface in Fig. 44). Also note that targets with track angles in the range $90^\circ \leq \theta_T \leq 270^\circ$ are moving toward the MASAR flight path and those with track angles in the range $270^\circ \leq \theta_T \leq 90^\circ$ are moving away from the MASAR flight path.

The surfaces reveal that constant Z contours can be constructed by connecting points on the surface corresponding to targets which have a common component of velocity along the MASAR boresight. That is, MASAR cannot discriminate between these targets without some other scheme to resolve their ambiguity.

Figures 43 through 62 depict the response to target in clutter for Cases 1 through 20, respectively. For these figures, the presumed target's azimuth is at zero degrees. The optimum weights steer the MASAR boresight to this azimuth. Since the presumed targets are moving along the 180 degree track, this explains why this track traverses the

peak response and why the response is symmetric about it. It traverses the peak response because it is parallel to the boresight. It is the line of symmetry for the response surface for the reason given in the previous paragraph.

These effects are more dramatically revealed in Figures 63 through 67. These figures depict the response for selected cases in which the azimuth, θ_0, of the presumed target is other than at zero degrees. Close inspection reveals that the peak response is traversed along the track which equals 180 degrees plus θ_0. Also, the surfaces are symmetrical about this track. For example, in Figure 67, the peak response is traversed by the 240 degree track, which is also the line of symmetry. (Recall that the upper arrow points touch the 180 degree track.)

There are some central observations which can be made from these surfaces. First, since clutter is defined, here, to have zero velocity, those surfaces which show a strong response at zero speed do not depict desirable MASAR performance. Conversely, those surfaces which show a strongly attenuated response at zero speed depict very desirable MASAR performance.

Consider Figure 48, for example. This is for a two antenna, 25 pulse case. The performance is observed to be poor for the three mile per hour presumed target, but good for the 15 and 30 mile per hour presumed targets. In addition, for both the 15 and 30 mile per hour presumed targets, sharp rolloff in the response can be observed in both directions along the orthogonal contours through each target. By examining the cases which have shorter synthetic apertures, it can be seen

that this rolloff sharpens with longer apertures (cf., e.g., Figs. 46 through 48).

The surfaces for cases which used three and four antennas and long clutter correlation intervals depict very good performance for the three mile per hour target (see Figs. 50 through 58). However, faster targets get better response from the optimum weights. Also, it is difficult to determine whether a three mile per hour target is moving toward or away from the MASAR flight path. But, these are cases with much shorter aperture lengths than the cases shown in Figures 45 and 48. With longer apertures, perhaps even better performance would be observed for very slowly moving targets in terms of the rolloff in response.

Comparing Figures 59 through 61 with Figures 50 through 53, and Figure 62 with 51, reveals that performance declines with faster clutter decorrelation for constant processing intervals. This was also observed in the relative improvement curves.

A tabulation of the unnormalized response to other boresight targets for selected cases from Table I is provided in Appendix F. By examining these tables for the cases shown, one can see evidence of a very important observation: the calculated response for the presumed target is not necessarily the highest response of those calculated for the other boresight targets. (There are other targets which obtain a higher response than the presumed target with the optimum weights. This does not "violate" the "optimality" of the optimum weights; in fact, these tables illustrate the "optimality" and "drive home" its meaning.) Yet, with no other weights can one obtain a higher response for the presumed target than that which is obtained with the optimum weights. This is what is "optimal" about the optimum weights.

An example from Table XIV, for Case 5, is shown below. The calculated unnormalized response is shown for a 15 mph target moving along a 180° track. In each case, the calculation was performed using the optimum weights for a presumed target moving along the same track at 3, 15 and 30 mph:

unnormalized response for 15 mph target (dB)	presumed target (mph)	obtained from Table XIV (page)
-60.5	3	236
-57.1 (optimum)	15	239
-61.4	30	242

[Figures 43 through 67 follow on pages 127 through 151, respectively. The text continues with Chapter V, "Summary and Conclusions," on page 152.]

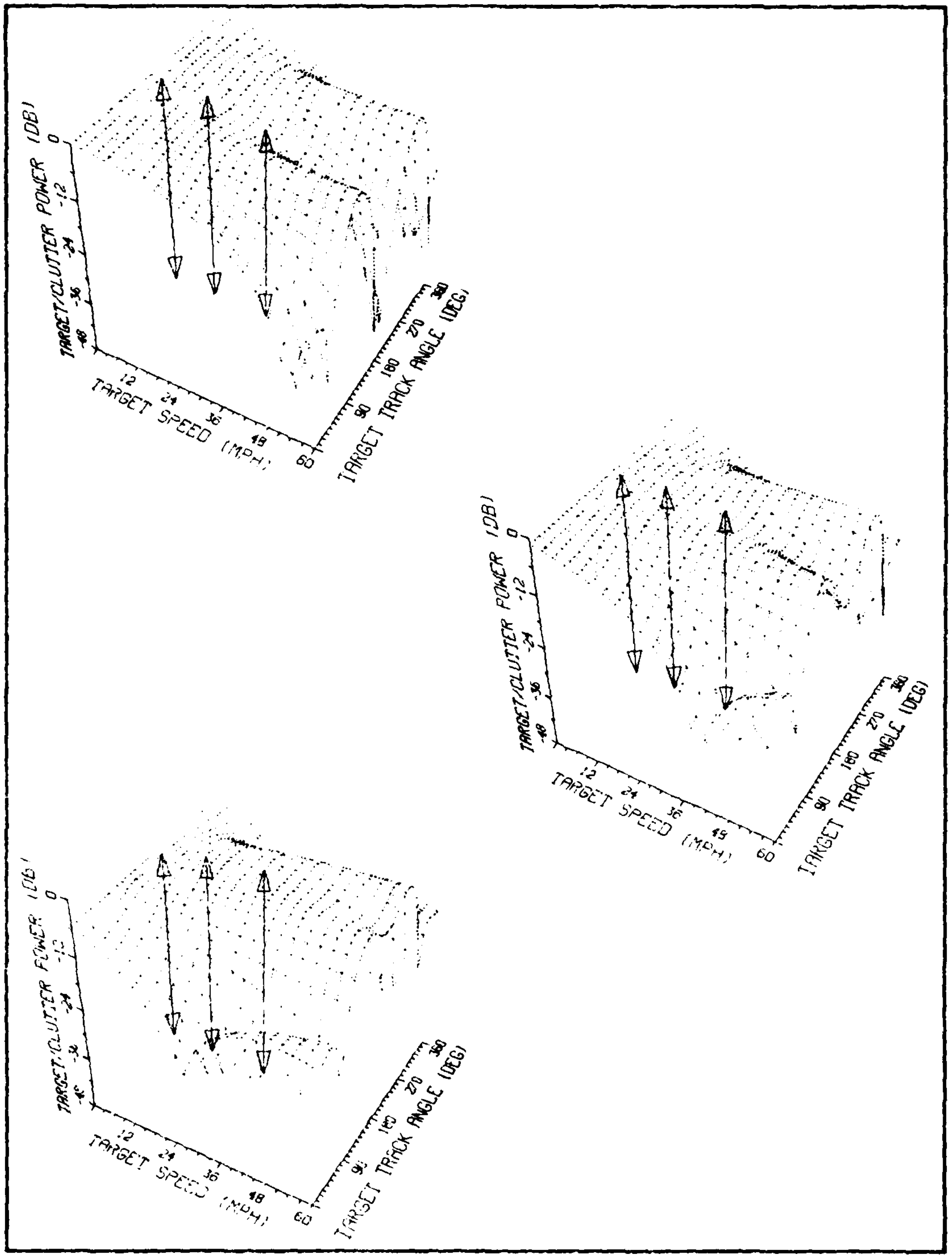

Figure 43. Response to Boresight Targets in Case 1 for Presumed Target at $\theta_0 = 0^\circ$, with $\theta_T = 180^\circ$ and $v_T = 3$ (top), 15 (middle) and 30 (bottom) mph.

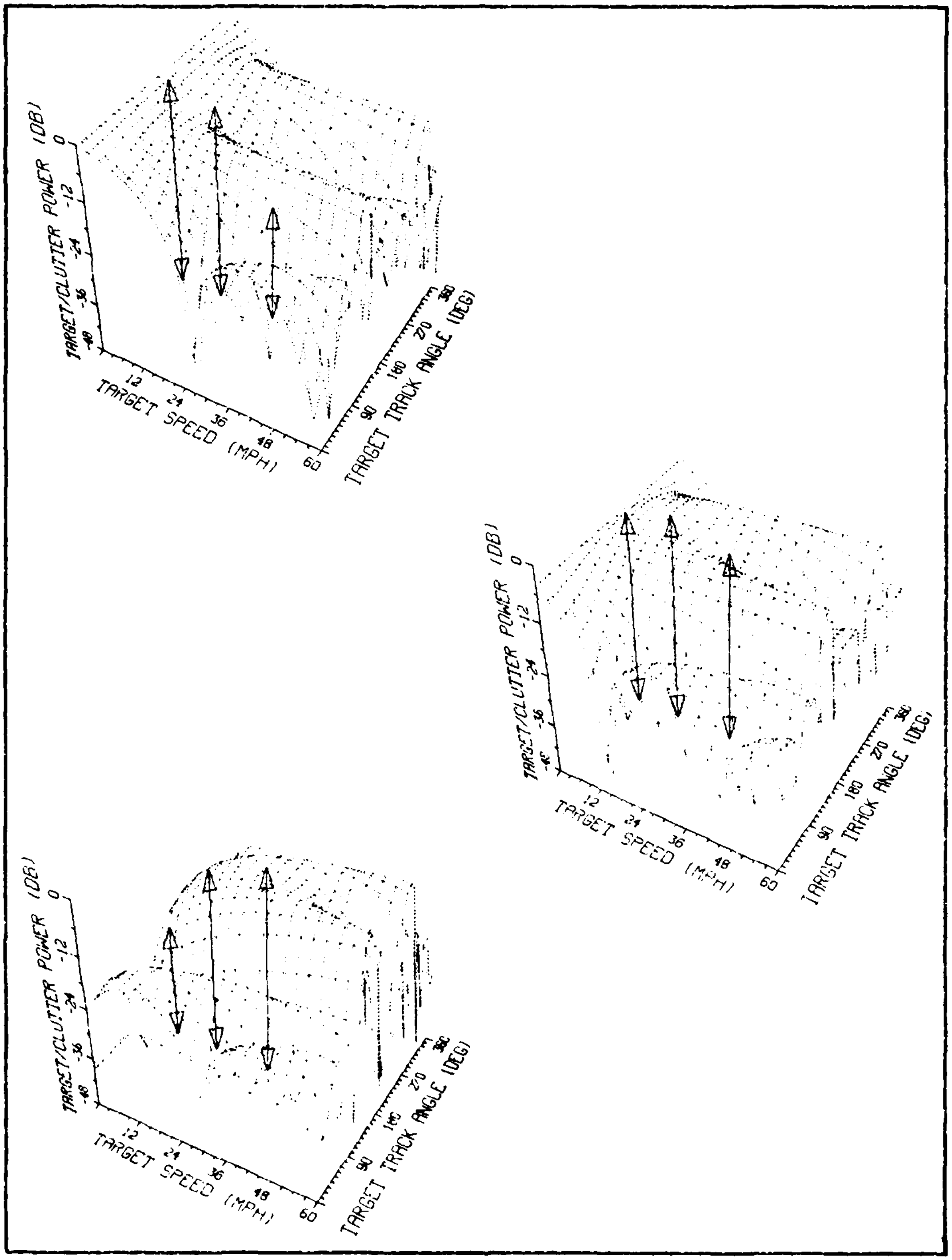

Figure 44. Response to Boresight Targets in Case 2 for Presumed Target at $\theta_0 = 0°$, with $\theta_T = 180°$ and $v_T = 3$ (top), 15 (middle) and 30 (bottom) mph.

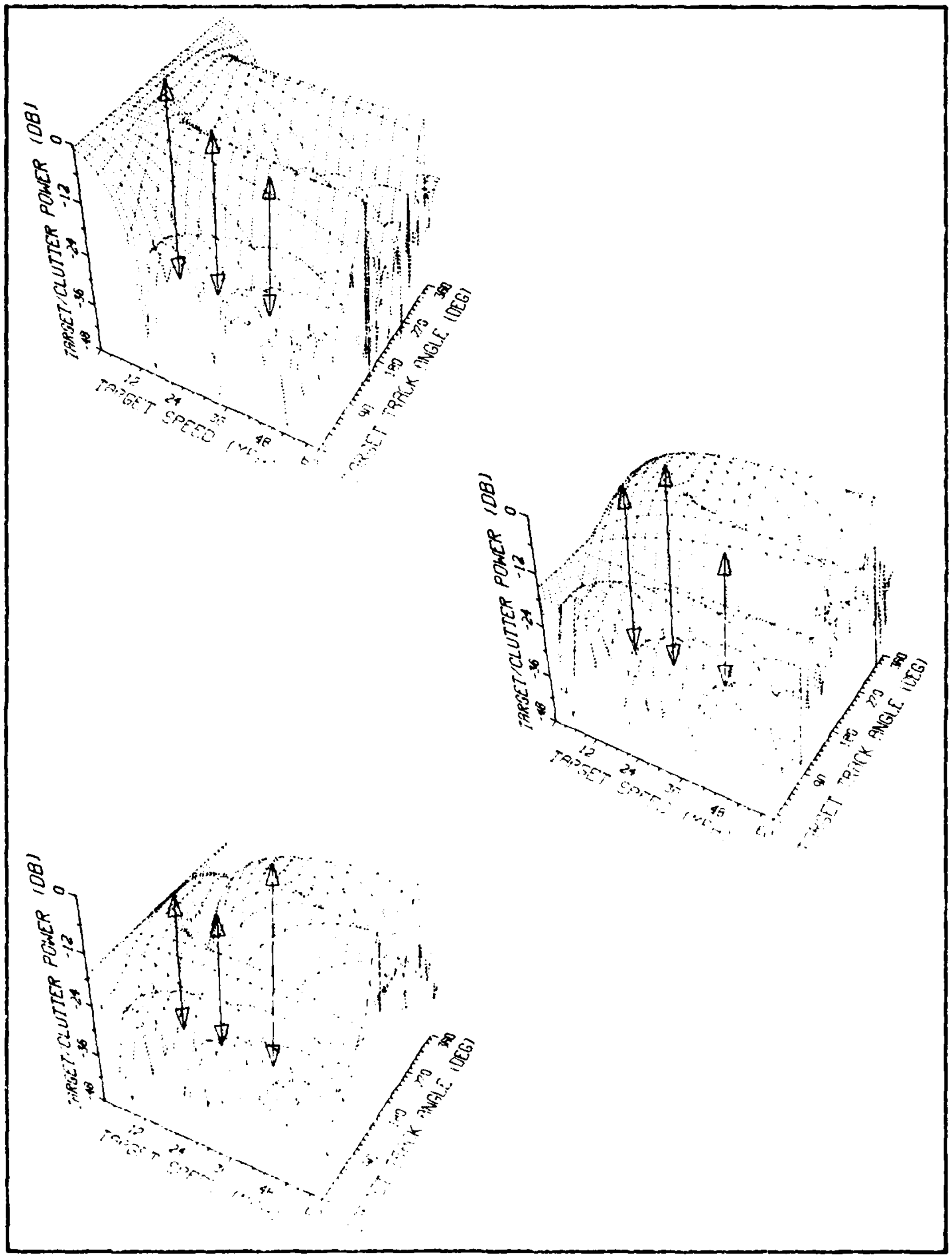

Figure 45. Response to Boresight Targets in Case 3 for Presumed Target at $\theta_0 = 0°$, with $\theta_T = 180°$ and $v_T = 3$ (top), 15 (middle) and 30 (bottom) mph.

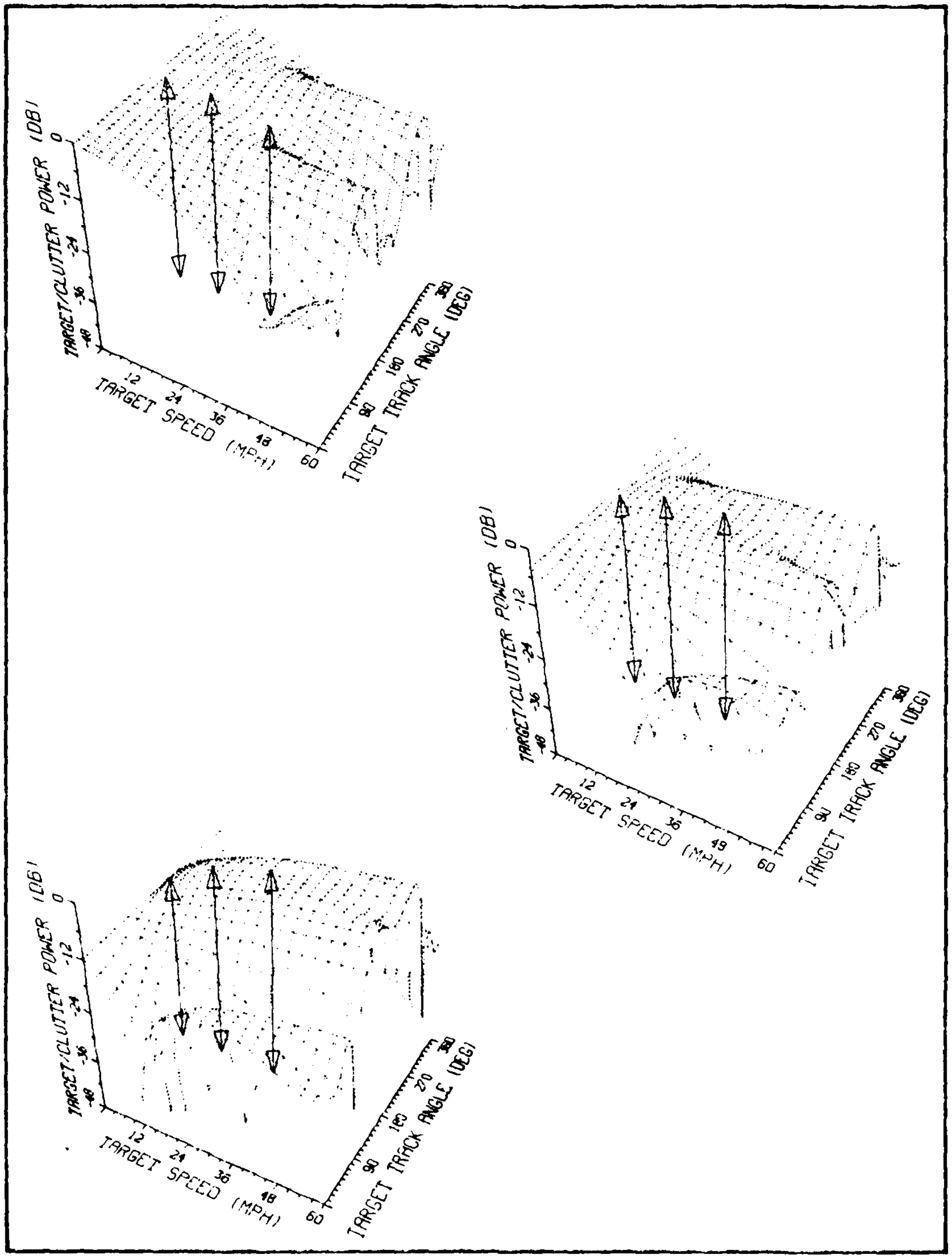

Figure 46. Response to Boresight Targets in Case 4 for Presumed Target at $\theta_0 = 0^\circ$, with $\theta_T = 180^\circ$ and $v_T = 3$ (top), 15 (middle) and 30 (bottom) mph.

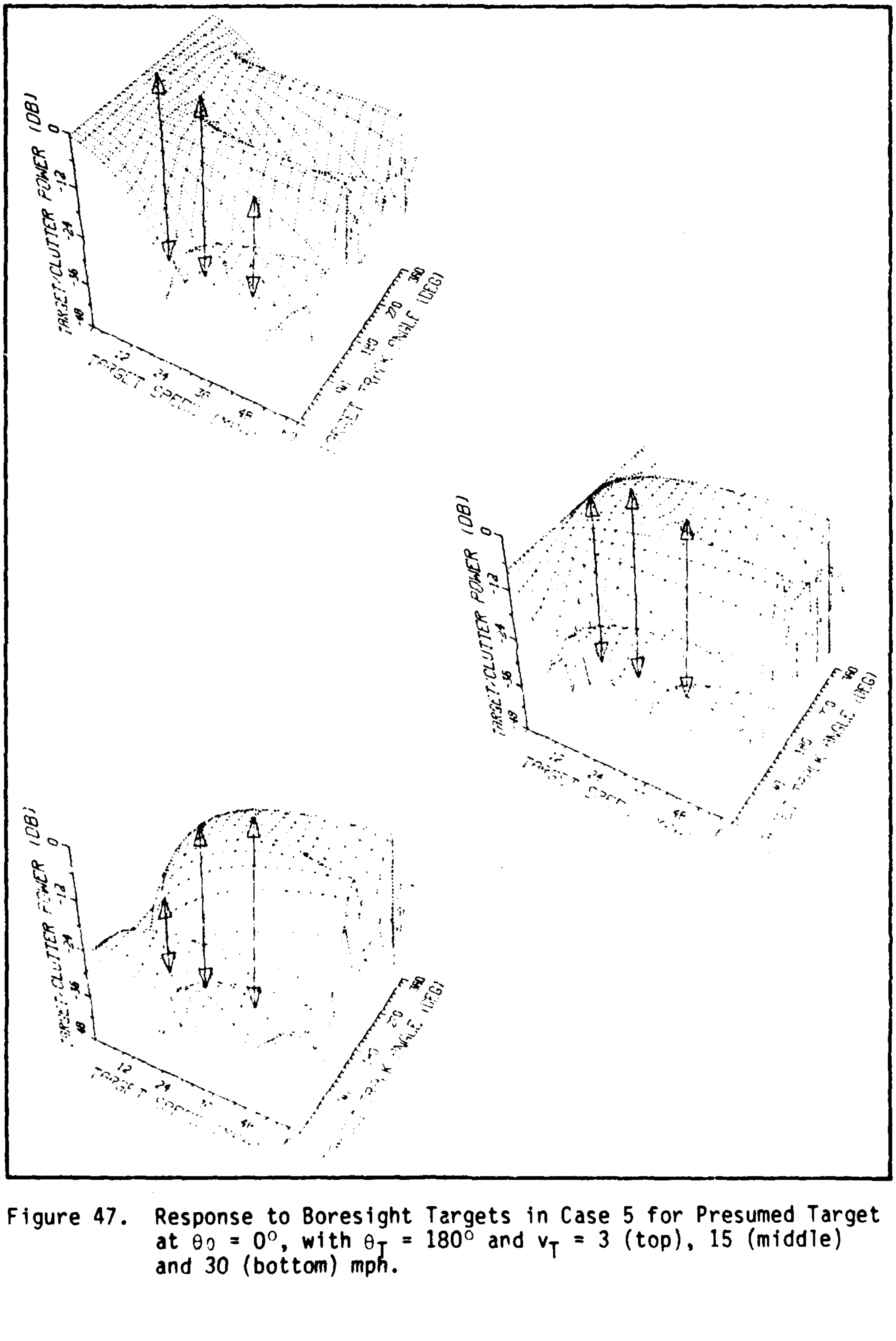

Figure 47. Response to Boresight Targets in Case 5 for Presumed Target at $\theta_0 = 0^\circ$, with $\theta_T = 180^\circ$ and $v_T = 3$ (top), 15 (middle) and 30 (bottom) mph.

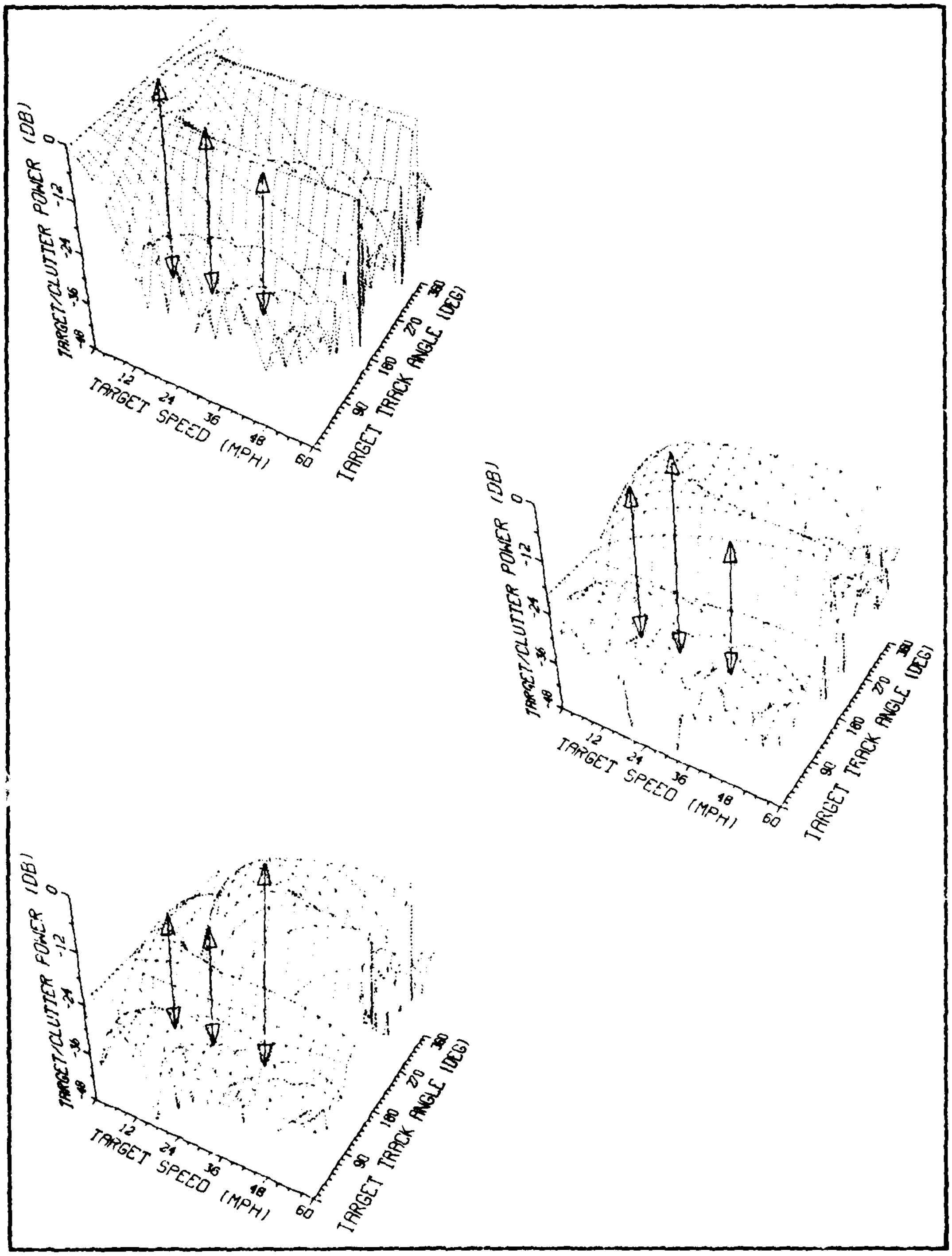

Figure 48. Response to Boresight Targets in Case 6 for Presumed Target at $\theta_0 = 0°$, with $\theta_T = 180°$ and $v_T = 3$ (top), 15 (middle) and 30 (bottom) mph.

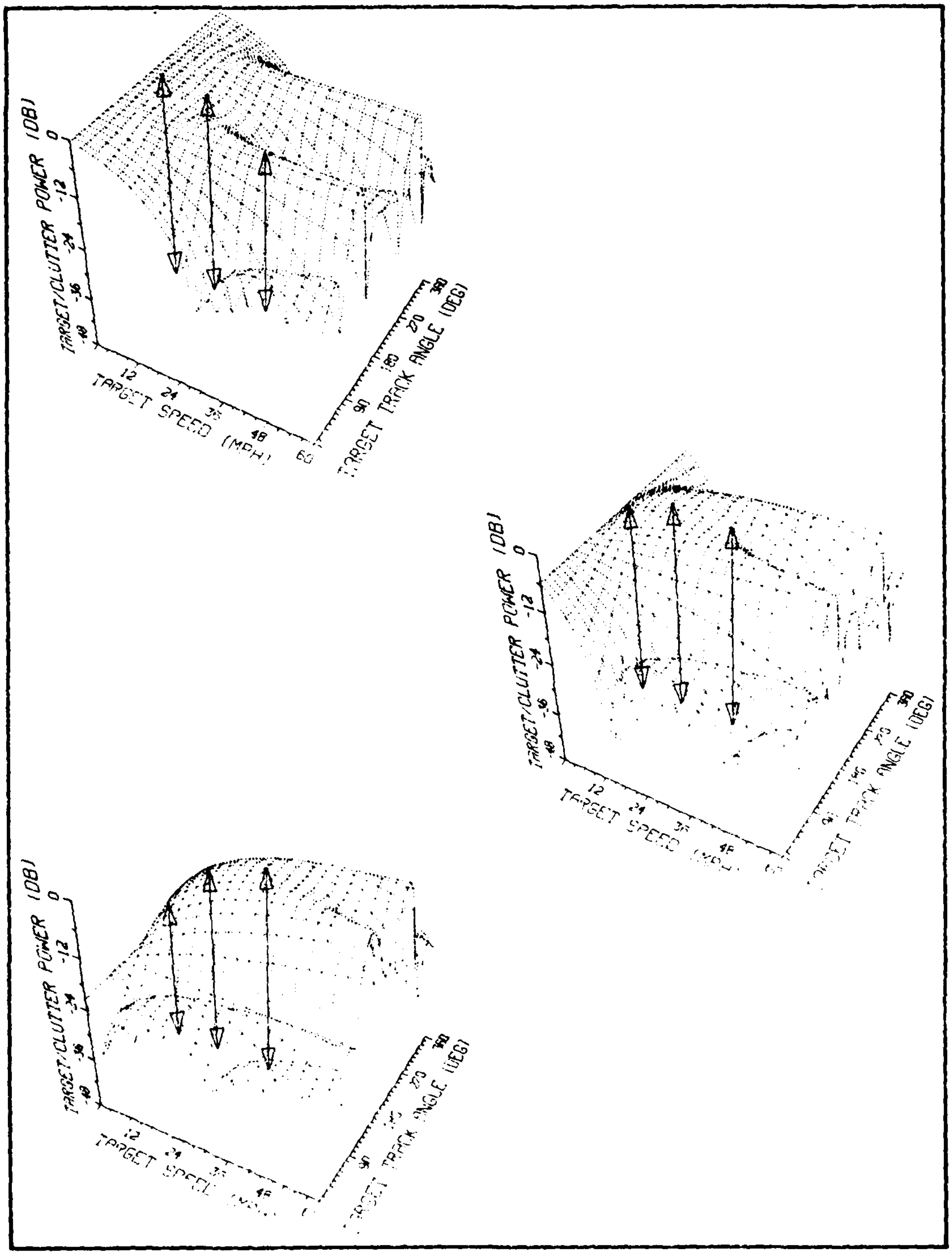

Figure 49. Response to Boresight Targets in Case 7 for Presumed Target at $\theta_0 = 0^{\circ}$, with $\theta_T = 180^{\circ}$ and $v_T = 3$ (top), 15 (middle) and 30 (bottom) mph.

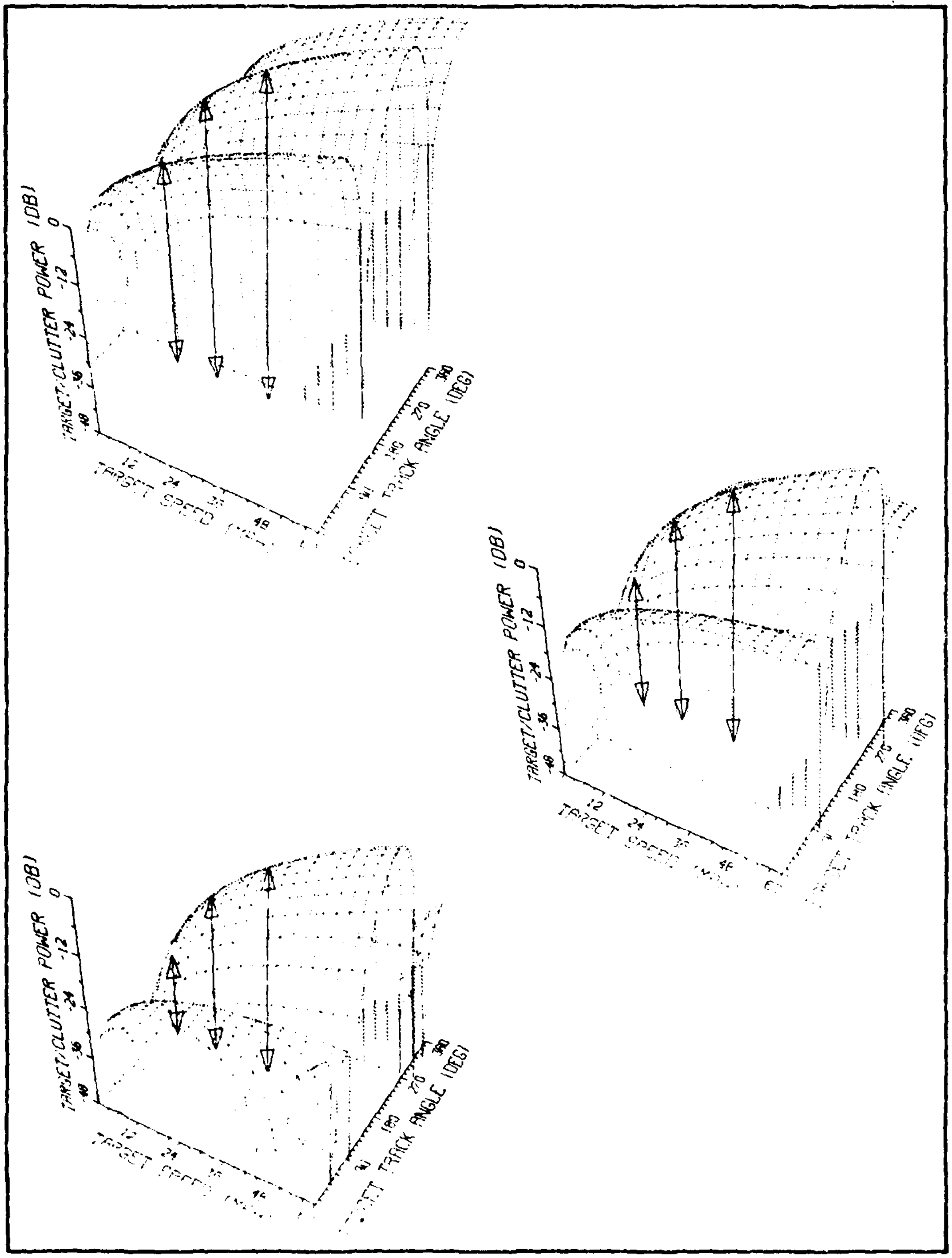

Figure 50. Response to Boresight Targets in Case 8 for Presumed Target at $\theta_0 = 0^\circ$, with $\theta_T = 180^\circ$ and v_T = 3 (top), 15 (middle) and 30 (bottom) mph.

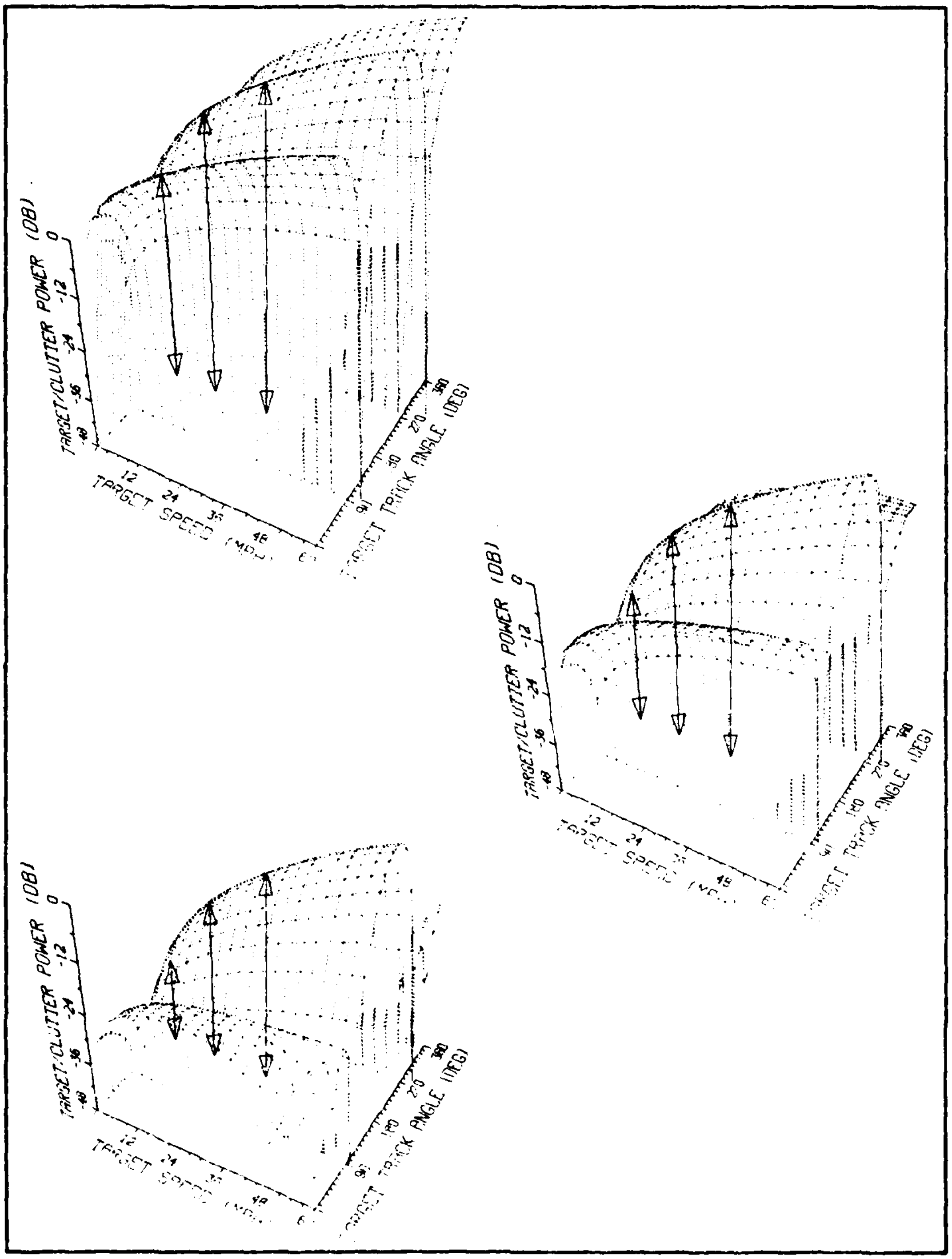

Figure 51. Response to Boresight Targets in Case 9 for Presumed Target at $\theta_0 = 0°$, with $\theta_T = 180°$ and $v_T = 3$ (top), 15 (middle) and 30 (bottom) mph.

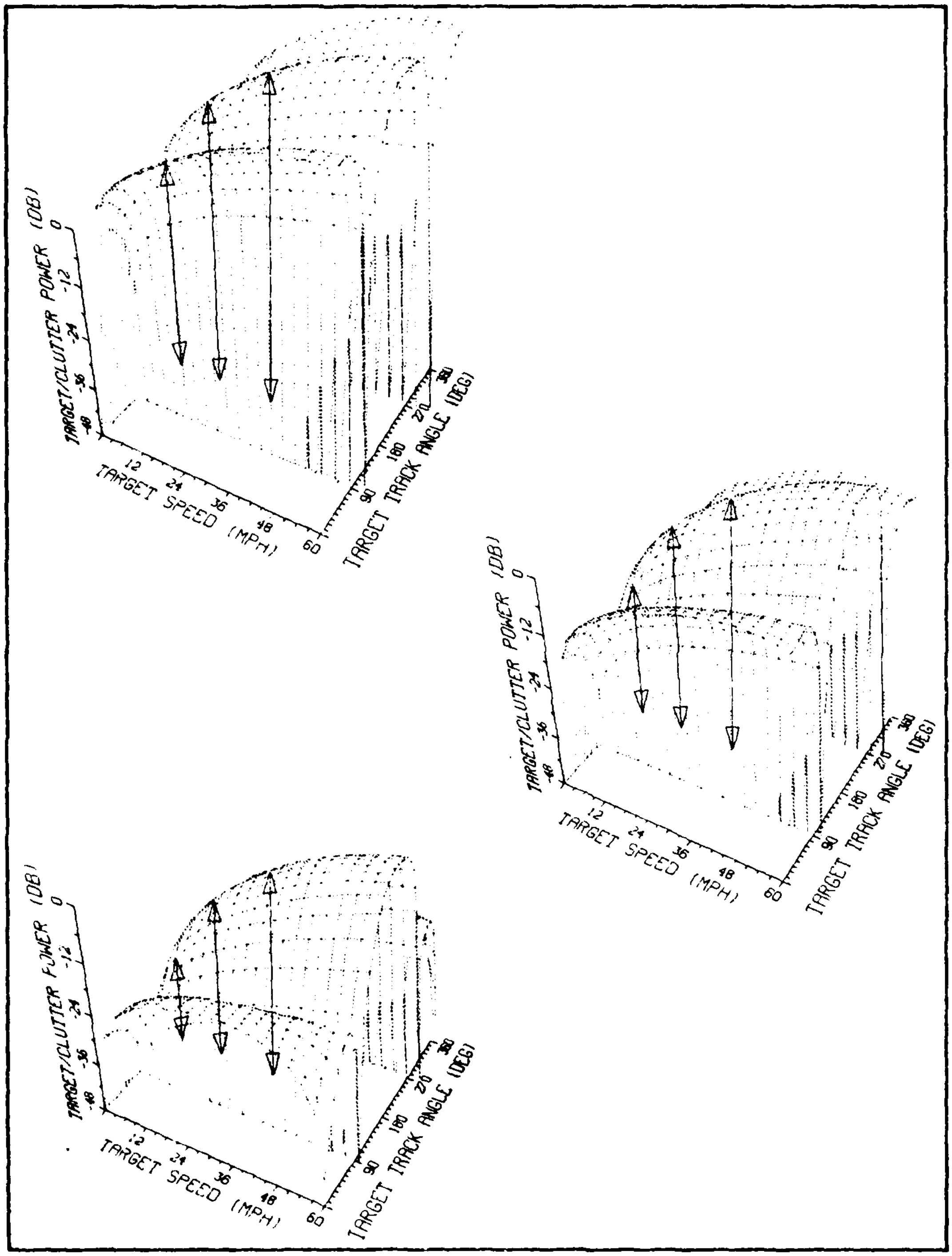

Figure 52. Response to Boresight Targets in Case 10 for Presumed Target at $\theta_0 = 0^{\circ}$, with $\theta_T = 180^{\circ}$ and $v_T = 3$ (top), 15 (middle) and 30 (bottom) mph.

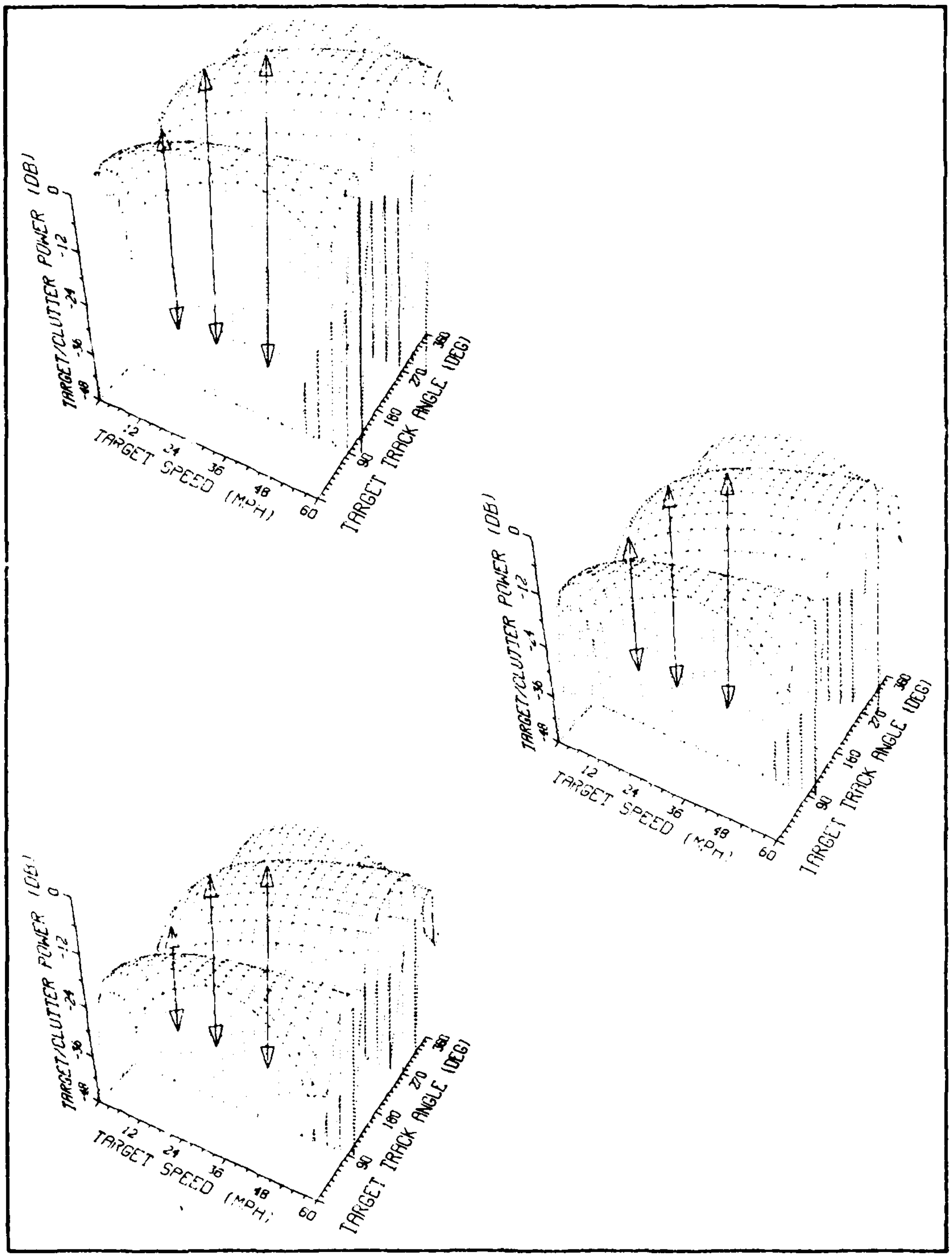

Figure 53. Response to Boresight Targets in Case 11 for Presumed Target at $\theta_0 = 0^\circ$, with $\theta_T = 180^\circ$ and $v_T = 3$ (top), 15 (middle) and 30 (bottom) mph.

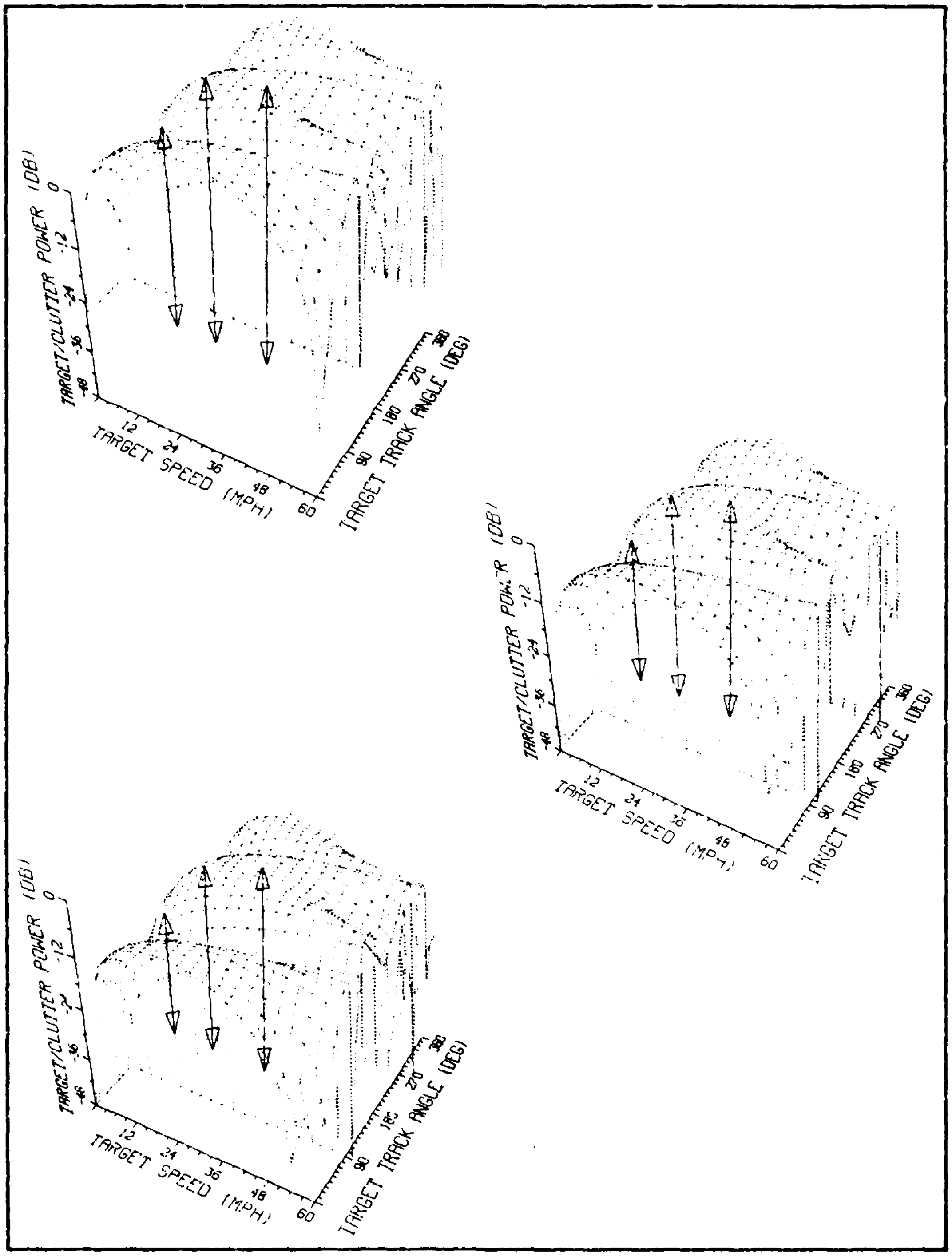

Figure 54. Response to Boresight Targets in Case 12 for Presumed Target at $\theta_0 = 0^o$, with $\theta_T = 180^o$ and $v_T = 3$ (top), 15 (middle) and 30 (bottom) mph.

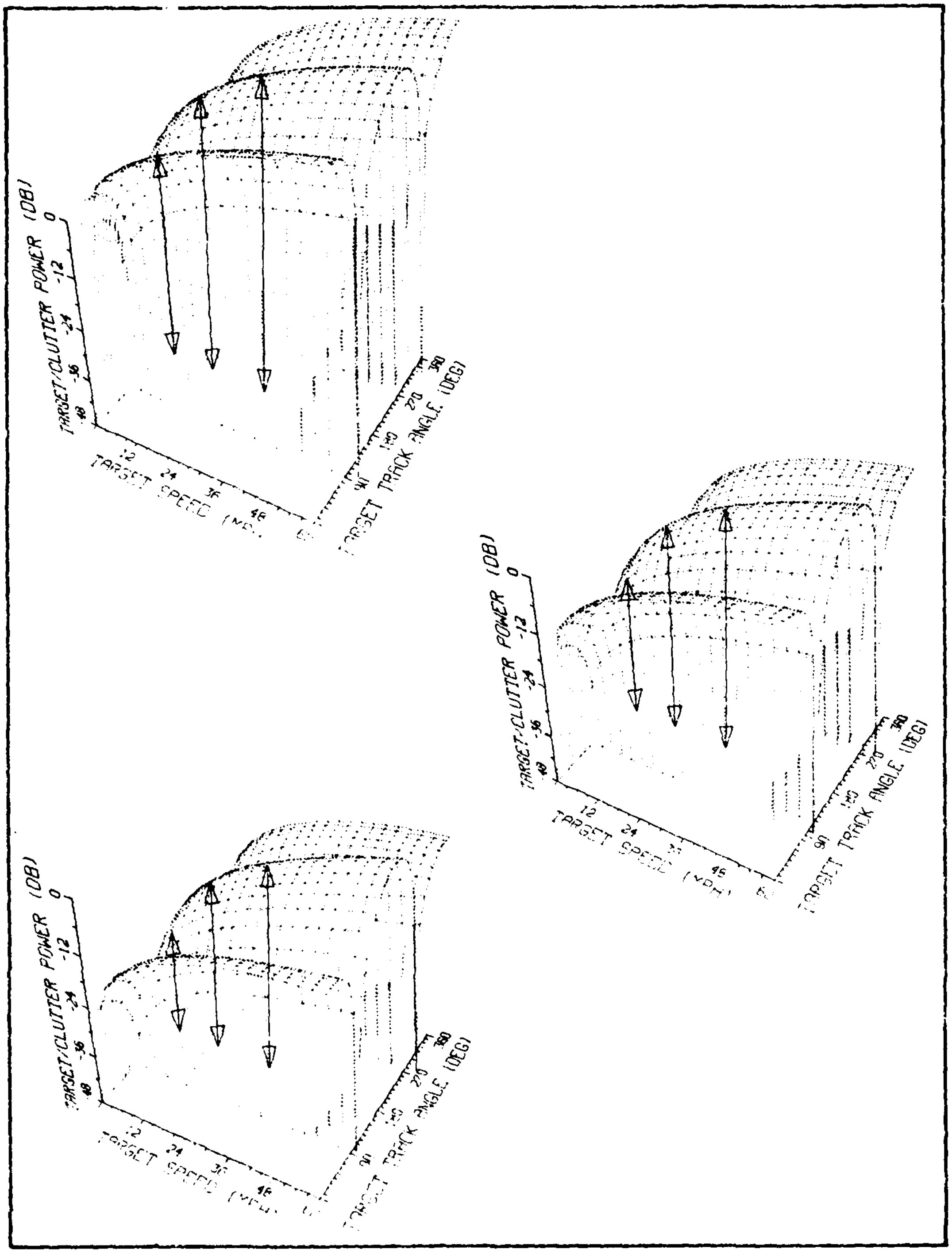

Figure 55. Response to Boresight Targets in Case 13 for Presumed Target at $\theta_0 = 0^{\circ}$, with $\theta_T = 180^{\circ}$ and $v_T = 3$ (top), 15 (middle) and 30 (bottom) mph.

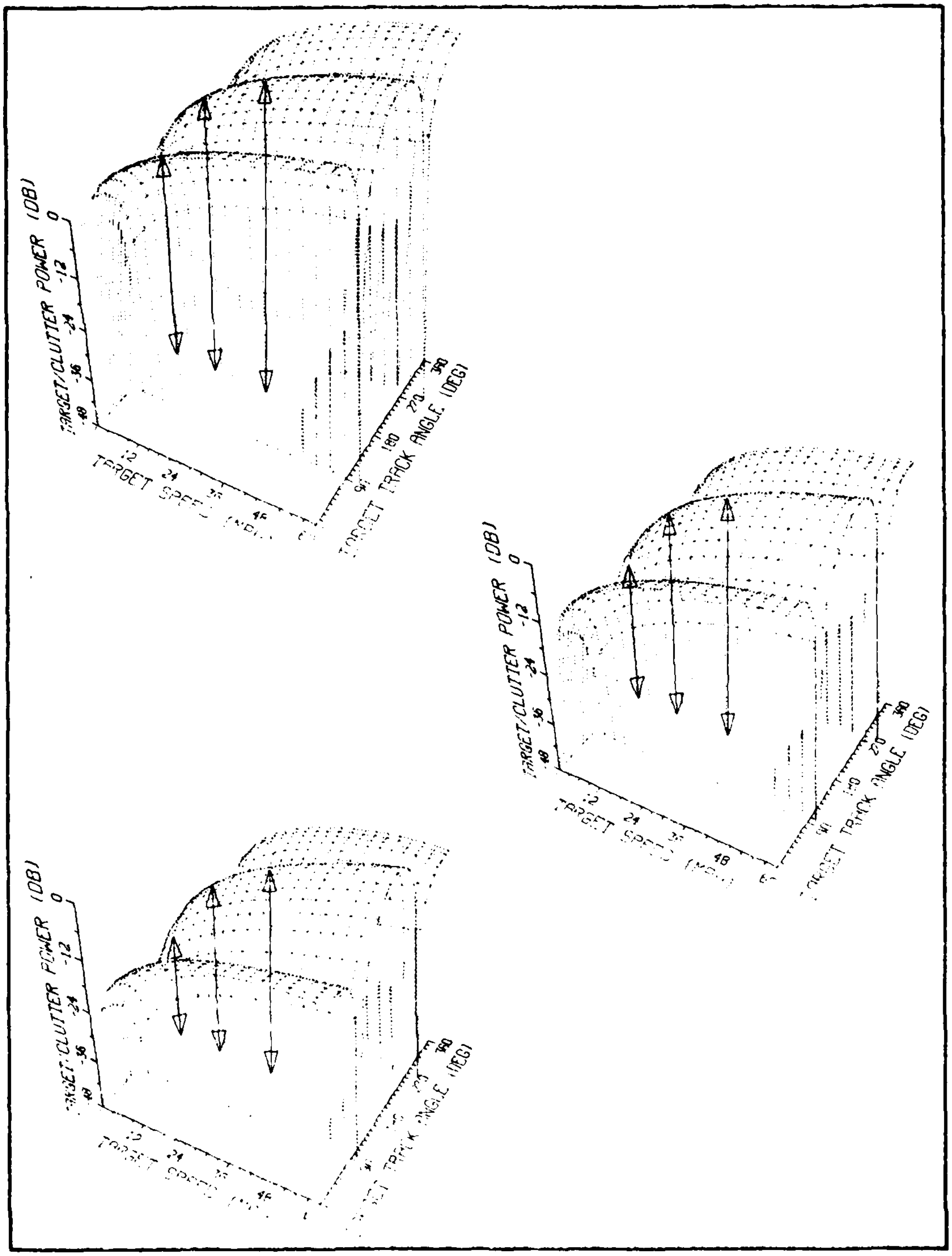

Figure 56. Response to Boresight Targets in Case 14 for Presumed Target at $\theta_0 = 0°$, with $\theta_T = 180°$ and v_T = 3 (top), 15 (middle) and 30 (bottom) mph.

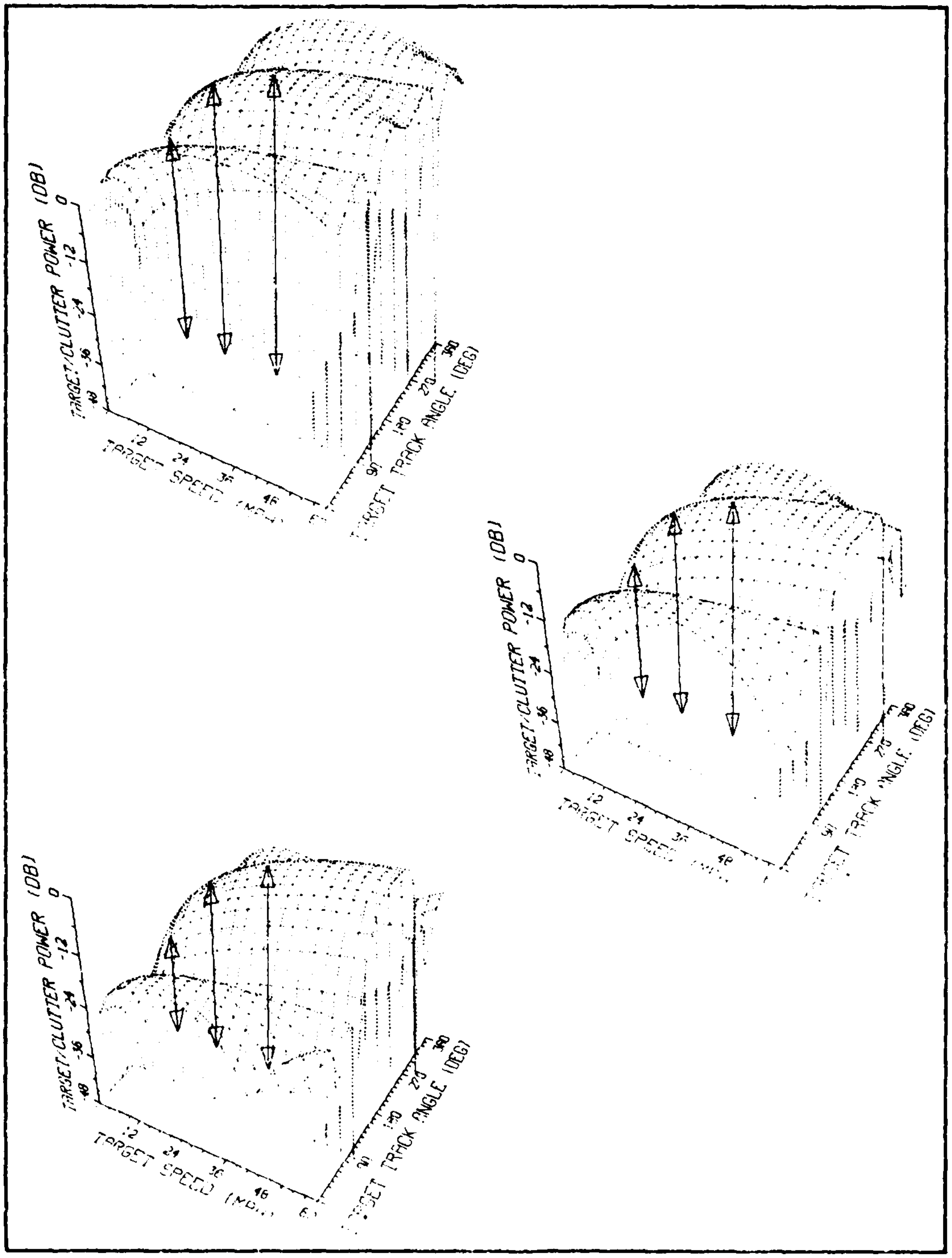

Figure 57. Response to Boresight Targets in Case 15 for Presumed Target at $\theta_0 = 0°$, with $\theta_T = 180°$ and $v_T = 3$ (top), 15 (middle) and 30 (bottom) mph.

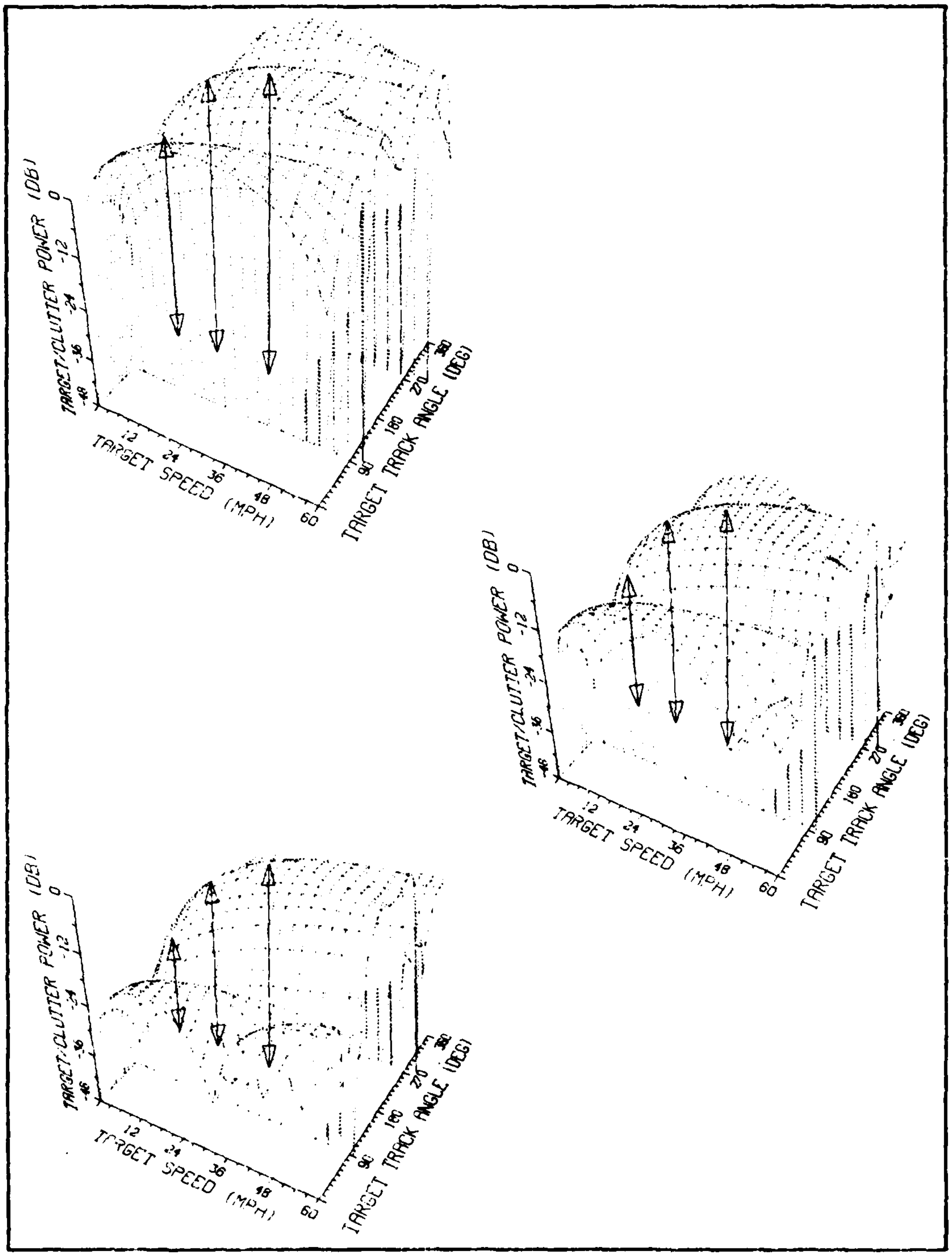

Figure 58. Response to Boresight Targets in Case 16 for Presumed Target at θ_0 = 0°, with θ_T = 180° and v_T = 3 (top), 15 (middle) and 30 (bottom) mph.

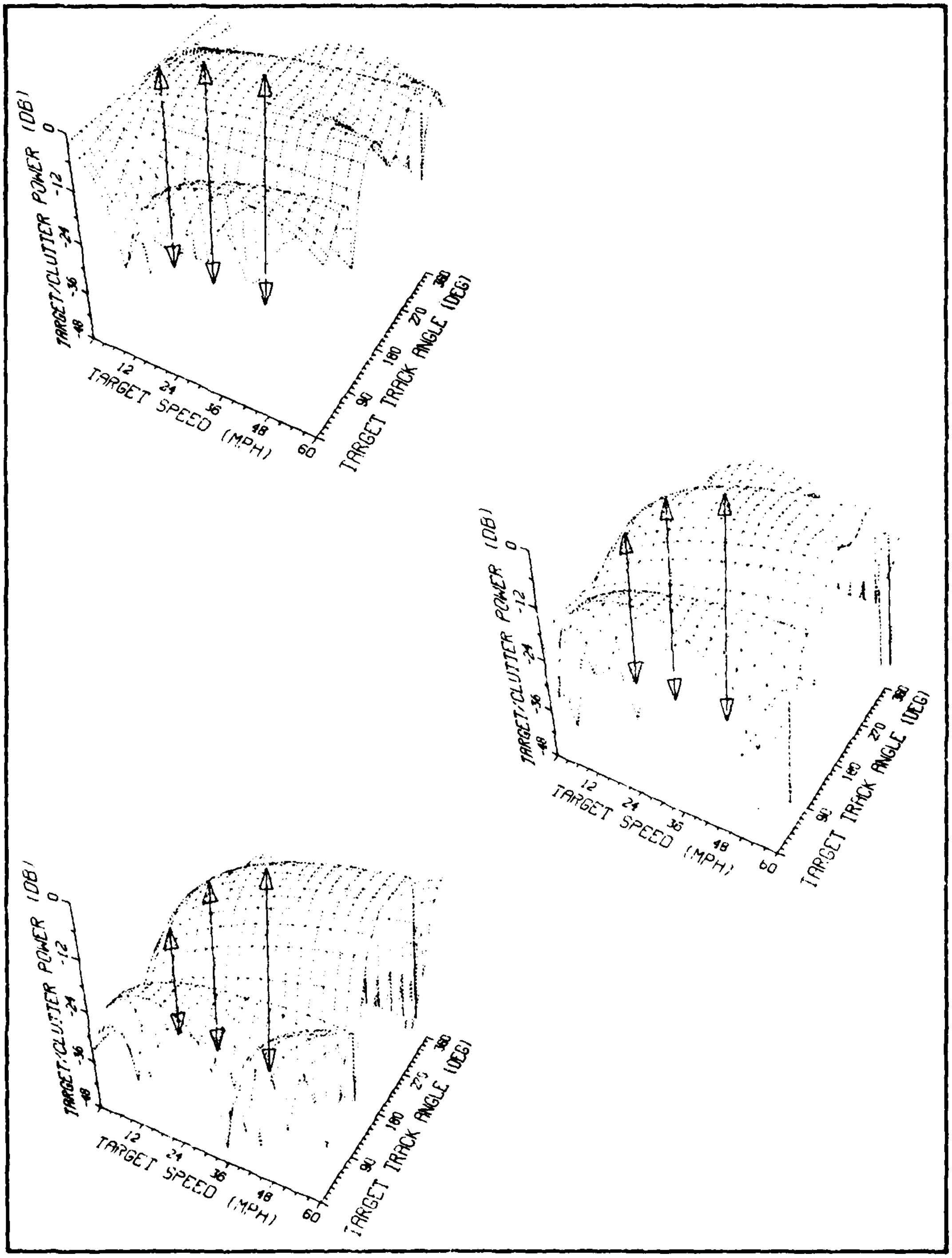

Figure 59. Response to Boresight Targets in Case 17 for Presumed Target at $\theta_0 = 0°$, with $\theta_T = 180°$ and $v_T = 3$ (top), 15 (middle) and 30 (bottom) mph.

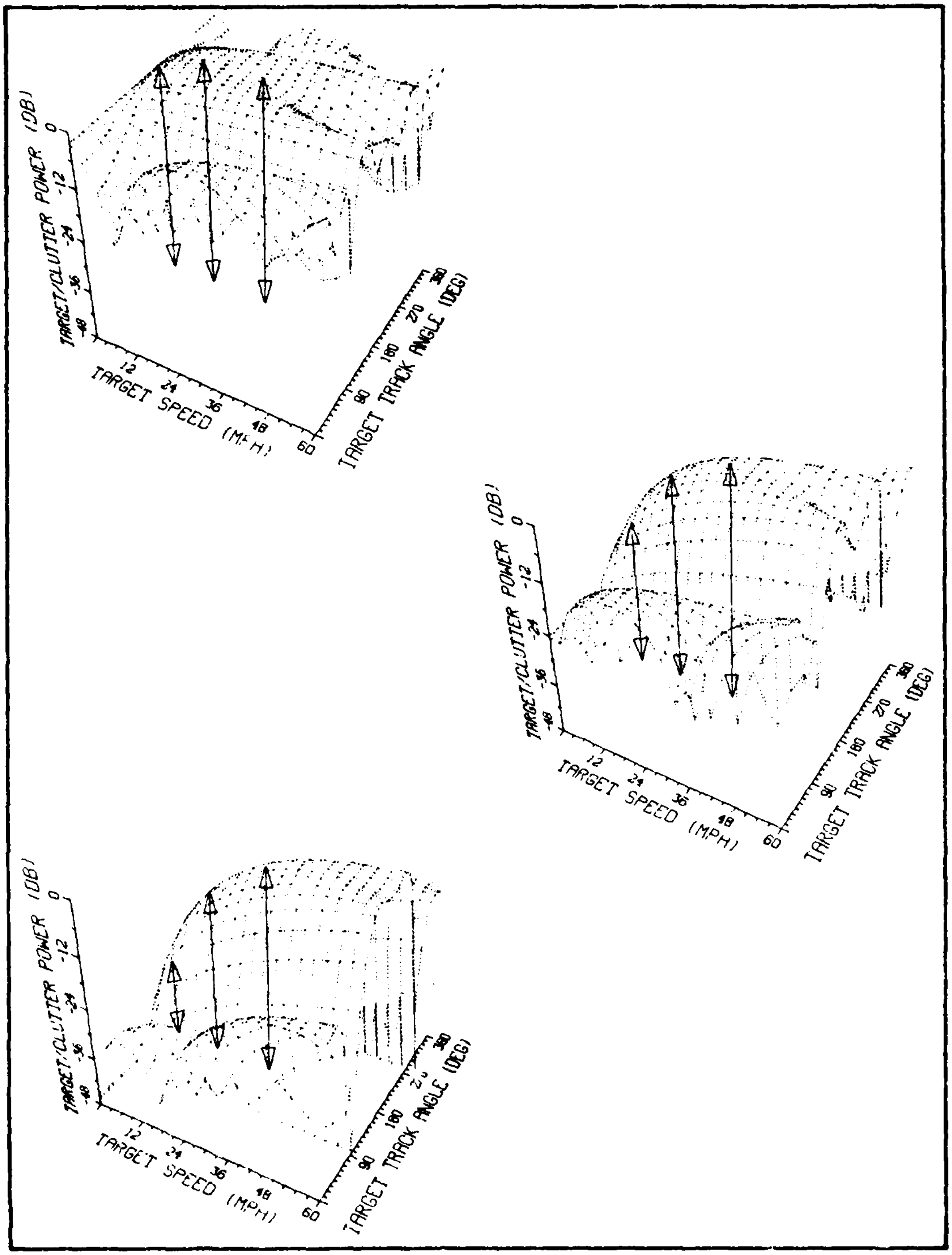

Figure 60. Response to Boresight Targets in Case 18 for Presumed Target at $\theta_0 = 0^o$, with $\theta_T = 180^o$ and v_T = 3 (top), 15 (middle) and 30 (bottom) mph.

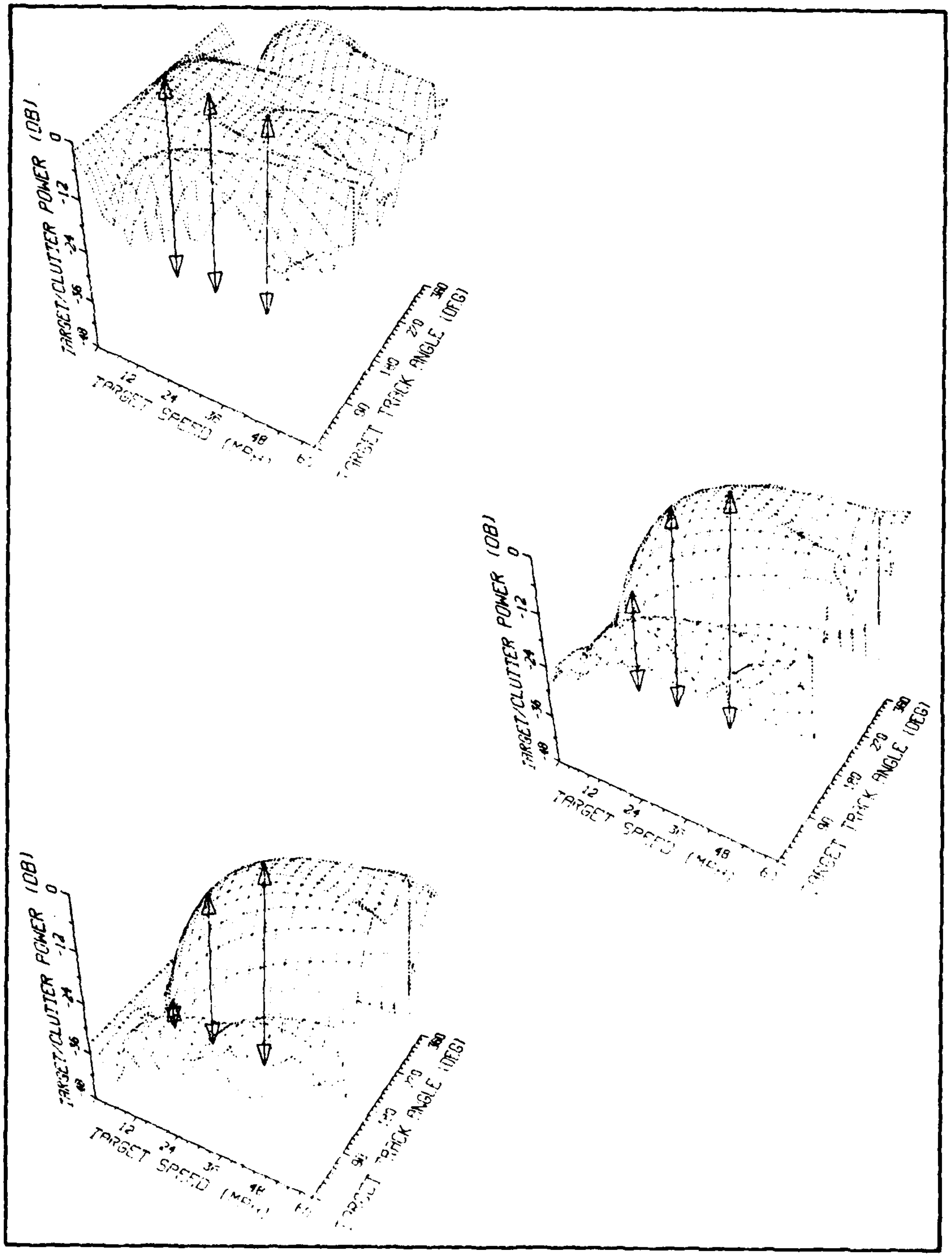

Figure 61. Response to Boresight Targets in Case 19 for Presumed Target at $\theta_0 = 0^\circ$, with $\theta_T = 180^\circ$ and $v_T = 3$ (top), 15 (middle) and 30 (bottom) mph.

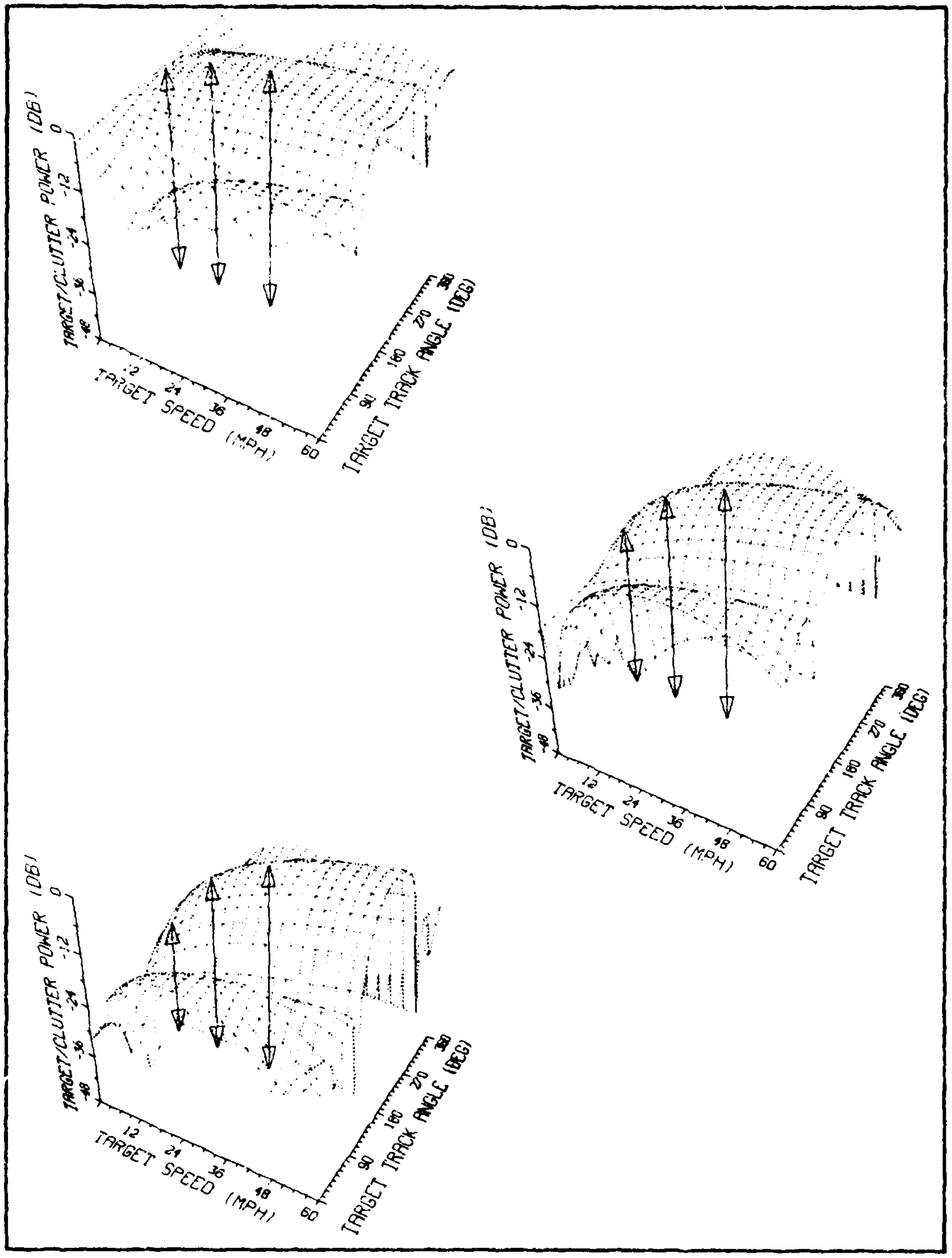

Figure 62. Response to Boresight Targets in Case 20 for Presumed Target at $\theta_0 = 0^o$, with $\theta_T = 180^o$ and $v_T = 3$ (top), 15 (middle) and 30 (bottom) mph.

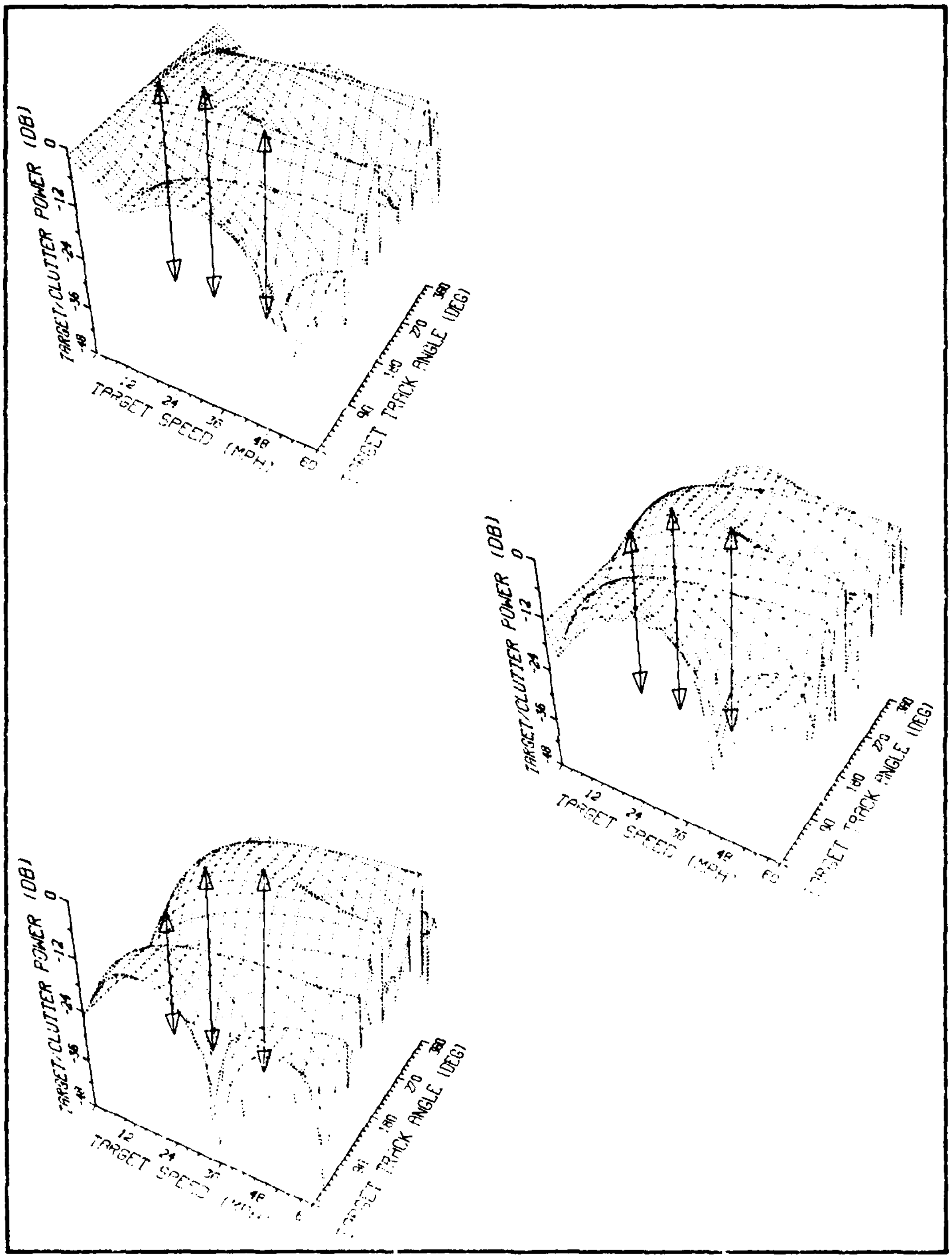

Figure 63. Response to Boresight Targets in Case 2 for Presumed Target at $\theta_0 = 30°$, with $\theta_T = 180°$ and $v_T = 3$ (top), 15 (middle) and 30 (bottom) mph.

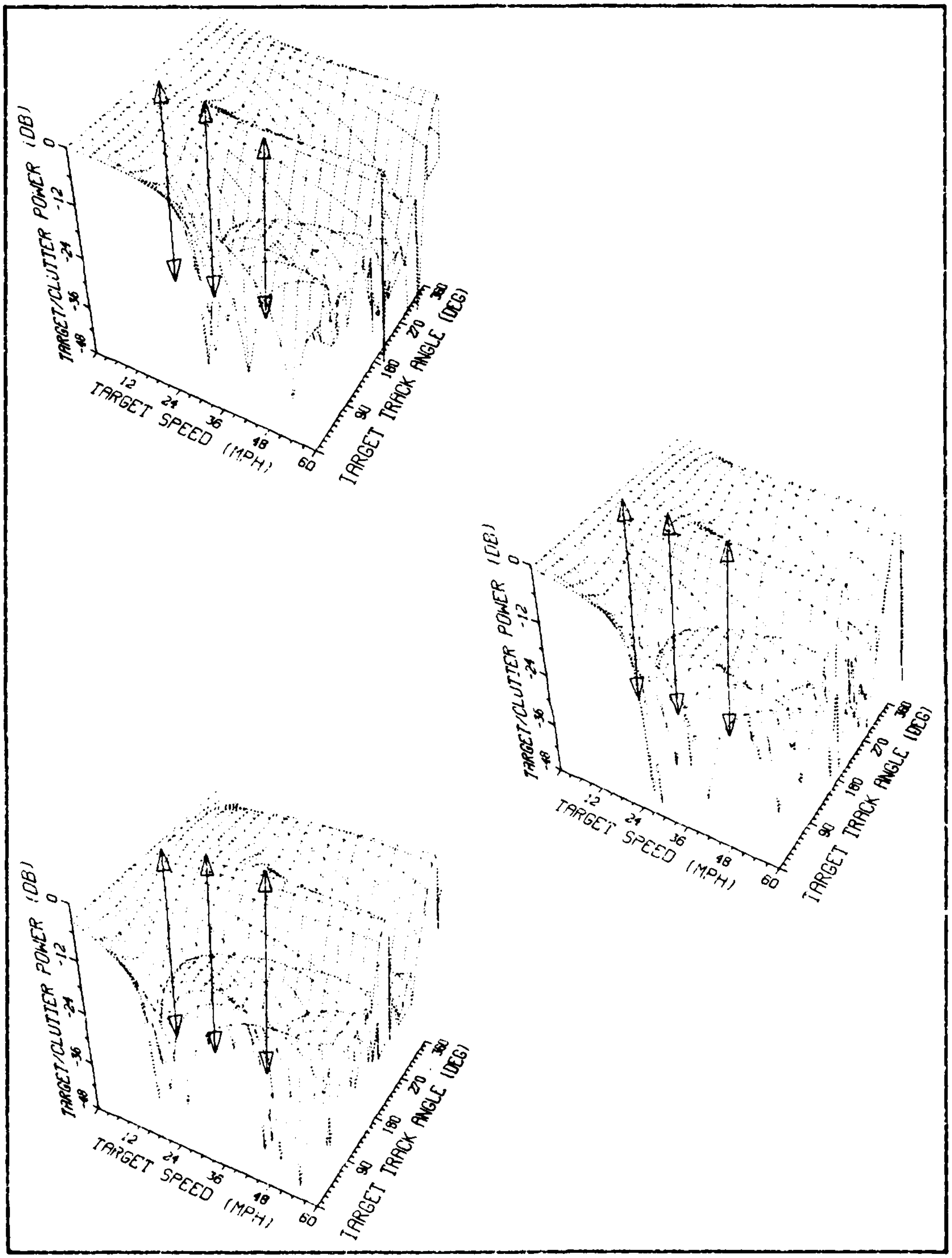

Figure 64. Response to Boresight Targets in Case 2 for Presumed Target at $\theta_0 = 60^\circ$, with $\theta_T = 180^\circ$ and $v_T = 3$ (top), 15 (middle) and 30 (bottom) mph.

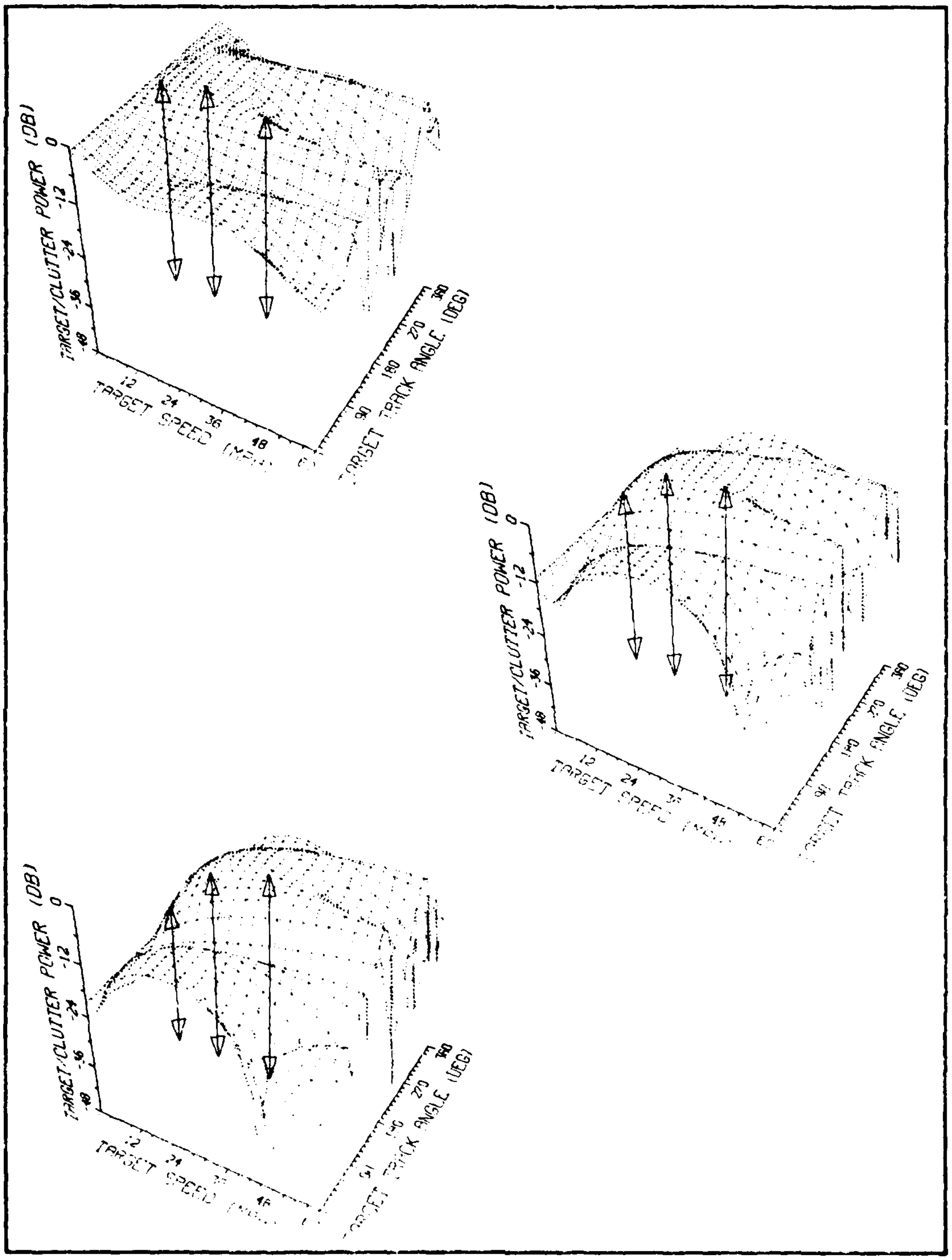

Figure 65. Response to Boresight Targets in Case 7 for Presumed Target at θ_0 = 30°, with θ_T = 180° and v_T = 3 (top), 15 (middle) and 30 (bottom) mph.

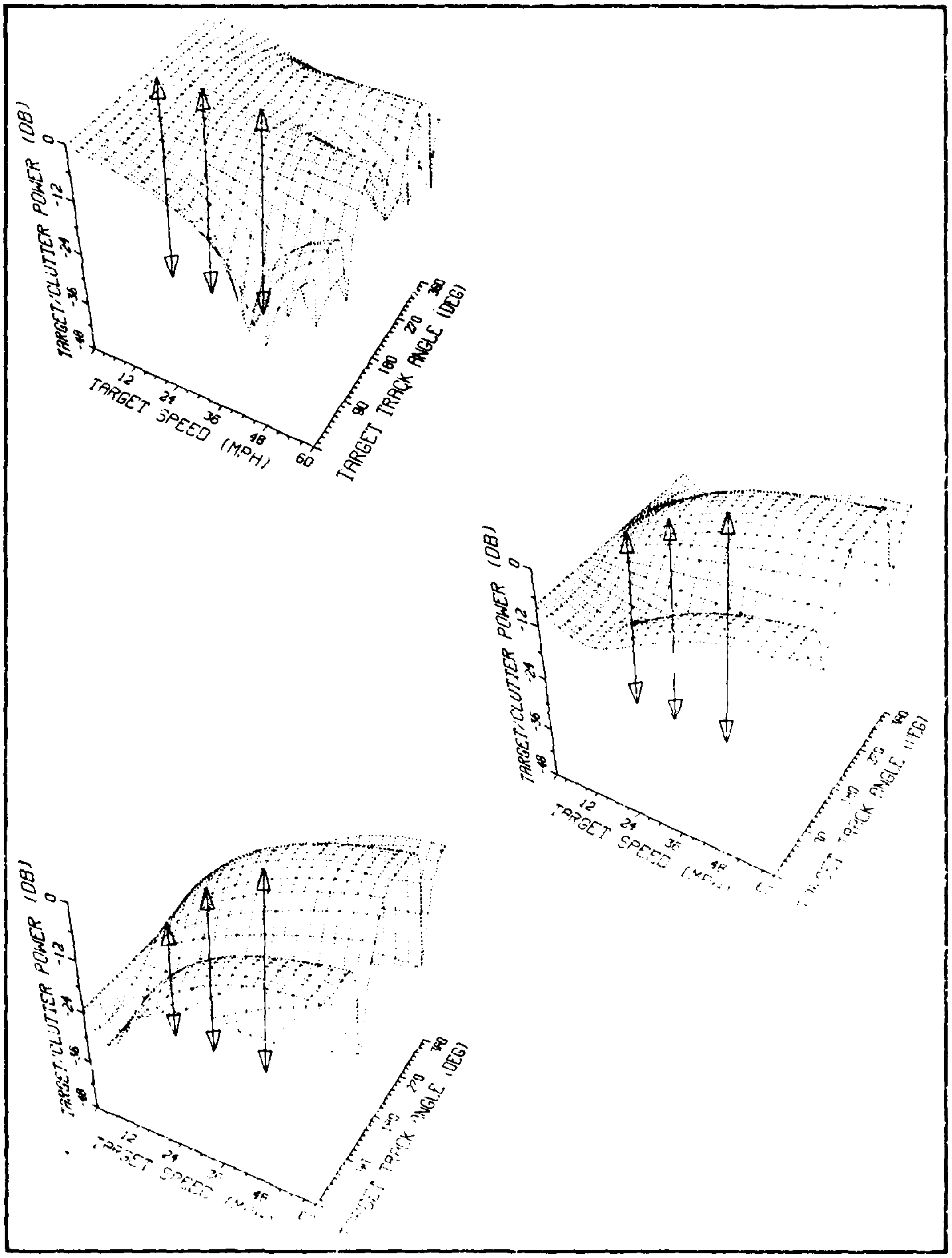

Figure 66. Response to Boresight Targets in Case 17 for Presumed Target at θ_0 = 30°, with θ_T = 180° and v_T = 3 (top), 15 (middle) and 30 (bottom) mph.

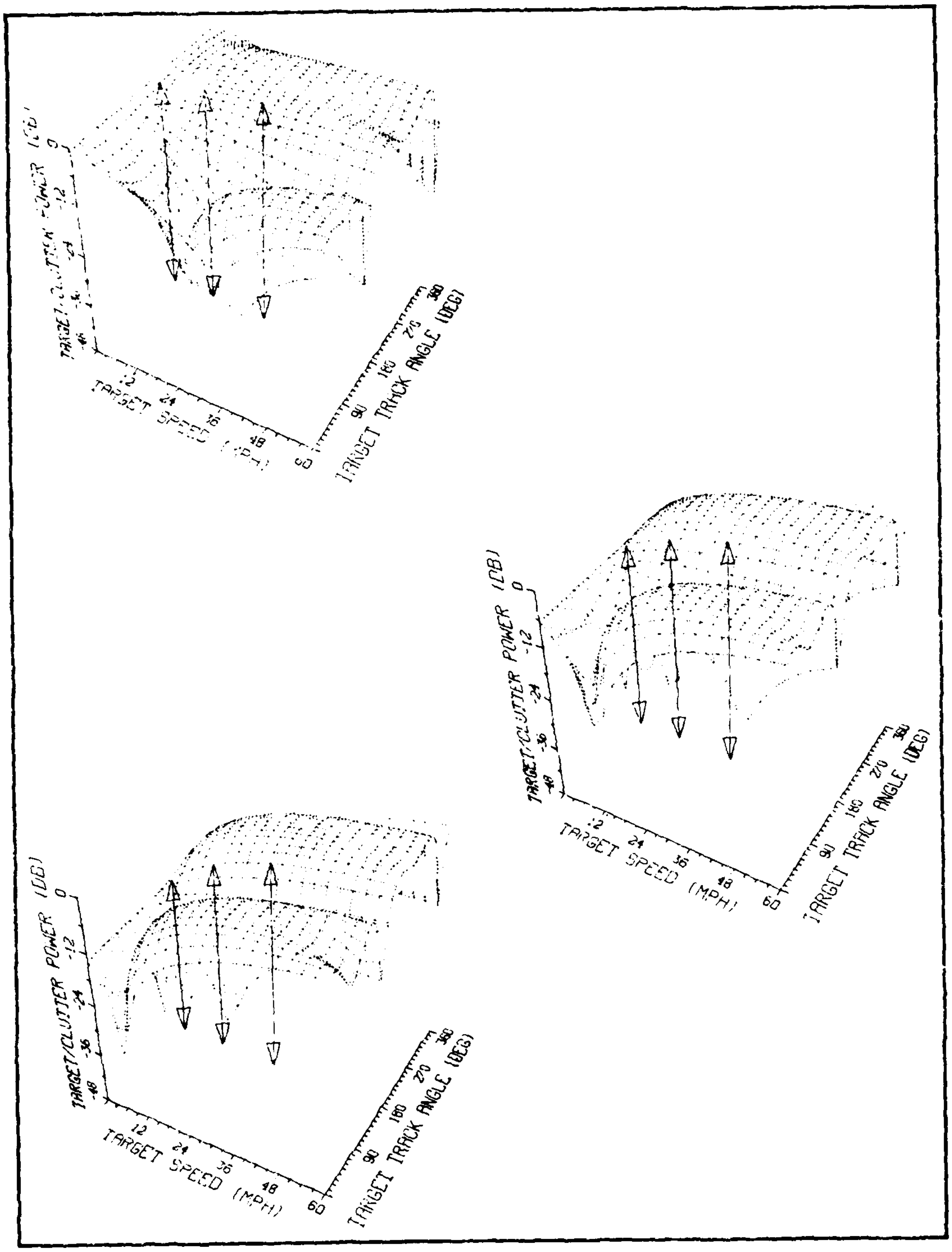

Figure 67. Response to Boresight Targets in Case 20 for Presumed Target at $\theta_0 = 60°$, with $\theta_T = 180°$ and $v_T = 3$ (top), 15 (middle) and 30 (bottom) mph.

V. Summary and Conclusions

Summary

In this work, the conceptualization and analysis of a new kind of synthetic aperture radar for detecting slowly moving targets in severe clutter environments has been done.

The radar consists of a multiplicity of antennas mounted longitudinally along the side of an aircraft which are pulsed sequentially as they are flown through common positions in space. Sequences of pulse returns are collected by each antenna and processed aboard the aircraft to form a multiplicity of synthetic arrays which are coincident in space but are displaced in time. The name applied to this radar in which a multiple of synthetic arrays are "arrested" in space is Multiple Arrested Synthetic Aperture Radar, or MASAR.

Central to the development of this new radar concept is the application of an optimal processing scheme never before applied in a synthetic aperture radar. This processing scheme optimizes the target to clutter power ratio for a given target in known clutter. The scheme treats the target and clutter as quadratic forms, the ratio of which is known to have extremal properties. These extremal properties are used to determine the optimum set of processing weights for MASAR.

Before the optimum weights could be determined, the MASAR target and clutter signal returns had to be formulated such that they could be [illegible] cast into [illegible]dratic form. This was a simple task for the target, [illegible] for the clutter. From basic principles, a new, though rudimen- [illegible] formulation of the cross-power correlation for clutter [illegible] applied to MASAR. This latter effort

is a principal part of this work. Without it, the analysis of MASAR presented here could not have been done.

The work concludes with the presentation of the results of a computer analysis of the performance of MASAR. This performance was investigated for the optimal weights and two other weighting schemes--weights based solely upon the target signal, and weights determined from the binomial coefficients of $(1-x)^{M-1}$ where M is the number of antennas used in the MASAR. The target weights contain maximum information about the target with no information on the nature of the clutter. The binomial weights effectively form MASAR into an M-stage synthetic aperture N-pulse clutter canceller, a subset of which is a two antenna MTI system well known as Displaced Phase Center Antenna, or DPCA.

The analysis was performed by drawing observations from three products of the computer results. The first was a set of curves which depicted relative MASAR improvement; the second, a set of curves which depicted the response of MASAR to the appearance of a target moving at the presumed velocity but at azimuths other than presumed; and the third, a set of three-dimensional surfaces which depicted the response of the optimal MASAR processor to the appearance of other targets at the presumed azimuth.

Conclusions

The analysis shows that the performance of MASAR with the optimum processor far surpasses that of the target and binomial processing schemes in terms of its improvement of the target to clutter power ratio for slowly moving targets. For example, for a target at a range of ten miles moving three miles per hour directly toward the MASAR flight path, the improvement of the optimum processor relative to the target and the

binomial processors is as follows:

M	N	length of synthetic aperture (feet)	Relative Improvement Optimum to Target (dB)	Optimum to Binomial (dB)
2	12	6	15	15
3	8	4	36	77
4	6	3	45	144+

where M and N are the number of antennas and number of pulses per antenna, respectively. This performance becomes less pronounced for more rapidly decorrelating clutter, but improves substantially with increasing numbers of antennas and longer apertures; moreso, it seems, with added antennas.

The performance also increases with longer time delay between the generation of succeeding synthetic apertures. For example, for the three antenna case just mentioned (but using broader beamwidth antennas), the following improvement was observed for the optimum processor tuned to a three mile per hour target relative to itself when tuned to a fixed target:

Inter-SAR Spacing (pulses)	Relative Improvement (dB)
1	16
7	33
13	38

The performance was also seen to increase with narrower real antenna beamwidths, but narrower beamwidths could become a limiting factor in the generation of longer synthetic apertures.

The optimum MASAR processor does an excellent job of steering the peak response toward the presumed target. (In one case it was seen to suppress a grating lobe; see Figure 42.) Its response to targets not within the synthetic mainbeam falls off very rapidly with long synthetic apertures, similar to the beamsharpening obtained from long antenna

arrays. With care to choose the pulse repetition frequency to avoid grating lobes, the location of slowly moving targets can be accurately determined.

From the three-dimensional surfaces which depict the response of MASAR to other targets at the presumed azimuth, it can be seen that the performance of MASAR with two antennas is poor for very slow targets. However, the performance of MASAR with three and four antennas becomes very good for very slow targets.

These response surfaces provide strong evidence to suggest that with long synthetic arrays, very good discrimination of the target's velocity component parallel to the MASAR boresight can be achieved with a simple threshold test of the output of the optimum MASAR processor. For example, from the response surfaces for Case 11 (Figure 53) where only four antennas and six pulses were used, the response for the target presumed to be moving directly toward the MASAR platform at three miles per hour rises more than 48 dB above the response for a fixed target or for a target moving parallel to the track of the MASAR platform.

Recognizing the limitations of the analysis performed here, nonetheless, the optimum MASAR scheme shows promise as an improved airborne slowly moving target indicating radar.

VI. Recommendations for Further Study

The reader will, at this point, realize that there seems to be an almost limitless number of variations on the work that's been presented. Some of these variations are proposed here.

Some simple extensions of this work would be to study the effect of varying the other system parameters on the performance of MASAR; the underlying question being, "how can the system parameters be preselected to achieve peak performance?" Those not varied were the radar frequency, pulse repetition frequency, platform velocity and pulsewidth. The range parameter was not varied either; but, upon inspection of the generating equations for the target signal vector and clutter cross-power correlation matrix, it can be seen that the range becomes a factor only when attempting to generate long synthetic apertures. Certainly, the performance of MASAR with very long synthetic apertures would be of interest.

More difficult, challenging extensions to this work would be the consideration of any one, or combinations of the proposals below.

1. More complicated targets: consider targets that fluctuate and have spatial extent; consider multiple targets.

2. More complicated clutter: try adding spatial correlation; e.g., instead of (58) where the spatial correlation is totally uncorrelated everywhere except at point, try incorporating gaussian spatial correlation:

$$\langle \chi_1 \chi_2^* \rangle = e^{-\frac{(\tau_1 - \tau_2)^2}{2T^2}} \, e^{-\frac{(x_1 - x_2)^2 + (y_1 - y_2)^2}{2L^2}} \tag{165}$$

where L is the spatial correlation interval. Further, L may be chosen

to have different components in both the X and Y directions; i.e.,

$$\langle \chi_1 \chi_2^* \rangle = e^{-\frac{(\tau_1 - \tau_2)^2}{2T^2}} e^{-\left[\frac{(x_1-x_2)^2}{2L_x^2} + \frac{(y_1-y_2)^2}{2L_y^2}\right]} \tag{166}$$

The sensitivity of the MASAR response to varying spatial correlations could then be examined. Any other choice could be made for $\langle \chi_1 \chi_2^* \rangle$ so long as it satisfied the properties of a correlation function. A topological weighting N(x,y) could be included also. Whatever the choice, serious consideration should be given to the stochastic properties propounded in the introductory section to the clutter model (pp. 35-38).

Clutter with inherent motion could also be addressed to simulate the effects of blowing trees or variable sea states. Perhaps a way to do this would be to use a v_T that is some function of time in (53) and (54) in conjunction with (60).

3. Noise: the analysis could be extended to include noise. First, consider additive zero mean white gaussian noise. Add the noise term to (42). Proceed by optimizing the target to mean clutter-plus-noise power ratio.

A further extension would be to include nonwhite noise in the analysis. Nonwhite noise is considered to be the sum of a white noise component and a colored noise component. Antennas and RF components in the radar receiver are known to shape the noise spectrum. Also, interfering targets or jammers are sources of nonwhite noise in radar.

4. More complicated antennas: incorporate antennas that have more variation in their patterns, both in amplitude and phase. An error analysis could be performed to determine the effects on achievable performance when the antenna patterns are imprecisely known.

5. Second time around returns: extend the analysis to include second time around clutter returns [3:350-352] in the clutter cross-power correlation. Since MASAR processes a multiplicity of pulses for each range cell, the optimization should be able to compensate for this additional clutter. The degree of effectiveness for varying system parameters (antennas, pulses, etc.) would be interesting to study. More specifically, it would be interesting to study what effect this added clutter has on MASAR improvement. (Note that, with the choice of parameters used in this study, a seven antenna MASAR would begin to have problems at a range of ten miles. Succeeding antennas would receive energy from the preceeding pulse which came from scatterers in the range bin of interest.)

6. Switching transmitter frequencies between synthetic apertures: the problem with second time around returns might be alleviated by a MASAR scheme which transmitted different frequencies on each antenna. This scheme might have other interesting effects which could be studied.

7. RF and PRF instabilities: study the effects of instabilities in the master oscillator and pulse repetition section of the transmitter on MASAR performance.

8. Other radar waveforms: The analysis in this work was greatly simplified by the choice of a gaussian-shaped radar pulse. A more ambitious project would be to investigate other waveforms. For example, the effects of a linear frequency modulated pulse, or a long pulse with pulse compression, on achievable MASAR performance could be studied.

9. Build MASAR: construct an actual system and test the MASAR concept.

Bibliography

1. Fred M. Staudaher, "Airborne MTI", Chapter 18 in the Radar Handbook, Merrill I. Skolnik, ed., McGraw-Hill, New York: 1970.

2. B. E. Nichols, ed., "Multiple Antenna Surveillance Radar (MASAR) Experiment Phase I Concept Validation System," Lincoln Laboratories, Massachusetts Institute of Technology, TST-16, 13 January 1978.

3. Fred E. Nathanson, Radar Design Principles, McGraw-Hill, New York: 1969.

4. William W. Schrader, "MTI Radar," Chapter 17 in the Radar Handbook, Merrill I. Skolnik, ed., McGraw-Hill, New York: 1970.

5. G. N. Tsandoulas, "Tolerance Control in an Array Antenna," Microwave Journal, Vol. 20, No. 10, October 1977, pp. 24ff.

6. Kiyo Tomiyasu, "Tutorial Review of Synthetic-Aperture Radar (SAR) With Applications to Imaging of the Ocean Surface", Proceedings of the IEEE, Vol. 66, No. 5, May 1978, pp. 567-583.

7. Carlyle J. Sletten and F. Sheppard Holt, Air Force Cambridge Research Laboratories, Microwave Physics Laboratory, Private Communication (1975).

8. Walter Chudleigh and Stephen Moulton, Control Data Corporation, Private Communication (1975).

9. Felix R. Gantmacher, A Theory of Matrices (1954, in Russian) translated into English as a two volume set entitled The Theory of Matrices, by K.A. Hirsch, Chelsea Publishing Co., New York, 1959, Vol. 1.

10. ________________, and M.G. Krein, Oscillation Matrices and Kernels and Small Vibrations of Dynamic Systems, second edition, Moscow: Gostekhizdat, 1950. (In Russian).

11. D. K. Cheng and F. I. Tseng, "Gain Optimization for Arbitrary Antenna Arrays", IEEE Transaction on Antennas and Propagation, AP-13, No. 6, November 1965, pp. 973-974.

12. ________________________, "Maximisation of Directive Gain for Circular and Elliptical Arrays", Proceedings of the IEE (England), Vol. 114, No. 5, May 1967, pp. 589-596.

13. Roger F. Harrington, "Antenna Excitation for Maximum Gain," IEEE AP-13, No. 6, November 1965, pp. 896-903.

14. John F. McIlvenna and Charles J. Drane, "Gain Maximization and Controlled Null Placement Simultaneously Achieved in Aerial Array Patterns", AFCRL-69-0257, June 1969. Also published in, The Radio and Electronic Engineer, Vol. 39, No. 1, pp.49-57, January 1970.

15. ____________________, "Maximum Gain, Mutual Coupling and Pattern Control in Array Antennas", The Radio and Electronic Engineer, Vol. 41, No. 12, December 1971, pp. 569-572.

16. William B. Goggins, Jr. and John K. Schindler, "Processing for Maximum Signal-to-Clutter in AMTI Radars", AFCRL-TR-74-0577, 19 November 1974.

17. D. O. North, "Analysis of the Factors Which Determine Signal/Noise Discrimination in Radar," Proc. IRE, Vol. 51, July 1963, pp. 1016-1028.

18. J. L. Lawson and G. E. Uhlenbeck, Threshold Signals, MIT Radiation Laboratory Series, Vol. 24, McGraw-Hill, New York: 1950.

19. J. V. Difranco and W. L. Rubin, Radar Detection, Prentice-Hall, Englewood Cliffs, NJ: 1968.

20. Gwilym M. Jenkins and Donald G. Watts, Spectral Analysis and its Applications, Holden-Day, San Francisco: 1968.

21. Donald G. Childers, ed., Modern Spectrum Analysis, IEEE Press, New York: 1978.

22. Petr Beckmann and Andre Spizzicino, The Scattering of Electromagnetic Waves From Rough Surfaces, Macmillan, New York: 1963.

23. Julius Adams Stratton, Electromagnetic Theory, McGraw-Hill, New York: 1941.

24. A. M. Yaglom, An Introduction to the Theory of Stationary Random Functions, translated and edited by Richard A. Silverman, Prentice-Hall, Englewood Cliffs, NJ:1962.

25. Eugene Wong, Stochastic Processes in Information and Dynamical Systems, McGraw-Hill, New York: 1971.

26. Athanasios Papoulis, The Fourier Integral and its Appli ations, McGraw-Hill, New York: 1962.

27. Milton Abramowitz and Irene A. Stegun, Handbook of Mathematical Functions, National Bureau of Standards, U.S. Government Printing Office, Washington D.C.

28. E. Oran Brigham, The Fast Fourier Transform, Prentice-Hall, Englewood Cliffs, NJ: 1974.

29. Daniel T. Finkbeiner, II, Introduction to Matrices and Linear Transformations, second edition, Freeman, San Francisco: 1966.

30. Germund Dahlquist, and Ake Bjorck, Numerical Methods, translated by Ned Anderson, Prentice-Hall, Englewood Cliffs, NJ: 1974.

31. Theodore C. Cheston and Joe Frank, "Array Antennas," Chapter 11 in the Radar Handbook, Merrill I. Skolnik, ed., McGraw-Hill, New York: 1970.

32. Philip J Davis and Philip Rabinowitz, Methods of Numerical Integration, Academic Press, New York: 1975.

Appendix A

Extremal Properties Of The Ratio Of Two Quadratic Forms : A Special Case

In this appendix, the extremal properties of the ratio

$$\frac{x^\dagger A x}{x^\dagger B x}$$

will be addressed for the special case when $A = aa^\dagger$ and B is hermitian and positive definite. Here, both x and a are N X 1 column vectors. Complex-valued elements are assumed throughout. The dagger, †, denotes the conjugate-transpose.

The reader is referred to reference [9:317-326] wherein it is shown that the maximum value of the ratio of two quadratic forms is the dominant eigenvalue of the generalized eigenproblem

$$Ax = \lambda Bx \tag{A.1}$$

The ratio can be obtained by premultiplying (A.1) by the vector $x^\dagger$

$$x^\dagger A x = \lambda x^\dagger B x \tag{A.2}$$

and then dividing by the scalar $x^\dagger Bx$

$$\frac{x^\dagger A x}{x^\dagger B x} = \lambda \tag{A.3}$$

This ratio attains its maximum, λ_D, equal to the dominant eigenvalue of (A.1), when x is the eigenvector, x_D, associated with λ_D.

It will be shown here, for $A = aa^\dagger$, and B Hermitian and positive definite, that (A.1) has only one nonzero eigenvalue; it is equal to $a^\dagger B^{-1} a$, is dominant, and has associated eigenvector $B^{-1}a$ [12:section 10].

First, the following theorem will be proven:

Theorem: If P and Q are respectively m x n and n x m matrices, then

$$(-1)^n\lambda^n\det(PQ-\lambda I_m) = (-1)^m\lambda^m\det(PQ-\lambda I_n) \qquad (A.4)$$

where I_m and I_n are m x m and n x n identity matrices, respectively. That is, the nonzero eigenvalues of PQ are the same as those for QP.

Proof: Observe, for Z an appropriately dimensioned null matrix,

$$\begin{bmatrix} PQ-\lambda I_m & P \\ Z_{n\times m} & \lambda I_n \end{bmatrix} \begin{bmatrix} -I_m & Z_{m\times n} \\ Q & I_n \end{bmatrix} = \begin{bmatrix} \lambda I_m & P \\ \lambda Q & \lambda I_n \end{bmatrix} \qquad (A.5)$$

and

$$\begin{bmatrix} I_m & Z_{m\times n} \\ Q & -I_n \end{bmatrix} \begin{bmatrix} \lambda I_m & P \\ Z_{n\times m} & QP-\lambda I_n \end{bmatrix} = \begin{bmatrix} \lambda I_m & P \\ \lambda Q & \lambda I_n \end{bmatrix} \qquad (A.6)$$

Hence, the left hand sides of (A.5) and (A.6) are equal and so are their determinants.

In order to evaluate these determinants, the following is noted [29:104,107]: Since the determinant of an n x n matrix A is an algebraic sum of all products of n terms which can be formed by selecting exactly one term from each row and each column of A, and if A can be partitioned as

$$A = \left(\begin{array}{c|c} F & Z \\ \hline G & H \end{array}\right) \qquad (A.7)$$

where F is a square matrix and Z is a null matrix, then

$$\det A = \det F \det H \qquad (A.8)$$

Thus, using (A.8) with (A.5) and (A.6),

$$\det(PQ-\lambda I_m)\det(\lambda I_n)\det(-I_m)\det(I_n)$$

$$= \det(I_m)\det(-I_n)\det(\lambda I_m)\det(QP-\lambda I_n) \quad \text{(A.9)}$$

That is,

$$(-1)^m \lambda^n \det(PQ-\lambda I_m) = (-1)^n \lambda^m \det(PQ-\lambda I_n) \quad \text{(A.10)}$$

Multiply through by $(-1)^{n-m}$,

$$(-1)^n \lambda^n \det(PQ-\lambda I_m) = (-1)^{2n-m} \lambda^m \det(PQ-\lambda I_n) \quad \text{(A.11)}$$

But $(-1)^{2n} = 1$ for all n an integer, and $(-1)^{-m} = (-1)^m$. Hence, the theorem is proven.

Now, from (A.1)

$$B^{-1}Ax = \lambda x \quad \text{(A.12)}$$

or

$$(B^{-1}A-\lambda I_N)x = 0 \quad \text{(A.13)}$$

from which the eigenvalues can be obtained as roots of

$$\det(B^{-1}A-\lambda I_N) = 0 \quad \text{(A.14)}$$

But, $A = aa^{\dagger}$, so

$$\det(B^{-1}aa^{\dagger}-\lambda I_N) = 0 \quad \text{(A.15)}$$

Now the above theorem is applied with $m = 1$, $n = N$, $P = a^{\dagger}$ is $1 \times N$, and $Q = B^{-1}a$ is $N \times 1$:

$$(-1)\lambda \det(B^{-1}aa^{\dagger}-\lambda I_n)$$
$$= (-1)^N \lambda^N \det(a^{\dagger}B^{-1}a-\lambda I_1) = 0 \quad \text{(A.16)}$$

or

$$\det(B^{-1}aa^{\dagger}-\lambda I_N)$$
$$= (-1)^{N-1} \lambda^{N-1} \det(a^{\dagger}B^{-1}a-\lambda I_1) = 0 \quad \text{(A.17)}$$

From (A.17) two results follow: N-1 eigenvalues of (A.1) are identically zero and the remaining nonzero eigenvalue is

$$\lambda = a^{\dagger}B^{-1}a \quad \text{(A.18)}$$

which must be real-valued.

To show this is the dominant eigenvalue (i.e., $\lambda = \lambda_D > 0$), choose a nonzero vector

$$x = B^{-1}a \quad \text{(A.19)}$$

Then

$$Bx = a \quad \text{(A.20)}$$

and

$$x^{\dagger}B^{\dagger} = a^{\dagger} \quad \text{(A.21)}$$

So, from (A.18)

$$\lambda = x^{\dagger}B^{\dagger}B^{-1}Bx = x^{\dagger}Bx > 0 \quad \text{(A.22)}$$

since B is Hermitian and positive definite; thus, in (A.18)

$$\lambda = \lambda_D = a^{\dagger}B^{-1}a \quad \text{(A.23)}$$

AD-A101 143 AIR FORCE INST OF TECH WRIGHT-PATTERSON AFB OH SCHOO--ETC F/G 17/9
MULTIPLE ARRESTED SYNTHETIC APERTURE RADAR.(U)
MAY 81 J S SHUSTER
UNCLASSIFIED AFIT/DS/EE/81-3 NL

3 OF 5
AD A
101143

Direct substitution of (A.19) in (A.1) obtains

$$aa^{\dagger}(B^{-1}a) = a^{\dagger}B^{-1}aB(B^{-1}a) \tag{A.24}$$

or

$$a\lambda_D = \lambda_D a \tag{A.25}$$

an identity. Thus, in (A.19),

$$x = x_D = B^{-1}a \tag{A.26}$$

Q.E.D.

Appendix B

Computational Notes

Solving for the Dominant Eigenvector and Eigenvalue

The target signal vector, a, is generated using (50), (53), (54) and (127). The clutter cross-power correlation matrix B, is generated using (126) and (140) through (148). As discussed in Chapter II, the solution for the dominant eigenvector (the optimum weights) is obtained from the set of simultaneous equations described by (8),

$$Bw_D = a \tag{B.1}$$

Since B is Hermitian and positive definite, it can be decomposed into the product of two triangular matrices, each the conjugate-transpose of the other; i.e.,

$$B = LL^{\dagger} \tag{B.2}$$

where L denotes a lower triangular matrix. This is known as the Choleski decomposition [30:158]. The solution for w_D is then easily obtained. From (B.1) with (B.2)

$$LL^{\dagger}w_D = a \tag{B.3}$$

Let

$$L^{\dagger}w_D = y \tag{B.4}$$

where y is a column vector. The system

$$Ly = a \tag{B.5}$$

is easily solved for y by forward substitution. Finally,

$$L^{\dagger} w_D = y \tag{B.6}$$

is easily solved for w_D by backward substitution. The dominant eigenvalue λ_D--the maximum target to mean clutter power ratio--is then easily obtained with (9).

<u>Gauss-Quadrature Integration of Equation (97)</u>

The solution of (97) leads to a mathematical fork in the road. One fork leads to the solution in closed form. This was the route taken in the main body of this work. The other fork leads to a numerical integration technique. Equation (97) is of the form which can be integrated directly by Gaussian quadrature using Chebyshev polynomials of the First Kind. Using equation [25.4.38] of Abramowitz and Stegun [27:889] one obtains

$$I = \frac{\pi}{N} \sum_{i=1}^{N} f(\eta_i) \; e^{jz\eta_i} \tag{B.7}$$

where I is described by (107), f(η) by (108), z by (109), and where the collocation points are found from

$$\eta_i = \cos \frac{(2i-1)\pi}{2N} \tag{B.8}$$

The problem in using this solution stems from the factor, z, in the complex exponential. It becomes large in magnitude as the antenna separation increases. This makes the integrand of (107) highly oscilla-

tory for even moderate antenna spacings. The consequence is that a large number of collocation points are required before the sum in (B.7) converges.

The convergence of (B.7) was compared with that of the closed form solution, (126), for the following system parameters:

wavelength = 1 foot (frequency = 1 GHz)

range = 10 miles

pulsewidth = .5 μsec

antennas: cosine and cosine-cubed patterns.

The following convergence was obtained for the antenna spacings, d, shown:

d (feet)	value of N required in (B.7) to converge to 4 significant digits	value of r required in (126) to converge to 8 significant digits
10	82	9
100	674	15
1000	convergence not obtained at 100,000	35

<u>The Evaluation of Equation (126)</u>

For the system parameters shown in Table I in the text, evaluation of the clutter cross-power correlation via (126) requires computation of the Bessel function of the First Kind for orders zero to 22. This provided accuracy to 10^{-5}--the factor $1/(r-s)!s!$ in (125) obviates the need for larger orders.

To obtain the cross-power correlation between two antennas for a radar wavelength of 1 foot, the argument of the Bessel functions, $2k_0d$, ranges from zero, when the antennas are spatially collocated, to 157.08 when the antennas are spaced 12.5 feet apart (maximum antenna spacing

for Cases 3 and 6).

The Bessel function routines of the International Mathematical and Statistical Libraries (IMSL) proved to be quite inadequate for this sort of use. Instead, following a discussion by Abramowitz and Stegun [27:385-386] a machine algorithm was developed employing the recurrence relation

$$J_{n-1}(x) + J_{n+1}(x) = \frac{2n}{x} J_n(x) \qquad [27:(9.1.27)]$$

in the direction of <u>decreasing</u> n, with the normalization factor obtained from the relation

$$J_0 + 2J_2 + 2J_4 + \cdots = 1 \qquad [27:(9.1.46)]$$

which avoids the severe accumulation of rounding errors.

Appendix C

Choice of the PRF

One consideration in choosing the PRF in pulsed radars is so that the targets of interest will have speeds below the first blind speed. A target moving so that the phase change in its signal return is exactly 360 degrees is moving at the first blind speed. The speed of the target must be such that its radial distance to the radar changes by one-half wavelength in an interpulse period. Blind speeds can occur, then, at

$$V_B = \frac{1}{2} n\lambda f_{PRF} \tag{C.1}$$

where $n = 1,2,3, \ldots ,$

λ is the wavelength,

and f_{PRF} is the pulse repetition frequency.

But, as will be seen, this is not the concern here. The more important factor for the analysis presented here is to chose the PRF so that the first synthetic array grating lobe [31:8; 6:568] lies outside the half-space within 90 degrees either side of abeam to starboard. For MASAR, the first grating lobes occur at

$$\sin\theta_g = \pm \frac{\lambda}{2\delta} \tag{C.2}$$

where θ_g is the angle off abeam to starboard,

λ is the wavelength,

and

d is the spacing between synthetic elements.

If $d < \lambda/2$ grating lobes do not occur. Choosing $d = \lambda/2$ positions the

first grating lobes at the azimuthal extremities of the half-space. But,

$$d = \frac{v_R}{f_{PRF}} \tag{C.3}$$

where v_R is the radar platform velocity. Thus

$$f_{PRF} = \frac{2v_R}{\lambda} \tag{C.4}$$

must be the minimum effective PRF for each synthetic array. Note that, for MASAR with two antennas, the PRF must be twice this value. In general, for MASAR with M antennas. the PRF must be

$$f_{PRF} = 2M \frac{v_R}{\lambda} \tag{C.5}$$

This ensures that the spacing of the synthetic elements of each synthetic aperture are no farther apart than $\lambda/2$ in space.

It must be emphasized that this choice of the PRF places the first grating lobes at the azimuthal extremeties of the half space. This causes some (explainable) anomalies to occur in the results when an isotropic antenna is used or when the presumed target is azimuthally positioned well off the perpendicular bisector of the MASAR observation interval. Most of these are explained in Chapter IV, Analysis of MASAR Performance.

To avoid the few anomalies that do occur as a consequence of the grating lobes, the PRF would have to be increased--perhaps doubled. If this were done, and the same number of pulses per antenna were used, the effective aperture length generated would be unacceptably short. If the number of pulses per antenna were increased to obtain apertures of reasonable length, the computer memory and central processing unit require-

ments of the MASAR computer model would become too excessive.

Hence, for MASAR with two antennas, using the parameter values given on page 66 in Chapter IV, the PRF must be 2640 Hz. Then, the effective PRF for each synthetic array is 1320 Hz. (With this in (C.1), the first blind speed occurs at 450 mph.)

Appendix D

Expressions For The Target Power Using Target And Binomial Weights

Here, approximate expressions are obtained for the target signal power, $w^{+}Aw$, using the target weights and the binomial weights, respectively. These expressions are useful in interpreting the results of the analysis in Chapter IV.

The Target Weighted Target Signal Power.

The generating function for the target signal (50) is repeated here for convenience:

$$\alpha_n^m = g^m(\theta_n^m) e^{-\frac{(r_n^m - R_0)^2}{2\sigma^2} - j2k_0 r_n^m} \tag{D.1}$$

where the constant factor in (50) is set to unity for simplicity, and where

$$\left(r_n^m\right)^2 = \left[R_0 \cos\theta_0 + v_T \cos\theta_T \left(\tau_n^m - \frac{\tau_N^M}{2}\right)\right]^2 + \left[R_0 \sin\theta_0 + v_R\left(\frac{\tau_N^1}{2} - \tau_n^1\right) + v_T \sin\theta_T \left(\tau_n^m - \frac{\tau_N^M}{2}\right)\right]^2 \tag{53}$$

and

$$\theta_n^m = \tan^{-1}\left[\frac{R_0 \sin\theta_0 + v_R\left(\frac{\tau_N^1}{2} - \tau_n^1\right) + v_T \sin\theta_T\left(\tau_n^m - \frac{\tau_N^M}{2}\right)}{R_0 \cos\theta_0 + v_T \cos\theta_T\left(\tau_n^m - \frac{\tau_N^M}{2}\right)}\right] \tag{54}$$

w_T is the target signal vector for a target presumed at θ_0. Recalling (29), $A = aa^{+}$; a is the target signal vector for an arbitrary target, obtained by letting θ_0 vary, i.e., $\theta_0 = \theta$. Then, notationally,

$$w_{T_i} = \alpha_n^m = g^m(\theta_n^m)\, e^{-\frac{(r_n^m - R_0)^2}{2\sigma^2} - j2k_0 r_n^m} \tag{D.2}$$

and

$$a_i = \tilde{\alpha}_n^m = g^m(\tilde{\theta}_n^m)\, e^{-\frac{(\tilde{r}_n^m - R_0)^2}{2\sigma^2} - j2k_0 \tilde{r}_n^m} \tag{D.3}$$

where $\tilde{r}_n^m, \tilde{\theta}_n^m$ are r_n^m, θ_n^m evaluated at $\theta_0 = \theta$.

The expression to be obtained is

$$\begin{aligned} w_T^\dagger A w_T &= w_T^\dagger a a^\dagger w = |w_T^\dagger a|^2 \\ &= \left|\sum_{n=1}^{N} \sum_{m=1}^{M} \alpha_n^{m*} \tilde{\alpha}_n^m\right|^2 \\ &= \left|\sum_{n=1}^{N} \sum_{m=1}^{M} g^{m*}(\theta_n^m) g^m(\tilde{\theta}_n^m) \right. \\ &\quad \left. \bullet\, e^{-\frac{1}{2\sigma^2}\left[(r_n^m - R_0)^2 + (\tilde{r}_n^m - R_0)^2\right] + j2k_0(r_n^m - \tilde{r}_n^m)}\right|^2 \end{aligned} \tag{D.4}$$

By expanding (53), combining terms, and factoring out an R_0^2, one obtains

$$\begin{aligned} r_n^m = R_0 \Big[1 &+ 2\frac{v_T}{R_0}\tau_b \cos(\theta_0 - \theta_T) + 2\frac{v_R}{R_0}\tau_a \sin\theta_0 \\ &+ 2\frac{v_R v_T}{R_0^2}\tau_a\tau_b \sin\theta_T + \left(\frac{v_T \tau_b}{R_0}\right)^2 + \left(\frac{v_R \tau_a}{R_0}\right)^2 \Big]^{1/2} \end{aligned} \tag{D.5}$$

where

$$\tau_a = \frac{\tau_N^1}{2} - \tau_n^1 \tag{D.6}$$

and

$$\tau_b = \tau_n^m - \frac{\tau_N^M}{2} \tag{D.7}$$

The radical in (D.5) is then expanded using the Taylor series for $(1+x)^{\frac{1}{2}}$ to obtain

$$r_n^m \cong R_0 + v_R \tau_a \sin\theta_0 + v_T \tau_b \cos(\theta_0 - \theta_T) \tag{D.8}$$

where the small terms (those containing negative powers of R_0) are ignored. The last term in (D.8) is the correction term for the moving target.

Using (34), τ_a can be converted from (D.6) to

$$\tau_a = \left[\frac{N-1}{2} - (n-1)\right] \frac{M}{f_{PRF}} \tag{D.9}$$

Similarly, τ_b can be converted from (D.7) to

$$\tau_b = \frac{M(n-1) + (m-1)K}{f_{PRF}} - \frac{M(N-1) - (M-1)K}{2f_{PRF}} \tag{D.10}$$

With (D.8), (D.9), (D.10), and the values for the parameters used in any of the twenty cases in the main text (see p.66 and Table I, p.67), the real term in the exponent of (D.4) is very small. So its associated factor can be taken to be unity. Furthermore, from (54) when the target speed v_T is small, $\theta_n^m \simeq \theta_0$ and $\tilde{\theta}_n^m \simeq \theta$. Hence, (D.4) can be written

$$w_T^{\dagger} A w_T \cong \left| \sum_{n=1}^{N} \sum_{m=1}^{M} g^{m*}(\theta_0) g^m(\theta)\ e^{j2k_0(r_n^m - \tilde{r}_n^m)} \right|^2 \quad \text{(D.11)}$$

Now consider $r_n^m - \tilde{r}_n^m$:

$$\begin{aligned} r_n^m - \tilde{r}_n^m &= v_R \left(\frac{N-1}{2}\right) \frac{M}{f_{PRF}} (\sin\theta_0 - \sin\theta) \\ &+ v_T \frac{M(N-1) - (M-1)K}{2 f_{PRF}} [\cos(\theta-\theta_T) - \cos(\theta_0-\theta_T)] \\ &+ \frac{(n-1)M}{f_{PRF}} \Big\{ v_R (\sin\theta - \sin\theta_0) \\ &- v_T [\cos(\theta-\theta_T) - \cos(\theta_0-\theta_T)] \Big\} \\ &+ v_T \frac{(m-1)K}{f_{PRF}} [\cos(\theta_0-\theta_T) - \cos(\theta-\theta_T)] \end{aligned} \quad \text{(D.12)}$$

Denoting Δr_N^M for the sum of the first two terms in (D.12), $(n-1)\Delta r_a$ for the third term and $(m-1)\Delta r_b$ for the last term, an abbreviated notation for (D.12) is

$$r_n^m - \tilde{r}_n^m = \Delta r_N^M + (n-1)\Delta r_a + (m-1)\Delta r_b \quad \text{(D.13)}$$

Since the antenna patterns are progressive, even powers of the cosine, i.e.,

$$g^m(\theta) = \cos^{2(m-1)} \cos^{2J}\theta \quad \text{(D.14)}$$

where J = 0,1,2 or 3 depending on the Case in Table I, then (D.11) can be written, using (D.13), as

$$w_T^{\dagger} A w_T \cong (\cos\theta_0 \cos\theta)^{4J} \left| e^{j2k_0 \Delta r_N^M} \sum_{n=1}^{N} e^{j2k_0 (n-1)\Delta r_a} \right.$$

$$\left. \bullet \sum_{m=1}^{M} \left(\cos\theta_0 \cos\theta e^{jk_0 \Delta r_b}\right)^{2(m-1)} \right|^2 \qquad \text{(D.16)}$$

The summations in (D.16) are those of a geometric series, i.e.,

$$\sum_{n=1}^{N} x^{n-1} = \frac{1-x^N}{1-x} \qquad \text{(D.17)}$$

If $x = (pe^{jy})^2$ then

$$\left| \sum_{m=1}^{M} (pe^{jy})^{2(m-1)} \right|^2 = \frac{1-(pe^{jy})^{2M}}{1-(pe^{jy})^2} \cdot \frac{1-(pe^{-jy})^{2M}}{1-(pe^{-jy})^2}$$

$$= \frac{1-p^{2M}e^{j2My}-p^{2M}e^{-j2My}+p^{4M}}{1-p^2e^{j2y}-p^2\, e^{-j2y}+p^4}$$

$$= \frac{1+p^{4M}-2p^{2M}\cos 2My}{1+p^4-2p^2\cos 2y} \qquad \text{(D.18)}$$

Now, if $p = 1$ in (D.18),

$$\left| \sum_{n=1}^{N} e^{j2(n-1)y} \right|^2 = \frac{1-\cos 2Ny}{1-\cos 2y} = \left[\frac{\sin Ny}{\sin y}\right]^2 \qquad \text{(D.19)}$$

Using (D.18) and (D.19), (D.16) can be written

$$w_T^\dagger A w_T \cong \left[\frac{\sin N k_0 \Delta r_a}{\sin k_0 \Delta r_a}\right]^2 (\cos\theta_0 \cos\theta)^{4J}$$

$$\bullet \left[\frac{1+(\cos\theta_0\cos\theta)^{4M} - 2(\cos\theta_0\cos\theta)^{2M}\cos 2Mk_0\Delta r_b}{1+(\cos\theta_0\cos\theta)^4 - 2(\cos\theta_0\cos\theta)^2 \cos 2k_0\Delta r_b}\right] \quad (D.20)$$

which can be written, using $k_0 = 2\pi/\lambda_0$,

$$w_T^\dagger A w_T = \left\{ \frac{\sin\left[\frac{\pi N}{f_{PRF}} \left(\frac{2Mv_R}{\lambda_0}\right)\Psi\right]}{\sin\left[\frac{\pi}{f_{PRF}} \left(\frac{2Mv_R}{\lambda_0}\right)\Psi\right]} \right\}^2 (\cos\theta_0 \cos\theta)^{4J}$$

$$\bullet \left\{ \frac{1+(\cos\theta_0\cos\theta)^{4M} - 2(\cos\theta_0\cos\theta)^{2M}\cos\left[\frac{2\pi K}{f_{PRF}}\left(\frac{2Mv_R}{\lambda_0}\right)\phi\right]}{1+(\cos\theta_0\cos\theta)^4 - 2(\cos\theta_0\cos\theta)^2 \cos\left[\frac{2\pi K}{f_{PRF}}\left(\frac{2v_R}{\lambda_0}\right)\phi\right]} \right\} \quad (D.21)$$

where K is defined by (1) and where

$$\Psi = (\sin\theta - \sin\theta_0) - \frac{v_T}{v_R}\left[\cos(\theta-\theta_T) - \cos\theta_0 - \theta_T)\right] \quad (D.22)$$

and

$$\phi = \frac{v_T}{v_R}\left[\cos(\theta_0 - \theta_T) - \cos(\theta - \theta_T)\right] \quad (D.23)$$

This describes the target signal power obtained with the MASAR target processor when the processor is tuned to a target at azimuth θ_0 but receives a signal from a target at azimuth θ.

Akin to conventional array antenna theory [31:7-15] , the first factor of (D.21)--in braces, squared--can be interpreted as the "combined array factor" of the MASAR target processor. The second and third factors of (D.21)--the factor to the 4J power times the factor in braces--can be interpreted as the "combined element factor" of the MASAR target processor.

The Binomially Weighted Target Power.

Recall that the binomial processor weights for an M antenna, N pulse MASAR are obtained from the binomial coefficients of $(1-x)^{M-1}$, repeated N times (see page 71). Then the binomial processor target power can be written

$$w_B^\dagger A w_B = |w_B^\dagger a|^2$$

$$= \left|\sum_{n=1}^{N} \sum_{m=1}^{M} (-1)^{m-1} \binom{M}{m} \alpha_n^m \right|^2 \tag{D.24}$$

where $\binom{M}{m}$ is the binomial coefficient.

From (D.1), (D.9), (D.10), assuming $(r_n^m - R_0)^2 << 2\sigma^2$ and v_T small (so that $\theta_n^m \simeq \theta_0 = \theta$ for the arbitrary target), α_n^m can be written

$$\alpha_n^m =$$

$$e^{-j2k_0\left[R_0 + \frac{M(N-1)}{2} \frac{V_R}{f_{PRF}} \sin\theta - \left\{\frac{M(N-1) - (M-1)K}{2}\right\} \frac{V_T}{f_{PRF}} \cos(\theta-\theta_T)\right]}$$

$$\bullet\ g^m(\theta) e^{-j\frac{2k_0}{f_{PRF}} (m-1) K v_T \cos(\theta-\theta_T)}$$

$$\bullet\ e^{j2k_0 (n-1) \frac{M v_R}{f_{PRF}} \left[\sin\theta - \frac{v_T}{v_R} \cos(\theta-\theta_T)\right]} \tag{D.25}$$

With this, the target power can be written

$$w_B^{\dagger} A w_B = \left| \sum_{n=1}^{N} e^{j2k_0 (n-1) \frac{M v_R}{f_{PRF}} [\sin\theta - \frac{v_T}{v_R} \cos(\theta - \theta_T)]} \right.$$

$$\left. \cdot \sum_{m=1}^{M} (-1)^{m-1} \binom{M}{m} g^m(\theta) e^{-j2k_0 (m-1) K v_T \cos(\theta - \theta_T)} \right|^2 \qquad \text{(D.26)}$$

Recalling (D.19), the summation on n can be written

$$w_B^{\dagger} A w_B = \left[\frac{\sin\{\frac{\pi N}{f_{PRF}} (\frac{2Mv_R}{\lambda_0}) [\sin\theta - \frac{v_T}{v_R} \cos(\theta - \theta_T)]\}}{\sin\{\frac{\pi}{f_{PRF}} (\frac{2Mv_R}{\lambda_0}) [\sin\theta - \frac{v_T}{v_R} \cos(\theta - \theta_T)]\}} \right]^2$$

$$\cdot \left| \sum_{m=1}^{M} (-1)^{m-1} \binom{M}{m} g^m(\theta) e^{-j2k_0 (m-1) K v_T \cos(\theta - \theta_T)} \right|^2 \qquad \text{(D.27)}$$

Here, as for the target-processor target power, the first factor can be interpreted as the "array factor" and the second can be interpreted as the "combined element factor" of the MASAR binomial processor.

Appendix E

Tabulations of the

Optimum and Target

Weights

for Selected Cases

from Table I

TABLE III

WEIGHTS FOR CASE 1

PRESUMED TARGET SPEED(MPH)	TRACK ANGLE(DEG)	AZIMUTH(DEG)
0.	180.	0.

NO.	OPTIMUM WEIGHTS MAGNITUDE	PHASE(DEG)	TARGET WEIGHTS MAGNITUDE	PHASE(DEG)
1	12.00300771	-.68341734	1.00000000	0.00000000
2	90.87445755	179.37387162	1.00000000	0.00000000
3	1.00000836	.04254855	1.00000000	.01039809
4	80.63419126	179.40618641	1.00000000	.01039809
5	4.46199932	-.63623480	1.00000000	.01733026
6	86.05688060	179.39957161	1.00000000	.01733026
7	1.92698991	-.40591871	1.00000000	.02079617
8	82.97627893	179.41129350	1.00000000	.02079617
9	1.92698672	-.43158511	1.00000000	.02079617
10	82.97627809	179.41050734	1.00000000	.02079617
11	4.46199925	-.62450543	1.00000000	.01733026
12	86.05688113	179.40037731	1.00000000	.01733026
13	1.00000000	0.00000000	1.00000000	.01039809
14	80.63419073	179.40549713	1.00000000	.01039809
15	12.00300649	-.67898249	1.00000000	0.00000000
16	90.87445710	179.37466358	1.00000000	0.00000000
NORMALIZATION FACTORS	.10712833E-08	-134.65550075	.10000000E+01	44.72969905

TABLE III (CONTINUED)

WEIGHTS FOR CASE 1

SPEED(MPH)	PRESUMED TARGET TRACK ANGLE(DEG)	AZIMUTH(DEG)
3.	180.	0.

	OPTIMUM WEIGHTS		TARGET WEIGHTS	
NO.	MAGNITUDE	PHASE(DEG)	MAGNITUDE	PHASE(DEG)
1	3.94822416	-100.25292875	1.00000000	-18.30066064
2	26.92301599	95.40721477	1.00000000	-17.08061663
3	1.00000000	0.00000000	1.00000000	-15.85017437
4	23.49898452	104.56577947	1.00000000	-14.63013036
5	1.96925066	-117.19899791	1.00000001	-13.40315418
6	25.47072055	99.95372986	1.00000001	-12.18311034
7	1.42570239	-3.60390518	1.00000001	-10.95960025
8	24.23125845	110.36324109	1.00000001	-9.73955607
9	1.43093000	-132.45838142	1.00000001	-8.51951206
10	24.50052330	104.69755952	1.00000001	-7.29946805
11	2.02746936	-17.52747908	1.00000001	-6.08288996
12	25.20418284	115.70748044	1.00000000	-4.86284612
13	1.13435008	-138.12150868	1.00000000	-3.64973411
14	23.72160058	109.88196082	1.00000000	-2.42968993
15	3.96180444	-36.74982172	1.00000000	-1.22004401
16	26.69257013	120.84658035	1.00000000	0.00000000
NORMALIZATION FACTORS	.36611041E-08	-62.01544263	.99999999E+00	53.88002945

TABLE III (CONTINUED)

WEIGHTS FOR CASE 1

PRESUMED TARGET SPEED(MPH)	TRACK ANGLE(DEG)	AZIMUTH(DEG)
15.	180.	0.

NO.	OPTIMUM WEIGHTS MAGNITUDE	PHASE(DEG)	TARGET WEIGHTS MAGNITUDE	PHASE(DEG)
1	2.20775140	-152.40681862	1.00000000	-91.50330272
2	7.76245666	47.33758410	1.00000003	-85.40308250
3	1.00000000	0.00000000	1.00000006	-79.29246437
4	5.10366003	84.14591597	1.00000008	-73.19224432
5	1.63928615	-141.30393718	1.00000010	-67.08509194
6	7.18658667	70.07588651	1.00000012	-60.98487189
7	1.35794850	13.31931452	1.00000013	-54.88118559
8	5.47750307	112.75436944	1.00000013	-48.78096538
9	1.41864700	-129.43777586	1.00000013	-42.68074499
10	6.72049177	92.65594111	1.00000012	-36.58052478
11	1.69938064	24.72043392	1.00000012	-30.48377065
12	6.01369195	139.68676343	1.00000010	-24.38355044
13	1.20471896	-117.52057287	1.00000008	-18.29026239
14	6.19114640	116.03221970	1.00000006	-12.19004218
15	2.27383436	30.24850553	1.00000003	-6.10022005
16	6.79205668	165.75431780	1.00000000	0.00000000

NORMALIZATION FACTORS

.15637251E-07	-52.13101849	.99999987E+00	90.48135057

TABLE III (CONTINUED)

WEIGHTS FOR CASE 1

PRESUMED TARGET

SPEED(MPH)	TRACK ANGLE(DEG)	AZIMUTH(DEG)
30.	180.	0.

	OPTIMUM WEIGHTS		TARGET WEIGHTS	
NO.	MAGNITUDE	PHASE(DEG)	MAGNITUDE	PHASE(DEG)
1	2.45778041	-137.91230828	1.00000000	176.99339407
2	6.52085334	49.39894537	1.00000013	-170.80616567
3	1.00000000	0.00000000	1.00000024	-158.59532716
4	3.51229897	101.63743230	1.00000033	-146.39488673
5	1.46528726	-93.43651580	1.00000041	-134.18751413
6	5.40092409	97.77307608	1.00000046	-121.98707404
7	1.04223433	36.59363132	1.00000050	-109.78316752
8	3.82367953	149.02995088	1.00000052	-97.58272726
9	1.31995203	-43.42964852	1.00000052	-85.38228666
10	5.23469721	146.95844572	1.00000050	-73.18184623
11	1.46658851	89.46156174	1.00000046	-60.98487189
12	3.92105883	-154.40983769	1.00000040	-48.78443163
13	1.37662560	-14.91640270	1.00000033	-36.59092303
14	5.08626794	-171.80044399	1.00000024	-24.39048277
15	2.62202942	122.56677574	1.00000013	-12.20044043
16	5.21217754	-95.81948412	1.00000000	0.00000000

NORMALIZATION FACTORS

.23828419E-07	-89.08324850	.99999948E+00	136.23300226

TABLE IV

WEIGHTS FOR CASE 3

	PRESUMED TARGET	
SPEED(MPH)	TRACK ANGLE(DEG)	AZIMUTH(DEG)
0.	180.	0.

	OPTIMUM WEIGHTS		TARGET WEIGHTS	
NO.	MAGNITUDE	PHASE(DEG)	MAGNITUDE	PHASE(DEG)
1	4.56915471	-179.48039882	1.00000001	-.00000000
2	24.94115219	.70908499	1.00000000	0.00000000
3	1.00000272	-.00939451	1.00000001	.03985930
4	18.67493711	.86494491	1.00000000	.03985930
5	3.01907409	-179.52450968	1.00000001	.07625286
6	24.21250455	.78219173	1.00000000	.07625286
7	1.52000905	.16101435	1.00000001	.10918016
8	18.32592421	.95275749	1.00000001	.10918016
9	2.72093027	-179.51708029	1.00000001	.13864137
10	23.97456849	.84057895	1.00000001	.13864137
11	1.72609228	.18655562	1.00000001	.16463667
12	18.14388414	1.02219050	1.00000001	.16463667
13	2.56592077	-179.50820568	1.00000001	.18716572
14	23.82834567	.88591870	1.00000001	.18716572
15	1.84660948	.19672128	1.00000001	.20622902
16	18.02526082	1.07435081	1.00000001	.20622902
17	2.47156194	-179.50129174	1.00000001	.22182606
18	23.73262900	.91839838	1.00000001	.22182606
19	1.91892781	.20208789	1.00000001	.23395719
20	17.95045424	1.10924060	1.00000001	.23395719
21	2.41874369	-179.49678129	1.00000001	.24262223
22	23.67719674	.93797419	1.00000001	.24262223
23	1.95349968	.20470032	1.00000001	.24782136
24	17.91387266	1.12671103	1.00000001	.24782136
25	2.40160399	-179.49471953	1.00000001	.24955440
26	23.65895669	.94458074	1.00000001	.24955440
27	1.95349948	.20504941	1.00000001	.24782136
28	17.91387265	1.12665649	1.00000001	.24782136
29	2.41874329	-179.49514153	1.00000001	.24262223
30	23.67719688	.93818869	1.00000001	.24262223
31	1.91892722	.20317926	1.00000001	.23395719
32	17.95045421	1.10907421	1.00000001	.23395719
33	2.47156112	-179.49812082	1.00000001	.22182606
34	23.73262919	.91882176	1.00000001	.22182606
35	1.84660849	.19869518	1.00000001	.20622902
36	18.02526078	1.07406482	1.00000001	.20622902
37	2.56591950	-179.50371142	1.00000001	.18716572
38	23.82834576	.88654055	1.00000001	.18716572
39	1.72609087	.18968476	1.00000001	.16463667
40	18.14388412	1.02177432	1.00000001	.16463667
41	2.72092851	-179.51156576	1.00000001	.13864137

TABLE IV (CONTINUED)

WEIGHTS FOR CASE 3

SPEED(MPH)	PRESUMED TARGET TRACK ANGLE(DEG)	AZIMUTH(DEG)
0.	180.	0.

	OPTIMUM WEIGHTS		TARGET WEIGHTS	
NO.	MAGNITUDE	PHASE(DEG)	MAGNITUDE	PHASE(DEG)
42	23.97456827	.84138608	1.00000001	.13864137
43	1.52000718	.16586655	1.00000001	.10918016
44	18.32592429	.95220309	1.00000001	.10918016
45	3.01907180	-179.51844770	1.00000001	.07625286
46	24.21250372	.78317305	1.00000000	.07625286
47	1.00000000	0.00000000	1.00000001	.03985930
48	18.67493737	.86426795	1.00000000	.03985930
49	4.56915208	-179.47559640	1.00000001	-.00000000
50	24.94115035	.71025213	1.00000000	0.00000000

NORMALIZATION FACTORS

.42627857E-08	43.73644710	.99999999E+00	44.50137416

TABLE IV (CONTINUED)

WEIGHTS FOR CASE 3

SPEED(MPH)	PRESUMED TARGET TRACK ANGLE(DEG)	AZIMUTH(DEG)
3.	180.	0.

NO.	OPTIMUM WEIGHTS MAGNITUDE	OPTIMUM WEIGHTS PHASE(DEG)	TARGET WEIGHTS MAGNITUDE	TARGET WEIGHTS PHASE(DEG)
1	6.37932958	-178.84497662	1.00000001	-59.78215780
2	37.50813762	2.01716587	1.00000000	-58.56211362
3	1.00000000	0.00000000	1.00000002	-57.30221031
4	29.44569576	4.82226410	1.00000001	-56.08216614
5	3.94774301	-173.77611109	1.00000003	-54.82572874
6	36.33015612	6.92087077	1.00000002	-53.60568490
7	1.57212725	6.49403939	1.00000004	-52.35271359
8	29.20551055	9.68766447	1.00000003	-51.13266941
9	3.42101901	-168.57049191	1.00000004	-49.88316419
10	35.87134539	11.85848008	1.00000004	-48.66312001
11	1.71043861	12.77279100	1.00000005	-47.41708070
12	29.15571227	14.48900950	1.00000005	-46.19703686
13	3.11865752	-162.91611524	1.00000005	-44.95446363
14	35.55918791	16.84234701	1.00000005	-43.73441946
15	1.76087486	19.36074189	1.00000006	-42.49531232
16	29.14765058	19.24552805	1.00000006	-41.27526814
17	2.92163107	-156.73881847	1.00000006	-40.03962709
18	35.34020883	21.86575425	1.00000006	-38.81958308
19	1.78143561	26.18882362	1.00000006	-37.58740794
20	29.15223798	23.96751062	1.00000006	-36.36736376
21	2.80537376	-150.11106222	1.00000007	-35.13865471
22	35.20350598	26.91715844	1.00000007	-33.91861053
23	1.78929745	33.17401038	1.00000007	-32.69336773
24	29.16042407	28.66268465	1.00000007	-31.47332355
25	2.76402476	-143.22581826	1.00000007	-30.25154650
26	35.14715845	31.98237973	1.00000007	-29.03150249
27	1.79004278	40.24084576	1.00000007	-27.81319136
28	29.16918504	33.33769828	1.00000007	-26.59314735
29	2.79662517	-136.35398541	1.00000007	-25.37830247
30	35.17155620	37.04591562	1.00000006	-24.15825829
31	1.78374384	47.32410917	1.00000006	-22.94687932
32	29.17830748	37.99904287	1.00000006	-21.72683531
33	2.90432343	-129.77363350	1.00000006	-20.51892227
34	35.27801514	42.09221391	1.00000006	-19.29887826
35	1.76498941	54.37745103	1.00000006	-18.09443146
36	29.19033009	42.65408029	1.00000005	-16.87438745
37	3.09316644	-123.70219232	1.00000006	-15.67340657
38	35.47006001	47.10719671	1.00000005	-14.45336239
39	1.71693630	61.41745919	1.00000005	-13.25584760
40	29.21360971	47.31281837	1.00000004	-12.03580376
41	3.38786208	-118.27552975	1.00000005	-10.84175488

TABLE IV (CONTINUED)

WEIGHTS FOR CASE 3

PRESUMED TARGET SPEED(MPH)	TRACK ANGLE(DEG)	AZIMUTH(DEG)
3.	180.	0.

NO.	OPTIMUM WEIGHTS MAGNITUDE	PHASE(DEG)	TARGET WEIGHTS MAGNITUDE	PHASE(DEG)
42	35.75994595	52.08050815	1.00000004	-9.62171070
43	1.58292555	68.79359481	1.00000004	-8.43112808
44	29.27600123	51.99285032	1.00000003	-7.21108407
45	3.90704274	-113.65168044	1.00000003	-6.02396736
46	36.20182979	57.01158351	1.00000002	-4.80392335
47	1.03514635	81.89547317	1.00000003	-3.62027289
48	29.52284053	56.74524436	1.00000001	-2.40022872
49	6.31894904	-111.64762745	1.00000002	-1.22004401
50	37.36489724	61.94750361	1.00000000	0.00000000

NORMALIZATION FACTORS

.27688200E-08	13.93052332	.99999993E+00	74.39245306

TABLE IV (CONTINUED)

WEIGHTS FOR CASE 3

SPEED(MPH)	PRESUMED TARGET TRACK ANGLE(DEG)	AZIMUTH(DEG)
15.	180.	0.

NO.	OPTIMUM WEIGHTS MAGNITUDE	PHASE(DEG)	TARGET WEIGHTS MAGNITUDE	PHASE(DEG)
1	2.89075008	-24.60123201	1.00000000	61.08921167
2	9.16509241	175.41756945	1.00000010	67.18943188
3	1.31426959	124.85908973	1.00000022	73.32951140
4	5.85728964	-143.00625889	1.00000031	79.42973161
5	2.13075891	-16.33050668	1.00000042	85.56634504
6	8.24230322	-162.49701487	1.00000050	91.66656509
7	1.66486781	132.83914084	1.00000060	97.79971244
8	6.57361699	-116.08678940	1.00000067	103.89993265
9	1.77259371	-7.09065107	1.00000076	110.02961408
10	7.48569643	-139.73604143	1.00000083	116.12983413
11	1.90601484	141.10038964	1.00000090	122.25604964
12	7.31345923	-92.22641422	1.00000096	128.35626986
13	1.47591289	.37448565	1.00000103	134.47901929
14	6.75554896	-115.71913532	1.00000108	140.57923950
15	2.09194907	150.55969805	1.00000113	146.69852285
16	7.97810257	-70.06660162	1.00000118	152.79874306
17	1.23040199	4.72365886	1.00000122	158.91456032
18	6.07062308	-90.11277938	1.00000126	165.01478070
19	2.22808033	160.75645255	1.00000129	171.12713205
20	8.52495224	-48.96797304	1.00000132	177.22735209
21	1.05906237	4.52741366	1.00000134	-176.66376265
22	5.46594469	-62.56502650	1.00000136	-170.56354260
23	2.31322252	171.27149229	1.00000137	-164.45812326
24	8.92640419	-28.57121731	1.00000138	-158.35790304
25	1.00000000	0.00000000	1.00000139	-152.25594979
26	4.99245748	-32.73544827	1.00000139	-146.15572957
27	2.34490151	-178.24279737	1.00000138	-140.05724240
28	9.16027590	-8.64656972	1.00000137	-133.95702219
29	1.07926258	-5.07164510	1.00000136	-127.86200110
30	4.72438836	-.63591233	1.00000134	-121.76178088
31	2.32072085	-168.10350578	1.00000132	-115.67022571
32	9.20696446	10.98295442	1.00000129	-109.57000550
33	1.28268135	-6.57709248	1.00000126	-103.48191641
34	4.74588760	32.74634727	1.00000122	-97.38169620
35	2.23905597	-158.63991241	1.00000118	-91.29707303
36	9.04932380	30.49335520	1.00000113	-85.19685281
37	1.57383897	-3.88504604	1.00000108	-79.11569607
38	5.10438458	65.39583101	1.00000103	-73.01547585
39	2.09927967	-150.22619656	1.00000097	-66.93778485
40	8.67396782	50.11507125	1.00000090	-60.83756464
41	1.92381418	1.71110151	1.00000084	-54.76333972

TABLE IV (CONTINUED)

WEIGHTS FOR CASE 3

PRESUMED TARGET SPEED(MPH)	TRACK ANGLE(DEG)	AZIMUTH(DEG)
15.	180.	0.

	OPTIMUM WEIGHTS		TARGET WEIGHTS	
NO.	MAGNITUDE	PHASE(DEG)	MAGNITUDE	PHASE(DEG)
42	5.77297401	95.50745916	1.00000076	-48.66311951
43	1.89972863	-143.21286318	1.00000069	-42.59236084
44	8.07370248	70.24346528	1.00000060	-36.49214063
45	2.32987751	8.73134438	1.00000052	-30.42484788
46	6.67554305	122.60043224	1.00000042	-24.32462767
47	1.62044175	-136.37323098	1.00000033	-18.26080101
48	7.25655150	91.88517888	1.00000022	-12.16058079
49	2.99512364	11.73256938	1.00000012	-6.10022005
50	7.85253079	147.67990388	1.00000000	0.00000000

NORMALIZATION FACTORS

.13933465E-07	73.78063214	.99999861E+00	-166.04323167

TABLE IV (CONTINUED)

WEIGHTS FOR CASE 3

PRESUMED TARGET SPEED(MPH)	TRACK ANGLE(DEG)	AZIMUTH(DEG)
30.	180.	0.

	OPTIMUM WEIGHTS		TARGET WEIGHTS	
NO.	MAGNITUDE	PHASE(DEG)	MAGNITUDE	PHASE(DEG)
1	2.83637213	3.17761544	1.00000000	0.00000000
2	7.51718548	-166.55235924	1.00000043	12.20044043
3	1.93890761	141.74493849	1.00000087	24.44073999
4	4.62428517	-99.87118256	1.00000126	36.64118025
5	1.76950984	15.55899782	1.00000166	48.87801357
6	5.77749165	-128.67581214	1.00000202	61.07845400
7	2.71775207	155.94195354	1.00000238	73.31182173
8	6.64299790	-56.96903179	1.00000270	85.51226182
9	1.00000000	0.00000000	1.00000302	97.74216330
10	3.66527169	-79.22811314	1.00000331	109.94260373
11	2.97614333	172.31464929	1.00000359	122.16903929
12	7.78753868	-22.47710574	1.00000384	134.36947972
13	1.27129487	-41.68227953	1.00000409	146.59244936
14	2.77655000	5.10859291	1.00000431	158.79288945
15	2.71370369	-171.88887539	1.00000451	171.01239318
16	7.68024720	10.30997577	1.00000469	-176.78716639
17	2.15166256	-42.55490686	1.00000486	-164.57112892
18	4.53066902	74.63803013	1.00000501	-152.37068832
19	2.01443553	-160.67411415	1.00000514	-140.15811693
20	6.33424456	44.87278705	1.00000525	-127.95767650
21	2.85391050	-29.30712172	1.00000534	-115.74857103
22	6.62883069	116.55456768	1.00000541	-103.54813043
23	1.17173618	-168.57793763	1.00000547	-91.34249121
24	4.16048641	88.40840356	1.00000550	-79.14205095
25	3.14324911	-12.84678236	1.00000552	-66.93987748
26	7.90991608	150.86184120	1.00000552	-54.73943688
27	1.15833511	145.90030159	1.00000550	-42.54072966
28	2.63137204	166.23136822	1.00000547	-30.34028923
29	2.94838626	3.36657148	1.00000541	-18.14504793
30	7.98702759	-176.71814681	1.00000534	-5.94460733
31	2.03527680	136.49992653	1.00000525	6.24716789
32	4.10836144	-114.19262197	1.00000514	18.44760831
33	2.32123573	15.87286229	1.00000501	30.63591762
34	6.81399498	-143.33818862	1.00000486	42.83635821
35	2.81553973	146.95576291	1.00000470	55.02120126
36	6.38501530	-70.29536689	1.00000451	67.22164152
37	1.49396302	14.83530881	1.00000431	79.40301899
38	4.67372932	-104.01268632	1.00000409	91.60345925
39	3.17555127	161.90945494	1.00000385	103.78137030
40	7.87576140	-36.24720221	1.00000359	115.98181073
41	1.21405634	-19.29737211	1.00000332	128.15625586

TABLE IV (CONTINUED)

WEIGHTS FOR CASE 3

SPEED(MPH)	PRESUMED TARGET TRACK ANGLE(DEG)	AZIMUTH(DEG)
30.	180.	0.

	OPTIMUM WEIGHTS		TARGET WEIGHTS	
NO.	MAGNITUDE	PHASE(DEG)	MAGNITUDE	PHASE(DEG)
42	2.56169206	-37.40905894	1.00000302	140.35669612
43	3.00967127	177.12030269	1.00000271	152.52767500
44	8.08312494	-4.58782198	1.00000238	164.72811542
45	1.97681544	-36.57256205	1.00000204	176.89562822
46	3.35084064	57.13507352	1.00000166	-170.90393135
47	2.33234663	-170.07215869	1.00000128	-158.73988464
48	6.88140586	28.12644175	1.00000087	-146.53944422
49	3.05875088	-31.31153343	1.00000046	-134.37886359
50	5.88850897	108.12980336	1.00000001	-122.17842316

NORMALIZATION FACTORS

.20386522E-07	-83.53472506	.99999448E+00	105.59058582

TABLE V

WEIGHTS FOR CASE 4

SPEED(MPH)	PRESUMED TARGET TRACK ANGLE(DEG)	AZIMUTH(DEG)
0.	180.	0.

NO.	OPTIMUM WEIGHTS MAGNITUDE	PHASE(DEG)	TARGET WEIGHTS MAGNITUDE	PHASE(DEG)
1	10.89505423	-.03483478	1.00000000	0.00000000
2	19.16823395	179.96830298	1.00000000	0.00000000
3	2.78855783	179.95104272	1.00000000	.01039809
4	1.47351957	-179.91829483	1.00000000	.01039809
5	5.40391582	-.03045785	1.00000000	.01733026
6	12.40148998	179.98048293	1.00000000	.01733026
7	1.00000005	.00442153	1.00000000	.02079617
8	6.63924472	179.99993901	1.00000000	.02079617
9	1.00000000	0.00000000	1.00000000	.02079617
10	6.63924466	179.99904082	1.00000000	.02079617
11	5.40391583	-.02969766	1.00000000	.01733026
12	12.40149001	179.98092743	1.00000000	.01733026
13	2.78855781	179.95210185	1.00000000	.01039809
14	1.47351944	-179.92105682	1.00000000	.01039809
15	10.89505423	-.03464523	1.00000000	0.00000000
16	19.16823395	179.96844737	1.00000000	0.00000000
	NORMALIZATION FACTORS			
	.14760360E-07	-135.24608411	.10000000E+01	44.72969905

TABLE V (CONTINUED)

WEIGHTS FOR CASE 4

PRESUMED TARGET SPEED(MPH)	TRACK ANGLE(DEG)	AZIMUTH(DEG)
3.	180.	0.

	OPTIMUM WEIGHTS		TARGET WEIGHTS	
NO.	MAGNITUDE	PHASE(DEG)	MAGNITUDE	PHASE(DEG)
1	4.96915915	141.93739208	1.00000000	-18.30066064
2	8.50860587	-45.21844726	1.00000000	-17.08061663
3	2.41798913	-109.57316205	1.00000000	-15.85017437
4	2.14143034	23.16580449	1.00000000	-14.63013036
5	2.83234797	160.44603686	1.00000001	-13.40315418
6	5.65827603	-37.61232475	1.00000001	-12.18311034
7	2.85429584	-146.02547672	1.00000001	-10.95960025
8	4.15671457	-1.17921593	1.00000001	-9.73955607
9	1.36842417	-159.45639679	1.00000001	-8.51951206
10	3.18240629	-28.17196351	1.00000001	-7.29946805
11	3.79314277	-173.33514277	1.00000001	-6.08288996
12	6.34301088	-13.32342775	1.00000001	-4.86284612
13	1.45449790	-81.36297103	1.00000000	-3.64973411
14	1.00000000	0.00000000	1.00000000	-2.42968993
15	5.37677304	165.21022354	1.00000000	-1.22004401
16	8.88276824	-22.87212820	1.00000000	0.00000000

NORMALIZATION FACTORS

.33738621E-07	92.94817429	.99999999E+00	53.88002945

TABLE V (CONTINUED)

WEIGHTS FOR CASE 4

SPEED(MPH)	PRESUMED TARGET TRACK ANGLE(DEG)	AZIMUTH(DEG)
15.	180.	0.

NO.	OPTIMUM WEIGHTS MAGNITUDE	OPTIMUM WEIGHTS PHASE(DEG)	TARGET WEIGHTS MAGNITUDE	TARGET WEIGHTS PHASE(DEG)
1	2.03737885	126.70191893	1.00000000	-91.50330272
2	2.69941109	-70.43552918	1.00000003	-85.40308250
3	2.37949174	-168.16442235	1.00000006	-79.29246437
4	2.30563614	3.20712663	1.00000008	-73.19224432
5	2.01310785	154.25337780	1.00000010	-67.08509194
6	2.42883651	-47.15227275	1.00000012	-60.98487189
7	3.24782024	-163.54867696	1.00000013	-54.88118559
8	3.49529304	8.15193321	1.00000013	-48.78096538
9	1.62798423	178.88296028	1.00000013	-42.68074499
10	1.82739265	-26.47436660	1.00000013	-36.58052478
11	3.49119928	-158.59339444	1.00000012	-30.48377065
12	4.04901998	12.85061454	1.00000010	-24.38355044
13	1.02760666	-147.66413931	1.00000008	-18.29026239
14	1.00000000	0.00000000	1.00000006	-12.19004218
15	3.10778567	-158.56661047	1.00000003	-6.10022005
16	3.97997882	13.35158786	1.00000000	0.00000000
NORMALIZATION FACTORS	.13546009E-06	120.87198825	.99999987E+00	90.48135057

TABLE V (CONTINUED)

WEIGHTS FOR CASE 4

PRESUMED TARGET SPEED(MPH)	TRACK ANGLE(DEG)	AZIMUTH(DEG)
30.	180.	0.

	OPTIMUM WEIGHTS		TARGET WEIGHTS	
NO.	MAGNITUDE	PHASE(DEG)	MAGNITUDE	PHASE(DEG)
1	1.55113351	-112.52582195	1.00000000	176.99339407
2	1.84445954	51.98908353	1.00000013	-170.80616567
3	1.81758806	-45.72555802	1.00000024	-158.59532716
4	1.74025236	130.82805717	1.00000033	-146.39488673
5	1.85241792	-72.88471162	1.00000041	-134.18751413
6	2.07794589	91.55025397	1.00000046	-121.98707404
7	2.59316556	-19.77632580	1.00000050	-109.78316752
8	2.73860585	156.48372195	1.00000052	-97.58272726
9	1.62492381	-38.19708942	1.00000052	-85.38228666
10	1.78293384	125.12615727	1.00000050	-73.18184623
11	2.83773396	5.34339132	1.00000046	-60.98487189
12	3.20455959	-178.92436097	1.00000041	-48.78443163
13	1.00000000	0.00000000	1.00000033	-36.59092303
14	1.05858576	160.04204764	1.00000024	-24.39048277
15	2.44100847	26.68524808	1.00000013	-12.20044043
16	2.99751247	-157.84602143	1.00000000	0.00000000

NORMALIZATION FACTORS

.26048798E-06	-21.37429669	.99999948E+00	136.23300226

TABLE VI

WEIGHTS FOR CASE 5

SPEED(MPH)	PRESUMED TARGET TRACK ANGLE(DEG)	AZIMUTH(DEG)
0.	180.	0.

NO.	OPTIMUM WEIGHTS MAGNITUDE	PHASE(DEG)	TARGET WEIGHTS MAGNITUDE	PHASE(DEG)
1	2.99774678	.07801748	1.00000000	0.00000000
2	5.04757338	-179.91610617	1.00000000	0.00000000
3	1.65563138	-179.93044475	1.00000001	.02252905
4	1.00000001	-.00000393	1.00000000	.02252905
5	2.66337737	.08029232	1.00000001	.04159234
6	4.73361116	-179.90244073	1.00000000	.04159234
7	1.82268600	-179.93197598	1.00000001	.05718939
8	1.16294327	-.03340174	1.00000001	.05718939
9	2.56345516	.08158530	1.00000001	.06932052
10	4.63508534	-179.89318515	1.00000001	.06932052
11	1.88495506	-179.93280572	1.00000001	.07798556
12	1.22459307	-.05278057	1.00000001	.07798556
13	2.52646008	.08220084	1.00000001	.08318469
14	4.59837257	-179.88852549	1.00000001	.08318469
15	1.90227620	-179.93307029	1.00000001	.08491773
16	1.24179333	-.05915182	1.00000001	.08491773
17	2.52646009	.08220314	1.00000001	.08318469
18	4.59837257	-179.88852377	1.00000001	.08318469
19	1.88495505	-179.93280019	1.00000001	.07798556
20	1.22459307	-.05276945	1.00000001	.07798556
21	2.56345516	.08159381	1.00000001	.06932052
22	4.63508535	-179.89317909	1.00000001	.06932052
23	1.82268600	-179.93196950	1.00000001	.05718939
24	1.16294326	-.03338616	1.00000001	.05718939
25	2.66337737	.08031173	1.00000001	.04159234
26	4.73361117	-179.90242756	1.00000000	.04159234
27	1.65563138	-179.93044794	1.00000001	.02252905
28	1.00000000	0.00000000	1.00000000	.02252905
29	2.99774679	.07805107	1.00000000	0.00000000
30	5.04757339	-179.91608329	1.00000000	0.00000000

NORMALIZATION FACTORS

.64655533E-07	-135.43465481	.99999999E+00	44.66601083

TABLE VI (CONTINUED)

WEIGHTS FOR CASE 5

PRESUMED TARGET

SPEED(MPH)	TRACK ANGLE(DEG)	AZIMUTH(DEG)
3.	180.	0.

	OPTIMUM WEIGHTS		TARGET WEIGHTS	
NO.	MAGNITUDE	PHASE(DEG)	MAGNITUDE	PHASE(DEG)
1	2.80117128	31.72040574	1.00000000	-35.38127694
2	4.57304974	-156.21453549	1.00000000	-34.16123310
3	1.68239798	165.14368375	1.00000001	-32.91865988
4	1.09780632	-24.19841441	1.00000001	-31.69861570
5	2.69765705	47.30864848	1.00000002	-30.45950856
6	4.38517543	-145.26214741	1.00000002	-29.23946438
7	1.91935825	163.42855738	1.00000002	-28.00382333
8	1.35801602	-27.25711140	1.00000002	-26.78377932
9	2.76024259	56.69257886	1.00000002	-25.55160418
10	4.39155069	-137.45988201	1.00000002	-24.33156000
11	2.00594255	164.73976249	1.00000003	-23.10285095
12	1.46317181	-26.68695330	1.00000003	-21.88280677
13	2.83039532	63.06001671	1.00000003	-20.65756397
14	4.44057917	-131.42709736	1.00000003	-19.43751980
15	2.00895315	167.98672952	1.00000003	-18.21574274
16	1.47727576	-23.91598038	1.00000003	-16.99569874
17	2.88315411	67.33471885	1.00000003	-15.77738760
18	4.50233891	-126.75603078	1.00000003	-14.55734359
19	1.94451731	173.01422715	1.00000003	-13.34249871
20	1.41574078	-19.16981608	1.00000003	-12.12245453
21	2.91234167	69.65812606	1.00000002	-10.91107557
22	4.56815497	-123.40250729	1.00000002	-9.69103156
23	1.80777974	-179.71173696	1.00000002	-8.48311851
24	1.27207847	-11.89851542	1.00000002	-7.26307450
25	2.92606982	69.45143508	1.00000002	-6.05862770
26	4.64622185	-121.68155235	1.00000001	-4.83858369
27	1.55357205	-168.55624548	1.00000001	-3.63760281
28	1.00000000	0.00000000	1.00000001	-2.41755864
29	3.04095235	64.07748435	1.00000001	-1.22004384
30	4.84358028	-122.89056624	1.00000000	0.00000000

NORMALIZATION FACTORS

.71459916E-07	-159.85326754	.99999997E+00	62.35664930

TABLE VI (CONTINUED)

WEIGHTS FOR CASE 5

PRESUMED TARGET SPEED(MPH)	TRACK ANGLE(DEG)	AZIMUTH(DEG)
15.	180.	0.

	OPTIMUM WEIGHTS		TARGET WEIGHTS	
NO.	MAGNITUDE	PHASE(DEG)	MAGNITUDE	PHASE(DEG)
1	1.53478381	51.08897507	1.00000000	-176.90638572
2	1.93334390	-149.49522108	1.00000006	-170.80616551
3	1.79685390	108.95466647	1.00000013	-164.68341608
4	1.60307449	-81.61320526	1.00000018	-158.58319586
5	1.98182572	89.38583655	1.00000023	-152.46391252
6	2.09488359	-109.36717819	1.00000028	-146.36369230
7	2.39082506	117.21857739	1.00000032	-140.24787504
8	2.32988764	-73.55516988	1.00000036	-134.14765466
9	2.37705357	115.85859689	1.00000039	-128.03530332
10	2.40654178	-78.23841142	1.00000042	-121.93508327
11	2.60528826	128.63274009	1.00000044	-115.82619801
12	2.63956414	-62.89261913	1.00000046	-109.72597796
13	2.73674308	137.55016330	1.00000048	-103.62055862
14	2.81207562	-53.10387372	1.00000049	-97.52033841
15	2.53111893	141.93895742	1.00000049	-91.41838515
16	2.61641050	-50.70753786	1.00000049	-85.31816494
17	3.02329326	155.69144005	1.00000049	-79.21967776
18	3.22555548	-33.06095086	1.00000048	-73.11945755
19	2.21917610	157.23625737	1.00000046	-67.02443646
20	2.31031454	-36.97745446	1.00000044	-60.92421625
21	3.16894958	170.74905970	1.00000042	-54.83266108
22	3.54174719	-17.17992288	1.00000039	-48.73244086
23	1.70745768	175.65284094	1.00000036	-42.64435178
24	1.76284324	-20.97236818	1.00000032	-36.54413156
25	3.08900087	-177.45647280	1.00000028	-30.45950839
26	3.65308047	-5.10520853	1.00000023	-24.35928818
27	1.01639266	-158.10071171	1.00000018	-18.27813143
28	1.00000000	0.00000000	1.00000013	-12.17791121
29	2.67287753	-171.59584837	1.00000007	-6.10022021
30	3.44563574	1.56632189	1.00000000	0.00000000

NORMALIZATION FACTORS

.16521836E-06 168.43025061 .99999951E+00 133.11920369

TABLE VI (CONTINUED)

WEIGHTS FOR CASE 5

PRESUMED TARGET SPEED(MPH)	TRACK ANGLE(DEG)	AZIMUTH(DEG)
30.	180.	0.

NO.	OPTIMUM WEIGHTS MAGNITUDE	PHASE(DEG)	TARGET WEIGHTS MAGNITUDE	PHASE(DEG)
1	1.67094934	76.90597554	1.00000000	6.18722856
2	2.06993355	-119.15188770	1.00000025	18.38766899
3	1.97378723	150.75946733	1.00000050	30.61063863
4	1.90716845	-33.76933495	1.00000072	42.81107873
5	1.71414691	123.04738099	1.00000092	55.03058245
6	1.96936689	-76.20877855	1.00000110	67.23102288
7	2.77378849	-179.75313946	1.00000127	79.44706036
8	2.94360378	-5.16510680	1.00000142	91.64750095
9	1.39059254	176.73216074	1.00000155	103.86007234
10	1.40101301	-26.56924174	1.00000166	116.06051277
11	3.09291078	-148.59093339	1.00000175	128.26961825
12	3.45387103	24.49810204	1.00000183	140.47005884
13	1.42217903	-112.25874331	1.00000188	152.67569806
14	1.17736627	55.71850134	1.00000192	164.87613833
15	2.99502814	-116.21872314	1.00000194	177.07831180
16	3.45906513	54.80876011	1.00000194	-170.72124761
17	2.08607660	-56.31185823	1.00000192	-158.52254039
18	2.00800652	120.76910693	1.00000188	-146.32209996
19	2.54700351	-82.10365939	1.00000183	-134.12685866
20	3.00170024	86.13169375	1.00000175	-121.92641806
21	2.80051116	-18.46168964	1.00000166	-109.73464284
22	2.99614778	158.40066335	1.00000155	-97.53420241
23	1.84708269	-44.78571810	1.00000142	-85.34589311
24	2.18120915	119.47979920	1.00000127	-73.14545251
25	3.11932207	11.12703266	1.00000111	-60.96060947
26	3.56938939	-173.09273968	1.00000092	-48.76016920
27	1.00000000	0.00000000	1.00000072	-36.57879174
28	1.13889212	157.43533605	1.00000050	-24.37835148
29	2.74110848	34.17277505	1.00000026	-12.20044043
30	3.39818476	-150.62708590	1.00000000	0.00000000

NORMALIZATION FACTORS

.21707100E-06	56.86372775	.99999806E+00	-138.42760345

TABLE VII

WEIGHTS FOR CASE 6

PRESUMED TARGET

SPEED(MPH)	TRACK ANGLE(DEG)	AZIMUTH(DEG)
0.	180.	0.

NO.	OPTIMUM WEIGHTS MAGNITUDE	OPTIMUM WEIGHTS PHASE(DEG)	TARGET WEIGHTS MAGNITUDE	TARGET WEIGHTS PHASE(DEG)
1	2.91459993	.12663419	1.00000001	0.00000000
2	4.92301099	-179.86285051	1.00000000	0.00000000
3	1.64522093	-179.88382302	1.00000001	.03985930
4	1.00000001	-.00000532	1.00000000	.03985930
5	2.56957219	.12986114	1.00000002	.07625286
6	4.59814233	-179.83807849	1.00000001	.07625286
7	1.82603289	-179.88629018	1.00000002	.10918016
8	1.17670487	-.06539074	1.00000001	.10918016
9	2.45336031	.13217689	1.00000002	.13864137
10	4.48333331	-179.81733777	1.00000001	.13864137
11	1.90728466	-179.88809431	1.00000002	.16463667
12	1.25729149	-.11578101	1.00000002	.16463667
13	2.39379428	.13390401	1.00000002	.18716572
14	4.42408996	-179.80102480	1.00000002	.18716572
15	1.95167357	-179.88939086	1.00000002	.20622902
16	1.30147054	-.15283811	1.00000002	.20622902
17	2.36046343	.13511394	1.00000002	.22182606
18	4.39086694	-179.78930046	1.00000002	.22182606
19	1.97617796	-179.89023455	1.00000003	.23395719
20	1.32589078	-.17727762	1.00000002	.23395719
21	2.34311330	.13583285	1.00000003	.24262223
22	4.37355683	-179.78224189	1.00000003	.24262223
23	1.98723690	-179.89064995	1.00000003	.24782136
24	1.33691774	-.18942857	1.00000003	.24782136
25	2.33770031	.13607220	1.00000003	.24955440
26	4.36815431	-179.77988482	1.00000003	.24955440
27	1.98723689	-179.89064702	1.00000003	.24782136
28	1.33691774	-.18942330	1.00000003	.24782136
29	2.34311331	.13583517	1.00000003	.24262223
30	4.37355684	-179.78223998	1.00000003	.24262223
31	1.97617795	-179.89022613	1.00000003	.23395719
32	1.32589077	-.17726232	1.00000002	.23395719
33	2.36046344	.13511929	1.00000002	.22182606
34	4.39086696	-179.78929624	1.00000002	.22182606
35	1.95167356	-179.88937827	1.00000002	.20622902
36	1.30147052	-.15281458	1.00000002	.20622902
37	2.39379430	.13391403	1.00000002	.18716572
38	4.42408998	-179.80101736	1.00000002	.18716572
39	1.90728464	-179.88808035	1.00000002	.16463667
40	1.25729147	-.11575318	1.00000002	.16463667
41	2.45336033	.13219456	1.00000002	.13864137

TABLE VII (CONTINUED)

WEIGHTS FOR CASE 6

SPEED(MPH)	PRESUMED TARGET TRACK ANGLE(DEG)	AZIMUTH(DEG)
0.	180.	0.

NO.	OPTIMUM WEIGHTS MAGNITUDE	OPTIMUM WEIGHTS PHASE(DEG)	TARGET WEIGHTS MAGNITUDE	TARGET WEIGHTS PHASE(DEG)
42	4.48333333	-179.81732542	1.00000001	.13864137
43	1.82603287	-179.88628031	1.00000002	.10918016
44	1.17670485	-.06536647	1.00000001	.10918016
45	2.56957221	.12989086	1.00000002	.07625286
46	4.59814235	-179.83805854	1.00000001	.07625286
47	1.64522091	-179.88382732	1.00000001	.03985930
48	1.00000000	0.00000000	1.00000000	.03985930
49	2.91459994	.12667680	1.00000001	0.00000000
50	4.92301101	-179.86282150	1.00000000	0.00000000
NORMALIZATION FACTORS	.65914253E-07	-135.66512214	.99999997E+00	44.50137416

TABLE VII (CONTINUED)

WEIGHTS FOR CASE 6

SPEED(MPH)	PRESUMED TARGET TRACK ANGLE(DEG)	AZIMUTH(DEG)
3.	180.	0.

	OPTIMUM WEIGHTS		TARGET WEIGHTS	
NO.	MAGNITUDE	PHASE(DEG)	MAGNITUDE	PHASE(DEG)
1	2.77047250	13.56913461	1.00000001	-59.78215780
2	4.54318816	-175.08470590	1.00000000	-58.56211362
3	1.76431087	143.53575119	1.00000002	-57.30221031
4	1.16877391	-46.78972601	1.00000002	-56.08216614
5	2.64107661	31.05897503	1.00000003	-54.82572874
6	4.29252819	-163.15240875	1.00000003	-53.60568490
7	2.05466828	140.70680419	1.00000004	-52.35271359
8	1.48963656	-51.19277788	1.00000004	-51.13266941
9	2.69874428	42.38418494	1.00000005	-49.88316419
10	4.25201493	-154.14192300	1.00000005	-48.66312001
11	2.20012615	140.72402328	1.00000006	-47.41708070
12	1.66214234	-52.11054601	1.00000005	-46.19703686
13	2.78010476	50.92009734	1.00000006	-44.95446363
14	4.26665947	-146.60891571	1.00000006	-43.73441946
15	2.27456731	142.28121949	1.00000007	-42.49531232
16	1.75736855	-51.21858697	1.00000007	-41.27526814
17	2.86019767	57.79531818	1.00000007	-40.03962709
18	4.30619407	-140.06062011	1.00000007	-38.81958308
19	2.30298247	144.89261294	1.00000008	-37.58740794
20	1.80058477	-49.11455556	1.00000008	-36.36736376
21	2.93215541	63.50951782	1.00000008	-35.13865471
22	4.35972414	-134.27734848	1.00000008	-33.91861053
23	2.29716467	148.35173870	1.00000008	-32.69336773
24	1.80400329	-46.04466697	1.00000008	-31.47332355
25	2.99300084	68.29515726	1.00000008	-30.25154650
26	4.42164136	-129.16061852	1.00000008	-29.03150249
27	2.26299079	152.58791208	1.00000008	-27.81319136
28	1.77383899	-42.09253728	1.00000008	-26.59314735
29	3.04036989	72.23978429	1.00000008	-25.37830247
30	4.48802953	-124.68195555	1.00000008	-24.15825829
31	2.20257144	157.62767051	1.00000008	-22.94687932
32	1.71238688	-37.23055340	1.00000007	-21.72683531
33	3.07158743	75.32388667	1.00000007	-20.51892227
34	4.55557281	-120.86811668	1.00000007	-19.29887826
35	2.11459691	163.60718929	1.00000007	-18.09443146
36	1.61823049	-31.30719708	1.00000007	-16.87438745
37	3.08363340	77.40723491	1.00000006	-15.67340657
38	4.62155409	-117.81064454	1.00000006	-14.45336239
39	1.99322436	170.84436384	1.00000006	-13.25584760
40	1.48485612	-23.95786351	1.00000005	-12.03580376
41	3.07453030	78.14255659	1.00000005	-10.84175488

TABLE VII (CONTINUED)

WEIGHTS FOR CASE 6

SPEED(MPH)	PRESUMED TARGET TRACK ANGLE(DEG)	AZIMUTH(DEG)
3.	180.	0.

NO.	OPTIMUM WEIGHTS MAGNITUDE	OPTIMUM WEIGHTS PHASE(DEG)	TARGET WEIGHTS MAGNITUDE	TARGET WEIGHTS PHASE(DEG)
42	4.68549251	-115.71161947	1.00000004	-9.62171070
43	1.82347813	-179.94757562	1.00000005	-8.43112808
44	1.29567196	-14.32067346	1.00000003	-7.21108407
45	3.05210342	76.67677949	1.00000004	-6.02396736
46	4.75816917	-115.03298931	1.00000002	-4.80392335
47	1.55548526	-166.93481052	1.00000003	-3.62027289
48	1.00000000	0.00000000	1.00000001	-2.40022872
49	3.13086003	70.12161556	1.00000002	-1.22004401
50	4.94697792	-117.20250253	1.00000000	0.00000000
NORMALIZATION FACTORS	.70549754E-07	-152.41919522	.99999992E+00	74.39245306

TABLE VII (CONTINUED)

WEIGHTS FOR CASE 6

PRESUMED TARGET SPEED(MPH)	TRACK ANGLE(DEG)	AZIMUTH(DEG)
15.	180.	0.

	OPTIMUM WEIGHTS		TARGET WEIGHTS	
NO.	MAGNITUDE	PHASE(DEG)	MAGNITUDE	PHASE(DEG)
1	2.16959515	-68.09447250	1.00000000	61.08921167
2	2.89241866	91.80187647	1.00000010	67.18943188
3	2.73676241	5.17168204	1.00000022	73.32951140
4	2.47796048	178.10153221	1.00000031	79.42973161
5	2.45198472	-33.88417294	1.00000042	85.56634504
6	2.85808208	122.56427037	1.00000051	91.66656509
7	3.85807930	15.98903893	1.00000060	97.79971244
8	3.83933599	-171.14595554	1.00000068	103.89993265
9	2.46759048	-5.23699080	1.00000077	110.02961408
10	2.60366253	149.96076731	1.00000084	116.12983413
11	4.54705844	28.88414112	1.00000091	122.25604964
12	4.75028090	-158.78902566	1.00000097	128.35626986
13	2.44691370	25.91259862	1.00000104	134.47901929
14	2.28921788	-177.63449775	1.00000109	140.57923950
15	4.90962047	42.69843708	1.00000114	146.69852285
16	5.30086775	-145.77629900	1.00000119	152.79874306
17	2.59797874	58.78456598	1.00000123	158.91456032
18	2.22067600	-138.35839204	1.00000127	165.01478070
19	4.99036861	57.18743770	1.00000130	171.12713205
20	5.52384162	-132.31290622	1.00000133	177.22735209
21	2.99874317	89.08489176	1.00000135	-176.66376265
22	2.61263762	-100.55270493	1.00000137	-170.56354260
23	4.82345853	72.37792831	1.00000139	-164.45812326
24	5.44398013	-118.39231802	1.00000139	-158.35790304
25	3.57054118	114.36901756	1.00000140	-152.25594979
26	3.34630574	-71.51424615	1.00000140	-146.15572957
27	4.44590515	88.45790865	1.00000139	-140.05724240
28	5.09181278	-103.88766826	1.00000139	-133.95702219
29	4.17734004	135.15421662	1.00000137	-127.86200110
30	4.18585634	-49.72797177	1.00000135	-121.76178088
31	3.90184548	105.78586686	1.00000133	-115.67022571
32	4.50843287	-88.54469243	1.00000130	-109.57000550
33	4.69523075	152.69160866	1.00000127	-103.48191641
34	4.95543858	-32.32010727	1.00000123	-97.38169620
35	3.24270300	124.97017750	1.00000119	-91.29707303
36	3.74652078	-71.91239924	1.00000114	-85.19685281
37	5.02230687	167.87634652	1.00000109	-79.11569607
38	5.53085419	-17.65975812	1.00000104	-73.01547585
39	2.52338786	147.05519346	1.00000098	-66.93778485
40	2.86839039	-53.17113138	1.00000091	-60.83756464
41	5.06982802	-178.91720515	1.00000084	-54.76333972

TABLE VII (CONTINUED)

WEIGHTS FOR CASE 6

SPEED(MPH)	PRESUMED TARGET TRACK ANGLE(DEG)	AZIMUTH(DEG)
15.	180.	0.

NO.	OPTIMUM WEIGHTS MAGNITUDE	PHASE(DEG)	TARGET WEIGHTS MAGNITUDE	PHASE(DEG)
42	5.81261455	-5.09210220	1.00000076	-48.66311951
43	1.79096265	174.05149532	1.00000069	-42.59236084
44	1.93862868	-30.67594919	1.00000060	-36.49214063
45	4.74667107	-168.01509704	1.00000052	-30.42484788
46	5.70671590	5.22609269	1.00000042	-24.32462767
47	1.05802051	-148.13394234	1.00000033	-18.26080101
48	1.00000000	0.00000000	1.00000022	-12.16058079
49	3.93346442	-162.23538082	1.00000012	-6.10022005
50	5.10802100	11.25380388	1.00000000	0.00000000
NORMALIZATION FACTORS	.11325996E-06	-141.22048192	.99999860E+00	-166.04323167

TABLE VII (CONTINUED)

WEIGHTS FOR CASE 6

SPEED(MPH)	PRESUMED TARGET TRACK ANGLE(DEG)	AZIMUTH(DEG)
30.	180.	0.

NO.	OPTIMUM WEIGHTS MAGNITUDE	PHASE(DEG)	TARGET WEIGHTS MAGNITUDE	PHASE(DEG)
1	1.41282726	-163.80858682	1.00000000	0.00000000
2	1.71726725	-.92521464	1.00000043	12.20044043
3	1.80850994	-98.07035154	1.00000087	24.44073999
4	1.76840879	75.96020286	1.00000126	36.64118025
5	1.50957248	-112.03777758	1.00000166	48.87801357
6	1.60874754	49.26401423	1.00000202	61.07845400
7	2.42070405	-71.58444458	1.00000238	73.31182173
8	2.57667655	101.50725743	1.00000271	85.51226182
9	1.51807261	-57.59543801	1.00000303	97.74216330
10	1.45774174	107.86358940	1.00000332	109.94260373
11	2.44598697	-42.00231478	1.00000360	122.16903929
12	2.72161112	129.47541899	1.00000385	134.36947972
13	1.72438030	-4.47635870	1.00000410	146.59244936
14	1.69959755	167.60645173	1.00000431	158.79288945
15	2.01476592	-7.50452766	1.00000452	171.01239318
16	2.30106368	161.32561016	1.00000470	-176.78716639
17	1.99177387	40.09207178	1.00000487	-164.57112892
18	2.13085032	-146.42573473	1.00000502	-152.37068832
19	1.37880987	40.08040634	1.00000515	-140.15811693
20	1.54325750	-155.74686687	1.00000526	-127.95767650
21	2.06033333	79.03176285	1.00000535	-115.74857103
22	2.34140348	-109.15999673	1.00000542	-103.54813043
23	1.12669639	114.39860739	1.00000548	-91.34249121
24	1.08314700	-80.31860262	1.00000552	-79.14205095
25	1.80745388	118.12248977	1.00000554	-66.93987748
26	2.13269557	-73.68791264	1.00000554	-54.73943688
27	1.60985881	178.33801378	1.00000552	-42.54072966
28	1.62854665	-8.98488704	1.00000548	-30.34028923
29	1.32832806	167.11594592	1.00000542	-18.14504793
30	1.53552478	-31.68555888	1.00000535	-5.94460733
31	2.17808055	-139.97769806	1.00000526	6.24716789
32	2.36522694	32.56408319	1.00000515	18.44760831
33	1.13537626	-119.55212157	1.00000502	30.63591762
34	1.01852532	40.51051096	1.00000487	42.83635821
35	2.44946398	-105.71722954	1.00000471	55.02120126
36	2.75982327	65.17721929	1.00000452	67.22164152
37	1.68178634	-56.14584155	1.00000432	79.40301899
38	1.55609179	118.50479584	1.00000410	91.60345925
39	2.31549773	-73.19887825	1.00000386	103.78137030
40	2.66082696	95.47473654	1.00000360	115.98181073
41	2.37564765	-16.78998340	1.00000333	128.15625586

TABLE VII (CONTINUED)

WEIGHTS FOR CASE 6

PRESUMED TARGET SPEED(MPH)	TRACK ANGLE(DEG)	AZIMUTH(DEG)
30.	180.	0.

NO.	OPTIMUM WEIGHTS MAGNITUDE	PHASE(DEG)	TARGET WEIGHTS MAGNITUDE	PHASE(DEG)
42	2.48525445	159.74417422	1.00000303	140.35669612
43	1.79923896	-39.47930683	1.00000272	152.52767500
44	2.07942673	126.09642535	1.00000238	164.72811542
45	2.72513195	12.45326732	1.00000204	176.89562822
46	3.08432758	-171.68015706	1.00000166	-170.90393135
47	1.00000000	0.00000000	1.00000129	-158.73988464
48	1.13474041	159.89346097	1.00000087	-146.53944422
49	2.43054420	34.56878525	1.00000046	-134.37886359
50	3.00024104	-150.11223677	1.00000001	-122.17842316

NORMALIZATION FACTORS

.24772400E-06	178.71257053	.99999446E+00	105.59058582

TABLE VIII

WEIGHTS FOR CASE 8

PRESUMED TARGET SPEED(MPH)	TRACK ANGLE(DEG)	AZIMUTH(DEG)
0.	180.	0.

NO.	OPTIMUM WEIGHTS MAGNITUDE	PHASE(DEG)	TARGET WEIGHTS MAGNITUDE	PHASE(DEG)
1	1.21824557	-13.85562327	1.00000000	0.00000000
2	2.03327532	167.70581175	1.00000000	0.00000000
3	1.00000212	-11.00503316	1.00000000	0.00000000
4	6.36797205	156.76598194	1.00000000	.01039809
5	16.79316350	-20.31395700	1.00000000	.01039809
6	11.05986277	160.98274081	1.00000000	.01039809
7	10.71709038	-43.57674808	1.00000000	.01733026
8	30.30994821	139.53347698	1.00000000	.01733026
9	20.63957222	-39.14400462	1.00000000	.01733026
10	11.75644106	101.69462155	1.00000000	.02079617
11	31.90461723	-79.94925261	1.00000000	.02079617
12	21.29647076	99.22031713	1.00000000	.02079617
13	11.75620528	-112.70085646	1.00000000	.02079617
14	31.90398309	68.94331459	1.00000000	.02079617
15	21.29603975	-110.22615102	1.00000000	.02079617
16	10.71680609	32.56921076	1.00000000	.01733026
17	30.30909996	-150.54093320	1.00000000	.01733026
18	20.63899120	28.13658921	1.00000000	.01733026
19	6.36788556	-167.77382140	1.00000000	.01039809
20	16.79295412	9.30656308	1.00000000	.01039809
21	11.05972797	-171.98999168	1.00000000	.01039809
22	1.21823856	2.84781414	1.00000000	0.00000000
23	2.03326759	-178.71227203	1.00000000	0.00000000
24	1.00000000	0.00000000	1.00000000	0.00000000
	NORMALIZATION FACTORS			
	.96392561E-05	50.21719908	.10000000E+01	44.72969905

TABLE VIII (CONTINUED)

WEIGHTS FOR CASE 8

PRESUMED TARGET

SPEED(MPH)	TRACK ANGLE(DEG)	AZIMUTH(DEG)
3.	180.	0.

	OPTIMUM WEIGHTS		TARGET WEIGHTS	
NO.	MAGNITUDE	PHASE(DEG)	MAGNITUDE	PHASE(DEG)
1	1.49784630	-38.08075775	1.00000000	-18.70734187
2	2.28485690	143.22101799	1.00000000	-17.89397908
3	1.00346847	-35.94002971	1.00000000	-17.08061647
4	7.20395758	126.81821828	1.00000001	-16.25685576
5	20.48458536	-47.47239056	1.00000001	-15.44349315
6	13.94371659	134.85149059	1.00000001	-14.63013036
7	8.04495731	-108.33157768	1.00000001	-13.80983558
8	24.17008321	79.02346780	1.00000001	-12.99647296
9	16.93018576	-97.87784261	1.00000001	-12.18311017
10	7.52006530	22.84002319	1.00000001	-11.36628147
11	27.70176118	-171.78426273	1.00000001	-10.55291869
12	21.01906901	3.91507624	1.00000001	-9.73955607
13	5.54481797	-58.40883972	1.00000001	-8.92619345
14	21.87198691	142.49517760	1.00000001	-8.11283067
15	17.10513732	-32.00519476	1.00000001	-7.29946805
16	6.77034910	69.84270993	1.00000001	-6.48957135
17	20.95653479	-117.34189863	1.00000001	-5.67620857
18	14.85562792	59.70932859	1.00000001	-4.86284595
19	7.10936651	-162.29957620	1.00000001	-4.05641533
20	20.34891454	12.74006860	1.00000001	-3.24305255
21	13.87947641	-169.27442385	1.00000000	-2.42968976
22	1.49486845	3.68974920	1.00000000	-1.62672540
23	2.27888488	-178.24801693	1.00000000	-.81336262
24	1.00000000	0.00000000	1.00000000	0.00000000

NORMALIZATION FACTORS

.12601428E-03	148.49713539	.99999999E+00	54.08337006

TABLE VIII (CONTINUED)

WEIGHTS FOR CASE 8

PRESUMED TARGET

SPEED(MPH)	TRACK ANGLE(DEG)	AZIMUTH(DEG)
15.	180.	0.

NO.	OPTIMUM WEIGHTS MAGNITUDE	OPTIMUM WEIGHTS PHASE(DEG)	TARGET WEIGHTS MAGNITUDE	TARGET WEIGHTS PHASE(DEG)
1	1.57979009	-6.10498996	1.00000000	-93.53670985
2	2.33432467	177.19271617	1.00000002	-89.46989626
3	1.00000000	0.00000000	1.00000004	-85.40308284
4	10.00477068	152.95066343	1.00000006	-81.32587150
5	25.86257667	-20.77058211	1.00000008	-77.25905791
6	16.90107861	162.16408940	1.00000009	-73.19224449
7	16.73570082	-59.36634712	1.00000011	-69.11849890
8	50.51330996	123.96934297	1.00000012	-65.05168548
9	35.29429295	-54.62611585	1.00000013	-60.98487189
10	10.11290923	92.61283643	1.00000013	-56.91459239
11	31.33714484	-104.65466614	1.00000014	-52.84777913
12	22.65609419	69.08562843	1.00000014	-48.78096554
13	9.82366629	-5.20721015	1.00000014	-44.71415212
14	30.41138925	-167.24675537	1.00000014	-40.64733854
15	22.02070209	19.25330465	1.00000013	-36.58052512
16	16.54210608	147.21331458	1.00000013	-32.51717778
17	50.00377817	-36.07328872	1.00000012	-28.45036419
18	34.95841161	142.54217398	1.00000011	-24.38355077
19	9.97573099	-65.09290901	1.00000009	-20.32366918
20	25.82510223	108.64026675	1.00000008	-16.25685593
21	16.88782596	-74.28485908	1.00000006	-12.19004234
22	1.58292195	93.90845403	1.00000005	-8.13362701
23	2.34161685	-89.48873750	1.00000002	-4.06681359
24	1.00443165	87.56860766	1.00000000	0.00000000
NORMALIZATION FACTORS	.88994598E-03	91.88727867	.99999986E+00	91.49805414

TABLE VIII (CONTINUED)

WEIGHTS FOR CASE 8

PRESUMED TARGET SPEED(MPH)	TRACK ANGLE(DEG)	AZIMUTH(DEG)
30.	180.	0.

NO.	OPTIMUM WEIGHTS MAGNITUDE	PHASE(DEG)	TARGET WEIGHTS MAGNITUDE	PHASE(DEG)
1	1.62129406	-7.29535101	1.00000000	172.92658048
2	2.36140603	176.57921591	1.00000009	-178.93979268
3	1.00000000	0.00000000	1.00000017	-170.80616584
4	11.21527609	150.93662209	1.00000025	-162.66214075
5	28.31064427	-22.91722906	1.00000031	-154.52851374
6	18.28426573	160.04921847	1.00000037	-146.39488673
7	19.61538461	-59.84142825	1.00000042	-138.25432772
8	59.92099392	124.09461773	1.00000046	-130.12070088
9	42.05314570	-54.31493484	1.00000049	-121.98707404
10	10.04719555	72.81136211	1.00000052	-113.84998111
11	35.55904595	-119.55562676	1.00000053	-105.71635410
12	26.52280064	56.68417858	1.00000054	-97.58272726
13	9.96406004	49.31453818	1.00000054	-89.44910025
14	35.34264949	-118.21241442	1.00000053	-81.31547324
15	26.38298085	65.56797010	1.00000052	-73.18184623
16	19.57068354	-178.17625464	1.00000049	-65.05168548
17	59.80912473	-2.10434273	1.00000046	-56.91805847
18	41.98113408	176.30868779	1.00000042	-48.78443163
19	11.22142011	-28.97463988	1.00000037	-40.65773662
20	28.34313371	144.88272038	1.00000031	-32.52410961
21	18.31054186	-38.07999776	1.00000025	-24.39048277
22	1.62631911	129.26482718	1.00000017	-16.26725385
23	2.37074040	-54.61899716	1.00000009	-8.13362701
24	1.00493748	121.94504553	1.00000000	0.00000000

NORMALIZATION FACTORS

.28502611E-02	77.44463939	.99999946E+00	138.26640906

TABLE IX

WEIGHTS FOR CASE 10

PRESUMED TARGET SPEED(MPH)	TRACK ANGLE(DEG)	AZIMUTH(DEG)
0.	180.	0.

	OPTIMUM WEIGHTS		TARGET WEIGHTS	
NO.	MAGNITUDE	PHASE(DEG)	MAGNITUDE	PHASE(DEG)
1	1.14576544	-1.55551970	1.00000000	0.00000000
2	1.97654959	179.30319919	1.00000000	0.00000000
3	1.00000000	0.00000000	1.00000000	0.00000000
4	5.07546545	173.30318752	1.00000000	.01039809
5	14.05717738	-5.05790526	1.00000000	.01039809
6	9.45358348	175.63002432	1.00000000	.01039809
7	6.00095259	-21.11493832	1.00000000	.01733026
8	17.59149149	160.88222124	1.00000000	.01733026
9	12.16330881	-18.28700152	1.00000000	.01733026
10	3.93697637	115.75775692	1.00000000	.02079617
11	10.10625947	-73.22525886	1.00000000	.02079617
12	6.62640124	102.15097975	1.00000000	.02079617
13	3.93709707	-110.09215330	1.00000000	.02079617
14	10.10637616	78.89065502	1.00000000	.02079617
15	6.62639432	-96.48561040	1.00000000	.02079617
16	6.00127642	26.78616388	1.00000000	.01733026
17	17.59236655	-155.21066905	1.00000000	.01733026
18	12.16389693	23.95873054	1.00000000	.01733026
19	5.07561399	-167.62998912	1.00000000	.01039809
20	14.05752226	10.73163487	1.00000000	.01039809
21	9.45379475	-169.95614102	1.00000000	.01039809
22	1.14578380	7.22917789	1.00000000	0.00000000
23	1.97657675	-173.62809278	1.00000000	0.00000000
24	1.00001182	5.67662722	1.00000000	0.00000000

NORMALIZATION FACTORS

.83346794E-05	41.87646824	.10000000E+01	44.72969905

TABLE IX (CONTINUED)

WEIGHTS FOR CASE 10

PRESUMED TARGET SPEED(MPH)	TRACK ANGLE(DEG)	AZIMUTH(DEG)
3.	180.	0.

NO.	OPTIMUM WEIGHTS MAGNITUDE	PHASE(DEG)	TARGET WEIGHTS MAGNITUDE	PHASE(DEG)
1	1.53782532	-23.35024886	1.00000000	-38.22804669
2	2.30964945	157.64449579	1.00000002	-27.65433149
3	1.00038385	-21.55434105	1.00000002	-17.08061663
4	8.06442509	148.22658967	1.00000001	-35.77756042
5	22.37708803	-28.79307915	1.00000002	-25.20384556
6	15.05026611	152.46135100	1.00000002	-14.63013036
7	8.16435484	-61.43518810	1.00000001	-33.33054023
8	25.37867388	123.45710659	1.00000002	-22.75682537
9	17.99629269	-54.60406670	1.00000002	-12.18311017
10	6.33989392	65.80298916	1.00000002	-30.88698629
11	19.62827731	-136.79842203	1.00000003	-20.31327110
12	14.42591965	35.02802586	1.00000002	-9.73955624
13	6.32596420	-86.79121801	1.00000002	-28.44689811
14	19.58332095	115.85362847	1.00000003	-17.87318308
15	14.39462394	-55.95809741	1.00000002	-7.29946805
16	8.13572511	40.38259554	1.00000002	-26.01027617
17	25.30071137	-144.49177458	1.00000002	-15.43656098
18	17.94382927	33.57693001	1.00000001	-4.86284612
19	8.05009943	-169.39423791	1.00000002	-23.57711999
20	22.34364117	7.59959411	1.00000002	-13.00340496
21	15.02978488	-173.66627313	1.00000001	-2.42968993
22	1.53657649	2.00504067	1.00000002	-21.14743005
23	2.30825028	-179.08424844	1.00000002	-10.57371503
24	1.00000000	0.00000000	1.00000000	0.00000000
NORMALIZATION FACTORS	.14209824E-02	151.10130100	.99999997E+00	63.84372247

TABLE IX (CONTINUED)

WEIGHTS FOR CASE 10

SPEED(MPH)	PRESUMED TARGET TRACK ANGLE(DEG)	AZIMUTH(DEG)
15.	180.	0.

	OPTIMUM WEIGHTS		TARGET WEIGHTS	
NO.	MAGNITUDE	PHASE(DEG)	MAGNITUDE	PHASE(DEG)
1	1.58651945	-61.74528893	1.00000000	168.85976689
2	2.34513170	121.01898896	1.00000045	-138.27165797
3	1.00424974	-56.56063820	1.00000056	-85.40308300
4	9.78668920	101.62342285	1.00000014	-178.92939476
5	25.58953768	-73.38929998	1.00000051	-126.06081963
6	16.79279826	108.90859854	1.00000053	-73.19224449
7	15.50778155	-105.77961832	1.00000025	-166.72202216
8	46.20882338	76.91988404	1.00000055	-113.85344720
9	32.14323453	-101.92533295	1.00000049	-60.98487189
10	12.31653702	51.90169953	1.00000035	-154.51811565
11	32.73355606	-141.27916367	1.00000056	-101.64954085
12	22.07033600	32.60386274	1.00000043	-48.78096554
13	12.34734166	-107.19781562	1.00000043	-142.31767522
14	32.93333955	85.83818395	1.00000056	-89.44910025
15	22.23165721	-88.14002647	1.00000035	-36.58052512
16	15.41528184	50.50365389	1.00000049	-130.12070121
17	45.89568649	-132.19983489	1.00000055	-77.25212591
18	31.91431446	46.64170275	1.00000025	-24.38355077
19	9.67718236	-157.48978755	1.00000054	-117.92719262
20	25.31261676	17.37266318	1.00000051	-65.05861765
21	16.61663488	-164.99394930	1.00000014	-12.19004234
22	1.57487299	5.35114568	1.00000056	-105.73715044
23	2.33154375	-177.50352088	1.00000045	-52.86857530
24	1.00000000	0.00000000	1.00000000	0.00000000

NORMALIZATION FACTORS

.90085564E-02	-166.16918771	.99999943E+00	140.29981585

TABLE IX (CONTINUED)

WEIGHTS FOR CASE 10

SPEED(MPH)	PRESUMED TARGET TRACK ANGLE(DEG)	AZIMUTH(DEG)
30.	180.	0.

NO.	OPTIMUM WEIGHTS MAGNITUDE	PHASE(DEG)	TARGET WEIGHTS MAGNITUDE	PHASE(DEG)
1	1.60404573	-6.74960765	1.00000000	-22.28046622
2	2.34910745	176.80526141	1.00000181	83.45668405
3	1.00000000	0.00000000	1.00000223	-170.80616567
4	10.83226051	154.71162684	1.00000054	2.13081272
5	27.51063571	-20.19971986	1.00000203	107.86796300
6	17.80990876	162.25295388	1.00000213	-146.39488690
7	19.11518691	-48.68384874	1.00000101	26.53862558
8	56.95573246	133.30610148	1.00000217	132.27577586
9	39.58973426	-45.83396046	1.00000196	-121.98707387
10	13.89496601	116.22312765	1.00000140	50.94297236
11	36.42138287	-75.68528191	1.00000225	156.68012263
12	24.32440940	98.69430008	1.00000172	-97.58272709
13	13.87057491	-32.47963502	1.00000172	75.34385338
14	36.34649495	159.44178529	1.00000225	-178.91899651
15	24.27211700	-14.92959475	1.00000140	-73.18184623
16	19.07961969	132.48175326	1.00000196	99.74126799
17	56.84707383	-49.49990982	1.00000217	-154.52158174
18	39.51331549	129.64324858	1.00000101	-48.78443146
19	10.81971666	-70.96104583	1.00000213	124.13521685
20	27.48889268	103.93858616	1.00000203	-130.12763288
21	17.79934985	-78.51862944	1.00000054	-24.39048260
22	1.60536492	90.47982652	1.00000223	148.52569945
23	2.35238331	-93.06388929	1.00000181	-105.73715027
24	1.00191515	83.75623755	1.00000000	0.00000000

NORMALIZATION FACTORS

.28764706E-01	153.91317689	.99999774E+00	-124.13006768

TABLE X

WEIGHTS FOR CASE 11

PRESUMED TARGET

SPEED(MPH)	TRACK ANGLE(DEG)	AZIMUTH(DEG)
0.	180.	0.

	OPTIMUM WEIGHTS		TARGET WEIGHTS	
NO.	MAGNITUDE	PHASE(DEG)	MAGNITUDE	PHASE(DEG)
1	1.37924485	105.52579462	1.00000000	0.00000000
2	3.19697329	-73.34808926	1.00000000	.00000000
3	2.91672022	109.87699807	1.00000000	0.00000000
4	1.00073571	-66.31781758	1.00000000	0.00000000
5	6.20268552	-94.15381249	1.00000000	.00693217
6	20.94133736	86.61614959	1.00000000	.00693217
7	20.38261712	-98.08358328	1.00000000	.00693217
8	5.82438001	68.32906773	1.00000000	.00693217
9	12.15590591	66.35332787	1.00000000	.01039809
10	49.34184402	-112.57702244	1.00000000	.01039809
11	67.45361091	70.72789884	1.00000000	.01039809
12	30.63036011	-105.79028874	1.00000000	.01039809
13	12.15314339	-132.61330023	1.00000000	.01039809
14	49.32620120	46.32170951	1.00000000	.01039809
15	67.42283005	-136.98062581	1.00000000	.01039809
16	30.61207444	39.53867744	1.00000000	.01039809
17	6.19945313	27.87605157	1.00000000	.00693217
18	20.92575673	-152.89433420	1.00000000	.00693217
19	20.35936566	31.81136695	1.00000000	.00693217
20	5.81368813	-134.56951071	1.00000000	.00693217
21	1.37864811	-171.82325091	1.00000000	0.00000000
22	3.19492665	7.04391338	1.00000000	.00000000
23	2.91461253	-176.18817357	1.00000000	0.00000000
24	1.00000000	0.00000000	1.00000000	0.00000000

NORMALIZATION FACTORS

.54675140E-04	77.90210816	.10000000E+01	44.74009713

TABLE X (CONTINUED)

WEIGHTS FOR CASE 11

PRESUMED TARGET SPEED(MPH)	TRACK ANGLE(DEG)	AZIMUTH(DEG)
3.	180.	0.

NO.	OPTIMUM WEIGHTS MAGNITUDE	PHASE(DEG)	TARGET WEIGHTS MAGNITUDE	PHASE(DEG)
1	2.18520513	64.78757355	1.00000000	-14.03050661
2	4.17855372	-124.84122980	1.00000000	-13.42048444
3	3.30978779	50.02637575	1.00000000	-12.81046260
4	1.00115115	-132.50349982	1.00000000	-12.20044060
5	9.35913977	-140.85965315	1.00000000	-11.58348642
6	29.76079853	31.64251532	1.00000000	-10.97346442
7	29.57033703	-176.60769554	1.00000000	-10.36344241
8	14.28333978	-36.03778186	1.00000000	-9.75342041
9	19.30053895	26.99577806	1.00000000	-9.13993232
10	78.10157905	-153.52589457	1.00000001	-8.52991031
11	106.70827110	30.38621324	1.00000001	-7.91988831
12	48.62989215	-144.89036112	1.00000001	-7.30986631
13	19.29774331	-159.46476829	1.00000001	-6.69984430
14	78.08813961	21.05607272	1.00000001	-6.08982213
15	106.69953587	-162.85663134	1.00000001	-5.47980029
16	48.63161229	12.42033175	1.00000000	-4.86977829
17	9.35662042	8.38964875	1.00000000	-4.26322220
18	29.74346408	-164.11789510	1.00000000	-3.65320019
19	29.52725992	44.15483867	1.00000000	-3.04317802
20	14.26362172	-96.34352937	1.00000000	-2.43315618
21	2.18528105	162.75595115	1.00000000	-1.83006601
22	4.17708435	-7.63691589	1.00000000	-1.22004418
23	3.30728216	177.48159669	1.00000000	-.61002217
24	1.00000000	0.00000000	1.00000000	0.00000000

NORMALIZATION FACTORS

.39240964E-01	-158.67250951	.99999999E+00	51.75535060

TABLE X (CONTINUED)

WEIGHTS FOR CASE 11

SPEED(MPH)	PRESUMED TARGET TRACK ANGLE(DEG)	AZIMUTH(DEG)
15.	180.	0.

NO.	OPTIMUM WEIGHTS MAGNITUDE	OPTIMUM WEIGHTS PHASE(DEG)	TARGET WEIGHTS MAGNITUDE	TARGET WEIGHTS PHASE(DEG)
1	2.15513623	-163.87232712	1.00000000	-70.15253255
2	4.15924000	7.06643717	1.00000001	-67.10242236
3	3.30420007	-177.68445971	1.00000002	-64.05231234
4	1.00000000	0.00000000	1.00000003	-61.00220215
5	9.43558497	-7.71260752	1.00000005	-57.94515995
6	29.96689704	165.32806914	1.00000005	-54.89504976
7	29.09805830	-41.08846643	1.00000006	-51.84493974
8	13.31804512	98.82068654	1.00000007	-48.79482955
9	19.44078709	161.00841345	1.00000007	-45.74125344
10	78.68675654	-19.53867966	1.00000007	-42.69114342
11	107.54048735	163.88361429	1.00000008	-39.64103322
12	48.95462277	-11.96178773	1.00000008	-36.59092320
13	19.44467704	-25.15691802	1.00000008	-33.54081318
14	78.70462223	155.40061162	1.00000008	-30.49070299
15	107.53002011	-28.01495331	1.00000007	-27.44059296
16	48.92992938	147.83268927	1.00000007	-24.39048277
17	9.43734755	143.54431404	1.00000007	-21.34383883
18	29.98483591	-29.47312681	1.00000006	-18.29372864
19	29.17239025	176.94249612	1.00000005	-15.24361862
20	13.36608222	36.88428054	1.00000005	-12.19350843
21	2.15411472	-60.36703826	1.00000004	-9.15033024
22	4.15846643	128.73409521	1.00000003	-6.10022021
23	3.30449843	-46.49680010	1.00000001	-3.05011002
24	1.00027179	135.82563172	1.00000000	0.00000000
	NORMALIZATION FACTORS			
	.22668009E+00	69.11166184	.99999992E+00	79.81636349

TABLE X (CONTINUED)

WEIGHTS FOR CASE 11

PRESUMED TARGET SPEED(MPH)	TRACK ANGLE(DEG)	AZIMUTH(DEG)
30.	180.	0.

NO.	OPTIMUM WEIGHTS MAGNITUDE	PHASE(DEG)	TARGET WEIGHTS MAGNITUDE	PHASE(DEG)
1	2.13260979	-165.27321074	1.00000000	-140.30506460
2	4.14890505	6.37099393	1.00000005	-134.20484455
3	3.30332572	-177.93407708	1.00000010	-128.10462434
4	1.00000000	0.00000000	1.00000014	-122.00440412
5	9.48953779	-7.30400908	1.00000018	-115.89725174
6	30.09542517	166.36332121	1.00000021	-109.79703153
7	28.49497916	-38.19572113	1.00000024	-103.69681148
8	12.28249540	100.87191235	1.00000026	-97.59659126
9	19.51281548	162.22632162	1.00000028	-91.49290513
10	79.03563313	-18.27987508	1.00000029	-85.39268492
11	108.18766673	164.81120776	1.00000030	-79.29246470
12	49.28855131	-11.44446510	1.00000031	-73.19224449
13	19.52422369	-23.66414742	1.00000031	-67.09202411
14	79.07868644	156.88915845	1.00000030	-60.99180389
15	108.08807207	-26.17286621	1.00000029	-54.89158385
16	49.15551040	150.09362905	1.00000028	-48.79136363
17	9.49271338	145.76933114	1.00000026	-42.69460950
18	30.14409400	-27.78332152	1.00000024	-36.59438929
19	28.76602351	176.86977754	1.00000021	-30.49416907
20	12.48912427	37.21774920	1.00000018	-24.39394886
21	2.12834009	-56.56345420	1.00000014	-18.30066064
22	4.14374899	131.96368975	1.00000010	-12.20044043
23	3.30221216	-43.64520856	1.00000005	-6.10022021
24	1.00033142	138.46166937	1.00000000	0.00000000

NORMALIZATION FACTORS

.49201438E+00	70.67149442	.99999969E+00	114.89262968

TABLE XI

WEIGHTS FOR CASE 17

SPEED(MPH)	PRESUMED TARGET TRACK ANGLE(DEG)	AZIMUTH(DEG)
0.	180.	0.

NO.	OPTIMUM WEIGHTS MAGNITUDE	PHASE(DEG)	TARGET WEIGHTS MAGNITUDE	PHASE(DEG)
1	6.38902541	-.01665903	1.00000000	0.00000000
2	20.33210521	179.98364683	1.00000000	0.00000000
3	15.95555528	-.01555233	1.00000000	0.00000000
4	6.49832476	179.98223047	1.00000000	.01039809
5	19.61531963	-.01741560	1.00000000	.01039809
6	13.22287777	179.98109105	1.00000000	.01039809
7	2.74721497	-.02381101	1.00000000	.01733026
8	7.02716780	179.97585172	1.00000000	.01733026
9	5.72980993	-.01786805	1.00000000	.01733026
10	1.00000000	0.00000000	1.00000000	.02079617
11	1.60125579	-179.99143413	1.00000000	.02079617
12	1.49912085	.02052395	1.00000000	.02079617
13	3.78032142	179.98789449	1.00000000	.02079617
14	10.94315880	-.01241474	1.00000000	.02079617
15	6.67542452	179.98324880	1.00000000	.02079617
16	6.80831920	-.01528691	1.00000000	.01733026
17	17.67043394	179.98499324	1.00000000	.01733026
18	12.65721924	-.01290096	1.00000000	.01733026
19	9.00888017	179.98352990	1.00000000	.01039809
20	26.35932460	-.01661384	1.00000000	.01039809
21	17.66814200	179.98208749	1.00000000	.01039809
22	7.06936796	-.01640813	1.00000000	0.00000000
23	21.59802739	179.98388544	1.00000000	0.00000000
24	16.61363859	-.01537358	1.00000000	0.00000000
	NORMALIZATION FACTORS			
	.96150024E-07	44.73412878	.10000000E+01	44.72969905

TABLE XI (CONTINUED)

WEIGHTS FOR CASE 17

PRESUMED TARGET SPEED(MPH)	TRACK ANGLE(DEG)	AZIMUTH(DEG)
3.	180.	0.

	OPTIMUM WEIGHTS		TARGET WEIGHTS	
NO.	MAGNITUDE	PHASE(DEG)	MAGNITUDE	PHASE(DEG)
1	3.84860368	124.97068864	1.00000000	-18.70734187
2	9.24223073	-37.50971869	1.00000000	-17.89397908
3	6.50365033	154.18835183	1.00000000	-17.08061647
4	6.51831389	-74.64314245	1.00000001	-16.25685576
5	23.28241296	103.00447533	1.00000001	-15.44349315
6	17.28067511	-78.32834763	1.00000001	-14.63013036
7	2.47586679	99.20951557	1.00000001	-13.80983558
8	1.00000000	0.00000000	1.00000001	-12.99647296
9	2.33774476	-117.64141857	1.00000001	-12.18311017
10	2.86257986	-111.56713956	1.00000001	-11.36628147
11	13.98593408	81.34247706	1.00000001	-10.55291869
12	11.50340300	-97.24984730	1.00000001	-9.73955607
13	2.39693998	-17.86906136	1.00000001	-8.92619345
14	10.82098036	129.39541975	1.00000001	-8.11283067
15	8.80560020	-59.43814586	1.00000001	-7.29946805
16	3.31928791	170.01575952	1.00000001	-6.48957135
17	9.26708496	33.71215175	1.00000001	-5.67620857
18	7.69656823	-132.33492852	1.00000001	-4.86284595
19	6.40093290	-44.13603056	1.00000001	-4.05641533
20	22.24411332	128.95590974	1.00000001	-3.24305255
21	16.29075448	-53.86711369	1.00000000	-2.42968976
22	3.69379061	144.97696382	1.00000000	-1.62672540
23	8.85700567	-16.61831041	1.00000000	-.81336262
24	6.28435954	175.65676052	1.00000000	0.00000000

NORMALIZATION FACTORS

.25802649E-06	-138.36363249	.99999999E+00	54.08337006

TABLE XI (CONTINUED)

WEIGHTS FOR CASE 17

SPEED(MPH)	PRESUMED TARGET TRACK ANGLE(DEG)	AZIMUTH(DEG)
15.	180.	0.

NO.	OPTIMUM WEIGHTS MAGNITUDE	OPTIMUM WEIGHTS PHASE(DEG)	TARGET WEIGHTS MAGNITUDE	TARGET WEIGHTS PHASE(DEG)
1	1.75195088	-78.88955827	1.00000000	-93.53670985
2	3.14039213	111.20655501	1.00000002	-89.46989626
3	1.64470373	-57.48710828	1.00000004	-85.40308284
4	3.80587952	83.24282019	1.00000006	-81.32587150
5	13.29726276	-93.03504514	1.00000008	-77.25905791
6	9.82072428	88.20260945	1.00000009	-73.19224449
7	2.08100020	-117.83580284	1.00000011	-69.11849890
8	3.84046548	21.67011258	1.00000012	-65.05168548
9	2.62768423	175.84486433	1.00000013	-60.98487189
10	2.56914805	65.73210749	1.00000013	-56.91459239
11	9.46122770	-95.47651264	1.00000014	-52.84777913
12	7.29877326	90.13499637	1.00000014	-48.78096554
13	2.34314253	-157.82736955	1.00000014	-44.71415212
14	8.03220057	-2.88083774	1.00000014	-40.64733854
15	6.09596396	168.93293270	1.00000013	-36.58052512
16	2.03956204	30.06966379	1.00000013	-32.51717778
17	5.24823426	-109.25925470	1.00000012	-28.45036419
18	4.06802617	87.34980985	1.00000011	-24.38355077
19	3.54115241	179.14680377	1.00000009	-20.32366918
20	12.31831197	-6.90373682	1.00000008	-16.25685593
21	9.05746563	170.95560923	1.00000006	-12.19004234
22	1.52345960	-14.81303242	1.00000005	-8.13362701
23	2.36169654	169.55541755	1.00000002	-4.06681359
24	1.00000000	0.00000000	1.00000000	0.00000000
	NORMALIZATION FACTORS			
	.23253800E-05	11.64770746	.99999986E+00	91.49805414

TABLE XI (CONTINUED)

WEIGHTS FOR CASE 17

SPEED(MPH)	PRESUMED TARGET TRACK ANGLE(DEG)	AZIMUTH(DEG)
30.	180.	0.

NO.	OPTIMUM WEIGHTS MAGNITUDE	PHASE(DEG)	TARGET WEIGHTS MAGNITUDE	PHASE(DEG)
1	1.67147447	-103.50212419	1.00000000	172.92658048
2	2.93996232	86.01225219	1.00000009	-178.93979268
3	1.49319073	-84.00269215	1.00000017	-170.80616584
4	4.14425160	55.13334035	1.00000025	-162.66214075
5	13.78637481	-120.22921442	1.00000031	-154.52851374
6	9.99959280	61.48162939	1.00000037	-146.39488673
7	2.60482633	-139.50955733	1.00000042	-138.25432772
8	5.73480900	11.94975418	1.00000046	-130.12070088
9	3.80280285	175.73536123	1.00000049	-121.98707404
10	3.32349815	59.72235275	1.00000052	-113.84998111
11	10.72790244	-104.11111065	1.00000053	-105.71635410
12	7.86714779	81.74947804	1.00000054	-97.58272726
13	3.24499989	-146.84245194	1.00000054	-89.44910025
14	10.14779959	15.55928464	1.00000053	-81.31547324
15	7.34438547	-171.08977358	1.00000052	-73.18184623
16	2.52839892	54.06330827	1.00000049	-65.05168548
17	6.12805023	-96.18259887	1.00000046	-56.91805847
18	4.31698599	98.50346686	1.00000042	-48.78443163
19	3.95870679	-143.62737538	1.00000037	-40.65773662
20	13.12274829	30.88460644	1.00000031	-32.52410961
21	9.49319623	-151.17764026	1.00000025	-24.39048277
22	1.48837962	13.51789470	1.00000017	-16.26725385
23	2.34408406	-173.32127223	1.00000009	-8.13362701
24	1.00000000	0.00000000	1.00000000	0.00000000

NORMALIZATION FACTORS

.50217630E-05	5.50820620	.99999946E+00	138.26640906

TABLE XII

WEIGHTS FOR CASE 2

SPEED(MPH)	PRESUMED TARGET TRACK ANGLE(DEG)	AZIMUTH(DEG)
0.	180.	30.

NO.	OPTIMUM WEIGHTS MAGNITUDE	OPTIMUM WEIGHTS PHASE(DEG)	TARGET WEIGHTS MAGNITUDE	TARGET WEIGHTS PHASE(DEG)
1	2.71140734	-132.29278585	1.33342172	.00000000
2	1.00926901	105.44049271	1.00000000	0.00000000
3	6.51789090	47.99687707	1.33345757	-176.97649766
4	5.77189519	-125.47774923	1.00003635	-176.97649766
5	9.67435849	-131.45212071	1.33348789	6.04440562
6	9.84374115	51.71391275	1.00006857	6.04440562
7	12.37688169	49.38581907	1.33351271	-170.93729066
8	13.39675047	-128.78890511	1.00009665	-170.93729066
9	14.37150536	-129.72015130	1.33353201	12.07841383
10	16.00432105	51.42717699	1.00012059	12.07841383
11	15.89315545	51.20995944	1.33354579	-164.90848124
12	18.00153529	-128.11747644	1.00014040	-164.90848124
13	16.71693022	-127.84620512	1.33355406	18.10202429
14	19.08141316	52.46951386	1.00015608	18.10202429
15	17.05924494	53.10345549	1.33355682	-158.89006957
16	19.52994502	-126.90186090	1.00016762	-158.89006957
17	16.70703181	-125.94737510	1.33355406	24.11523683
18	19.06843253	53.72612263	1.00017502	24.11523683
19	15.87429678	54.99402558	1.33354579	-152.88205616
20	17.97679597	-125.68980043	1.00017829	-152.88205616
21	14.34596879	-124.07927347	1.33353201	30.11805128
22	15.97078614	54.76111291	1.00017742	30.11805128
23	12.34742753	56.80937474	1.33351271	-146.88444117
24	13.35801336	-125.03026136	1.00017242	-146.88444117
25	9.64558195	-122.35901037	1.33348790	36.11046698
26	9.80578760	54.45541441	1.00016328	36.11046698
27	6.49411697	58.18342643	1.33345758	-140.89722460
28	5.74039194	-128.38094299	1.00015001	-140.89722460
29	2.69997197	-121.53547893	1.33342175	42.09248392
30	1.00000000	0.00000000	1.00013260	42.09248392

NORMALIZATION FACTORS

.16846121E-07	-8.38783933	.74987431E+00	-156.35900170

TABLE XII (CONTINUED)

WEIGHTS FOR CASE 2

PRESUMED TARGET SPEED(MPH)	TRACK ANGLE(DEG)	AZIMUTH(DEG)
3.	180.	30.

NO.	OPTIMUM WEIGHTS MAGNITUDE	OPTIMUM WEIGHTS PHASE(DEG)	TARGET WEIGHTS MAGNITUDE	TARGET WEIGHTS PHASE(DEG)
1	1.08344118	-157.85087513	1.33342117	-1.05655398
2	1.00000000	0.00000000	1.00000000	0.00000000
3	2.56750413	23.89261917	1.33345786	-175.92000570
4	2.97482712	-163.53845781	1.00003693	-174.86344635
5	3.77129319	-154.05349570	1.33348891	9.21396330
6	4.56909600	20.77444441	1.00006962	10.27052751
7	4.81286756	27.72531640	1.33351432	-165.65464698
8	5.96738045	-156.44900955	1.00009809	-164.59807774
9	5.58359936	-150.49292349	1.33353408	19.47416330
10	7.00879222	25.76337830	1.00012232	20.53073756
11	6.17420603	31.23585164	1.33354820	-155.39960571
12	7.81466484	-152.27301855	1.00014232	-154.34302658
13	6.49761114	-147.04130783	1.33355668	29.72404534
14	8.27167277	29.50511455	1.00015809	30.78062950
15	6.63495005	34.65912910	1.33355952	-145.15488256
16	8.48241667	-148.82617727	1.00016963	-144.09829354
17	6.50521568	-143.65965789	1.33355671	39.96360959
18	8.34552895	32.68285880	1.00017694	41.02020381
19	6.19018684	38.00085515	1.33354827	-134.92047787
20	7.96275362	-145.92976863	1.00018001	-133.86387862
21	5.60660423	-140.38318270	1.33353418	50.19285539
22	7.23109872	35.17976374	1.00017886	51.24945950
23	4.84580385	41.17477765	1.33351445	-124.69639113
24	6.26557694	-144.02650485	1.00017347	-123.63978216
25	3.80976290	-137.39403690	1.33348908	60.41178240
26	4.94460580	35.86918000	1.00016385	61.46839656
27	2.62199700	43.59084185	1.33345807	-114.48262352
28	3.43628718	-146.09996818	1.00015000	-113.42600450
29	1.11872275	-135.92954782	1.33342142	70.62039061
30	1.56766848	20.75792355	1.00013193	71.67701449

NORMALIZATION FACTORS

.84993210E-07 -50.23815085 .74987279E+00 -170.62248314

TABLE XII (CONTINUED)

WEIGHTS FOR CASE 2

PRESUMED TARGET

SPEED(MPH)	TRACK ANGLE(DEG)	AZIMUTH(DEG)
15.	180.	30.

	OPTIMUM WEIGHTS		TARGET WEIGHTS	
NO.	MAGNITUDE	PHASE(DEG)	MAGNITUDE	PHASE(DEG)
1	1.00000000	0.00000000	1.33341890	-5.28277393
2	1.15272544	176.24118087	1.00000000	0.00000000
3	2.39106318	-176.15796156	1.33345909	-171.69403654
4	3.02348001	1.95070086	1.00003930	-166.41123813
5	3.54551718	8.82849338	1.33349310	21.89220054
6	4.55850842	-172.66056139	1.00007397	27.17502359
7	4.56930071	-166.28327385	1.33352095	-144.52406237
8	5.92899721	12.40772105	1.00010402	-139.24121484
9	5.35020472	18.77033802	1.33354263	49.05717423
10	6.98050291	-162.44789951	1.00012944	54.34004640
11	5.94905091	-156.22155033	1.33355813	-117.36408949
12	7.79264115	22.61191785	1.00015023	-112.08119284
13	6.28961775	28.84141701	1.33356747	76.21214664
14	8.26700881	-152.30182156	1.00016640	81.49506759
15	6.42549093	-146.10962990	1.33357064	-90.21411790
16	8.46986280	32.75490630	1.00017793	-84.93117213
17	6.29659429	38.93531221	1.33356764	103.35711725
18	8.32607846	-142.21341712	1.00018485	108.64008732
19	5.96322768	-136.00988602	1.33355847	-63.07414809
20	7.90956093	42.81443990	1.00018713	-57.79115338
21	5.37045420	48.98026507	1.33354313	130.49208591
22	7.15271515	-132.25514211	1.00018479	135.77510526
23	4.59665290	-125.99621402	1.33352163	-35.94418041
24	6.15296929	52.67885496	1.00017783	-30.66113641
25	3.57660159	58.84163240	1.33349395	157.61705277
26	4.82914685	-122.67456694	1.00016623	162.90012108
27	2.43107661	-116.30689975	1.33346012	-8.82421486
28	3.33590473	61.83282640	1.00015001	-3.54112208
29	1.02534482	67.38320746	1.33342011	-175.26798315
30	1.49766764	-116.08429006	1.00012917	-169.98486573

NORMALIZATION FACTORS

.29904465E-06 107.19927541 .74986654E+00 132.32357383

TABLE XII (CONTINUED)

WEIGHTS FOR CASE 2

	PRESUMED TARGET	
SPEED(MPH)	TRACK ANGLE(DEG)	AZIMUTH(DEG)
30.	180.	30.

NO.	OPTIMUM WEIGHTS MAGNITUDE	OPTIMUM WEIGHTS PHASE(DEG)	TARGET WEIGHTS MAGNITUDE	TARGET WEIGHTS PHASE(DEG)
1	1.00000000	0.00000000	1.33341596	-10.56555457
2	1.11280115	178.53747995	1.00000000	0.00000000
3	2.45724025	-169.95916934	1.33346073	-166.41156938
4	3.07201755	8.54198071	1.00004242	-155.84596653
5	3.74624665	22.33761689	1.33349864	37.74001306
6	4.78801083	-159.00484573	1.00007969	48.30566386
7	4.91957168	-145.58859320	1.33352970	-118.11080776
8	6.36428137	33.12618649	1.00011182	-107.54510868
9	5.86743413	46.89564697	1.33355389	86.03596849
10	7.64557872	-134.34103449	1.00013880	96.60171552
11	6.58353678	-120.79279136	1.33357122	-69.81965868
12	8.62642186	58.00357801	1.00016064	-59.25386354
13	7.02617342	71.67543585	1.33358169	134.32231123
14	9.24793726	-109.49763079	1.00017733	144.88815447
15	7.17708927	-95.91278678	1.33358530	-21.53812230
16	9.48612864	82.93989863	1.00018888	-10.97223094
17	7.03667497	96.49809547	1.33358204	-177.40095908
18	9.33884138	-84.61918231	1.00019528	-166.83501961
19	6.60414892	-71.03017153	1.33357193	26.73380088
20	8.80392018	107.87953261	1.00019654	37.29978863
21	5.89713486	121.28202599	1.33355496	-129.13384242
22	7.90351428	-59.76713552	1.00019265	-118.56780672
23	4.95769250	-46.21813508	1.33353112	74.99611085
24	6.69051968	132.77704314	1.00018361	85.56219466
25	3.78945371	145.86395831	1.33350043	-80.87633930
26	5.17072468	-35.05500963	1.00016943	-70.31020738
27	2.50870911	-21.73699148	1.33346288	123.24880712
28	3.49410340	157.50021807	1.00015011	133.81498698
29	1.03296634	168.34272062	1.33341847	-32.62845006
30	1.55310570	-11.66947176	1.00012564	-22.06222208
	NORMALIZATION FACTORS			
	.26581714E-06	53.58549204	.74985830E+00	61.00610526

TABLE XIII

WEIGHTS FOR CASE 20

PRESUMED TARGET SPEED(MPH)	TRACK ANGLE(DEG)	AZIMUTH(DEG)
0.	180.	60.

	OPTIMUM WEIGHTS		TARGET WEIGHTS	
NO.	MAGNITUDE	PHASE(DEG)	MAGNITUDE	PHASE(DEG)
1	1.00000000	0.00000000	64.00787339	0.00000000
2	3.65185768	-162.97779319	16.00131220	0.00000000
3	4.74301424	30.25356427	4.00016402	0.00000000
4	2.09537893	-140.54986905	1.00000000	0.00000000
5	2.10449611	153.06671736	64.01051124	-43.02152686
6	8.53146090	-29.45175206	16.00223410	-43.02152686
7	11.21234923	149.89404946	4.00046010	-43.02152686
8	4.81242848	-29.66945385	1.00009042	-43.02152686
9	2.69114394	-33.96710222	64.01235516	-86.04392024
10	10.16297076	150.05495752	16.00295755	-86.04392024
11	12.86199915	-27.19537666	4.00070658	-86.04392024
12	5.43416149	154.65906541	1.00016844	-86.04392024
13	2.64891624	145.81260587	64.01340510	-129.06717980
14	9.92862295	-37.69746544	16.00348252	-129.06717980
15	12.52765625	140.12272612	4.00090344	-129.06717980
16	5.29176644	-41.07066689	1.00023406	-129.06717980
17	2.22447577	-42.50202495	64.01366102	-172.09130622
18	9.05445971	140.37515494	16.00380899	-172.09130622
19	11.93508326	-38.38978413	4.00105069	-172.09130622
20	5.13501839	141.90627089	1.00028728	-172.09130622
21	1.12950917	117.05882499	64.01312292	144.88370100
22	4.08763216	-76.98094057	16.00393696	144.88370100
23	5.19337832	91.64308815	4.00114831	144.88370100
24	2.24541605	-96.62195548	1.00032809	144.88370100
NORMALIZATION FACTORS				
	.27433707E-05	-15.31012076	.39054580E-02	-27.69362938

TABLE XIII (CONTINUED)

WEIGHTS FOR CASE 20

SPEED(MPH)	PRESUMED TARGET TRACK ANGLE(DEG)	AZIMUTH(DEG)
3.	180.	60.

	OPTIMUM WEIGHTS		TARGET WEIGHTS	
NO.	MAGNITUDE	PHASE(DEG)	MAGNITUDE	PHASE(DEG)
1	1.05771667	-174.51020990	64.00779945	-.91501448
2	3.36231820	15.94285772	16.00130140	-.61000960
3	3.77661856	-153.74599487	4.00016286	-.30500488
4	1.48919460	35.14405910	1.00000000	0.00000000
5	2.59249960	1.68968099	64.01043857	-42.71654075
6	10.71557400	178.37334525	16.00222039	-42.41153335
7	14.21322742	-2.93879660	4.00045741	-42.10652612
8	6.12019518	176.84857538	1.00008984	-41.80151872
9	2.78707623	-174.37719614	64.01227764	-84.51891359
10	10.54326925	11.80421059	16.00293940	-84.21390384
11	13.44701853	-164.56133766	4.00070197	-83.90889410
12	5.72784352	17.31138891	1.00016718	-83.60388419
13	2.83862663	-1.34651012	64.01331661	-126.32213317
14	10.82098556	172.80834430	16.00345841	-126.01712091
15	13.84454638	-10.44163628	4.00089654	-125.71210865
16	5.89858566	168.06658506	1.00023202	-125.40709639
17	2.58389186	-175.62129494	64.01355543	-168.12619932
18	10.67972335	8.05823952	16.00377738	-167.82118455
19	14.17208616	-170.32928183	4.00104110	-167.51616977
20	6.10585256	10.15716881	1.00028437	-167.21115500
21	1.00000000	0.00000000	64.01299411	150.06888812
22	3.10655560	168.99896769	16.00389632	150.37390525
23	3.41574840	-22.26734761	4.00113566	150.67892237
24	1.32704419	147.78656823	1.00032422	150.98393966

NORMALIZATION FACTORS

.42255262E-05	134.29074367	.39054633E-02	-30.28616996

TABLE XIII (CONTINUED)

WEIGHTS FOR CASE 20

PRESUMED TARGET SPEED(MPH)	TRACK ANGLE(DEG)	AZIMUTH(DEG)
15.	180.	60.

NO.	OPTIMUM WEIGHTS MAGNITUDE	PHASE(DEG)	TARGET WEIGHTS MAGNITUDE	PHASE(DEG)
1	1.04020771	122.07316632	64.00750323	-4.57507677
2	3.31132564	-56.85735408	16.00125810	-3.05005085
3	3.65761798	124.15639640	4.00015821	-1.52502526
4	1.39871158	-54.83271170	1.00000000	0.00000000
5	2.45894513	-41.90389394	64.01014800	-41.49659531
6	10.36325806	133.98104687	16.00216560	-39.97155765
7	13.87998098	-47.89445945	4.00044666	-38.44652049
8	6.00217142	131.38900705	1.00008750	-36.92148317
9	2.37109318	155.29320159	64.01196799	-78.41888331
10	9.09854825	-16.34176347	16.00286693	-76.89383391
11	11.75765650	168.00716614	4.00068357	-75.36878468
12	5.04570950	-10.26091508	1.00016213	-73.84373579
13	2.41797063	-34.16644754	64.01296315	-115.34194060
14	9.33315650	137.41918004	16.00336208	-113.81687947
15	12.09534336	-46.99000175	4.00086895	-112.29181867
16	5.19583074	131.17048487	1.00022387	-110.76675788
17	2.46869466	164.32323814	64.01313343	-152.26576718
18	10.41110843	-11.58392627	16.00365101	-150.74069431
19	13.94410197	170.20611439	4.00100277	-149.21562161
20	6.02742302	-9.19808224	1.00027272	-147.69054892
21	1.00000000	0.00000000	64.01247885	170.80963679
22	3.10712364	178.92629526	16.00373373	172.33472155
23	3.34388380	-1.97140594	4.00108505	173.85980615
24	1.24834887	177.18343687	1.00030869	175.38489042
NORMALIZATION FACTORS	.12230442E-04	169.54337855	.39054844E-02	-40.65633802

TABLE XIII (CONTINUED)

WEIGHTS FOR CASE 20

	PRESUMED TARGET	
SPEED(MPH)	TRACK ANGLE(DEG)	AZIMUTH(DEG)
30.	180.	60.

	OPTIMUM WEIGHTS		TARGET WEIGHTS	
NO.	MAGNITUDE	PHASE(DEG)	MAGNITUDE	PHASE(DEG)
1	1.00938954	94.93979208	64.00713198	-9.15016428
2	3.28856560	-85.80092230	16.00120381	-6.10010890
3	3.72370117	93.52249261	4.00015237	-3.05005403
4	1.45621563	-86.88293885	1.00000000	0.00000000
5	2.19650286	-64.33752707	64.00978506	-39.97166092
6	9.40000394	111.08867139	16.00209723	-36.92158341
7	12.68847562	-71.03143041	4.00043326	-33.87150642
8	5.50759723	108.07618631	1.00008460	-30.82143025
9	2.03043547	140.64134996	64.01158193	-70.79383565
10	7.83784011	-29.59671829	16.00277662	-67.74373585
11	10.19186884	155.28589860	4.00066065	-64.69363673
12	4.38693181	-22.92844057	1.00015584	-61.64353844
13	2.06091558	-45.09111912	64.01252252	-101.61668831
14	7.97394942	124.81491452	16.00324196	-98.56656639
15	10.39086281	-60.40607158	4.00083453	-95.51644513
16	4.48008757	117.44738440	1.00021369	-92.46632488
17	2.22710209	160.37187637	64.01260680	-132.44021874
18	9.53039953	-15.29911201	16.00349322	-129.39007469
19	12.85233634	166.56064946	4.00095489	-126.33993164
20	5.57082212	-12.82368004	1.00025817	-123.28978892
21	1.00000000	0.00000000	64.01183478	-163.26442726
22	3.20474434	-179.65131948	16.00353041	-160.21426108
23	3.56720674	.79562772	4.00102174	-157.16409573
24	1.37372026	-178.92318138	1.00028927	-154.11393106

NORMALIZATION FACTORS

.22371891E-04	-179.01067871	.39055108E-02	-53.61905973

Appendix F

Tabulations of the
Unnormalized Response to
Other Boresight Targets
for Selected Cases
from Table I

TABLE XIV

CASE 5
UNNORMALIZED RESPONSE
TO OTHER BORESIGHT TARGETS

PRESUMED TARGET

SPEED (MPH)	TRACK (DEGREES)	AZIMUTH (DEGREES)	EIGENVALUE (dB)
3.	180.	0.	-58.5

TARGET TRACK (DEGREES)

TARGET SPEED (MPH)	0	10	20	30	40	50	60	70	80
	90	100	110	120	130	140	150	160	170
	180	190	200	210	220	230	240	250	260
	270	280	290	300	310	320	330	340	350
0.	-58.9	-58.9	-58.9	-58.9	-58.9	-58.9	-58.9	-58.9	-58.9
	-58.9	-58.9	-58.9	-58.9	-58.9	-58.9	-58.9	-58.9	-58.9
	-58.9	-58.9	-58.9	-58.9	-58.9	-58.9	-58.9	-58.9	-58.9
	-58.9	-58.9	-58.9	-58.9	-58.9	-58.9	-58.9	-58.9	-58.9
3.	-59.6	-59.6	-59.5	-59.5	-59.4	-59.3	-59.2	-59.1	-59.0
	-58.9	-58.8	-58.7	-58.7	-58.6	-58.6	-58.6	-58.6	-58.6
	-58.5	-58.6	-58.6	-58.6	-58.6	-58.6	-58.7	-58.7	-58.8
	-58.9	-59.0	-59.1	-59.2	-59.3	-59.4	-59.5	-59.5	-59.6
6.	-60.6	-60.6	-60.5	-60.3	-60.1	-59.8	-59.6	-59.3	-59.1
	-58.9	-58.7	-58.6	-58.5	-58.5	-58.5	-58.5	-58.5	-58.5
	-58.5	-58.5	-58.5	-58.5	-58.5	-58.5	-58.5	-58.6	-58.7
	-58.9	-59.1	-59.3	-59.6	-59.8	-60.1	-60.3	-60.5	-60.6
9.	-62.0	-62.0	-61.7	-61.4	-61.0	-60.5	-60.0	-59.6	-59.2
	-58.9	-58.7	-58.5	-58.5	-58.5	-58.6	-58.7	-58.7	-58.8
	-58.8	-58.8	-58.7	-58.7	-58.6	-58.5	-58.5	-58.5	-58.7
	-58.9	-59.2	-59.6	-60.0	-60.5	-61.0	-61.4	-61.7	-62.0
12.	-64.0	-63.9	-63.5	-62.9	-62.2	-61.4	-60.6	-59.9	-59.3
	-58.9	-58.6	-58.5	-58.5	-58.7	-58.9	-59.1	-59.3	-59.4
	-59.5	-59.4	-59.3	-59.1	-58.9	-58.7	-58.5	-58.5	-58.6
	-58.9	-59.3	-59.9	-60.6	-61.4	-62.2	-62.9	-63.5	-63.9
15.	-66.7	-66.4	-65.8	-64.8	-63.6	-62.4	-61.3	-60.3	-59.5
	-58.9	-58.6	-58.5	-58.6	-58.9	-59.3	-59.8	-60.1	-60.4
	-60.5	-60.4	-60.1	-59.8	-59.3	-58.9	-58.6	-58.5	-58.6
	-58.9	-59.5	-60.3	-61.3	-62.4	-63.6	-64.8	-65.8	-66.4
18.	-70.4	-70.0	-68.9	-67.3	-65.5	-63.7	-62.0	-60.7	-59.6
	-58.9	-58.5	-58.5	-58.8	-59.3	-60.0	-60.7	-61.4	-61.8
	-62.0	-61.8	-61.4	-60.7	-60.0	-59.3	-58.8	-58.5	-58.5
	-58.9	-59.6	-60.7	-62.0	-63.7	-65.5	-67.3	-68.9	-70.0

TABLE XIV (CONTINUED)

CASE 5
UNNORMALIZED RESPONSE
TO OTHER BORESIGHT TARGETS

PRESUMED TARGET

SPEED (MPH)	TRACK (DEGREES)	AZIMUTH (DEGREES)	EIGENVALUE (dB)
3.	180.	0.	-58.5

TARGET TRACK (DEGREES)

TARGET SPEED (MPH)	0	10	20	30	40	50	60	70	80
	90	100	110	120	130	140	150	160	170
	180	190	200	210	220	230	240	250	260
	270	280	290	300	310	320	330	340	350
21.	-76.4	-75.6	-73.5	-70.7	-67.9	-65.2	-63.0	-61.1	-59.8
	-58.9	-58.5	-58.6	-59.1	-59.9	-61.0	-62.1	-63.1	-63.8
	-64.0	-63.8	-63.1	-62.1	-61.0	-59.9	-59.1	-58.6	-58.5
	-58.9	-59.8	-61.1	-63.0	-65.2	-67.9	-70.7	-73.5	-75.6
24.	-88.8	-87.1	-81.6	-75.8	-71.0	-67.1	-64.0	-61.6	-59.9
	-58.9	-58.5	-58.7	-59.5	-60.7	-62.2	-63.9	-65.4	-66.5
	-66.9	-66.5	-65.4	-63.9	-62.2	-60.7	-59.5	-58.7	-58.5
	-58.9	-59.9	-61.6	-64.0	-67.1	-71.0	-75.8	-81.6	-87.1
27.	-80.1	-81.3	-86.0	-85.7	-75.6	-69.5	-65.2	-62.2	-60.1
	-58.9	-58.5	-58.9	-59.9	-61.6	-63.8	-66.2	-68.7	-70.6
	-71.3	-70.6	-68.7	-66.2	-63.8	-61.6	-59.9	-58.9	-58.5
	-58.9	-60.1	-62.2	-65.2	-69.5	-75.6	-85.7	-86.0	-81.3
30.	-75.2	-75.7	-77.6	-83.4	-83.6	-72.6	-66.7	-62.8	-60.3
	-58.9	-58.5	-59.0	-60.5	-62.8	-65.8	-69.6	-73.8	-77.7
	-79.5	-77.7	-73.8	-69.6	-65.8	-62.8	-60.5	-59.0	-58.5
	-58.9	-60.3	-62.8	-66.7	-72.6	-83.6	-83.4	-77.6	-75.7
33.	-73.1	-73.4	-74.3	-77.0	-86.4	-77.0	-68.4	-63.5	-60.5
	-58.9	-58.5	-59.3	-61.2	-64.2	-68.6	-74.8	-84.5	-86.9
	-84.2	-86.9	-84.5	-74.8	-68.6	-64.2	-61.2	-59.3	-58.5
	-58.9	-60.5	-63.5	-68.4	-77.0	-86.4	-77.0	-74.3	-73.4
36.	-72.5	-72.5	-72.8	-74.2	-78.8	-84.4	-70.4	-64.2	-60.7
	-58.9	-58.5	-59.5	-62.0	-66.0	-72.5	-85.4	-80.6	-76.3
	-75.2	-76.3	-80.6	-85.5	-72.5	-66.0	-62.0	-59.5	-58.5
	-58.9	-60.7	-64.2	-70.4	-84.4	-78.8	-74.2	-72.8	-72.5
39.	-72.9	-72.7	-72.5	-72.9	-75.3	-87.4	-73.0	-65.1	-60.9
	-58.9	-58.6	-59.9	-62.9	-68.3	-79.0	-80.8	-74.2	-72.3
	-71.8	-72.3	-74.2	-80.8	-79.0	-68.3	-62.9	-59.9	-58.6
	-58.9	-60.9	-65.1	-73.0	-87.4	-75.3	-72.9	-72.5	-72.7

TABLE XIV (CONTINUED)

CASE 5
UNNORMALIZED RESPONSE
TO OTHER BORESIGHT TARGETS

PRESUMED TARGET SPEED (MPH)	TRACK (DEGREES)	AZIMUTH (DEGREES)	EIGENVALUE (dB)
3.	180.	0.	-58.5

TARGET TRACK (DEGREES)

TARGET SPEED (MPH)	0 / 90 / 180 / 270	10 / 100 / 190 / 280	20 / 110 / 200 / 290	30 / 120 / 210 / 300	40 / 130 / 220 / 310	50 / 140 / 230 / 320	60 / 150 / 240 / 330	70 / 160 / 250 / 340	80 / 170 / 260 / 350
42.	-74.3	-73.9	-73.1	-72.5	-73.5	-80.1	-76.4	-66.0	-61.2
	-58.9	-58.6	-60.2	-64.0	-71.3	-88.3	-74.6	-71.5	-70.5
	-70.3	-70.5	-71.5	-74.6	-88.3	-71.3	-64.0	-60.2	-58.6
	-58.9	-61.2	-66.0	-76.4	-80.1	-73.5	-72.5	-73.1	-73.9
45.	-77.0	-76.2	-74.5	-72.9	-72.7	-76.5	-81.4	-67.1	-61.4
	-58.9	-58.7	-60.6	-65.4	-75.8	-78.6	-71.8	-70.2	-69.9
	-70.0	-69.9	-70.2	-71.8	-78.6	-75.8	-65.4	-60.6	-58.7
	-58.9	-61.4	-67.1	-81.4	-76.5	-72.7	-72.9	-74.5	-76.2
48.	-81.6	-80.2	-77.1	-74.1	-72.5	-74.4	-88.8	-68.3	-61.7
	-58.9	-58.7	-61.1	-66.9	-83.6	-74.1	-70.4	-70.0	-70.3
	-70.6	-70.3	-70.0	-70.4	-74.1	-83.6	-66.9	-61.1	-58.7
	-58.9	-61.7	-68.3	-88.8	-74.4	-72.5	-74.1	-77.1	-80.2
51.	-88.3	-86.9	-81.5	-76.1	-72.9	-73.2	-85.4	-69.6	-62.0
	-58.9	-58.8	-61.6	-68.9	-85.4	-71.7	-70.0	-70.6	-71.7
	-72.2	-71.7	-70.6	-70.0	-71.7	-85.4	-68.9	-61.6	-58.8
	-58.9	-62.0	-69.6	-85.4	-73.2	-72.9	-76.1	-81.5	-86.9
54.	-83.6	-85.5	-88.0	-79.4	-73.9	-72.6	-80.1	-71.2	-62.3
	-58.9	-58.9	-62.2	-71.3	-77.9	-70.5	-70.2	-72.0	-74.2
	-75.1	-74.2	-72.0	-70.2	-70.5	-77.9	-71.3	-62.2	-58.9
	-58.9	-62.3	-71.2	-80.1	-72.6	-73.9	-79.4	-88.0	-85.5
57.	-79.0	-80.0	-84.6	-84.7	-75.6	-72.5	-77.1	-73.0	-62.6
	-58.9	-59.0	-62.9	-74.6	-74.3	-70.0	-71.2	-74.6	-78.4
	-80.2	-78.4	-74.6	-71.2	-70.0	-74.3	-74.6	-62.9	-59.0
	-58.9	-62.6	-73.0	-77.1	-72.5	-75.6	-84.7	-84.6	-80.0
60.	-76.6	-77.1	-79.7	-88.0	-78.2	-72.8	-75.2	-75.2	-62.9
	-58.9	-59.1	-63.6	-79.5	-72.1	-70.1	-73.0	-78.9	-84.7
	-85.3	-84.7	-78.9	-73.0	-70.1	-72.1	-79.5	-63.6	-59.1
	-58.9	-62.9	-75.2	-75.2	-72.8	-78.2	-88.0	-79.7	-77.1

TABLE XIV (CONTINUED)

CASE 5
UNNORMALIZED RESPONSE
TO OTHER BORESIGHT TARGETS

PRESUMED TARGET

SPEED (MPH)	TRACK (DEGREES)	AZIMUTH (DEGREES)	EIGENVALUE (dB)
15.	180.	0.	-57.1

TARGET TRACK (DEGREES)

TARGET SPEED (MPH)	0 90 180 270	10 100 190 280	20 110 200 290	30 120 210 300	40 130 220 310	50 140 230 320	60 150 240 330	70 160 250 340	80 170 260 350
0.	-64.5	-64.5	-64.5	-64.5	-64.5	-64.5	-64.5	-64.5	-64.5
	-64.5	-64.5	-64.5	-64.5	-64.5	-64.5	-64.5	-64.5	-64.5
	-64.5	-64.5	-64.5	-64.5	-64.5	-64.5	-64.5	-64.5	-64.5
	-64.5	-64.5	-64.5	-64.5	-64.5	-64.5	-64.5	-64.5	-64.5
3.	-68.1	-68.1	-67.9	-67.6	-67.2	-66.7	-66.2	-65.6	-65.1
	-64.5	-64.0	-63.5	-63.1	-62.8	-62.5	-62.2	-62.1	-62.0
	-61.9	-62.0	-62.1	-62.2	-62.5	-62.8	-63.1	-63.5	-64.0
	-64.5	-65.1	-65.6	-66.2	-66.7	-67.2	-67.6	-67.9	-68.1
6.	-73.7	-73.4	-72.8	-71.9	-70.7	-69.4	-68.1	-66.8	-65.6
	-64.5	-63.5	-62.7	-61.9	-61.3	-60.9	-60.5	-60.2	-60.1
	-60.0	-60.1	-60.2	-60.5	-60.9	-61.3	-61.9	-62.7	-63.5
	-64.5	-65.6	-66.8	-68.1	-69.4	-70.7	-71.9	-72.8	-73.4
9.	-86.0	-85.0	-82.4	-79.2	-76.1	-73.1	-70.5	-68.2	-66.2
	-64.5	-63.1	-61.9	-60.9	-60.2	-59.6	-59.1	-58.9	-58.7
	-58.6	-58.7	-58.9	-59.1	-59.6	-60.2	-60.9	-61.9	-63.1
	-64.5	-66.2	-68.2	-70.5	-73.1	-76.1	-79.2	-82.4	-85.0
12.	-82.0	-82.8	-85.5	-93.5	-87.6	-78.9	-73.7	-69.8	-66.9
	-64.5	-62.6	-61.2	-60.0	-59.2	-58.6	-58.1	-57.9	-57.7
	-57.7	-57.7	-57.9	-58.1	-58.6	-59.2	-60.0	-61.2	-62.6
	-64.5	-66.9	-69.8	-73.7	-78.9	-87.6	-93.5	-85.5	-82.8
15.	-75.6	-75.9	-76.8	-79.0	-84.3	-92.6	-78.1	-71.7	-67.6
	-64.5	-62.2	-60.5	-59.3	-58.4	-57.8	-57.4	-57.2	-57.1
	-57.1	-57.1	-57.2	-57.4	-57.8	-58.4	-59.3	-60.5	-62.2
	-64.5	-67.6	-71.7	-78.1	-92.6	-84.3	-79.0	-76.8	-75.9
18.	-73.3	-73.4	-73.9	-74.9	-77.3	-83.9	-86.0	-74.0	-68.3
	-64.5	-61.8	-59.9	-58.6	-57.8	-57.3	-57.0	-56.9	-56.9
	-56.9	-56.9	-56.9	-57.0	-57.3	-57.8	-58.6	-59.9	-61.8
	-64.5	-68.3	-74.0	-86.0	-83.9	-77.3	-74.9	-73.9	-73.4

TABLE XIV (CONTINUED)

CASE 5
UNNORMALIZED RESPONSE
TO OTHER BORESIGHT TARGETS

PRESUMED TARGET SPEED (MPH)	TRACK (DEGREES)	AZIMUTH (DEGREES)	EIGENVALUE (dB)
15.	180.	0.	-57.1

TARGET TRACK (DEGREES)

TARGET SPEED (MPH)	0 / 90 / 180 / 270	10 / 100 / 190 / 280	20 / 110 / 200 / 290	30 / 120 / 210 / 300	40 / 130 / 220 / 310	50 / 140 / 230 / 320	60 / 150 / 240 / 330	70 / 160 / 250 / 340	80 / 170 / 260 / 350
21.	-72.8	-72.8	-72.8	-73.2	-74.5	-77.9	-92.2	-77.0	-69.1
	-64.5	-61.5	-59.4	-58.1	-57.3	-57.0	-56.9	-56.9	-57.0
	-57.0	-57.0	-56.9	-56.9	-57.0	-57.3	-58.1	-59.4	-61.5
	-64.5	-69.1	-77.0	-92.2	-77.9	-74.5	-73.2	-72.8	-72.8
24.	-73.5	-73.3	-73.0	-72.8	-73.2	-75.1	-82.0	-81.1	-69.9
	-64.5	-61.1	-59.0	-57.7	-57.0	-56.9	-57.0	-57.2	-57.4
	-57.5	-57.4	-57.2	-57.0	-56.9	-57.0	-57.7	-59.0	-61.1
	-64.5	-69.9	-81.1	-82.0	-75.1	-73.2	-72.8	-73.0	-73.3
27.	-75.4	-75.0	-74.2	-73.2	-72.8	-73.6	-77.9	-88.0	-70.9
	-64.5	-60.8	-58.6	-57.3	-56.9	-57.0	-57.4	-57.9	-58.3
	-58.4	-58.3	-57.9	-57.4	-57.0	-56.9	-57.3	-58.6	-60.8
	-64.5	-70.9	-88.0	-77.9	-73.6	-72.8	-73.2	-74.2	-75.0
30.	-79.0	-78.3	-76.6	-74.6	-73.1	-72.9	-75.6	-95.1	-71.9
	-64.5	-60.5	-58.2	-57.1	-56.9	-57.3	-58.1	-58.9	-59.6
	-59.8	-59.6	-58.9	-58.1	-57.3	-56.9	-57.1	-58.2	-60.5
	-64.5	-71.9	-95.1	-75.6	-72.9	-73.1	-74.6	-76.6	-78.3
33.	-86.2	-84.5	-80.8	-77.0	-74.1	-72.8	-74.2	-85.5	-73.0
	-64.5	-60.2	-57.9	-56.9	-57.0	-57.8	-59.1	-60.5	-61.5
	-61.9	-61.5	-60.5	-59.1	-57.8	-57.0	-56.9	-57.9	-60.2
	-64.5	-73.0	-85.5	-74.2	-72.8	-74.1	-77.0	-80.8	-84.5
36.	-90.8	-93.1	-89.6	-81.2	-75.9	-73.2	-73.3	-80.9	-74.3
	-64.5	-59.9	-57.6	-56.9	-57.3	-58.7	-60.6	-62.6	-64.3
	-64.9	-64.3	-62.6	-60.6	-58.7	-57.3	-56.9	-57.6	-59.9
	-64.5	-74.3	-80.9	-73.3	-73.2	-75.9	-81.2	-89.6	-93.1
39.	-81.9	-83.0	-88.1	-89.3	-78.8	-74.0	-72.9	-78.2	-75.7
	-64.5	-59.6	-57.4	-56.9	-57.8	-59.8	-62.6	-65.7	-68.5
	-69.6	-68.5	-65.7	-62.6	-59.8	-57.8	-56.9	-57.4	-59.6
	-64.5	-75.7	-78.2	-72.9	-74.0	-78.8	-89.3	-88.1	-83.0

TABLE XIV (CONTINUED)

CASE 5
UNNORMALIZED RESPONSE
TO OTHER BORESIGHT TARGETS

PRESUMED TARGET

SPEED (MPH)	TRACK (DEGREES)	AZIMUTH (DEGREES)	EIGENVALUE (dB)
15.	180.	0.	-57.1

TARGET TRACK (DEGREES)

TARGET SPEED (MPH)	0 90 180 270	10 100 190 280	20 110 200 290	30 120 210 300	40 130 220 310	50 140 230 320	60 150 240 330	70 160 250 340	80 170 260 350
42.	-78.1	-78.7	-81.1	-89.2	-83.6	-75.4	-72.8	-76.4	-77.4
	-64.5	-59.4	-57.2	-57.0	-58.4	-61.3	-65.4	-70.6	-76.5
	-79.7	-76.5	-70.6	-65.4	-61.3	-58.4	-57.0	-57.2	-59.4
	-64.5	-77.4	-76.4	-72.8	-75.4	-83.6	-89.2	-81.1	-78.7
45.	-76.4	-76.7	-77.9	-81.9	-92.5	-77.4	-73.0	-75.1	-79.3
	-64.5	-59.1	-57.0	-57.2	-59.3	-63.2	-69.6	-81.6	-84.8
	-80.0	-84.8	-81.6	-69.6	-63.2	-59.3	-57.2	-57.0	-59.1
	-64.5	-79.3	-75.1	-73.0	-77.4	-92.5	-81.9	-77.9	-76.7
48.	-75.9	-75.9	-76.4	-78.5	-87.6	-80.5	-73.5	-74.2	-81.7
	-64.5	-58.9	-56.9	-57.5	-60.4	-65.9	-77.4	-79.5	-72.9
	-71.6	-72.9	-79.5	-77.4	-65.9	-60.4	-57.5	-56.9	-58.9
	-64.5	-81.7	-74.2	-73.5	-80.5	-87.6	-78.5	-76.4	-75.9
51.	-76.4	-76.2	-75.9	-76.8	-81.8	-85.4	-74.3	-73.6	-84.9
	-64.5	-58.7	-56.9	-57.9	-61.7	-69.8	-86.3	-71.8	-69.1
	-68.5	-69.1	-71.8	-86.3	-69.8	-61.7	-57.9	-56.9	-58.7
	-64.5	-84.9	-73.6	-74.3	-85.4	-81.8	-76.8	-75.9	-76.2
54.	-77.8	-77.3	-76.3	-76.0	-78.7	-93.4	-75.4	-73.1	-89.5
	-64.5	-58.5	-56.9	-58.4	-63.5	-76.5	-74.0	-68.6	-67.3
	-67.1	-67.3	-68.6	-74.0	-76.5	-63.5	-58.4	-56.9	-58.5
	-64.5	-89.4	-73.1	-75.4	-93.4	-78.7	-76.0	-76.3	-77.3
57.	-80.4	-79.5	-77.5	-76.0	-77.0	-88.1	-76.9	-72.9	-95.8
	-64.5	-58.3	-56.9	-59.1	-65.7	-93.9	-69.9	-67.2	-66.9
	-66.9	-66.9	-67.2	-69.9	-94.0	-65.7	-59.1	-56.9	-58.3
	-64.5	-95.7	-72.9	-76.9	-88.1	-77.0	-76.0	-77.5	-79.5
60.	-84.1	-82.9	-79.7	-76.7	-76.1	-82.7	-79.0	-72.8	-93.2
	-64.5	-58.1	-57.0	-59.8	-68.8	-76.1	-67.9	-66.9	-67.3
	-67.7	-67.3	-66.9	-67.9	-76.1	-68.8	-59.8	-57.0	-58.1
	-64.5	-93.1	-72.8	-79.0	-82.7	-76.1	-76.7	-79.7	-82.9

TABLE XIV (CONTINUED)

CASE 5
UNNORMALIZED RESPONSE
TO OTHER BORESIGHT TARGETS

PRESUMED TARGET

SPEED (MPH)	TRACK (DEGREES)	AZIMUTH (DEGREES)	EIGENVALUE (dB)
30.	180.	0.	-55.5

TARGET TRACK (DEGREES)

TARGET SPEED (MPH)	0	10	20	30	40	50	60	70	80
	90	100	110	120	130	140	150	160	170
	180	190	200	210	220	230	240	250	260
	270	280	290	300	310	320	330	340	350
0.	-85.6	-85.6	-85.6	-85.6	-85.6	-85.6	-85.6	-85.6	-85.6
	-85.6	-85.6	-85.6	-85.6	-85.6	-85.6	-85.6	-85.6	-85.6
	-85.6	-85.6	-85.6	-85.6	-85.6	-85.6	-85.6	-85.6	-85.6
	-85.6	-85.6	-85.6	-85.6	-85.6	-85.6	-85.6	-85.6	-85.6
3.	-78.2	-78.3	-78.5	-78.8	-79.2	-79.9	-80.8	-82.0	-83.6
	-85.6	-88.3	-90.9	-91.2	-88.9	-86.4	-84.6	-83.4	-82.7
	-82.5	-82.7	-83.4	-84.6	-86.4	-88.9	-91.2	-90.9	-88.3
	-85.6	-83.6	-82.0	-80.8	-79.9	-79.2	-78.8	-78.5	-78.3
6.	-76.0	-76.0	-76.2	-76.4	-76.7	-77.3	-78.2	-79.7	-81.9
	-85.6	-91.0	-88.1	-82.5	-78.9	-76.5	-74.9	-73.8	-73.2
	-73.0	-73.2	-73.8	-74.9	-76.5	-78.9	-82.5	-88.0	-91.0
	-85.6	-81.9	-79.7	-78.2	-77.3	-76.7	-76.4	-76.2	-76.0
9.	-75.9	-75.9	-75.8	-75.7	-75.8	-76.1	-76.8	-78.1	-80.7
	-85.6	-90.9	-82.1	-76.8	-73.4	-71.2	-69.6	-68.5	-67.9
	-67.7	-67.9	-68.5	-69.6	-71.2	-73.4	-76.8	-82.1	-90.9
	-85.6	-80.7	-78.1	-76.8	-76.1	-75.8	-75.7	-75.8	-75.9
12.	-77.3	-77.2	-76.8	-76.4	-75.9	-75.7	-76.0	-77.1	-79.6
	-85.6	-87.8	-78.1	-73.0	-69.7	-67.5	-65.9	-64.9	-64.3
	-64.1	-64.3	-64.9	-65.9	-67.5	-69.7	-73.0	-78.1	-87.8
	-85.6	-79.6	-77.1	-76.0	-75.7	-75.9	-76.4	-76.8	-77.2
15.	-80.6	-80.2	-79.3	-78.1	-77.0	-76.1	-75.7	-76.4	-78.8
	-85.6	-84.6	-75.0	-70.1	-66.9	-64.7	-63.2	-62.2	-61.6
	-61.4	-61.6	-62.2	-63.2	-64.7	-66.9	-70.1	-75.0	-84.6
	-85.6	-78.8	-76.4	-75.7	-76.1	-77.0	-78.1	-79.3	-80.2
18.	-87.5	-86.6	-84.3	-81.5	-79.0	-77.0	-75.9	-76.0	-78.1
	-85.6	-81.9	-72.6	-67.7	-64.6	-62.4	-61.0	-60.1	-59.6
	-59.4	-59.6	-60.1	-61.0	-62.4	-64.6	-67.7	-72.6	-81.9
	-85.6	-78.1	-76.0	-75.9	-77.0	-79.0	-81.5	-84.3	-86.6

TABLE XIV (CONTINUED)

CASE 5
UNNORMALIZED RESPONSE
TO OTHER BORESIGHT TARGETS

PRESUMED TARGET

SPEED (MPH)	TRACK (DEGREES)	AZIMUTH (DEGREES)	EIGENVALUE (dB)
30.	180.	0.	-55.5

TARGET TRACK (DEGREES)

TARGET SPEED (MPH)									
	0	10	20	30	40	50	60	70	80
	90	100	110	120	130	140	150	160	170
	180	190	200	210	220	230	240	250	260
	270	280	290	300	310	320	330	340	350
21.	-92.8	-94.3	-95.0	-88.1	-82.4	-78.7	-76.4	-75.8	-77.5
	-85.6	-79.7	-70.6	-65.8	-62.7	-60.6	-59.3	-58.4	-58.0
	-57.8	-58.0	-58.4	-59.3	-60.6	-62.7	-65.8	-70.6	-79.7
	-85.6	-77.5	-75.8	-76.4	-78.7	-82.4	-88.1	-95.0	-94.3
24.	-83.4	-84.1	-86.8	-93.8	-88.9	-81.2	-77.3	-75.8	-77.0
	-85.6	-77.9	-68.9	-64.1	-61.1	-59.2	-57.9	-57.2	-56.8
	-56.7	-56.8	-57.2	-57.9	-59.2	-61.1	-64.1	-68.9	-77.9
	-85.6	-77.0	-75.8	-77.3	-81.2	-88.9	-93.8	-86.8	-84.1
27.	-79.6	-80.0	-81.3	-84.7	-94.2	-85.4	-78.7	-75.9	-76.7
	-85.6	-76.2	-67.4	-62.7	-59.8	-58.0	-56.9	-56.3	-56.0
	-55.9	-56.0	-56.3	-56.9	-58.0	-59.8	-62.7	-67.4	-76.2
	-85.6	-76.7	-75.9	-78.7	-85.4	-94.3	-84.7	-81.3	-80.0
30.	-77.8	-78.0	-78.7	-80.6	-85.6	-93.0	-80.6	-76.3	-76.3
	-85.6	-74.8	-66.1	-61.4	-58.7	-57.0	-56.2	-55.7	-55.5
	-55.5	-55.5	-55.7	-56.2	-57.0	-58.7	-61.4	-66.1	-74.8
	-85.6	-76.3	-76.3	-80.6	-93.0	-85.6	-80.6	-78.7	-78.0
33.	-77.4	-77.4	-77.6	-78.5	-81.4	-91.8	-83.3	-76.8	-76.1
	-85.6	-73.6	-64.9	-60.4	-57.8	-56.3	-55.7	-55.4	-55.4
	-55.4	-55.4	-55.4	-55.7	-56.3	-57.8	-60.4	-64.9	-73.6
	-85.6	-76.1	-76.8	-83.3	-91.8	-81.4	-78.5	-77.6	-77.4
36.	-77.9	-77.7	-77.4	-77.5	-79.1	-85.2	-87.5	-77.5	-75.9
	-85.6	-72.4	-63.8	-59.4	-57.0	-55.8	-55.4	-55.4	[illegible]
	-55.6	-55.6	-55.4	-55.4	-55.8	-57.0	-59.4	-63.8	[illegible]
	-85.6	-75.9	-77.5	-87.5	-85.2	-79.1	-77.5	-77.4	-77.7
39.	-79.5	-79.1	-78.2	-77.4	-77.9	-81.7	-94.0	-78.5	-75.8
	-85.6	-71.4	-62.8	-58.6	-56.4	-55.5	-55.4	-55.7	-56.1
	-56.3	-56.1	-55.7	-55.4	-55.5	-56.4	-58.6	-62.8	-71.4
	-85.6	-75.8	-78.5	-94.0	-81.7	-77.9	-77.4	-78.2	-79.1

TABLE XIV (CONTINUED)

CASE 5
UNNORMALIZED RESPONSE
TO OTHER BORESIGHT TARGETS

PRESUMED TARGET

SPEED (MPH)	TRACK (DEGREES)	AZIMUTH (DEGREES)	EIGENVALUE (dB)
30.	180.	0.	-55.5

TARGET TRACK (DEGREES)

TARGET SPEED (MPH)	0	10	20	30	40	50	60	70	80
	90	100	110	120	130	140	150	160	170
	180	190	200	210	220	230	240	250	260
	270	280	290	300	310	320	330	340	350
42.	-82.1	-81.5	-79.8	-78.0	-77.4	-79.6	-92.8	-79.7	-75.8
	-85.7	-70.4	-62.0	-57.8	-55.9	-55.4	-55.7	-56.4	-57.0
	-57.3	-57.0	-56.4	-55.7	-55.4	-55.9	-57.8	-62.0	-70.4
	-85.6	-75.8	-79.7	-92.8	-79.6	-77.4	-78.0	-79.8	-81.5
45.	-85.5	-84.8	-82.4	-79.4	-77.5	-78.3	-87.0	-81.2	-75.7
	-85.7	-69.5	-61.1	-57.2	-55.6	-55.5	-56.3	-57.4	-58.4
	-58.8	-58.4	-57.4	-56.3	-55.5	-55.6	-57.2	-61.1	-69.5
	-85.6	-75.7	-81.2	-87.0	-78.3	-77.5	-79.4	-82.4	-84.8
48.	-85.9	-86.3	-85.6	-81.7	-78.2	-77.6	-83.4	-83.1	-75.8
	-85.7	-68.7	-60.4	-56.7	-55.4	-55.8	-57.1	-58.9	-60.4
	-61.0	-60.4	-58.9	-57.1	-55.8	-55.4	-56.7	-60.4	-68.7
	-85.6	-75.8	-83.1	-83.4	-77.6	-78.2	-81.7	-85.6	-86.3
51.	-82.8	-83.7	-86.0	-84.6	-79.5	-77.4	-81.1	-85.7	-75.9
	-85.7	-67.9	-59.7	-56.3	-55.4	-56.3	-58.3	-61.0	-63.3
	-64.3	-63.3	-61.0	-58.3	-56.3	-55.4	-56.3	-59.7	-67.9
	-85.6	-75.9	-85.7	-81.1	-77.4	-79.5	-84.6	-86.0	-83.7
54.	-80.3	-80.9	-83.1	-86.4	-81.5	-77.6	-79.6	-89.2	-76.0
	-85.7	-67.2	-59.1	-55.9	-55.5	-57.0	-60.0	-63.9	-67.7
	-69.5	-67.7	-63.9	-60.0	-57.0	-55.5	-55.9	-59.1	-67.2
	-85.6	-76.0	-89.3	-79.6	-77.6	-81.5	-86.4	-83.1	-80.9
57.	-78.7	-79.1	-80.6	-84.6	-84.0	-78.2	-78.5	-94.0	-76.1
	-85.7	-66.5	-58.6	-55.7	-55.7	-58.1	-62.3	-68.5	-76.5
	-82.3	-76.5	-68.5	-62.3	-58.1	-55.7	-55.7	-58.6	-66.5
	-85.6	-76.1	-94.0	-78.5	-78.2	-84.0	-84.6	-80.6	-79.1
60.	-78.1	-78.2	-79.0	-81.9	-86.2	-79.2	-77.8	-94.9	-76.4
	-85.7	-65.9	-58.1	-55.5	-56.1	-59.5	-65.6	-77.9	-81.3
	-76.5	-81.3	-77.9	-65.6	-59.5	-56.1	-55.5	-58.1	-65.9
	-85.6	-76.4	-94.9	-77.8	-79.2	-86.2	-81.9	-79.0	-78.2

TABLE XV

CASE 11
UNNORMALIZED RESPONSE
TO OTHER BORESIGHT TARGETS

PRESUMED TARGET

SPEED (MPH)	TRACK (DEGREES)	AZIMUTH (DEGREES)	EIGENVALUE (dB)
3.	180.	0.	-17.5

TARGET TRACK (DEGREES)

TARGET SPEED (MPH)	0 90 180 270	10 100 190 280	20 110 200 290	30 120 210 300	40 130 220 310	50 140 230 320	60 150 240 330	70 160 250 340	80 170 260 350
0.	-83.0	-83.0	-83.0	-83.0	-83.0	-83.0	-83.0	-83.0	-83.0
	-83.0	-83.0	-83.0	-83.0	-83.0	-83.0	-83.0	-83.0	-83.0
	-83.0	-83.0	-83.0	-83.0	-83.0	-83.0	-83.0	-83.0	-83.0
	-83.0	-83.0	-83.0	-83.0	-83.0	-83.0	-83.0	-83.0	-83.0
3.	-18.0	-18.1	-18.5	-19.2	-20.2	-21.7	-23.9	-27.1	-33.0
	-82.9	-32.9	-27.0	-23.7	-21.4	-19.9	-18.8	-18.1	-17.7
	-17.5	-17.7	-18.1	-18.8	-19.9	-21.4	-23.7	-27.0	-32.9
	-83.1	-33.0	-27.1	-23.9	-21.7	-20.2	-19.2	-18.5	-18.1
6.	-12.2	-12.3	-12.7	-13.4	-14.4	-15.9	-18.0	-21.2	-27.0
	-82.9	-26.9	-20.9	-17.5	-15.3	-13.7	-12.6	-11.9	-11.5
	-11.3	-11.5	-11.9	-12.6	-13.7	-15.3	-17.5	-20.9	-26.9
	-83.2	-27.0	-21.2	-18.0	-15.9	-14.4	-13.4	-12.7	-12.3
9.	-9.0	-9.1	-9.5	-10.1	-11.1	-12.5	-14.6	-17.8	-23.5
	-82.8	-23.3	-17.3	-13.9	-11.7	-10.1	-9.0	-8.2	-7.8
	-7.7	-7.8	-8.2	-9.0	-10.1	-11.7	-13.9	-17.3	-23.3
	-83.3	-23.5	-17.8	-14.6	-12.5	-11.1	-10.1	-9.5	-9.1
12.	-6.8	-7.0	-7.3	-7.9	-8.8	-10.2	-12.2	-15.3	-21.1
	-82.7	-20.8	-14.8	-11.3	-9.1	-7.5	-6.4	-5.6	-5.2
	-5.1	-5.2	-5.6	-6.4	-7.5	-9.1	-11.3	-14.8	-20.8
	-83.4	-21.1	-15.3	-12.2	-10.2	-8.8	-7.9	-7.3	-7.0
15.	-5.3	-5.4	-5.7	-6.3	-7.2	-8.5	-10.4	-13.5	-19.2
	-82.6	-18.8	-12.8	-9.3	-7.1	-5.5	-4.4	-3.6	-3.2
	-3.1	-3.2	-3.6	-4.4	-5.5	-7.1	-9.3	-12.8	-18.8
	-83.5	-19.2	-13.5	-10.4	-8.5	-7.2	-6.3	-5.7	-5.4
18.	-4.1	-4.2	-4.5	-5.0	-5.9	-7.1	-9.0	-12.0	-17.6
	-82.5	-17.2	-11.1	-7.7	-5.4	-3.8	-2.7	-2.0	-1.6
	-1.4	-1.6	-2.0	-2.7	-3.8	-5.4	-7.7	-11.1	-17.2
	-83.6	-17.6	-12.0	-9.0	-7.1	-5.9	-5.0	-4.5	-4.2

TABLE XV (CONTINUED)

CASE 11
UNNORMALIZED RESPONSE
TO OTHER BORESIGHT TARGETS

PRESUMED TARGET

SPEED (MPH)	TRACK (DEGREES)	AZIMUTH (DEGREES)	EIGENVALUE (dB)
3.	180.	0.	-17.5

TARGET TRACK (DEGREES)

TARGET SPEED (MPH)	0 90 180 270	10 100 190 280	20 110 200 290	30 120 210 300	40 130 220 310	50 140 230 320	60 150 240 330	70 160 250 340	80 170 260 350
21.	-3.3	-3.3	-3.6	-4.1	-4.8	-6.0	-7.8	-10.8	-16.3
	-82.5	-15.8	-9.7	-6.3	-4.0	-2.4	-1.3	-.6	-.2
	-.0	-.2	-.6	-1.3	-2.4	-4.0	-6.3	-9.7	-15.8
	-83.7	-16.3	-10.8	-7.8	-6.0	-4.8	-4.1	-3.6	-3.3
24.	-2.6	-2.7	-2.9	-3.3	-4.0	-5.1	-6.8	-9.7	-15.2
	-82.4	-14.6	-8.5	-5.1	-2.8	-1.2	-.1	.6	1.0
	1.1	1.0	.6	-.1	-1.2	-2.8	-5.1	-8.5	-14.6
	-83.8	-15.2	-9.7	-6.8	-5.1	-4.0	-3.3	-2.9	-2.7
27.	-2.2	-2.2	-2.4	-2.7	-3.3	-4.4	-6.0	-8.8	-14.2
	-82.3	-13.6	-7.5	-4.0	-1.7	-.2	.9	1.6	2.0
	2.1	2.0	1.6	.9	-.2	-1.7	-4.0	-7.5	-13.6
	-83.9	-14.2	-8.8	-6.0	-4.4	-3.3	-2.7	-2.4	-2.2
30.	-1.9	-1.9	-2.1	-2.3	-2.8	-3.7	-5.3	-8.0	-13.4
	-82.3	-12.6	-6.5	-3.1	-.8	.7	1.8	2.5	2.9
	3.0	2.9	2.5	1.8	.7	-.8	-3.1	-6.5	-12.6
	-84.0	-13.4	-8.0	-5.3	-3.7	-2.8	-2.3	-2.1	-1.9
33.	-1.8	-1.8	-1.9	-2.0	-2.4	-3.2	-4.7	-7.3	-12.6
	-82.2	-11.8	-5.6	-2.2	.0	1.6	2.6	3.3	3.6
	3.7	3.6	3.3	2.6	1.6	.0	-2.2	-5.6	-11.8
	-84.1	-12.6	-7.3	-4.7	-3.2	-2.4	-2.0	-1.9	-1.8
36.	-1.9	-1.8	-1.8	-1.9	-2.1	-2.8	-4.1	-6.7	-11.9
	-82.1	-11.0	-4.8	-1.4	.8	2.3	3.3	3.9	4.3
	4.4	4.3	3.9	3.3	2.3	.8	-1.4	-4.8	-11.0
	-84.2	-11.9	-6.7	-4.1	-2.8	-2.1	-1.9	-1.8	-1.8
39.	-2.1	-2.0	-1.9	-1.8	-1.9	-2.4	-3.7	-6.1	-11.2
	-82.0	-10.3	-4.1	-.7	1.5	3.0	3.9	4.5	4.9
	5.0	4.9	4.5	3.9	3.0	1.5	-.7	-4.1	-10.3
	-84.3	-11.2	-6.1	-3.7	-2.4	-1.9	-1.8	-1.9	-2.0

TABLE XV (CONTINUED)

CASE 11
UNNORMALIZED RESPONSE
TO OTHER BORESIGHT TARGETS

PRESUMED TARGET			
SPEED (MPH)	TRACK (DEGREES)	AZIMUTH (DEGREES)	EIGENVALUE (dB)
3.	180.	0.	-17.5

TARGET TRACK (DEGREES)

TARGET SPEED (MPH)	0	10	20	30	40	50	60	70	80
	90	100	110	120	130	140	150	160	170
	180	190	200	210	220	230	240	250	260
	270	280	290	300	310	320	330	340	350
42.	-2.4	-2.3	-2.1	-1.9	-1.8	-2.2	-3.3	-5.6	-10.7
	-82.0	-9.6	-3.4	-.0	2.1	3.5	4.5	5.1	5.4
	5.5	5.4	5.1	4.5	3.5	2.1	-.0	-3.4	-9.6
	-84.5	-10.7	-5.6	-3.3	-2.2	-1.8	-1.9	-2.1	-2.3
45.	-3.0	-2.9	-2.5	-2.1	-1.8	-2.0	-2.9	-5.1	-10.1
	-81.9	-9.0	-2.8	.6	2.7	4.1	5.0	5.5	5.8
	5.9	5.8	5.5	5.0	4.1	2.7	.6	-2.8	-9.0
	-84.6	-10.1	-5.1	-2.9	-2.0	-1.8	-2.1	-2.5	-2.9
48.	-3.8	-3.6	-3.0	-2.4	-1.9	-1.9	-2.6	-4.7	-9.6
	-81.9	-8.4	-2.2	1.1	3.2	4.6	5.4	5.9	6.2
	6.2	6.2	5.9	5.4	4.6	3.2	1.1	-2.2	-8.4
	-84.7	-9.6	-4.7	-2.6	-1.9	-1.9	-2.4	-3.0	-3.6
51.	-4.9	-4.6	-3.8	-2.8	-2.1	-1.8	-2.4	-4.3	-9.1
	-81.8	-7.8	-1.7	1.6	3.7	5.0	5.8	6.2	6.5
	6.5	6.5	6.2	5.8	5.0	3.7	1.6	-1.7	-7.8
	-84.8	-9.1	-4.3	-2.4	-1.8	-2.1	-2.8	-3.8	-4.6
54.	-6.4	-5.9	-4.8	-3.5	-2.3	-1.8	-2.2	-4.0	-8.7
	-81.8	-7.3	-1.2	2.1	4.1	5.4	6.1	6.5	6.7
	6.8	6.7	6.5	6.1	5.4	4.1	2.1	-1.2	-7.3
	-85.0	-8.7	-4.0	-2.2	-1.8	-2.3	-3.5	-4.8	-5.9
57.	-8.4	-7.8	-6.1	-4.3	-2.7	-1.9	-2.0	-3.7	-8.3
	-81.7	-6.8	-.7	2.6	4.5	5.7	6.4	6.8	6.9
	7.0	6.9	6.8	6.4	5.7	4.5	2.6	-.7	-6.8
	-85.1	-8.3	-3.7	-2.0	-1.9	-2.7	-4.3	-6.1	-7.8
60.	-11.4	-10.4	-8.0	-5.3	-3.2	-2.0	-1.9	-3.4	-7.9
	-81.6	-6.4	-.2	3.0	4.9	6.0	6.6	6.9	7.1
	7.1	7.1	6.9	6.6	6.0	4.9	3.0	-.2	-6.4
	-85.2	-7.9	-3.4	-1.9	-2.0	-3.2	-5.3	-8.0	-10.4

TABLE XV (CONTINUED)

CASE 11
UNNORMALIZED RESPONSE
TO OTHER BORESIGHT TARGETS

PRESUMED TARGET

SPEED (MPH)	TRACK (DEGREES)	AZIMUTH (DEGREES)	EIGENVALUE (dB)
15.	180.	0.	-3.0

TARGET TRACK (DEGREES)

TARGET SPEED (MPH)									
	0	10	20	30	40	50	60	70	80
	90	100	110	120	130	140	150	160	170
	180	190	200	210	220	230	240	250	260
	270	280	290	300	310	320	330	340	350
0.	-82.9	-82.9	-82.9	-82.9	-82.9	-82.9	-82.9	-82.9	-82.9
	-82.9	-82.9	-82.9	-82.9	-82.9	-82.9	-82.9	-82.9	-82.9
	-82.9	-82.9	-82.9	-82.9	-82.9	-82.9	-82.9	-82.9	-82.9
	-82.9	-82.9	-82.9	-82.9	-82.9	-82.9	-82.9	-82.9	-82.9
3.	-18.1	-18.2	-18.6	-19.3	-20.3	-21.8	-24.0	-27.2	-33.1
	-82.8	-33.0	-27.1	-23.7	-21.5	-20.0	-18.9	-18.1	-17.7
	-17.6	-17.7	-18.1	-18.9	-20.0	-21.5	-23.7	-27.1	-33.0
	-83.0	-33.1	-27.2	-24.0	-21.8	-20.3	-19.3	-18.6	-18.2
6.	-12.4	-12.5	-12.9	-13.5	-14.6	-16.0	-18.1	-21.3	-27.1
	-82.7	-26.9	-21.0	-17.6	-15.4	-13.8	-12.7	-11.9	-11.5
	-11.4	-11.5	-11.9	-12.7	-13.8	-15.4	-17.6	-21.0	-26.9
	-83.2	-27.1	-21.3	-18.1	-16.0	-14.6	-13.5	-12.9	-12.5
9.	-9.2	-9.3	-9.7	-10.3	-11.3	-12.7	-14.7	-17.9	-23.6
	-82.6	-23.4	-17.4	-14.0	-11.7	-10.1	-9.0	-8.3	-7.8
	-7.7	-7.8	-8.3	-9.0	-10.1	-11.7	-14.0	-17.4	-23.4
	-83.2	-23.6	-17.9	-14.7	-12.7	-11.3	-10.3	-9.7	-9.3
12.	-7.1	-7.2	-7.5	-8.1	-9.0	-10.4	-12.4	-15.5	-21.2
	-82.5	-20.8	-14.8	-11.4	-9.1	-7.5	-6.4	-5.6	-5.2
	-5.0	-5.2	-5.6	-6.4	-7.5	-9.1	-11.4	-14.8	-20.8
	-83.3	-21.2	-15.5	-12.4	-10.4	-9.0	-8.1	-7.5	-7.2
15.	-5.6	-5.7	-6.[illegible]	-6.5	-7.4	-8.7	-10.6	-13.7	-19.3
	-82.5	-18.9	-12.8	-9.3	-7.1	-5.4	-4.3	-3.6	-3.1
	-3.0	-3.1	-3.6	-4.3	-5.4	-7.1	-9.3	-12.8	-18.9
	-83.5	-19.3	-13.7	-10.6	-8.7	-7.4	-6.5	-6.0	-5.7
18.	-4.5	-4.6	-4.8	-5.3	-6.1	-7.3	-9.2	-12.2	-17.8
	-82.3	-17.2	-11.1	-7.7	-5.4	-3.8	-2.6	-1.9	-1.5
	-1.3	-1.5	-1.9	-2.6	-3.8	-5.4	-7.7	-11.1	-17.2
	-83.5	-17.8	-12.2	-9.2	-7.3	-6.1	-5.3	-4.8	-4.6

TABLE XV (CONTINUED)

CASE 11
UNNORMALIZED RESPONSE
TO OTHER BORESIGHT TARGETS

PRESUMED TARGET

SPEED (MPH)	TRACK (DEGREES)	AZIMUTH (DEGREES)	EIGENVALUE (dB)
15.	180.	0.	-3.0

TARGET TRACK (DEGREES)

TARGET SPEED (MPH)	0	10	20	30	40	50	60	70	80
	90	100	110	120	130	140	150	160	170
	180	190	200	210	220	230	240	250	260
	270	280	290	300	310	320	330	340	350
21.	-3.7	-3.7	-4.0	-4.4	-5.1	-6.3	-8.1	-11.0	-16.5
	-82.3	-15.9	-9.7	-6.3	-4.0	-2.4	-1.2	-.5	-.1
	.1	-.1	-.5	-1.2	-2.4	-4.0	-6.3	-9.7	-15.9
	-83.7	-16.5	-11.0	-8.1	-6.3	-5.1	-4.4	-4.0	-3.7
24.	-3.1	-3.2	-3.3	-3.7	-4.4	-5.4	-7.1	-9.9	-15.4
	-82.2	-14.7	-8.5	-5.0	-2.7	-1.1	-.0	.7	1.1
	1.3	1.1	.7	-.0	-1.1	-2.7	-5.0	-8.5	-14.7
	-83.8	-15.4	-9.9	-7.1	-5.4	-4.4	-3.7	-3.3	-3.2
27.	-2.7	-2.8	-2.9	-3.2	-3.7	-4.7	-6.3	-9.0	-14.4
	-82.1	-13.6	-7.4	-4.0	-1.7	-.1	1.0	1.7	2.1
	2.3	2.1	1.7	1.0	-.1	-1.7	-4.0	-7.4	-13.6
	-83.9	-14.4	-9.0	-6.3	-4.7	-3.7	-3.2	-2.9	-2.8
30.	-2.5	-2.6	-2.6	-2.8	-3.3	-4.1	-5.6	-8.2	-13.5
	-82.1	-12.7	-6.5	-3.0	-.7	.9	1.9	2.6	3.0
	3.2	3.0	2.6	1.9	.9	-.7	-3.0	-6.5	-12.7
	-84.0	-13.5	-8.2	-5.6	-4.1	-3.3	-2.8	-2.6	-2.6
33.	-2.5	-2.5	-2.5	-2.6	-2.9	-3.6	-5.0	-7.5	-12.8
	-82.0	-11.8	-5.6	-2.1	.2	1.7	2.8	3.4	3.8
	3.9	3.8	3.4	2.8	1.7	.2	-2.1	-5.6	-11.8
	-84.2	-12.8	-7.5	-5.0	-3.6	-2.9	-2.6	-2.5	-2.5
36.	-2.7	-2.7	-2.6	-2.5	-2.7	-3.2	-4.5	-6.9	-12.1
	-81.9	-11.0	-4.8	-1.3	.9	2.5	3.5	4.1	4.5
	4.6	4.5	4.1	3.5	2.5	.9	-1.3	-4.8	-11.0
	-84.3	-12.1	-6.9	-4.5	-3.2	-2.7	-2.5	-2.6	-2.7
39.	-3.1	-3.0	-2.8	-2.6	-2.6	-2.9	-4.0	-6.4	-11.4
	-81.8	-10.3	-4.1	-.6	1.6	3.1	4.1	4.8	5.1
	5.2	5.1	4.8	4.1	3.1	1.6	-.6	-4.1	-10.3
	-84.5	-11.4	-6.4	-4.0	-2.9	-2.6	-2.6	-2.8	-3.0

TABLE XV (CONTINUED)

CASE 11
UNNORMALIZED RESPONSE
TO OTHER BORESIGHT TARGETS

PRESUMED TARGET

SPEED (MPH)	TRACK (DEGREES)	AZIMUTH (DEGREES)	EIGENVALUE (dB)
15.	180.	0.	-3.0

TARGET TRACK (DEGREES)

TARGET SPEED (MPH)	0 / 90 / 180 / 270	10 / 100 / 190 / 280	20 / 110 / 200 / 290	30 / 120 / 210 / 300	40 / 130 / 220 / 310	50 / 140 / 230 / 320	60 / 150 / 240 / 330	70 / 160 / 250 / 340	80 / 170 / 260 / 350
42.	-3.6	-3.5	-3.1	-2.7	-2.5	-2.7	-3.7	-5.9	-10.8
	-81.7	-9.6	-3.4	.1	2.3	3.7	4.7	5.3	5.6
	5.7	5.6	5.3	4.7	3.7	2.3	.1	-3.4	-9.6
	-84.6	-10.8	-5.9	-3.7	-2.7	-2.5	-2.7	-3.1	-3.5
45.	-4.5	-4.3	-3.7	-3.1	-2.6	-2.6	-3.4	-5.4	-10.3
	-81.7	-9.0	-2.8	.7	2.9	4.3	5.2	5.8	6.1
	6.2	6.1	5.8	5.2	4.3	2.9	.7	-2.8	-9.0
	-84.7	-10.3	-5.4	-3.4	-2.6	-2.6	-3.1	-3.7	-4.3
48.	-5.6	-5.3	-4.5	-3.5	-2.8	-2.5	-3.1	-5.0	-9.8
	-81.6	-8.4	-2.2	1.3	3.4	4.8	5.7	6.2	6.5
	6.6	6.5	6.2	5.7	4.8	3.4	1.3	-2.2	-8.4
	-84.8	-9.8	-5.0	-3.1	-2.5	-2.8	-3.5	-4.5	-5.3
51.	-7.2	-6.7	-5.6	-4.2	-3.1	-2.5	-2.9	-4.7	-9.3
	-81.5	-7.8	-1.6	1.8	3.9	5.2	6.1	6.6	6.8
	6.9	6.8	6.6	6.1	5.2	3.9	1.8	-1.6	-7.8
	-85.0	-9.3	-4.7	-2.9	-2.5	-3.1	-4.2	-5.6	-6.7
54.	-9.4	-8.7	-7.0	-5.1	-3.5	-2.6	-2.7	-4.3	-8.9
	-81.5	-7.3	-1.1	2.3	4.3	5.6	6.4	6.9	7.1
	7.2	7.1	6.9	6.4	5.6	4.3	2.3	-1.1	-7.3
	-85.2	-8.9	-4.3	-2.7	-2.6	-3.5	-5.1	-7.0	-8.7
57.	-12.8	-11.7	-9.0	-6.3	-4.1	-2.8	-2.6	-4.0	-8.5
	-81.4	-6.8	-.6	2.7	4.8	6.0	6.7	7.1	7.3
	7.4	7.3	7.1	6.7	6.0	4.8	2.7	-.6	-6.8
	-85.3	-8.5	-4.0	-2.6	-2.8	-4.1	-6.3	-9.0	-11.7
60.	-18.1	-16.3	-12.0	-7.8	-4.8	-3.0	-2.5	-3.8	-8.1
	-81.3	-6.3	-.1	3.2	5.1	6.3	7.0	7.3	7.5
	7.5	7.5	7.3	7.0	6.3	5.1	3.2	-.1	-6.3
	-85.5	-8.1	-3.8	-2.5	-3.0	-4.8	-7.8	-12.0	-16.3

TABLE XV (CONTINUED)

CASE 11
UNNORMALIZED RESPONSE
TO OTHER BORESIGHT TARGETS

	PRESUMED TARGET		
SPEED (MPH)	TRACK (DEGREES)	AZIMUTH (DEGREES)	EIGENVALUE (dB)
30.	180.	0.	3.2

TARGET TRACK (DEGREES)

TARGET SPEED (MPH)	0 / 90 / 180 / 270	10 / 100 / 190 / 280	20 / 110 / 200 / 290	30 / 120 / 210 / 300	40 / 130 / 220 / 310	50 / 140 / 230 / 320	60 / 150 / 240 / 330	70 / 160 / 250 / 340	80 / 170 / 260 / 350
0.	-82.8	-82.8	-82.8	-82.8	-82.8	-82.8	-82.8	-82.8	-82.8
	-82.8	-82.8	-82.8	-82.8	-82.8	-82.8	-82.8	-82.8	-82.8
	-82.8	-82.8	-82.8	-82.8	-82.8	-82.8	-82.8	-82.8	-82.8
	-82.8	-82.8	-82.8	-82.8	-82.8	-82.8	-82.8	-82.8	-82.8
3.	-18.4	-18.5	-18.9	-19.6	-20.6	-22.1	-24.2	-27.5	-33.3
	-82.7	-33.2	-27.3	-23.9	-21.7	-20.2	-19.1	-18.3	-17.9
	-17.8	-17.9	-18.3	-19.1	-20.2	-21.7	-23.9	-27.3	-33.2
	-82.9	-33.3	-27.5	-24.2	-22.1	-20.6	-19.6	-18.9	-18.5
6.	-12.7	-12.8	-13.2	-13.8	-14.8	-16.3	-18.4	-21.6	-27.3
	-82.6	-27.1	-21.2	-17.8	-15.5	-14.0	-12.8	-12.1	-11.7
	-11.5	-11.7	-12.1	-12.8	-14.0	-15.5	-17.8	-21.2	-27.1
	-83.1	-27.3	-21.6	-18.4	-16.3	-14.8	-13.8	-13.2	-12.8
9.	-9.5	-9.7	-10.0	-10.6	-11.6	-13.0	-15.0	-18.1	-23.9
	-82.5	-23.6	-17.6	-14.1	-11.9	-10.3	-9.1	-8.4	-7.9
	-7.8	-7.9	-8.4	-9.1	-10.3	-11.9	-14.1	-17.6	-23.6
	-83.1	-23.9	-18.1	-15.0	-13.0	-11.6	-10.6	-10.0	-9.7
12.	-7.5	-7.6	-7.9	-8.5	-9.4	-10.7	-12.7	-15.8	-21.4
	-82.4	-21.0	-15.0	-11.5	-9.2	-7.6	-6.5	-5.7	-5.3
	-5.1	-5.3	-5.7	-6.5	-7.6	-9.2	-11.5	-15.0	-21.0
	-83.2	-21.4	-15.8	-12.7	-10.7	-9.4	-8.5	-7.9	-7.6
15.	-6.0	-6.1	-6.4	-6.9	-7.8	-9.0	-10.9	-13.9	-19.5
	-82.3	-19.0	-13.0	-9.5	-7.2	-5.5	-4.4	-3.6	-3.2
	-3.1	-3.2	-3.6	-4.4	-5.5	-7.2	-9.5	-13.0	-19.0
	-83.4	-19.5	-13.9	-10.9	-9.0	-7.8	-6.9	-6.4	-6.1
18.	-5.0	-5.1	-5.3	-5.8	-6.6	-7.7	-9.5	-12.5	-18.0
	-82.1	-17.4	-11.3	-7.8	-5.5	-3.8	-2.7	-1.9	-1.5
	-1.4	-1.5	-1.9	-2.7	-3.8	-5.5	-7.8	-11.3	-17.4
	-83.5	-18.0	-12.5	-9.5	-7.7	-6.6	-5.8	-5.3	-5.1

TABLE XV (CONTINUED)

CASE 11
UNNORMALIZED RESPONSE
TO OTHER BORESIGHT TARGETS

PRESUMED TARGET

SPEED (MPH)	TRACK (DEGREES)	AZIMUTH (DEGREES)	EIGENVALUE (dB)
30.	180.	0.	3.2

TARGET TRACK (DEGREES)

TARGET SPEED (MPH)	0 / 90 / 180 / 270	10 / 100 / 190 / 280	20 / 110 / 200 / 290	30 / 120 / 210 / 300	40 / 130 / 220 / 310	50 / 140 / 230 / 320	60 / 150 / 240 / 330	70 / 160 / 250 / 340	80 / 170 / 260 / 350
21.	-4.2	-4.3	-4.5	-4.9	-5.6	-6.7	-8.4	-11.3	-16.7
	-82.1	-16.0	-9.9	-6.4	-4.0	-2.4	-1.3	-.5	-.1
	.1	-.1	-.5	-1.3	-2.4	-4.0	-6.4	-9.9	-16.0
	-83.6	-16.7	-11.3	-8.4	-6.7	-5.6	-4.9	-4.5	-4.3
24.	-3.7	-3.8	-3.9	-4.3	-4.9	-5.8	-7.5	-10.2	-15.6
	-82.0	-14.8	-8.7	-5.1	-2.8	-1.2	-.0	.7	1.1
	1.3	1.1	.7	-.0	-1.2	-2.8	-5.1	-8.7	-14.8
	-83.7	-15.6	-10.2	-7.5	-5.9	-4.9	-4.3	-3.9	-3.8
27.	-3.5	-3.5	-3.6	-3.8	-4.3	-5.2	-6.7	-9.4	-14.7
	-81.9	-13.8	-7.6	-4.0	-1.7	-.1	1.0	1.8	2.2
	2.3	2.2	1.8	1.0	-.1	-1.7	-4.0	-7.6	-13.8
	-83.9	-14.7	-9.4	-6.7	-5.2	-4.3	-3.8	-3.6	-3.5
30.	-3.4	-3.4	-3.4	-3.5	-3.9	-4.6	-6.0	-8.6	-13.8
	-81.8	-12.8	-6.6	-3.1	-.7	.9	2.0	2.7	3.1
	3.2	3.1	2.7	2.0	.9	-.7	-3.1	-6.6	-12.8
	-84.0	-13.8	-8.6	-6.0	-4.6	-3.9	-3.5	-3.4	-3.4
33.	-3.5	-3.5	-3.4	-3.4	-3.6	-4.2	-5.5	-7.9	-13.0
	-81.7	-11.9	-5.7	-2.2	.1	1.7	2.8	3.5	3.9
	4.0	3.9	3.5	2.8	1.7	.1	-2.2	-5.7	-11.9
	-84.2	-13.0	-7.9	-5.5	-4.2	-3.6	-3.4	-3.4	-3.5
36.	-3.8	-3.7	-3.6	-3.4	-3.4	-3.9	-5.0	-7.3	-12.4
	-81.7	-11.2	-4.9	-1.4	.9	2.5	3.6	4.2	4.6
	4.7	4.6	4.2	3.6	2.5	.9	-1.4	-4.9	-11.2
	-84.4	-12.4	-7.3	-5.0	-3.9	-3.4	-3.4	-3.6	-3.7
39.	-4.4	-4.2	-3.9	-3.6	-3.4	-3.6	-4.6	-6.8	-11.7
	-81.6	-10.4	-4.2	-.6	1.7	3.2	4.2	4.9	5.2
	5.4	5.2	4.9	4.2	3.2	1.7	-.6	-4.2	-10.4
	-84.5	-11.7	-6.8	-4.6	-3.6	-3.4	-3.6	-3.9	-4.2

TABLE XV (CONTINUED)

CASE 11
UNNORMALIZED RESPONSE
TO OTHER BORESIGHT TARGETS

PRESUMED TARGET

SPEED (MPH)	TRACK (DEGREES)	AZIMUTH (DEGREES)	EIGENVALUE (dB)
30.	180.	0.	3.2

TARGET TRACK (DEGREES)

TARGET SPEED (MPH)	0 / 90 / 180 / 270	10 / 100 / 190 / 280	20 / 110 / 200 / 290	30 / 120 / 210 / 300	40 / 130 / 220 / 310	50 / 140 / 230 / 320	60 / 150 / 240 / 330	70 / 160 / 250 / 340	80 / 170 / 260 / 350
42.	-5.2	-5.0	-4.5	-3.9	-3.4	-3.5	-4.2	-6.3	-11.1
	-81.5	-9.7	-3.5	.1	2.3	3.8	4.8	5.4	5.8
	5.9	5.8	5.4	4.8	3.8	2.3	.1	-3.5	-9.7
	-84.7	-11.1	-6.3	-4.2	-3.5	-3.4	-3.9	-4.5	-5.0
45.	-6.3	-6.0	-5.3	-4.4	-3.6	-3.4	-4.0	-5.9	-10.6
	-81.4	-9.1	-2.8	.7	2.9	4.4	5.4	5.9	6.3
	6.4	6.3	5.9	5.4	4.4	2.9	.7	-2.8	-9.1
	-84.8	-10.6	-5.9	-4.0	-3.4	-3.6	-4.4	-5.3	-6.0
48.	-8.0	-7.5	-6.4	-5.0	-3.9	-3.4	-3.7	-5.5	-10.1
	-81.3	-8.5	-2.2	1.3	3.5	4.9	5.8	6.4	6.7
	6.8	6.7	6.4	5.8	4.9	3.5	1.3	-2.2	-8.5
	-85.0	-10.1	-5.5	-3.7	-3.4	-3.9	-5.0	-6.4	-7.5
51.	-10.4	-9.7	-7.9	-6.0	-4.4	-3.5	-3.6	-5.1	-9.7
	-81.3	-8.0	-1.7	1.8	4.0	5.4	6.2	6.8	7.0
	7.1	7.0	6.8	6.2	5.4	4.0	1.8	-1.7	-8.0
	-85.1	-9.7	-5.1	-3.6	-3.5	-4.4	-6.0	-7.9	-9.7
54.	-14.1	-12.9	-10.1	-7.2	-5.0	-3.6	-3.5	-4.8	-9.2
	-81.2	-7.4	-1.1	2.3	4.4	5.8	6.6	7.1	7.4
	7.4	7.4	7.1	6.6	5.8	4.4	2.3	-1.1	-7.4
	-85.4	-9.2	-4.8	-3.5	-3.6	-5.0	-7.2	-10.1	-12.9
57.	-19.8	-18.0	-13.4	-9.0	-5.8	-3.9	-3.4	-4.6	-8.8
	-81.1	-6.9	-.6	2.8	4.9	6.2	6.9	7.4	7.6
	7.7	7.6	7.4	6.9	6.2	4.9	2.8	-.6	-6.9
	-85.5	-8.8	-4.6	-3.4	-3.9	-5.8	-9.0	-13.4	-18.0
60.	-18.3	-20.3	-18.5	-11.4	-6.8	-4.3	-3.4	-4.3	-8.5
	-81.1	-6.5	-.2	3.2	5.3	6.5	7.2	7.6	7.8
	7.9	7.8	7.6	7.2	6.5	5.3	3.2	-.2	-6.5
	-85.7	-8.5	-4.3	-3.4	-4.3	-6.8	-11.4	-18.5	-20.3

TABLE XVI

CASE 2
UNNORMALIZED RESPONSE
TO OTHER BORESIGHT TARGETS

PRESUMED TARGET SPEED (MPH)	PRESUMED TARGET TRACK (DEGREES)	PRESUMED TARGET AZIMUTH (DEGREES)	EIGENVALUE (dB)
3.	180.	30.	-61.6

TARGET TRACK (DEGREES)

TARGET SPEED (MPH)	0 90 180 270	10 100 190 280	20 110 200 290	30 120 210 300	40 130 220 310	50 140 230 320	60 150 240 330	70 160 250 340	80 170 260 350
0.	-62.9	-62.9	-62.9	-62.9	-62.9	-62.9	-62.9	-62.9	-62.9
	-62.9	-62.9	-62.9	-62.9	-62.9	-62.9	-62.9	-62.9	-62.9
	-62.9	-62.9	-62.9	-62.9	-62.9	-62.9	-62.9	-62.9	-62.9
	-62.9	-62.9	-62.9	-62.9	-62.9	-62.9	-62.9	-62.9	-62.9
3.	-64.6	-64.8	-64.9	-64.9	-64.9	-64.8	-64.6	-64.4	-64.2
	-63.9	-63.5	-63.2	-62.9	-62.6	-62.4	-62.1	-61.9	-61.8
	-61.6	-61.5	-61.5	-61.5	-61.5	-61.5	-61.6	-61.8	-61.9
	-62.1	-62.4	-62.6	-62.9	-63.2	-63.5	-63.9	-64.2	-64.4
6.	-66.8	-67.2	-67.4	-67.5	-67.4	-67.2	-66.8	-66.3	-65.6
	-64.9	-64.2	-63.6	-62.9	-62.4	-61.9	-61.5	-61.1	-60.9
	-60.7	-60.6	-60.5	-60.5	-60.5	-60.6	-60.7	-60.9	-61.1
	-61.5	-61.9	-62.4	-62.9	-63.6	-64.2	-64.9	-65.6	-66.3
9.	-69.2	-69.7	-70.0	-70.1	-70.0	-69.7	-69.2	-68.4	-67.3
	-66.2	-65.0	-63.9	-62.9	-62.1	-61.4	-60.9	-60.5	-60.3
	-60.1	-60.0	-60.0	-59.9	-60.0	-60.0	-60.1	-60.3	-60.5
	-60.9	-61.4	-62.1	-62.9	-63.9	-65.0	-66.2	-67.3	-68.4
12.	-70.8	-70.9	-70.8	-70.8	-70.8	-70.9	-70.8	-70.3	-69.1
	-67.5	-65.8	-64.3	-62.9	-61.9	-61.1	-60.5	-60.1	-59.9
	-59.8	-59.8	-59.8	-59.8	-59.8	-59.8	-59.8	-59.9	-60.1
	-60.5	-61.1	-61.9	-62.9	-64.3	-65.8	-67.5	-69.1	-70.3
15.	-70.4	-69.7	-69.3	-69.1	-69.3	-69.7	-70.4	-70.9	-70.5
	-68.9	-66.7	-64.6	-62.9	-61.6	-60.7	-60.2	-59.9	-59.8
	-59.8	-59.9	-60.0	-60.0	-60.0	-59.9	-59.8	-59.8	-59.9
	-60.2	-60.7	-61.6	-62.9	-64.6	-66.7	-68.9	-70.5	-70.9
18.	-68.7	-67.8	-67.4	-67.2	-67.4	-67.8	-68.7	-69.9	-70.9
	-70.1	-67.7	-65.0	-62.9	-61.4	-60.5	-59.9	-59.8	-59.9
	-60.1	-60.4	-60.6	-60.6	-60.6	-60.4	-60.1	-59.9	-59.8
	-59.9	-60.5	-61.4	-62.9	-65.0	-67.7	-70.1	-70.9	-69.9

TABLE XVI (CONTINUED)

CASE 2
UNNORMALIZED RESPONSE
TO OTHER BORESIGHT TARGETS

PRESUMED TARGET SPEED (MPH)	TRACK (DEGREES)	AZIMUTH (DEGREES)	EIGENVALUE (dB)
3.	180.	30.	-61.6

TARGET TRACK (DEGREES)

TARGET SPEED (MPH)									
	0	10	20	30	40	50	60	70	80
	90	100	110	120	130	140	150	160	170
	180	190	200	210	220	230	240	250	260
	270	280	290	300	310	320	330	340	350
21.	-67.1	-66.4	-66.0	-65.9	-66.0	-66.4	-67.1	-68.4	-70.1
	-70.8	-68.6	-65.5	-62.9	-61.2	-60.2	-59.8	-59.9	-60.2
	-60.7	-61.2	-61.6	-61.7	-61.6	-61.2	-60.7	-60.2	-59.9
	-59.8	-60.2	-61.2	-62.9	-65.5	-68.6	-70.8	-70.1	-68.4
24.	-65.9	-65.4	-65.2	-65.2	-65.2	-65.4	-65.9	-67.0	-68.8
	-70.8	-69.5	-65.9	-62.9	-61.0	-60.0	-59.8	-60.1	-60.8
	-61.6	-62.5	-63.1	-63.3	-63.1	-62.5	-61.6	-60.8	-60.1
	-59.8	-60.0	-61.0	-62.9	-65.9	-69.5	-70.8	-68.8	-67.0
27.	-65.3	-65.1	-65.0	-65.1	-65.0	-65.1	-65.3	-66.0	-67.6
	-70.1	-70.3	-66.3	-62.9	-60.9	-59.9	-59.9	-60.5	-61.6
	-62.9	-64.2	-65.2	-65.6	-65.2	-64.2	-62.9	-61.6	-60.5
	-59.9	-59.9	-60.9	-62.9	-66.3	-70.3	-70.1	-67.6	-66.0
30.	-65.0	-65.2	-65.4	-65.5	-65.4	-65.2	-65.0	-65.3	-66.6
	-69.1	-70.8	-66.8	-62.9	-60.7	-59.8	-60.0	-61.0	-62.7
	-64.7	-66.7	-68.2	-68.8	-68.2	-66.7	-64.7	-62.7	-61.0
	-60.0	-59.8	-60.7	-62.9	-66.8	-70.8	-69.1	-66.6	-65.3
33.	-65.2	-65.8	-66.3	-66.6	-66.3	-65.8	-65.2	-65.1	-65.8
	-68.1	-70.9	-67.3	-62.9	-60.6	-59.8	-60.3	-61.8	-64.2
	-67.1	-70.3	-72.9	-73.9	-72.9	-70.3	-67.1	-64.2	-61.8
	-60.3	-59.8	-60.6	-62.9	-67.3	-70.9	-68.1	-65.8	-65.1
36.	-65.9	-67.0	-67.9	-68.3	-67.9	-67.0	-65.9	-65.1	-65.3
	-67.2	-70.7	-67.8	-62.9	-60.4	-59.8	-60.7	-62.8	-66.1
	-70.5	-76.0	-81.1	-83.1	-81.1	-76.0	-70.5	-66.1	-62.8
	-60.6	-59.8	-60.4	-62.9	-67.8	-70.7	-67.2	-65.3	-65.1
39.	-66.9	-68.8	-70.4	-71.0	-70.4	-68.8	-66.9	-65.5	-65.1
	-66.5	-70.2	-68.3	-62.9	-60.3	-59.8	-61.1	-64.0	-68.7
	-75.8	-84.6	-80.8	-79.2	-80.8	-84.6	-75.8	-68.7	-64.0
	-61.1	-59.8	-60.3	-62.9	-68.3	-70.2	-66.5	-65.1	-65.5

TABLE XVI (CONTINUED)

CASE 2
UNNORMALIZED RESPONSE
TO OTHER BORESIGHT TARGETS

	PRESUMED TARGET		
SPEED (MPH)	TRACK (DEGREES)	AZIMUTH (DEGREES)	EIGENVALUE (dB)
3.	180.	30.	-61.6

TARGET TRACK (DEGREES)

TARGET SPEED (MPH)									
	0	10	20	30	40	50	60	70	80
	90	100	110	120	130	140	150	160	170
	180	190	200	210	220	230	240	250	260
	270	280	290	300	310	320	330	340	350
42.	-68.6	-71.6	-74.3	-75.4	-74.3	-71.6	-68.6	-66.2	-65.1
	-65.9	-69.5	-68.7	-62.9	-60.2	-59.9	-61.7	-65.6	-72.2
	-84.1	-78.0	-74.5	-73.7	-74.5	-78.0	-84.1	-72.2	-65.6
	-61.7	-59.9	-60.2	-62.9	-68.7	-69.5	-65.9	-65.1	-66.2
45.	-71.0	-75.9	-81.2	-83.6	-81.2	-75.9	-71.0	-67.3	-65.3
	-65.5	-68.8	-69.2	-62.9	-60.1	-60.1	-62.4	-67.5	-77.8
	-79.2	-73.4	-71.6	-71.2	-71.6	-73.4	-79.2	-77.8	-67.5
	-62.4	-60.1	-60.1	-62.9	-69.2	-68.8	-65.4	-65.3	-67.3
48.	-74.6	-84.1	-87.1	-84.3	-87.1	-84.1	-74.6	-68.9	-65.8
	-65.2	-68.2	-69.6	-62.9	-60.0	-60.3	-63.3	-70.0	-84.6
	-74.3	-71.1	-70.3	-70.1	-70.3	-71.1	-74.3	-84.7	-70.0
	-63.3	-60.3	-60.0	-62.9	-69.6	-68.1	-65.2	-65.8	-68.9
51.	-80.7	-84.6	-78.4	-77.1	-78.4	-84.6	-80.7	-71.1	-66.5
	-65.1	-67.5	-70.0	-62.9	-60.0	-60.5	-64.3	-73.5	-79.0
	-71.7	-70.1	-70.0	-70.0	-70.0	-70.1	-71.7	-79.0	-73.5
	-64.3	-60.5	-60.0	-62.9	-70.0	-67.5	-65.1	-66.5	-71.1
54.	-88.5	-77.5	-74.6	-73.9	-74.6	-77.5	-88.5	-74.3	-67.5
	-65.1	-67.0	-70.4	-62.9	-59.9	-60.8	-65.6	-78.5	-74.5
	-70.4	-70.0	-70.5	-70.8	-70.5	-70.0	-70.4	-74.5	-78.5
	-65.6	-60.8	-59.9	-62.9	-70.4	-66.9	-65.1	-67.5	-74.3
57.	-80.3	-74.2	-72.7	-72.4	-72.7	-74.2	-80.3	-79.2	-68.8
	-65.2	-66.5	-70.6	-62.9	-59.9	-61.1	-67.0	-84.5	-72.1
	-70.0	-70.6	-71.9	-72.5	-71.9	-70.6	-70.0	-72.1	-84.6
	-67.0	-61.1	-59.9	-62.9	-70.6	-66.5	-65.2	-68.8	-79.2
60.	-75.8	-72.6	-72.0	-72.0	-72.0	-72.6	-75.8	-87.6	-70.6
	-65.5	-66.0	-70.8	-62.9	-59.8	-61.5	-68.8	-80.4	-70.7
	-70.2	-72.0	-74.3	-75.4	-74.3	-72.0	-70.2	-70.7	-80.4
	-68.8	-61.5	-59.8	-62.9	-70.8	-66.0	-65.5	-70.6	-87.5

TABLE XVI (CONTINUED)

CASE 2
UNNORMALIZED RESPONSE
TO OTHER BORESIGHT TARGETS

PRESUMED TARGET

SPEED (MPH)	TRACK (DEGREES)	AZIMUTH (DEGREES)	EIGENVALUE (dB)
15.	180.	30.	-56.7

TARGET TRACK (DEGREES)

TARGET SPEED (MPH)									
	0	10	20	30	40	50	60	70	80
	90	100	110	120	130	140	150	160	170
	180	190	200	210	220	230	240	250	260
	270	280	290	300	310	320	330	340	350
0.	-70.0	-70.0	-70.0	-70.0	-70.0	-70.0	-70.0	-70.0	-70.0
	-70.0	-70.0	-70.0	-70.0	-70.0	-70.0	-70.0	-70.0	-70.0
	-70.0	-70.0	-70.0	-70.0	-70.0	-70.0	-70.0	-70.0	-70.0
	-70.0	-70.0	-70.0	-70.0	-70.0	-70.0	-70.0	-70.0	-70.0
3.	-76.6	-76.5	-76.4	-76.3	-76.4	-76.5	-76.6	-76.4	-75.7
	-74.5	-73.0	-71.5	-70.0	-68.7	-67.6	-66.6	-65.9	-65.2
	-64.7	-64.4	-64.2	-64.1	-64.2	-64.4	-64.7	-65.2	-65.9
	-66.6	-67.6	-68.7	-70.0	-71.5	-73.0	-74.5	-75.7	-76.4
6.	-70.4	-69.4	-68.8	-68.6	-68.8	-69.4	-70.4	-72.0	-74.1
	-76.3	-76.0	-73.1	-70.0	-67.6	-65.6	-64.1	-63.0	-62.1
	-61.5	-61.0	-60.8	-60.7	-60.8	-61.0	-61.5	-62.1	-63.0
	-64.1	-65.6	-67.6	-70.0	-73.1	-76.0	-76.3	-74.1	-72.0
9.	-65.7	-64.8	-64.4	-64.2	-64.4	-64.8	-65.7	-67.0	-69.1
	-72.2	-76.2	-74.7	-70.0	-66.5	-64.0	-62.2	-60.9	-60.0
	-59.3	-58.8	-58.6	-58.5	-58.6	-58.8	-59.3	-60.0	-60.9
	-62.2	-64.0	-66.5	-70.0	-74.7	-76.2	-72.2	-69.1	-67.0
12.	-62.9	-62.3	-61.9	-61.8	-61.9	-62.3	-62.9	-64.0	-65.8
	-68.6	-73.4	-76.1	-70.0	-65.6	-62.7	-60.7	-59.3	-58.4
	-57.8	-57.3	-57.1	-57.1	-57.1	-57.3	-57.8	-58.4	-59.3
	-60.7	-62.7	-65.6	-70.0	-76.1	-73.4	-68.6	-65.8	-64.0
15.	-61.3	-60.8	-60.5	-60.5	-60.5	-60.8	-61.3	-62.1	-63.6
	-66.1	-70.6	-76.6	-70.0	-64.7	-61.6	-59.5	-58.1	-57.3
	-56.7	-56.4	-56.2	-56.2	-56.2	-56.4	-56.7	-57.3	-58.1
	-59.5	-61.6	-64.7	-70.0	-76.6	-70.6	-66.1	-63.6	-62.1
18.	-60.3	-60.0	-59.9	-59.9	-59.9	-60.0	-60.3	-60.9	-62.1
	-64.2	-68.3	-76.1	-70.0	-64.0	-60.6	-58.5	-57.2	-56.5
	-56.1	-55.9	-55.8	-55.8	-55.8	-55.9	-56.1	-56.5	-57.2
	-58.5	-60.6	-64.0	-70.0	-76.1	-68.3	-64.2	-62.1	-60.9

TABLE XVI (CONTINUED)

CASE 2
UNNORMALIZED RESPONSE
TO OTHER BORESIGHT TARGETS

PRESUMED TARGET

SPEED (MPH)	TRACK (DEGREES)	AZIMUTH (DEGREES)	EIGENVALUE (dB)
15.	180.	30.	-56.7

TARGET TRACK (DEGREES)

TARGET SPEED (MPH)	0 90 180 270	10 100 190 280	20 110 200 290	30 120 210 300	40 130 220 310	50 140 230 320	60 150 240 330	70 160 250 340	80 170 260 350
21.	-59.8	-59.8	-59.9	-59.9	-59.9	-59.8	-59.8	-60.2	-61.0
	-62.8	-66.5	-74.7	-70.0	-63.3	-59.7	-57.7	-56.6	-56.0
	-55.8	-55.7	-55.8	-55.8	-55.8	-55.7	-55.8	-56.0	-56.6
	-57.7	-59.7	-63.3	-70.0	-74.7	-66.5	-62.8	-61.0	-60.2
24.	-59.9	-60.1	-60.4	-60.5	-60.4	-60.1	-59.9	-59.8	-60.3
	-61.8	-65.1	-73.2	-70.0	-62.6	-59.0	-57.1	-56.1	-55.7
	-55.8	-56.0	-56.1	-56.2	-56.1	-56.0	-55.8	-55.7	-56.1
	-57.1	-59.0	-62.6	-70.0	-73.2	-65.1	-61.8	-60.3	-59.8
27.	-60.3	-61.0	-61.5	-61.7	-61.5	-61.0	-60.3	-59.9	-59.9
	-61.0	-64.0	-71.7	-70.0	-62.0	-58.4	-56.6	-55.8	-55.8
	-56.1	-56.5	-56.9	-57.1	-56.9	-56.5	-56.1	-55.8	-55.8
	-56.6	-58.4	-62.0	-70.0	-71.7	-64.0	-61.0	-59.9	-59.9
30.	-61.2	-62.4	-63.3	-63.7	-63.3	-62.4	-61.2	-60.2	-59.8
	-60.5	-63.0	-70.4	-70.0	-61.5	-57.8	-56.2	-55.7	-56.0
	-56.7	-57.5	-58.2	-58.4	-58.2	-57.5	-56.7	-56.0	-55.7
	-56.2	-57.8	-61.5	-70.0	-70.4	-63.0	-60.5	-59.8	-60.2
33.	-62.6	-64.6	-66.1	-66.7	-66.1	-64.6	-62.6	-60.9	-59.9
	-60.1	-62.3	-69.2	-70.0	-61.0	-57.3	-55.9	-55.8	-56.5
	-57.7	-59.0	-60.0	-60.4	-60.0	-59.0	-57.7	-56.5	-55.8
	-55.9	-57.3	-61.0	-70.0	-69.2	-62.2	-60.1	-59.9	-60.9
36.	-64.7	-67.8	-70.6	-71.7	-70.6	-67.8	-64.7	-62.0	-60.3
	-59.9	-61.6	-68.1	-70.0	-60.5	-56.9	-55.8	-56.0	-57.3
	-59.1	-61.1	-62.6	-63.3	-62.6	-61.1	-59.1	-57.3	-56.0
	-55.8	-56.9	-60.5	-70.0	-68.1	-61.6	-59.9	-60.3	-62.0
39.	-67.8	-73.4	-80.1	-84.2	-80.1	-73.4	-67.8	-63.6	-60.9
	-59.8	-61.1	-67.2	-70.0	-60.1	-56.6	-55.7	-56.5	-58.4
	-61.0	-64.0	-66.6	-67.6	-66.6	-64.0	-61.0	-58.4	-56.5
	-55.7	-56.6	-60.1	-70.0	-67.2	-61.1	-59.8	-60.9	-63.6

TABLE XVI (CONTINUED)

CASE 2
UNNORMALIZED RESPONSE
TO OTHER BORESIGHT TARGETS

PRESUMED TARGET

SPEED (MPH)	TRACK (DEGREES)	AZIMUTH (DEGREES)	EIGENVALUE (dB)
15.	180.	30.	-56.7

TARGET TRACK (DEGREES)

TARGET SPEED (MPH)	0 90 180 270	10 100 190 280	20 110 200 290	30 120 210 300	40 130 220 310	50 140 230 320	60 150 240 330	70 160 250 340	80 170 260 350
42.	-72.6	-89.8	-81.9	-78.8	-81.9	-89.8	-72.6	-65.7	-61.7
	-59.9	-60.7	-66.4	-70.0	-59.6	-56.3	-55.8	-57.1	-59.8
	-63.7	-68.5	-73.5	-76.0	-73.5	-68.5	-63.7	-59.8	-57.1
	-55.8	-56.3	-59.6	-70.0	-66.4	-60.7	-59.9	-61.7	-65.7
45.	-84.0	-77.7	-72.8	-71.7	-72.8	-77.7	-84.0	-68.8	-62.9
	-60.1	-60.3	-65.6	-70.0	-59.3	-56.1	-55.9	-57.9	-61.7
	-67.6	-77.4	-93.4	-83.1	-93.4	-77.4	-67.6	-61.7	-57.9
	-55.9	-56.1	-59.3	-70.0	-65.6	-60.3	-60.1	-62.9	-68.8
48.	-80.8	-71.6	-69.4	-68.9	-69.4	-71.6	-80.8	-73.7	-64.4
	-60.5	-60.1	-65.0	-70.0	-58.9	-55.9	-56.2	-58.9	-64.2
	-74.2	-82.2	-73.3	-71.8	-73.3	-82.2	-74.2	-64.2	-58.9
	-56.2	-55.9	-58.9	-70.0	-65.0	-60.1	-60.5	-64.4	-73.7
51.	-73.1	-68.9	-67.8	-67.6	-67.8	-68.9	-73.1	-84.8	-66.4
	-61.0	-59.9	-64.4	-70.0	-58.6	-55.8	-56.6	-60.2	-67.7
	-99.1	-72.0	-68.8	-68.2	-68.8	-72.0	-99.2	-67.7	-60.2
	-56.6	-55.8	-58.6	-70.0	-64.4	-59.9	-61.0	-66.4	-84.8
54.	-69.8	-67.7	-67.4	-67.4	-67.4	-67.7	-69.8	-81.9	-69.2
	-61.7	-59.8	-63.8	-70.0	-58.3	-55.7	-57.1	-61.9	-73.5
	-74.6	-68.4	-66.9	-66.5	-66.9	-68.4	-74.6	-73.5	-61.9
	-57.1	-55.7	-58.3	-70.0	-63.8	-59.8	-61.7	-69.2	-81.9
57.	-68.1	-67.4	-67.8	-68.1	-67.8	-67.4	-68.1	-74.0	-73.3
	-62.6	-59.8	-63.3	-70.0	-58.0	-55.7	-57.7	-64.0	-91.1
	-69.8	-66.7	-66.1	-66.1	-66.1	-66.7	-69.8	-91.2	-64.0
	-57.7	-55.7	-58.0	-70.0	-63.3	-59.8	-62.6	-73.3	-74.0
60.	-67.4	-67.9	-69.1	-69.7	-69.1	-67.9	-67.4	-70.6	-81.0
	-63.7	-59.9	-62.9	-70.0	-57.7	-55.8	-58.4	-66.8	-77.4
	-67.5	-66.1	-66.4	-66.6	-66.4	-66.1	-67.5	-77.4	-66.8
	-58.4	-55.8	-57.7	-70.0	-62.9	-59.8	-63.7	-81.0	-70.6

TABLE XVI (CONTINUED)

CASE 2
UNNORMALIZED RESPONSE
TO OTHER BORESIGHT TARGETS

PRESUMED TARGET

SPEED (MPH)	TRACK (DEGREES)	AZIMUTH (DEGREES)	EIGENVALUE (dB)
30.	180.	30.	-54.9

TARGET TRACK (DEGREES)

TARGET SPEED (MPH)	0 90 180 270	10 100 190 280	20 110 200 290	30 120 210 300	40 130 220 310	50 140 230 320	60 150 240 330	70 160 250 340	80 170 260 350
0.	-79.9	-79.9	-79.9	-79.9	-79.9	-79.9	-79.9	-79.9	-79.9
	-79.9	-79.9	-79.9	-79.9	-79.9	-79.9	-79.9	-79.9	-79.9
	-79.9	-79.9	-79.9	-79.9	-79.9	-79.9	-79.9	-79.9	-79.9
	-79.9	-79.9	-79.9	-79.9	-79.9	-79.9	-79.9	-79.9	-79.9
3.	-75.5	-74.9	-74.6	-74.5	-74.6	-74.9	-75.5	-76.4	-77.5
	-78.9	-80.2	-80.8	-79.9	-78.2	-76.3	-74.7	-73.3	-72.3
	-71.5	-70.9	-70.6	-70.5	-70.6	-70.9	-71.5	-72.3	-73.3
	-74.7	-76.3	-78.2	-79.9	-80.8	-80.2	-78.9	-77.5	-76.4
6.	-70.4	-69.8	-69.5	-69.4	-69.5	-69.8	-70.4	-71.2	-72.6
	-74.5	-77.2	-80.2	-79.9	-76.3	-73.0	-70.5	-68.6	-67.2
	-66.2	-65.6	-65.2	-65.1	-65.2	-65.6	-66.2	-67.2	-68.6
	-70.5	-73.0	-76.3	-79.9	-80.2	-77.2	-74.5	-72.6	-71.2
9.	-67.7	-67.3	-67.0	-67.0	-67.0	-67.3	-67.7	-68.4	-69.6
	-71.4	-74.3	-78.7	-79.9	-74.5	-70.3	-67.4	-65.4	-63.9
	-62.8	-62.1	-61.7	-61.6	-61.7	-62.1	-62.8	-63.9	-65.4
	-67.4	-70.3	-74.5	-79.9	-78.7	-74.3	-71.4	-69.6	-68.4
12.	-66.3	-66.1	-65.9	-65.9	-65.9	-66.1	-66.3	-66.9	-67.8
	-69.4	-72.1	-77.1	-79.9	-72.9	-68.1	-65.1	-62.9	-61.4
	-60.4	-59.7	-59.3	-59.2	-59.3	-59.7	-60.4	-61.4	-62.9
	-65.1	-68.1	-72.9	-79.9	-77.1	-72.1	-69.4	-67.8	-66.9
15.	-65.8	-65.8	-65.8	-65.8	-65.8	-65.8	-65.8	-66.0	-66.6
	-67.9	-70.4	-75.5	-79.9	-71.4	-66.3	-63.2	-61.0	-59.6
	-58.6	-57.9	-57.6	-57.5	-57.6	-57.9	-58.6	-59.6	-61.0
	-63.2	-66.3	-71.4	-79.9	-75.5	-70.4	-67.9	-66.6	-66.0
18.	-65.9	-66.1	-66.4	-66.5	-66.4	-66.1	-65.9	-65.7	-66.0
	-67.0	-69.2	-74.2	-79.9	-70.2	-64.8	-61.6	-59.5	-58.1
	-57.2	-56.6	-56.3	-56.3	-56.3	-56.6	-57.2	-58.1	-59.5
	-61.6	-64.8	-70.2	-79.9	-74.2	-69.2	-67.0	-66.0	-65.7

TABLE XVI (CONTINUED)

CASE 2
UNNORMALIZED RESPONSE
TO OTHER BORESIGHT TARGETS

PRESUMED TARGET

SPEED (MPH)	TRACK (DEGREES)	AZIMUTH (DEGREES)	EIGENVALUE (dB)
30.	180.	30.	-54.9

TARGET TRACK (DEGREES)

TARGET SPEED (MPH)	0 90 180 270	10 100 190 280	20 110 200 290	30 120 210 300	40 130 220 310	50 140 230 320	60 150 240 330	70 160 250 340	80 170 260 350
21.	-66.6	-67.2	-67.8	-68.0	-67.8	-67.2	-66.6	-66.0	-65.8
	-66.3	-68.2	-73.0	-79.9	-69.0	-63.5	-60.3	-58.3	-57.0
	-56.2	-55.7	-55.5	-55.4	-55.5	-55.7	-56.2	-57.0	-58.3
	-60.3	-63.5	-69.0	-79.9	-73.0	-68.2	-66.3	-65.8	-66.0
24.	-67.9	-69.2	-70.2	-70.6	-70.2	-69.2	-67.9	-66.6	-65.9
	-65.9	-67.4	-72.0	-79.9	-68.0	-62.4	-59.2	-57.3	-56.1
	-55.5	-55.2	-55.0	-55.0	-55.0	-55.2	-55.5	-56.1	-57.3
	-59.2	-62.4	-68.0	-79.9	-72.0	-67.4	-65.9	-65.9	-66.6
27.	-69.9	-72.3	-74.2	-75.0	-74.2	-72.3	-69.9	-67.8	-66.3
	-65.8	-66.8	-71.1	-79.9	-67.1	-61.4	-58.3	-56.5	-55.5
	-55.0	-54.9	-54.9	-54.9	-54.9	-54.9	-55.0	-55.5	-56.5
	-58.3	-61.4	-67.1	-79.9	-71.1	-66.8	-65.8	-66.3	-67.8
30.	-73.2	-77.7	-82.4	-84.8	-82.4	-77.7	-73.2	-69.6	-67.0
	-65.8	-66.4	-70.3	-79.9	-66.2	-60.5	-57.5	-55.9	-55.1
	-54.9	-54.9	-55.0	-55.1	-55.0	-54.9	-54.9	-55.1	-55.9
	-57.5	-60.5	-66.2	-79.9	-70.3	-66.4	-65.8	-67.0	-69.6
33.	-78.8	-94.6	-88.7	-85.3	-88.7	-94.6	-78.8	-72.2	-68.1
	-66.0	-66.1	-69.7	-79.9	-65.4	-59.7	-56.8	-55.4	-54.9
	-54.9	-55.2	-55.5	-55.6	-55.5	-55.2	-54.9	-54.9	-55.4
	-56.8	-59.7	-65.4	-79.9	-69.7	-66.1	-66.0	-68.1	-72.2
36.	-98.2	-81.6	-77.5	-76.5	-77.5	-81.6	-98.2	-76.2	-69.7
	-66.5	-65.9	-69.1	-79.9	-64.7	-59.0	-56.3	-55.1	-54.9
	-55.2	-55.8	-56.3	-56.5	-56.3	-55.8	-55.2	-54.9	-55.1
	-56.2	-59.0	-64.7	-79.9	-69.1	-65.9	-66.5	-69.7	-76.2
39.	-81.8	-75.5	-73.6	-73.2	-73.6	-75.5	-81.8	-84.0	-71.9
	-67.1	-65.8	-68.6	-79.9	-64.0	-58.4	-55.8	-54.9	-55.1
	-55.8	-56.8	-57.5	-57.8	-57.5	-56.8	-55.8	-55.1	-54.9
	-55.8	-58.4	-64.0	-79.9	-68.6	-65.8	-67.1	-71.9	-84.0

AD-A101 143 AIR FORCE INST OF TECH WRIGHT-PATTERSON AFB OH SCHOO--ETC F/G 17/9
MULTIPLE ARRESTED SYNTHETIC APERTURE RADAR.(U)
MAY 81 J S SHUSTER
UNCLASSIFIED AFIT/DS/EE/81-3 NL

4 OF 5
AD A
101143

END
DATE
FILMED
7-81
DTIC

Cont

TABLE XVI (CONTINUED)

CASE 2
UNNORMALIZED RESPONSE
TO OTHER BORESIGHT TARGETS

PRESUMED TARGET

SPEED (MPH)	TRACK (DEGREES)	AZIMUTH (DEGREES)	EIGENVALUE (dB)
30.	180.	30.	-54.9

TARGET TRACK (DEGREES)

TARGET SPEED (MPH)	0 / 90 / 180 / 270	10 / 100 / 190 / 280	20 / 110 / 200 / 290	30 / 120 / 210 / 300	40 / 130 / 220 / 310	50 / 140 / 230 / 320	60 / 150 / 240 / 330	70 / 160 / 250 / 340	80 / 170 / 260 / 350
42.	-75.9	-72.8	-71.9	-71.6	-71.9	-72.8	-75.9	-92.0	-75.0
	-68.0	-65.8	-68.1	-79.9	-63.4	-57.8	-55.4	-54.9	-55.4
	-56.7	-58.1	-59.2	-59.7	-59.2	-58.1	-56.7	-55.4	-54.9
	-55.4	-57.8	-63.4	-79.9	-68.1	-65.8	-68.0	-75.0	-92.0
45.	-73.2	-71.6	-71.3	-71.3	-71.3	-71.6	-73.2	-79.7	-79.9
	-69.1	-65.8	-67.7	-79.9	-62.8	-57.3	-55.2	-55.0	-56.0
	-57.8	-59.9	-61.5	-62.2	-61.5	-59.9	-57.8	-56.0	-55.0
	-55.2	-57.3	-62.8	-79.9	-67.7	-65.8	-69.1	-79.9	-79.7
48.	-71.8	-71.3	-71.6	-71.9	-71.6	-71.3	-71.8	-75.4	-92.2
	-70.6	-66.0	-67.3	-79.9	-62.3	-56.8	-55.0	-55.2	-56.8
	-59.4	-62.3	-64.7	-65.7	-64.7	-62.3	-59.4	-56.8	-55.2
	-55.0	-56.8	-62.3	-79.9	-67.3	-66.0	-70.6	-92.2	-75.4
51.	-71.3	-71.8	-72.9	-73.4	-72.9	-71.8	-71.3	-73.1	-86.6
	-72.5	-66.3	-67.0	-79.9	-61.7	-56.4	-54.9	-55.6	-57.9
	-61.4	-65.6	-69.5	-71.3	-69.5	-65.6	-61.4	-57.9	-55.6
	-54.9	-56.4	-61.7	-79.9	-67.0	-66.3	-72.5	-86.6	-73.1
54.	-71.5	-73.2	-75.3	-76.3	-75.3	-73.2	-71.5	-71.9	-79.1
	-75.0	-66.7	-66.8	-79.9	-61.3	-56.1	-54.9	-56.1	-59.2
	-64.1	-70.7	-79.4	-85.9	-79.4	-70.7	-64.1	-59.2	-56.1
	-54.9	-56.1	-61.3	-79.9	-66.8	-66.7	-75.0	-79.1	-71.9
57.	-72.4	-75.8	-79.7	-81.8	-79.7	-75.8	-72.4	-71.3	-75.6
	-78.6	-67.1	-66.5	-80.0	-60.8	-55.8	-54.9	-56.8	-60.9
	-67.9	-81.9	-81.5	-77.5	-81.5	-81.9	-67.9	-60.9	-56.8
	-54.9	-55.8	-60.8	-79.9	-66.5	-67.1	-78.6	-75.6	-71.3
60.	-74.2	-80.3	-90.6	-102.8	-90.6	-80.3	-74.2	-71.4	-73.5
	-84.8	-67.7	-66.3	-80.0	-60.4	-55.5	-55.1	-57.6	-63.1
	-74.1	-80.1	-72.6	-71.3	-72.6	-80.1	-74.1	-63.1	-57.6
	-55.1	-55.5	-60.4	-79.9	-66.3	-67.7	-84.8	-73.5	-71.4

TABLE XVII

CASE 20
UNNORMALIZED RESPONSE
TO OTHER BORESIGHT TARGETS

PRESUMED TARGET

SPEED (MPH)	TRACK (DEGREES)	AZIMUTH (DEGREES)	EIGENVALUE (dB)
3.	180.	60.	-63.2

TARGET TRACK (DEGREES)

TARGET SPEED (MPH)	0 / 90 / 180 / 270	10 / 100 / 190 / 280	20 / 110 / 200 / 290	30 / 120 / 210 / 300	40 / 130 / 220 / 310	50 / 140 / 230 / 320	60 / 150 / 240 / 330	70 / 160 / 250 / 340	80 / 170 / 260 / 350
0.	-63.7	-63.7	-63.7	-63.7	-63.7	-63.7	-63.7	-63.7	-63.7
	-63.7	-63.7	-63.7	-63.7	-63.7	-63.7	-63.7	-63.7	-63.7
	-63.7	-63.7	-63.7	-63.7	-63.7	-63.7	-63.7	-63.7	-63.7
	-63.7	-63.7	-63.7	-63.7	-63.7	-63.7	-63.7	-63.7	-63.7
3.	-64.3	-64.4	-64.6	-64.7	-64.8	-64.9	-64.9	-64.9	-64.8
	-64.7	-64.6	-64.4	-64.3	-64.1	-63.9	-63.7	-63.5	-63.3
	-63.2	-63.0	-62.9	-62.8	-62.8	-62.7	-62.7	-62.7	-62.8
	-62.8	-62.9	-63.0	-63.2	-63.3	-63.5	-63.7	-63.9	-64.1
6.	-64.9	-65.3	-65.7	-66.0	-66.2	-66.3	-66.4	-66.3	-66.2
	-66.0	-65.7	-65.3	-64.9	-64.5	-64.1	-63.7	-63.3	-63.0
	-62.7	-62.5	-62.3	-62.1	-62.0	-61.9	-61.9	-61.9	-62.0
	-62.1	-62.3	-62.5	-62.7	-63.0	-63.3	-63.7	-64.1	-64.5
9.	-65.6	-66.3	-66.9	-67.5	-67.9	-68.2	-68.3	-68.2	-67.9
	-67.5	-66.9	-66.3	-65.6	-64.9	-64.3	-63.7	-63.2	-62.7
	-62.3	-62.0	-61.7	-61.5	-61.4	-61.3	-61.3	-61.3	-61.4
	-61.5	-61.7	-62.0	-62.3	-62.7	-63.2	-63.7	-64.3	-64.9
12.	-66.4	-67.4	-68.4	-69.4	-70.1	-70.7	-70.8	-70.7	-70.1
	-69.4	-68.4	-67.4	-66.4	-65.4	-64.5	-63.7	-63.0	-62.4
	-61.9	-61.5	-61.2	-61.0	-60.9	-60.8	-60.7	-60.8	-60.9
	-61.0	-61.2	-61.5	-61.9	-62.4	-63.0	-63.7	-64.5	-65.4
15.	-67.3	-68.8	-70.3	-71.9	-73.2	-74.1	-74.4	-74.1	-73.2
	-71.9	-70.3	-68.8	-67.3	-65.9	-64.7	-63.7	-62.8	-62.1
	-61.6	-61.1	-60.8	-60.6	-60.4	-60.4	-60.3	-60.4	-60.4
	-60.6	-60.8	-61.1	-61.6	-62.1	-62.8	-63.7	-64.7	-65.9
18.	-68.3	-70.4	-72.8	-75.4	-77.8	-79.6	-80.3	-79.6	-77.8
	-75.4	-72.8	-70.4	-68.3	-66.5	-65.0	-63.7	-62.7	-61.9
	-61.3	-60.8	-60.5	-60.3	-60.1	-60.0	-60.0	-60.0	-60.1
	-60.3	-60.5	-60.8	-61.3	-61.9	-62.7	-63.7	-65.0	-66.5

TABLE XVII (CONTINUED)

CASE 20
UNNORMALIZED RESPONSE
TO OTHER BORESIGHT TARGETS

PRESUMED TARGET

SPEED (MPH)	TRACK (DEGREES)	AZIMUTH (DEGREES)	EIGENVALUE (dB)
3.	180.	60.	-63.2

TARGET TRACK (DEGREES)

TARGET SPEED (MPH)	0	10	20	30	40	50	60	70	80
	90	100	110	120	130	140	150	160	170
	180	190	200	210	220	230	240	250	260
	270	280	290	300	310	320	330	340	350
21.	-69.5	-72.5	-76.2	-80.8	-84.9	-85.6	-85.2	-85.6	-84.9
	-80.8	-76.2	-72.5	-69.5	-67.1	-65.2	-63.7	-62.5	-61.6
	-61.0	-60.5	-60.2	-60.0	-59.9	-59.8	-59.8	-59.8	-59.9
	-60.0	-60.2	-60.5	-61.0	-61.6	-62.5	-63.7	-65.2	-67.1
24.	-70.8	-75.1	-81.3	-85.5	-81.2	-78.7	-77.9	-78.7	-81.2
	-85.5	-81.3	-75.1	-70.8	-67.8	-65.4	-63.7	-62.4	-61.4
	-60.7	-60.3	-60.0	-59.8	-59.7	-59.7	-59.7	-59.7	-59.7
	-59.8	-60.0	-60.3	-60.7	-61.4	-62.4	-63.7	-65.4	-67.8
27.	-72.5	-78.8	-85.6	-79.2	-75.5	-73.8	-73.3	-73.8	-75.5
	-79.2	-85.6	-78.8	-72.5	-68.5	-65.7	-63.7	-62.2	-61.2
	-60.5	-60.1	-59.8	-59.7	-59.6	-59.6	-59.6	-59.6	-59.6
	-59.7	-59.8	-60.1	-60.5	-61.2	-62.2	-63.7	-65.7	-68.5
30.	-74.4	-83.8	-80.1	-74.6	-72.0	-70.7	-70.4	-70.7	-72.0
	-74.6	-80.1	-83.8	-74.4	-69.3	-66.0	-63.7	-62.1	-61.0
	-60.3	-59.9	-59.7	-59.6	-59.6	-59.7	-59.7	-59.7	-59.6
	-59.6	-59.7	-59.9	-60.3	-61.0	-62.1	-63.7	-66.0	-69.3
33.	-77.0	-84.8	-75.6	-71.6	-69.6	-68.6	-68.3	-68.6	-69.6
	-71.6	-75.6	-84.8	-77.0	-70.2	-66.2	-63.7	-62.0	-60.9
	-60.2	-59.8	-59.6	-59.6	-59.7	-59.8	-59.8	-59.8	-59.7
	-59.6	-59.6	-59.8	-60.2	-60.9	-62.0	-63.7	-66.2	-70.2
36.	-80.3	-79.8	-72.6	-69.5	-67.9	-67.1	-66.8	-67.1	-67.9
	-69.5	-72.6	-79.8	-80.3	-71.1	-66.5	-63.7	-61.9	-60.7
	-60.0	-59.7	-59.6	-59.7	-59.8	-59.9	-60.0	-59.9	-59.8
	-59.7	-59.6	-59.7	-60.0	-60.7	-61.9	-63.7	-66.5	-71.1
39.	-84.4	-76.0	-70.5	-67.9	-66.6	-65.9	-65.7	-65.9	-66.6
	-67.9	-70.5	-76.0	-84.4	-72.3	-66.8	-63.7	-61.7	-60.5
	-59.9	-59.7	-59.7	-59.8	-60.0	-60.2	-60.2	-60.2	-60.0
	-59.8	-59.7	-59.7	-59.9	-60.5	-61.7	-63.7	-66.8	-72.3

TABLE XVII (CONTINUED)

CASE 20
UNNORMALIZED RESPONSE
TO OTHER BORESIGHT TARGETS

PRESUMED TARGET

SPEED (MPH)	TRACK (DEGREES)	AZIMUTH (DEGREES)	EIGENVALUE (dB)
3.	180.	60.	-63.2

TARGET TRACK (DEGREES)

TARGET SPEED (MPH)	0	10	20	30	40	50	60	70	80
	90	100	110	120	130	140	150	160	170
	180	190	200	210	220	230	240	250	260
	270	280	290	300	310	320	330	340	350
42.	-85.2	-73.3	-68.8	-66.7	-65.6	-65.1	-64.9	-65.1	-65.6
	-66.7	-68.8	-73.3	-85.2	-73.6	-67.2	-63.7	-61.6	-60.4
	-59.8	-59.6	-59.7	-60.0	-60.3	-60.5	-60.6	-60.5	-60.3
	-60.0	-59.7	-59.6	-59.8	-60.4	-61.6	-63.7	-67.2	-73.6
45.	-81.4	-71.3	-67.5	-65.7	-64.8	-64.5	-64.4	-64.5	-64.8
	-65.7	-67.5	-71.3	-81.4	-75.0	-67.5	-63.7	-61.5	-60.3
	-59.7	-59.6	-59.9	-60.2	-60.6	-60.9	-61.0	-60.9	-60.6
	-60.2	-59.9	-59.6	-59.7	-60.3	-61.5	-63.7	-67.5	-75.0
48.	-77.9	-69.7	-66.5	-65.0	-64.3	-64.1	-64.0	-64.1	-64.3
	-65.0	-66.5	-69.7	-77.9	-76.8	-67.8	-63.7	-61.4	-60.2
	-59.7	-59.7	-60.0	-60.5	-61.0	-61.3	-61.5	-61.3	-61.0
	-60.5	-60.0	-59.7	-59.7	-60.2	-61.4	-63.7	-67.8	-76.8
51.	-75.3	-68.5	-65.7	-64.5	-64.0	-63.9	-63.9	-63.9	-64.0
	-64.5	-65.7	-68.5	-75.3	-79.0	-68.2	-63.7	-61.3	-60.1
	-59.6	-59.8	-60.2	-60.9	-61.5	-61.9	-62.1	-61.9	-61.5
	-60.9	-60.2	-59.8	-59.6	-60.1	-61.3	-63.7	-68.2	-79.0
54.	-73.3	-67.4	-65.1	-64.1	-63.9	-64.0	-64.0	-64.0	-63.9
	-64.1	-65.1	-67.4	-73.3	-81.6	-68.6	-63.7	-61.2	-60.0
	-59.6	-59.9	-60.5	-61.3	-62.0	-62.5	-62.7	-62.5	-62.0
	-61.3	-60.5	-59.9	-59.6	-60.0	-61.2	-63.7	-68.6	-81.6
57.	-71.7	-66.6	-64.6	-63.9	-64.0	-64.3	-64.4	-64.3	-64.0
	-63.9	-64.6	-66.6	-71.7	-84.4	-69.0	-63.7	-61.1	-59.9
	-59.6	-60.0	-60.8	-61.7	-62.6	-63.2	-63.5	-63.2	-62.6
	-61.7	-60.8	-60.0	-59.6	-59.9	-61.1	-63.7	-69.0	-84.4
60.	-70.4	-65.9	-64.2	-63.9	-64.3	-64.9	-65.1	-64.9	-64.3
	-63.9	-64.2	-65.9	-70.4	-85.7	-69.4	-63.7	-61.0	-59.8
	-59.7	-60.2	-61.1	-62.3	-63.3	-64.0	-64.3	-64.0	-63.3
	-62.3	-61.1	-60.2	-59.7	-59.8	-61.0	-63.7	-69.4	-85.7

TABLE XVII (CONTINUED)

CASE 20
UNNORMALIZED RESPONSE
TO OTHER BORESIGHT TARGETS

PRESUMED TARGET			
SPEED (MPH)	TRACK (DEGREES)	AZIMUTH (DEGREES)	EIGENVALUE (dB)
15.	180.	60.	-60.1

TARGET TRACK (DEGREES)

TARGET SPEED (MPH)									
	0	10	20	30	40	50	60	70	80
	90	100	110	120	130	140	150	160	170
	180	190	200	210	220	230	240	250	260
	270	280	290	300	310	320	330	340	350
0.	-66.4	-66.4	-66.4	-66.4	-66.4	-66.4	-66.4	-66.4	-66.4
	-66.4	-66.4	-66.4	-66.4	-66.4	-66.4	-66.4	-66.4	-66.4
	-66.4	-66.4	-66.4	-66.4	-66.4	-66.4	-66.4	-66.4	-66.4
	-66.4	-66.4	-66.4	-66.4	-66.4	-66.4	-66.4	-66.4	-66.4
3.	-68.6	-69.3	-70.1	-70.7	-71.2	-71.5	-71.6	-71.5	-71.2
	-70.7	-70.1	-69.3	-68.6	-67.8	-67.1	-66.4	-65.7	-65.2
	-64.7	-64.2	-63.9	-63.6	-63.4	-63.3	-63.2	-63.3	-63.4
	-63.6	-63.9	-64.2	-64.7	-65.2	-65.7	-66.4	-67.1	-67.8
6.	-71.6	-73.9	-76.6	-79.6	-82.6	-84.9	-85.9	-84.9	-82.6
	-79.6	-76.6	-73.9	-71.6	-69.6	-67.9	-66.4	-65.1	-64.1
	-63.2	-62.5	-62.0	-61.5	-61.2	-61.1	-61.0	-61.1	-61.2
	-61.5	-62.0	-62.5	-63.2	-64.1	-65.1	-66.4	-67.9	-69.6
9.	-76.2	-83.8	-88.8	-80.6	-77.0	-75.4	-74.9	-75.4	-77.0
	-80.6	-88.8	-83.8	-76.2	-71.8	-68.7	-66.4	-64.6	-63.2
	-62.0	-61.1	-60.4	-59.9	-59.6	-59.4	-59.3	-59.4	-59.6
	-59.9	-60.4	-61.1	-62.0	-63.2	-64.6	-66.4	-68.7	-71.8
12.	-85.9	-81.1	-74.3	-71.0	-69.3	-68.3	-68.0	-68.3	-69.3
	-71.0	-74.3	-81.1	-85.9	-74.7	-69.6	-66.4	-64.1	-62.3
	-61.0	-60.0	-59.2	-58.7	-58.3	-58.1	-58.0	-58.1	-58.3
	-58.7	-59.2	-60.0	-61.0	-62.3	-64.1	-66.4	-69.6	-74.7
15.	-82.7	-72.9	-68.9	-66.6	-65.3	-64.6	-64.3	-64.6	-65.3
	-66.6	-68.9	-72.9	-82.7	-79.2	-70.7	-66.4	-63.6	-61.6
	-60.1	-59.0	-58.2	-57.6	-57.2	-57.0	-56.9	-57.0	-57.2
	-57.6	-58.2	-59.0	-60.1	-61.6	-63.6	-66.4	-70.7	-79.2
18.	-74.9	-68.8	-65.6	-63.8	-62.6	-62.0	-61.8	-62.0	-62.6
	-63.8	-65.6	-68.8	-74.9	-87.6	-71.9	-66.4	-63.1	-60.9
	-59.3	-58.2	-57.3	-56.7	-56.4	-56.1	-56.1	-56.1	-56.4
	-56.7	-57.3	-58.2	-59.3	-60.9	-63.1	-66.4	-71.9	-87.6

TABLE XVII (CONTINUED)

CASE 20
UNNORMALIZED RESPONSE
TO OTHER BORESIGHT TARGETS

PRESUMED TARGET SPEED (MPH)	TRACK (DEGREES)	AZIMUTH (DEGREES)	EIGENVALUE (dB)
15.	180.	60.	-60.1

TARGET TRACK (DEGREES)

TARGET SPEED (MPH)	0 90 180 270	10 100 190 280	20 110 200 290	30 120 210 300	40 130 220 310	50 140 230 320	60 150 240 330	70 160 250 340	80 170 260 350
21.	-70.8	-66.0	-63.3	-61.7	-60.7	-60.2	-60.0	-60.2	-60.7
	-61.7	-63.3	-66.0	-70.8	-85.6	-73.3	-66.4	-62.7	-60.3
	-58.6	-57.4	-56.6	-56.0	-55.7	-55.4	-55.4	-55.4	-55.7
	-56.0	-56.6	-57.4	-58.6	-60.3	-62.7	-66.4	-73.3	-85.6
24.	-68.0	-63.9	-61.6	-60.1	-59.2	-58.7	-58.6	-58.7	-59.2
	-60.1	-61.6	-63.9	-68.0	-78.2	-74.9	-66.4	-62.3	-59.7
	-58.0	-56.8	-56.0	-55.4	-55.1	-54.9	-54.8	-54.9	-55.1
	-55.4	-56.0	-56.8	-58.0	-59.7	-62.3	-66.4	-74.9	-78.2
27.	-66.0	-62.3	-60.2	-58.8	-58.0	-57.6	-57.5	-57.6	-58.0
	-58.8	-60.2	-62.3	-66.0	-74.1	-77.0	-66.4	-61.9	-59.2
	-57.4	-56.2	-55.4	-54.9	-54.6	-54.5	-54.4	-54.5	-54.6
	-54.9	-55.4	-56.2	-57.4	-59.2	-61.9	-66.4	-77.0	-74.1
30.	-64.3	-61.0	-59.0	-57.8	-57.1	-56.8	-56.6	-56.8	-57.1
	-57.8	-59.0	-61.0	-64.3	-71.3	-79.6	-66.4	-61.5	-58.7
	-56.9	-55.8	-55.0	-54.5	-54.3	-54.1	-54.1	-54.1	-54.3
	-54.5	-55.0	-55.8	-56.9	-58.7	-61.5	-66.4	-79.6	-71.3
33.	-63.0	-59.9	-58.1	-57.0	-56.4	-56.1	-56.0	-56.1	-56.4
	-57.0	-58.1	-59.9	-63.0	-69.2	-83.3	-66.4	-61.2	-58.3
	-56.5	-55.3	-54.6	-54.2	-54.0	-53.9	-53.9	-53.9	-54.0
	-54.2	-54.6	-55.3	-56.5	-58.3	-61.2	-66.4	-83.3	-69.3
36.	-61.8	-58.9	-57.3	-56.4	-55.9	-55.6	-55.5	-55.6	-55.9
	-56.4	-57.3	-58.9	-61.8	-67.6	-88.6	-66.4	-60.8	-57.9
	-56.1	-55.0	-54.3	-54.0	-53.8	-53.8	-53.7	-53.8	-53.8
	-54.0	-54.3	-55.0	-56.1	-57.9	-60.8	-66.4	-88.6	-67.6
39.	-60.8	-58.2	-56.7	-55.9	-55.5	-55.3	-55.2	-55.3	-55.5
	-55.9	-56.7	-58.2	-60.8	-66.2	-90.0	-66.4	-60.5	-57.5
	-55.7	-54.7	-54.1	-53.8	-53.7	-53.7	-53.7	-53.7	-53.7
	-53.8	-54.1	-54.7	-55.7	-57.5	-60.5	-66.4	-90.0	-66.2

TABLE XVII (CONTINUED)

CASE 20
UNNORMALIZED RESPONSE
TO OTHER BORESIGHT TARGETS

PRESUMED TARGET

SPEED (MPH)	TRACK (DEGREES)	AZIMUTH (DEGREES)	EIGENVALUE (dB)
15.	180.	60.	-60.1

TARGET TRACK (DEGREES)

TARGET SPEED (MPH)	0 90 180 270	10 100 190 280	20 110 200 290	30 120 210 300	40 130 220 310	50 140 230 320	60 150 240 330	70 160 250 340	80 170 260 350
42.	-60.0	-57.5	-56.2	-55.5	-55.2	-55.1	-55.1	-55.1	-55.2
	-55.5	-56.2	-57.5	-60.0	-65.0	-84.5	-66.4	-60.2	-57.1
	-55.4	-54.4	-53.9	-53.7	-53.7	-53.7	-53.7	-53.7	-53.7
	-53.7	-53.9	-54.4	-55.4	-57.1	-60.2	-66.4	-84.5	-65.0
45.	-59.2	-56.9	-55.7	-55.2	-55.1	-55.1	-55.2	-55.1	-55.1
	-55.2	-55.7	-56.9	-59.2	-64.0	-80.5	-66.4	-59.9	-56.8
	-55.1	-54.2	-53.8	-53.7	-53.7	-53.8	-53.9	-53.8	-53.7
	-53.7	-53.8	-54.2	-55.1	-56.8	-59.9	-66.4	-80.5	-64.0
48.	-58.6	-56.4	-55.4	-55.1	-55.2	-55.3	-55.4	-55.3	-55.2
	-55.1	-55.4	-56.4	-58.6	-63.0	-77.6	-66.4	-59.6	-56.5
	-54.8	-54.0	-53.7	-53.7	-53.9	-54.0	-54.1	-54.0	-53.9
	-53.7	-53.7	-54.0	-54.8	-56.5	-59.6	-66.4	-77.6	-63.0
51.	-58.0	-56.0	-55.2	-55.1	-55.4	-55.7	-55.8	-55.7	-55.4
	-55.1	-55.2	-56.0	-58.0	-62.2	-75.4	-66.4	-59.4	-56.2
	-54.6	-53.9	-53.7	-53.8	-54.0	-54.3	-54.3	-54.3	-54.0
	-53.8	-53.7	-53.9	-54.6	-56.2	-59.4	-66.4	-75.4	-62.2
54.	-57.5	-55.7	-55.1	-55.3	-55.8	-56.3	-56.5	-56.3	-55.8
	-55.3	-55.1	-55.7	-57.5	-61.5	-73.7	-66.4	-59.1	-55.9
	-54.4	-53.8	-53.7	-54.0	-54.3	-54.6	-54.7	-54.6	-54.3
	-54.0	-53.7	-53.8	-54.4	-55.9	-59.1	-66.4	-73.7	-61.5
57.	-57.0	-55.5	-55.1	-55.6	-56.4	-57.2	-57.5	-57.2	-56.4
	-55.6	-55.1	-55.5	-57.0	-60.8	-72.2	-66.4	-58.9	-55.7
	-54.2	-53.7	-53.8	-54.2	-54.6	-55.0	-55.1	-55.0	-54.6
	-54.2	-53.8	-53.7	-54.2	-55.7	-58.9	-66.4	-72.2	-60.8
60.	-56.6	-55.3	-55.2	-56.0	-57.3	-58.5	-59.0	-58.5	-57.3
	-56.0	-55.2	-55.3	-56.6	-60.2	-71.0	-66.4	-58.6	-55.5
	-54.1	-53.7	-53.9	-54.4	-55.0	-55.5	-55.6	-55.5	-55.0
	-54.4	-53.9	-53.7	-54.1	-55.5	-58.6	-66.4	-71.0	-60.2

TABLE XVII (CONTINUED)

CASE 20
UNNORMALIZED RESPONSE
TO OTHER BORESIGHT TARGETS

PRESUMED TARGET

SPEED (MPH)	TRACK (DEGREES)	AZIMUTH (DEGREES)	EIGENVALUE (dB)
30.	180.	60.	-56.5

TARGET TRACK (DEGREES)

TARGET SPEED (MPH)	0	10	20	30	40	50	60	70	80
	90	100	110	120	130	140	150	160	170
	180	190	200	210	220	230	240	250	260
	270	280	290	300	310	320	330	340	350
0.	-69.9	-69.9	-69.9	-69.9	-69.9	-69.9	-69.9	-69.9	-69.9
	-69.9	-69.9	-69.9	-69.9	-69.9	-69.9	-69.9	-69.9	-69.9
	-69.9	-69.9	-69.9	-69.9	-69.9	-69.9	-69.9	-69.9	-69.9
	-69.9	-69.9	-69.9	-69.9	-69.9	-69.9	-69.9	-69.9	-69.9
3.	-74.3	-76.2	-78.1	-80.0	-81.7	-83.0	-83.4	-83.0	-81.7
	-80.0	-78.1	-76.2	-74.3	-72.7	-71.2	-69.9	-68.8	-67.8
	-67.0	-66.4	-65.8	-65.4	-65.1	-64.9	-64.9	-64.9	-65.1
	-65.4	-65.8	-66.4	-67.0	-67.8	-68.8	-69.9	-71.2	-72.7
6.	-83.4	-91.2	-82.2	-78.0	-75.8	-74.6	-74.3	-74.6	-75.8
	-78.0	-82.2	-91.2	-83.4	-76.8	-72.8	-69.9	-67.8	-66.2
	-64.9	-63.8	-63.1	-62.5	-62.1	-61.8	-61.7	-61.8	-62.1
	-62.5	-63.1	-63.8	-64.9	-66.2	-67.8	-69.9	-72.8	-76.8
9.	-83.2	-75.1	-71.5	-69.3	-68.0	-67.3	-67.1	-67.3	-68.0
	-69.3	-71.5	-75.1	-83.2	-84.2	-74.6	-69.9	-66.9	-64.8
	-63.2	-61.9	-61.0	-60.3	-59.9	-59.6	-59.5	-59.6	-59.9
	-60.3	-61.0	-61.9	-63.2	-64.8	-66.9	-69.9	-74.6	-84.2
12.	-74.3	-69.5	-66.8	-65.1	-64.1	-63.5	-63.3	-63.5	-64.1
	-65.1	-66.8	-69.5	-74.3	-87.9	-76.9	-69.9	-66.1	-63.6
	-61.7	-60.4	-59.4	-58.7	-58.2	-57.9	-57.8	-57.9	-58.2
	-58.7	-59.4	-60.4	-61.7	-63.6	-66.1	-69.9	-76.9	-87.9
15.	-70.0	-66.1	-63.9	-62.4	-61.5	-61.0	-60.8	-61.0	-61.5
	-62.4	-63.9	-66.1	-70.0	-78.4	-80.1	-69.9	-65.4	-62.5
	-60.5	-59.1	-58.1	-57.3	-56.8	-56.6	-56.5	-56.6	-56.8
	-57.3	-58.1	-59.1	-60.5	-62.5	-65.4	-69.9	-80.1	-78.4
18.	-67.1	-63.8	-61.7	-60.4	-59.6	-59.1	-59.0	-59.1	-59.6
	-60.4	-61.7	-63.8	-67.1	-73.7	-84.8	-69.9	-64.7	-61.6
	-59.5	-58.0	-57.0	-56.2	-55.8	-55.5	-55.4	-55.5	-55.8
	-56.2	-57.0	-58.0	-59.5	-61.6	-64.7	-69.9	-84.8	-73.7

TABLE XVII (CONTINUED)

CASE 20
UNNORMALIZED RESPONSE
TO OTHER BORESIGHT TARGETS

	PRESUMED TARGET		
SPEED (MPH)	TRACK (DEGREES)	AZIMUTH (DEGREES)	EIGENVALUE (dB)
30.	180.	60.	-56.5

TARGET TRACK (DEGREES)

TARGET SPEED (MPH)	0 / 90 / 180 / 270	10 / 100 / 190 / 280	20 / 110 / 200 / 290	30 / 120 / 210 / 300	40 / 130 / 220 / 310	50 / 140 / 230 / 320	60 / 150 / 240 / 330	70 / 160 / 250 / 340	80 / 170 / 260 / 350
21.	-65.0	-62.0	-60.1	-58.9	-58.1	-57.7	-57.6	-57.7	-58.1
	-58.9	-60.1	-62.0	-65.0	-70.7	-91.5	-69.9	-64.1	-60.8
	-58.6	-57.1	-56.1	-55.3	-54.9	-54.6	-54.5	-54.6	-54.9
	-55.3	-56.1	-57.1	-58.6	-60.8	-64.1	-69.9	-91.5	-70.7
24.	-63.3	-60.5	-58.8	-57.7	-57.0	-56.7	-56.5	-56.7	-57.0
	-57.7	-58.8	-60.5	-63.3	-68.5	-87.0	-69.9	-63.5	-60.0
	-57.8	-56.3	-55.3	-54.6	-54.1	-53.9	-53.8	-53.9	-54.1
	-54.6	-55.3	-56.3	-57.8	-60.0	-63.5	-69.9	-87.0	-68.5
27.	-62.0	-59.3	-57.7	-56.7	-56.1	-55.8	-55.7	-55.8	-56.1
	-56.7	-57.7	-59.3	-62.0	-66.7	-81.5	-69.9	-63.0	-59.4
	-57.1	-55.6	-54.6	-53.9	-53.5	-53.3	-53.2	-53.3	-53.5
	-53.9	-54.6	-55.6	-57.1	-59.4	-63.0	-69.9	-81.5	-66.7
30.	-60.8	-58.4	-56.9	-56.0	-55.5	-55.2	-55.1	-55.2	-55.5
	-56.0	-56.9	-58.4	-60.8	-65.3	-77.9	-69.9	-62.5	-58.7
	-56.5	-55.0	-54.0	-53.4	-53.0	-52.8	-52.8	-52.8	-53.0
	-53.4	-54.0	-55.0	-56.5	-58.7	-62.5	-69.9	-77.9	-65.3
33.	-59.8	-57.5	-56.2	-55.4	-55.0	-54.8	-54.7	-54.8	-55.0
	-55.4	-56.2	-57.5	-59.8	-64.1	-75.4	-69.9	-62.0	-58.2
	-55.9	-54.5	-53.6	-53.0	-52.7	-52.5	-52.4	-52.5	-52.7
	-53.0	-53.6	-54.5	-55.9	-58.2	-62.0	-69.9	-75.4	-64.1
36.	-59.0	-56.8	-55.6	-54.9	-54.6	-54.5	-54.5	-54.5	-54.6
	-54.9	-55.6	-56.8	-59.0	-63.0	-73.4	-69.9	-61.5	-57.7
	-55.4	-54.0	-53.1	-52.6	-52.4	-52.2	-52.2	-52.2	-52.4
	-52.6	-53.1	-54.0	-55.4	-57.7	-61.5	-69.9	-73.4	-63.0
39.	-58.3	-56.2	-55.1	-54.6	-54.4	-54.4	-54.4	-54.4	-54.4
	-54.6	-55.1	-56.2	-58.3	-62.1	-71.8	-69.9	-61.1	-57.2
	-54.9	-53.6	-52.8	-52.4	-52.2	-52.1	-52.0	-52.1	-52.2
	-52.4	-52.8	-53.6	-54.9	-57.2	-61.1	-69.9	-71.8	-62.1

TABLE XVII (CONTINUED)

CASE 20
UNNORMALIZED RESPONSE
TO OTHER BORESIGHT TARGETS

PRESUMED TARGET

SPEED (MPH)	TRACK (DEGREES)	AZIMUTH (DEGREES)	EIGENVALUE (dB)
30.	180.	60.	-56.5

TARGET TRACK (DEGREES)

TARGET SPEED (MPH)									
	0	10	20	30	40	50	60	70	80
	90	100	110	120	130	140	150	160	170
	180	190	200	210	220	230	240	250	260
	270	280	290	300	310	320	330	340	350
42.	-57.6	-55.7	-54.8	-54.5	-54.4	-54.5	-54.5	-54.5	-54.4
	-54.5	-54.8	-55.7	-57.6	-61.3	-70.4	-69.9	-60.7	-56.7
	-54.5	-53.2	-52.5	-52.2	-52.0	-52.0	-52.0	-52.0	-52.0
	-52.2	-52.5	-53.2	-54.5	-56.7	-60.7	-69.9	-70.4	-61.3
45.	-57.0	-55.3	-54.6	-54.4	-54.6	-54.8	-54.9	-54.8	-54.6
	-54.4	-54.6	-55.3	-57.0	-60.6	-69.3	-69.9	-60.3	-56.3
	-54.1	-52.9	-52.3	-52.0	-52.0	-52.0	-52.0	-52.0	-52.0
	-52.0	-52.3	-52.9	-54.1	-56.3	-60.3	-69.9	-69.3	-60.6
48.	-56.5	-55.0	-54.4	-54.5	-54.9	-55.3	-55.4	-55.3	-54.9
	-54.5	-54.4	-55.0	-56.5	-59.9	-68.3	-69.9	-60.0	-55.9
	-53.8	-52.7	-52.1	-52.0	-52.0	-52.0	-52.1	-52.0	-52.0
	-52.0	-52.1	-52.7	-53.8	-55.9	-60.0	-69.9	-68.3	-59.9
51.	-56.1	-54.7	-54.4	-54.7	-55.4	-56.0	-56.2	-56.0	-55.4
	-54.7	-54.4	-54.7	-56.1	-59.3	-67.3	-69.9	-59.6	-55.6
	-53.5	-52.5	-52.0	-52.0	-52.1	-52.2	-52.2	-52.2	-52.1
	-52.0	-52.0	-52.5	-53.5	-55.6	-59.6	-69.9	-67.4	-59.3
54.	-55.7	-54.6	-54.5	-55.2	-56.2	-57.1	-57.5	-57.1	-56.2
	-55.2	-54.5	-54.6	-55.7	-58.7	-66.5	-69.9	-59.3	-55.2
	-53.2	-52.3	-52.0	-52.0	-52.2	-52.4	-52.5	-52.4	-52.2
	-52.0	-52.0	-52.3	-53.2	-55.2	-59.3	-69.9	-66.5	-58.7
57.	-55.4	-54.4	-54.7	-55.8	-57.3	-58.7	-59.2	-58.7	-57.3
	-55.8	-54.7	-54.4	-55.4	-58.3	-65.8	-69.9	-59.0	-54.9
	-53.0	-52.2	-52.0	-52.1	-52.4	-52.7	-52.8	-52.7	-52.4
	-52.1	-52.0	-52.2	-53.0	-54.9	-59.0	-69.9	-65.8	-58.3
60.	-55.1	-54.4	-55.0	-56.6	-58.8	-61.0	-62.0	-61.0	-58.8
	-56.6	-55.0	-54.4	-55.1	-57.8	-65.1	-69.9	-58.7	-54.6
	-52.8	-52.1	-52.0	-52.3	-52.7	-53.1	-53.2	-53.1	-52.7
	-52.3	-52.0	-52.1	-52.8	-54.6	-58.7	-69.9	-65.1	-57.8

VITA

Jerrold Stuart Shuster was born on 30 March 1940 in Flint, Michigan. He graduated from Flint Central High School in 1957 and attended Flint Junior College the following year. In the Fall of 1958 he transferred to the University of Michigan in Ann Arbor, from which he received the degrees of Bachelor of Science in Engineering (Electrical Engineering) and Bachelor of Science (Engineering Mathematics) in 1963. He received his commission in the USAF on 5 November 1963 as a distinguished graduate from Officer Training School at Lackland AFB, Texas. After an assignment at the Commumications Computer Programming Center at Tinker AFB, Oklahoma, he entered the Air Force Institute of Technology (AFIT) at Wright-Patterson AFB, Ohio in 1968 and obtained the degree of Master of Science in Electrical Engineering in 1970. He then spent a year at Tan Son Nhut AB, Republic of Vietnam, followed by two years with the 1st Aerospace Communications Group-Command at Offutt AFB, Nebraska. In July, 1973, he re-entered AFIT to obtain the degree of Doctor of Philosophy in Aerospace Engineering. He was admitted to Candidacy in 1975 and was assigned to the Microwave Physics Laboratory, Air Force Cambridge Research Laboratories at Hanscom AFB, Massachusetts until June 1979. He then transferred to the Air Force Weapons Laboratory at Kirtland AFB, New Mexico, where he is currently the Chief, EMP Interactions and Advanced Concepts Section of the Electromagnetics Technology Branch of the Applied Physics Division.

Permanent address: care of:
29 Burt Ct
Valley Stream, L.I., NY 11581

END

DATE FILMED

7 81

DTIC

AD-A101 143 MULTIPLE ARRESTED SYNTHETIC APERTURE RADAR(U) AIR FORCE 5/5
INST OF TECH WRIGHT-PATTERSON AFB OH SCHOOL OF
ENGINEERING J S SHUSTER MAY 81 AFIT/DS/EE/81-3

UNCLASSIFIED F/G 17/9 NL

END
DATE
FILMED
5 83
DTIC

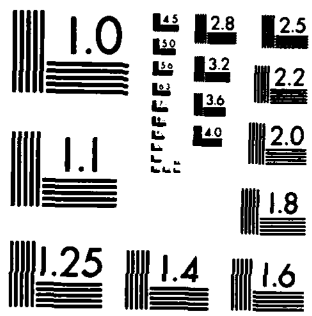

MICROCOPY RESOLUTION TEST CHART
NATIONAL BUREAU OF STANDARDS-1963-A

SUPPLEMENTARY

INFORMATION

AFIT/DS/EE/81-3

Corrected rept. no.

AD A101183

MULTIPLE ARRESTED

SYNTHETIC APERTURE RADAR

DISSERTATION

AFIT/DS/EE/81-3

Jerrold S. Shuster
Major USAF

Approved for public release; distribution unlimited